THE DEVELOPMENT OF PROXIMAL SENSING METHODS FOR SOIL MAPPING AND MONITORING, AND THEIR APPLICATION TO PRECISION IRRIGATION

A thesis presented in partial fulfilment of the requirements for the degree of

Doctor of Philosophy

in

Soil Science

at

Massey University, Palmerston North, New Zealand

Carolyn B Hedley

2009

Abstract

The potential of proximal soil sensing methods for high resolution investigation of soils in the landscape has been investigated. This addresses the need for improved environmental monitoring and management of soils within their environs. On-the-go electromagnetic (EM) mapping has been used to map soils, providing a high resolution (< 10m) spatially defined soil apparent electrical conductivity (EC_a) datalayer. Vis-NIR field spectroscopy has been trialled for in situ analysis of soil carbon, nitrogen and moisture.

The portable spectroradiometer has been used at 6 sites in the Taupo-Rotorua region for rapid, field analysis of soil carbon (R^2 calibration = 0.95, R^2 prediction = 0.75,) soil nitrogen (R^2 calibration = 0.95, R^2 prediction = 0.86) and moisture (R^2 calibration = 0.96, R^2 prediction = 0.70) by collecting reflectance spectra from the flat surface of a soil core; and at one Manawatu site for soil moisture (R^2 calibration = 0.79, R^2 prediction = 0.71), where the reflectance spectra were collected directly from a freshly cut in situ soil surface. EM mapping and Vis-NIR field spectroscopy were used in combination to spatially characterize soil moisture patterns at the Manawatu site.

Soil available water-holding capacity (AWC) of EC_a-defined zones has been assessed at six irrigated production farming sites. Two methods (predicted AWC v EC_a; estimated AWC v EC_a) have been used to relate soil EC_a to soil AWC to predict spatial AWC ($R^2 \geq$ 0.8 at 5 sites). Site-specific soil water balance models have been developed at all sites; and a wireless real-time soil moisture monitoring network has been trialled at two sites, to be used with the EC_a-AWC prediction model for the development of daily soil water status maps, for variable rate irrigation (VRI) scheduling. This digital, spatially defined soil water status information is available for upload to a sprinkler system modified for variable rate application.

The calculated water savings with VRI were 9–26% with equivalent energy savings and improved irrigation water use efficiency. Drainage and runoff were reduced by 0–55% during the period of irrigation, with the accompanying reduced risk of nitrogen

leaching. The reduction in virtual water content of product has also been assessed for VRI and compared with uniform rate irrigation (URI) at three study sites.

This study suggests that these proximal sensing methods provide a new improved way of monitoring and mapping soils. This facilitates soil inventory mapping, for example soil moisture and carbon mapping. In addition, these high resolution environmental monitoring and mapping techniques provide the information required for optimizing site-specific management of natural resources at the farm scale.

On-the-go electromagnetic (EM) mapping has enabled a step change in the pedological investigation of New Zealand soils. Resulting soil EC_a maps provide a tool for improving traditional soil map boundaries because they delineate soil zones primarily on a basis of soil texture and moisture in non-saline soils. In this study the maps have been used for site-specific irrigation management at the farm-scale, aiming to increase the energy efficiency of this land management operation. The study has developed a method for improved use of freshwaters by more accurate irrigation scheduling, based on high resolution characterization of spatial and temporal soil differences.

Acknowledgements

There are many. Firstly I would like to acknowledge the support of my three supervisors. Ian Yule, my chief supervisor and agricultural engineer who introduced me to sensor technologies and on-the-go mapping systems. Mike Tuohy, remote sensing expert, who introduced me to GIS and the enormous opportunities that it offers to a traditional soil science background. Alison Collins, soil and landscapes strategist, who provided much appreciated support, during her role as Science Leader of the Soil and Landscapes Group, in Landcare Research. Thank-you to all three of you for providing a well-balanced, supportive network of supervision.

I also acknowledge AGMARDT and NZVCC William Georgetti Scholarship funds for supporting this study. Thank-you Landcare Research for allowing me to take time out to pursue my interest in these new technologies, that offer so much to the study of soils in the immediate future. I especially thank Allan Hewitt for his support of this research.

I would also like to acknowledge Matt Irwin and Anne Sutherland for training me to use ArcGIS; Anne Austin for really helpful assistance with editing, Moira Hubbard for formatting, John Dando for top quality assistance with field and laboratory work, Greg Arnold (late) and Anne West for help with statistics, and Dave Scotter for assistance with soil water balance modelling and greatly appreciated soil water discussions. I would particularly like to thank Ian, Mike, Matt, Miles, John P, Ieda, Ina and Reddy for all those fun coffee breaks. I particularly enjoy the sense of humour of the NZCPA whanua.

Thank-you to previous NZCPA students – Callum Eastwood, Hayden Lawrence, Rob Murray and Stu Bradbury who helped me with EM mapping and other field-work before and during my PhD studies. I also really appreciated the collaboration and friendship of Bambang Kusumo, as he developed a new field method for collection and analysis of VIS-NIR reflectance spectra of soil cores as his PhD topic. To Stu – thanks for your help in EM mapping the Massey University farms. As the concept of variable rate

irrigation evolved in my mind as a soil-based decision support tool, so (I think) it developed in Stu's mind as a modification of a centre-pivot or lateral irrigator with individual sprinkler control. Stu went on to form a new company, Precision Irrigation, with George Ricketts; and it became apparent to us all, at roughly the same time, that we could combine forces and come up with a potentially really useful new technology to help address New Zealand's emerging problem of insufficient freshwater to maintain supply to the ever increasing demands for irrigation in drought-prone parts of the country. We hope to continue and expand this collaboration.

A huge thank-you to the land-owners and growers who welcomed me onto their land to conduct research in real production systems. I particularly thank Hew and Roger Dalrymple for providing field sites for my research at Waitatapia Station. Hew and Wayne Hosking helped to make this whole study possible by being open-minded about my objectives and freely providing any support if and when it was needed. Thank-you to Christine in the farm office, and Mr John Dalrymple Senior for his unfailing supply of daily rainfall data. Thank-you to all the Dalrymple family and all the staff at Waitatapia Station – it was a great place to undertake my field research.

Thanks also to Monty Spencer and other Wilcox Growers staff, for their enthusiastic encouragement to undertake some proximal sensing and irrigation efficiency studies at their Ohakune potato fields. Thanks to Todd White who included me in a Sustainable Farming Fund project in Canterbury and North Otago to evaluate soil variability with EMI survey for improved irrigation scheduling at four irrigated dairy farms.

Thanks to Dan Bloomer, who has done so much to promote best management practice for irrigation in New Zealand, for his support of my ideas.

Also, I must acknowledge every one of my teachers and colleagues through the years – from Southend High School, Essex, to the Soil Science Dept, Reading University, in England, to the Soil Science Departments at the Universities of Guelph, British Columbia and Saskatchewan; and most recently all the staff of the Soil and Earth Sciences Group at Massey University – a very special group of people.

.

So now I am left to thank my immediate family. Thank-you to my mother, the late Betty Hubbard, my father Bernard Hubbard and my brother Richard – who have always totally supported and encouraged me in each step that I have taken.

Our children have a name for their Dad, and I would like to acknowledge the tremendous guidance that Mike “Walking Textbook” Hedley has provided. He liberally hands out (in the words of his most recent PhD student, Bambang Kusumo) many brilliant ideas on a very regular basis. To have a Soil Science Walking Textbook at home was a great asset as I strived to develop a new and really useful soils-based method in my PhD studies. To Mike and our three children, of whom we are immensely proud – Frances, our food technologist and skier – Paul, our engineering geologist and cyclist and – Joanne, our environmentalist and gourmet cook extraordinaire, this effort is for you all.

This thesis is dedicated

to the memory of

Alan McRae

18 November 1948 – 19 April 2008

Farm Consultant

Lochalsh Agriculture Ltd

A great friend and visionary

who introduced me to the concept of participatory research

Table of Contents

List of Tables

List of Figures

CHAPTER ONE

Introduction, Aims and Objectives

Farming generates about 60% of New Zealand's foreign exchange (MfE, 2009). During the period of economic liberalisation from 1984 to 2004, substantial improvements occurred in agricultural productivity due to the removal of most agricultural sudsidies. This impacted on agriculture by shifting production away from sheep to dairy, deer and horticulture. From the 1990s to 2004 dairy cow numbers expanded by over 50%, deer numbers by more than 65%, the area under horticulture and grape vines rose by 20%, while sheep numbers declined by 28%. Total annual nitrogen fertiliser use increased by a factor of approximately six between 1990 and 2003 (PCE, 2004). Agricultural productivity improved substantially over this period as a result of technological changes: improved animal husbandry and breeding, effective targeting of investment, cost cutting, efficiency gains, and scale economies through expansion of average farm and orchard size. The United Nations Food and Agriculture Organisation's Agricultural Production Index 2006, shows production rates from pastoral farming in New Zealand increased by a massive 38% between 1990 and 2003, due to more intensive farming and more productivity per animal.

The period from 1984 to 2004 therefore marked a period of significant growth and wealth for the New Zealand agricultural sector. However toward the end of this period there was an increasing underlying awareness of the undesirable pressures being placed on the environment. In 2004 the "Growing for Good" Report (PCE, 2004) was released. It highlighted the fact that farming which underpins the New Zealand economy, also places intense pressures on the environment and natural capital. The Report observed that declining water quality was nationally widespread largely due to intensive farming, and highlighted the need to ensure that the natural capital of New Zealand farms be maintained for future generations.

Also in 2004 the government released a report on the economic value of irrigated land (MAF, 2004) acknowledging the significant increasing contribution of irrigation to

agriculture. This was estimated as a contribution of NZ$920 million at the farmgate (MAF, 2004), 12% of total agriculture and horticultural exports (assuming the extra production is all exported). This "good news" Report was accompanied by the "Water Programme of Action" (MfE, 2004) acknowledging that New Zealand's freshwater resources are under pressure. The "Water Programme of Action" Report states: "Significant growth in agricultural productivity is being supported by irrigation. The area of irrigated land has roughly doubled every ten years since the 1960s, and irrigation now accounts for nearly 80% of all water allocated in New Zealand." It suggests that future productivity gains will increasingly rely on irrigation – particularly in eastern regions predicted by the IPCC to become hotter and drier due to climate change (IPCC 3rd Assessment Report, McCarthy et al., 2001).

The "Growing for Good" Report and "Water Programme of Action" were released at the same time as New Zealand joined with most other developed countries of the world to acknowledge climate change and ratify the Kyoto Protocol; and in February 2005, the Kyoto Protocol came into force. This event represented a major milestone in international collaboration to address climate change, engaging the world in efforts to reduce greenhouse gas emissions.

The "Growing for Good" Report in 2004 probably marked a moment of realisation for many New Zealanders that it is not possible to target increased productivity year after year – that there is a limit to productive growth, and that we require sustainable systems to maintain natural capital for future generations.

Increasing agricultural productivity in New Zealand over this time period is paralleled by increasing greenhouse gas emissions, the agricultural sector contributing 48% of New Zealand's total emissions in 2007, an increase of 12% from the 1990 level (MfE, 2009), primarily due to increased methane emissions from enteric fermentation processes in ruminant animals. This exemplifies the link between the drive for increased agricultural productivity, its dependence on new irrigation schemes, and associated increased greenhouse gas emissions.

The country is faced with addressing the potential deleterious long-term impacts of its own success story - an impressive level of increased agricultural productivity. In

addition its commitment to address the obvious signs of global climate change due to anthropogenic greenhouse gas emissions, along with 189 other Kyoto Protocol signatories can be addressed simultaneously. The issues are intimately linked. More productivity = more energy consumption = more greenhouse gas emissions.

This situation, explained here for New Zealand, but mirrored in one way or another around the world, sets the scene for the current research topic. How can we address the unprecedented demand on our freshwaters for irrigation? How can we improve the energy efficiency of our agricultural systems, and therefore also minimise greenhouse gas emissions? How do we address the potential impacts on New Zealand primary production outlined in the IPCC Third Assessment Report for New Zealand (McCarthy et al., 2001) of increasing temperatures, and increased incidence of floods and droughts within the next 100 years? How do we help the New Zealand economy to adapt rapidly to change – climate change, global financial changes etc? How do we address the future challenges of maintaining a soil resource for global food supply (Lal 2009).

During the last decade, there has been a marked change in global awareness toward understanding the importance of total energy efficiency of food production. In the United Kingdom the “Buy British” campaign was found to be flawed when British tomatoes grown in heated glasshouses turned out to require more total energy input to reach UK supermarkets than outdoor grown Spanish tomatoes. The food miles debate used to disadvantage food being transported long distances was shown to be misleading; with New Zealand sheep, beef and dairy cows (produced on all-year round pastoral systems with little or no supplementary feed) being able to be transported to Europe from New Zealand with lower overall energy input than the same product produced in Europe, where animals are housed over winter months with significant supplementary feed (Basset-Mens et al., 2009). However Basset-Mens et al. (2009) caution that this remarkable eco-efficiency of New Zealand’s traditional low input system (e.g. no N fertiliser, no brought-in feed supplement, stocking rate of 2.3 cows/ha for dairy farming) is very quickly eroded with intensification of this traditional pasture-based system by increasing stocking numbers with increased use of fertiliser N and maize silage supplementary feed.

Precision agriculture is an enabling technology. It uses new technologies, such as global positioning systems (GPS), sensors, satellite or aerial imagery and geographic information tools (GIS) to understand variations in the natural landscape. It pre-supposes that in-field variability exists, and that if this can be measured and monitored, then site-specific management practices can be adopted to more accurately apply inputs (e.g. seed, nitrogen fertiliser) for improved overall energy efficiency. It enables changes during the growing season to be assessed and responded to in real-time if necessary (using, for example, visible and near infra-red sensors), and aims for optimal use of resources, e.g. freshwaters for irrigation. A study, conducted between 1998–2001 in Canterbury, New Zealand, showed potential financial and environmental gains from the adoption of site-specific farming methods (Craighead and Yule, 2001); and Yule et al (2008) discuss potential precision agriculture applications to dairy farming, including site-specific pasture management and GPS tracking of fertiliser application.

1.1. Aims and Objectives

Therefore this thesis aims to investigate the potential application of precision agriculture technologies to improve eco-efficiency of agricultural production systems. Could precision agriculture help to optimise irrigation water use efficiency? Could it be used to help the agricultural sector adhere to quality assurance schemes? Could it be used to help determine eco-efficiency of production more accurately? Could it be used to help auditability and traceability of primary products for life cycle analysis? Could it be used to monitor and understand declining soil quality (due to intensification) and declining soil carbon levels observed by researchers, and perhaps linked to climate change (Schipper et al., 2007; Bellamy et al., 2005)?

The specific aims of this thesis are:

- A comprehensive literature review of (i) relevant publications on the emerging global freshwater crisis, and opportunities for improving freshwater use efficiency, and of (ii) proximal sensing, geostatistical and GIS methods for acquisition and handling of high resolution spatial data, with particular emphasis on those methods relevant to mapping and monitoring soil variability and other properties pertinent to this study

- Assess the potential of two proximal sensing methods (EM mapping and Vis-NIR field spectroscopy) for mapping soil variability and specific soil properties (carbon, nitrogen, moisture)
- Develop proximal sensing methods for mapping soil water status
- Use soil water status maps to develop an integrated decision support tool for precision application of irrigation water, suited to immediate commercial uptake
- Assess the potential benefits of this soil-based decision support tool, for precision irrigation within New Zealand

This thesis presents a comprehensive literature review in Chapter 2 of new and on-the-horizon ground-based sensors available to precision agriculture. The review targets sensors suited to monitoring and mapping soils and soil properties in the landscape, with an emphasis on soil moisture mapping for irrigation. It reviews existing methodologies for simultaneous acquisition of precise location **(**RTK-DGPS [cm accuracy]; GPS [metre accuracy]**)** with sensor data for on-the-go mapping of soil variability and specific soil properties, such as soil carbon, nitrogen and moisture. It also introduces some geostatistical concepts, essential for interpolation of sensor data across a landscape. Geostatistical concepts have rapidly evolved since the 1980s, enabled by improved computer power and software handling of new high density sensor data from field-scale experiments.

Chapter 3 describes a field trial of two proximal (ground-based) sensors for (i) field analysis of soil carbon, nitrogen and moisture and herbage nitrogen; and (ii) mapping of soil variability, at three farms in the Taupo-Rotorua region. A portable spectroradiometer is used for (i), and an on-the-go electromagnetic (EM) mapping system is used for (ii). Chapter 3 presents a geostatistical analysis of the collected EM sensor data.

Chapter 4 describes the use of the portable spectroradiometer and on-the-go EM mapping system for field estimation of soil moisture and mapping soil variability, respectively, at a Manawatu farm [Manawatu maize 1]. The portable spectroradiometer is used to collect diffuse reflectance spectra from a soil surface. The EM sensor records apparent soil electrical conductivity (EC_a), which is related to soil texture and soil available water-holding (AWC) properties. A link is made between EM

mapping and soil AWC maps, and discussed in the context of irrigation scheduling. Spatial variability of soil moisture is assessed by TDR survey.

Chapter 5 introduces a soil water balance model to be used in conjunction with the AWC map so that soil water supply and crop water demand can be assessed, using the same research site used in Chapter 4. It also evaluates the efficiency of the irrigator system and reports the distribution uniformity coefficient for the centre-pivot irrigation system at this study site. This acknowledges that irrigation water use efficiency audits should include an evaluation of the performance of the irrigation system as well as efficacy of irrigation scheduling.

Chapter 6 presents results from the second year of field trials at the Manawatu farm. The experiment is conducted using half of the previous site and a new adjacent field, used for wheat production in the previous year but under irrigated maize cultivation for the year of investigation [Manawatu maize 2]. A method is developed for adding a daily time-step to the AWC map to produce a daily soil water status map. It presents soil moisture monitoring data of 50 positions at the study site to support the temporal stability of soil water status patterns. The data shows that there is significant spatial variability of soil moisture within each EC_a-defined zone at this study site, and the need for high density real-time soil moisture monitoring in each soil EC_a management zone is discussed, because soil water balance models cannot adequately account for site-specific factors such as ponding and impeded drainage. This chapter discusses that at this site the null hypothesis of precision agriculture (Whelan and McBratney, 2000) applies where variability within each zone is greater than the variability between EC_a-defined management zones.

Chapter 7 develops the concept of variable rate irrigation. It presents soil water status maps for 2 study sites (Massey University pastoral farm [Manawatu pasture]; Manawatu maize field [Manawatu maize 1]) and potential water savings if variable rate irrigation was applied at each site. Variable rate irrigation (VRI), i.e. site specific irrigation scheduling based on soil zone differences, is defined and explained. Water savings of VRI are compared with uniform rate irrigation (URI). Deficit irrigation (DI) is also discussed.

Chapter 8 further develops the concept of VRI and assesses potential water savings at a new study site, an irrigated Canterbury dairy pastoral soil [Canterbury pasture], with varying stoniness. Other key performance indicators for assessing VRI are introduced: drainage and runoff, nitrogen leaching, irrigation water use efficiency (kg DM mm^{-1}) and energy usage (kg CO_2-eq).

Chapter 9 provides a final analysis of potential benefits of VRI, using three irrigated production system case studies [Canterbury pasture, Manawatu Sand Country maize, Ohakune potatoes]. It includes a discussion of the total ecosystem services value of New Zealand freshwaters; and in addition estimates the virtual water content of these three primary products. The chapter explains that the "value" of any product, in this case VRI, should be assessed not only by the benefit to the party who stands to gain directly (and usually financially) but by the wider ecological consequences of these decisions, and the social goals being served by the decisions (Costanza, 2006).

Chapter 10 summarises individual results and conclusions from the different pieces of research presented in Chapters 3 to 9. It provides some overall conclusions by comparing all results from all case studies. It also discusses future research gaps and needs.

This thesis does not attempt to answer all the questions posed in this Introduction. It aims to highlight some key precision and spatial technologies that show significant promise for future research into mapping and monitoring of soils and landscapes for optimising energy efficiencies of land use.

In particular, it aims to develop a spatial decision support tool for variable rate irrigation scheduling onto variable soils.

CHAPTER TWO

Literature Review

This review introduces the issue to be addressed in this research project: freshwater supply for irrigation. Section 2.1 summarises current literature on the topic of freshwater allocation at the local, national and global scale. A discussion is then provided on ways in which freshwater allocations can be managed more efficiently (Section 2.2). This leads to an introduction to precision agriculture methodology for assessing farm-scale variations (Section 2.2.1). Section 2.2.1 explains that precision agriculture relies on ground-based sensors for acquisition of high resolution land parameter maps. The concept, theory and summary chart of ground-based sensors for on-the-go proximal sensing is provided. A comprehensive review of ground-based sensors, available and becoming available, for soil studies at the landscape scale, is then provided (Section 2.3). The final part of the review (Section 2.4) summarises the potential uses of proximal sensing techniques, with actual examples from the literature and particular emphasis on those suited to assessing soil properties relating to freshwater supply for irrigation.

2.1. The Issue

An unprecedented demand by agriculture on global freshwater supplies is seen as the main cause of increasing global freshwater scarcity (Jury & Vaux, 2007). This is reflected in New Zealand where the area of irrigated land has roughly doubled every decade since the 1960s (PCE, 2004). Land-use intensification, and complementary developments such as plant breeding, has maintained global food production since the 1960s, a period commonly referred to as the Green Revolution (Swaminathan, 2007). However, land-use intensification has relied on increased use of irrigation and 70% of global freshwater extractions are now used for irrigation (UN/WWAP 2003; Mu et al., 2009). Some of this water is used inefficiently, and there is a need for research and technological advances to improve water use efficiency (Mu et al., 2009; Lal, 2009).

Water has traditionally been a readily available resource for all users, but as we move into the 21st Century, concepts of water metering, water trading, and water footprints (Chapagain & Hoekstra, 2004) are becoming a reality. The improved efficiency of irrigation water use would therefore impact favourably on global water scarcity issues. This research project aims to address this water-use efficiency issue by developing practical methods to monitor and map daily soil water status, allowing more precise irrigation scheduling, using the technological advantages of the 21st Century, which include, for example, (i) GPS control of equipment, (ii) a range of ground-based sensors that can be used for rapid acquisition of field data at the farm and catchment scale, and (iii) powerful geostatistical and GIS software for data analysis and mapping.

2.1.1. Freshwater Allocation – The Local Situation

Actual Scenario – summer 2008 in the Manawatu: no rain for 4 weeks – irrigation systems in the Manawatu Sand Country are hardly keeping up with daily evapotranspiration (E_t) demands of maize crops. Then the local council places a 50% restriction on allocated irrigation water. This restriction, at this growth stage, could impact on yields by 3–4 T ha^{-1}, which is more than NZ$1000 dollars lost return per hectare. It is essential to use the restricted irrigation water strategically, aiming for best conversion to dry matter production. Can this be addressed by site-specific management of the irrigated land, i.e. producing a map of soil variability, selecting irrigation management zones and variable rate precision placement of irrigation water?

This scenario exemplifies problems associated with an unprecedented increase in water demand by irrigators in the Rangitikei catchment over recent years. Horizons Regional Council are addressing this and other environmental issues in The One Plan, a resource management plan that acknowledges a public expectation for local natural resources to be used in an acceptable manner (Horizons Regional Council, 2008). Community and policy makers have identified four key environmental issues in our Region – water quality, water quantity, biodiversity, and sustainable land use. It is acknowledged that demand on surface and groundwater resources is one of the most critical issues to be dealt with by proposed regional plans. The One Plan states:

> The challenge for the Manawatu-Wanganui Region is to strike the ideal balance between using natural resources for economic and social well-being, while keeping the environment in good health. Horizons Regional Council's role is to find a satisfactory way to make this seemingly conflicting challenge a reality for the community.
>
> *(Horizons Regional Council, 2008)*

This plan has been prepared in accordance with the Resource Management Act 1991 (RMA) and defines how the natural and physical resources of the Manawatu-Wanganui Region will be cared for and managed. Identification of the four key environmental issues provides a working framework for progress to be made, and it is acknowledged that they have significant interconnections.

Agricultural water demand in our region has more than tripled since 1997, taking 80% of all allocations (Table 2.1). This unprecedented increase in demand on local freshwater has caused the Regional Council to define allocation volumes for water management zones where there is pressure from increased water take. The Council encourages water-use efficiency and accurately defines abstraction rates using telemetered water meters.

Table 2.1 Change in consented water abstraction volumes from 1997 to 2004, excluding hydroelectric power generation (Horizons Regional Council, 2008)

		1997 to 2004 percentage change in consented water takes		
Source	**Sector**	**1997 (m^3/d)**	**2004 (m^3/d)**	**Increase (%)**
Groundwater	**All Sectors**	287,000	425,000	+45%
Surface water	Agriculture	70,668	291,949	+313%
	Industry	38,835	56,003	+44%
	Water supply	162,024	219,088	+34%
	All Sectors	**271,527**	**567,040**	**+108%**

This is essential as reduced water levels adversely impact on stream life and recreational activities, such as fishing and swimming, as well as on cultural and spiritual values, and the ability of waterways to assimilate waste (Horizons Regional Council, 2008).

Proposed policies to manage freshwater allocations to consent holders will set maximum daily rate of abstraction, irrigation return periods, and seasonal or annual volumes. In addition, when allocations are made, the Regional Council proposes to:

- consider land use, crop water-use requirements, on-site physical factors such as soil water-holding capacity, and climatic factors such as rainfall variability and potential evapotranspiration (PET)
- assess applications either on the basis of an irrigation application efficiency of 80% (even if the actual system being used has a lower application efficiency) or on the basis of a higher efficiency where an application is for an irrigation system with a higher efficiency
- link actual irrigation use to soil moisture measurements in consent conditions.

In preparation for these proposed conditions, the Regional Council intends to set up a web-based information system for individual consent holders to monitor their water use on a daily basis. The website, Watermatters, monitors water zones to ensure water is being abstracted within predetermined water resource levels (www.horizons.govt.nz/watermatters). Abstracted water rates are telemetered from the irrigation systems, and these data are regularly checked by council staff with on-site monitoring. Such a system ensures efficient monitoring of the resources and could be used in the future for water trading or for determining charge-out rates for water usage.

2.1.2. Freshwater Allocation – The National Situation

New Zealand has an abundance of freshwater when compared with other countries, and allocated water comprises less than 5% of the national renewable freshwater resources (MfE, 2007). However, much of this renewable resource is not available to users, indeed water is not always in the right place at the right time.

Water will be fully allocated in most major New Zealand catchments by 2012 (Neilson, 2008), and Williams (2006) identified four core issues to be addressed in managing agriculture's escalating water demand:

- Allocation across competing purpose – after sufficient water is left in rivers, lakes and aquifers to maintain their ecological health
- Consents and tradable rights
- Charges for use
- Education and awareness

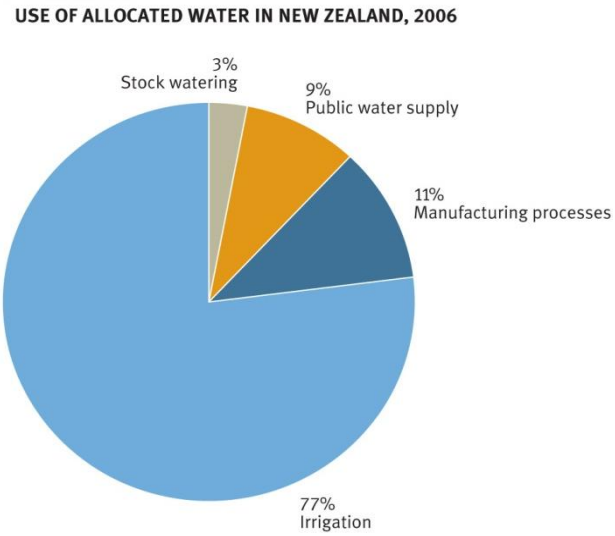

Fig. 2.1 Use of allocated water in New Zealand in 2006 (MfE 2007)

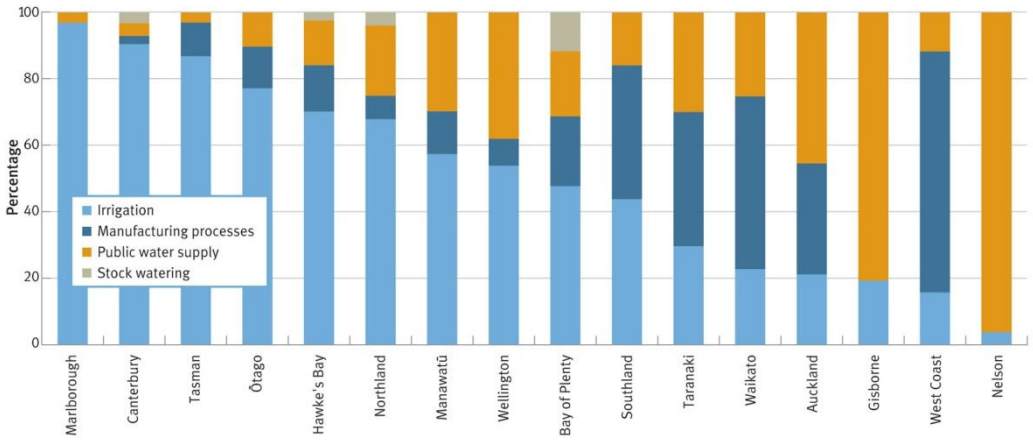

Fig. 2.2 Regional variations in the use of allocated water, 2006 (MfE 2007)

A national Sustainable Water Programme of Action was established in 2003 (MfE, 2004) as a response to obvious escalating pressures on freshwater resources, with

simultaneous declining water quality. The Programme acknowledged that significant growth in agricultural productivity was being supported by irrigation. Its aim was to ensure sustainable management of New Zealand's freshwater resources.

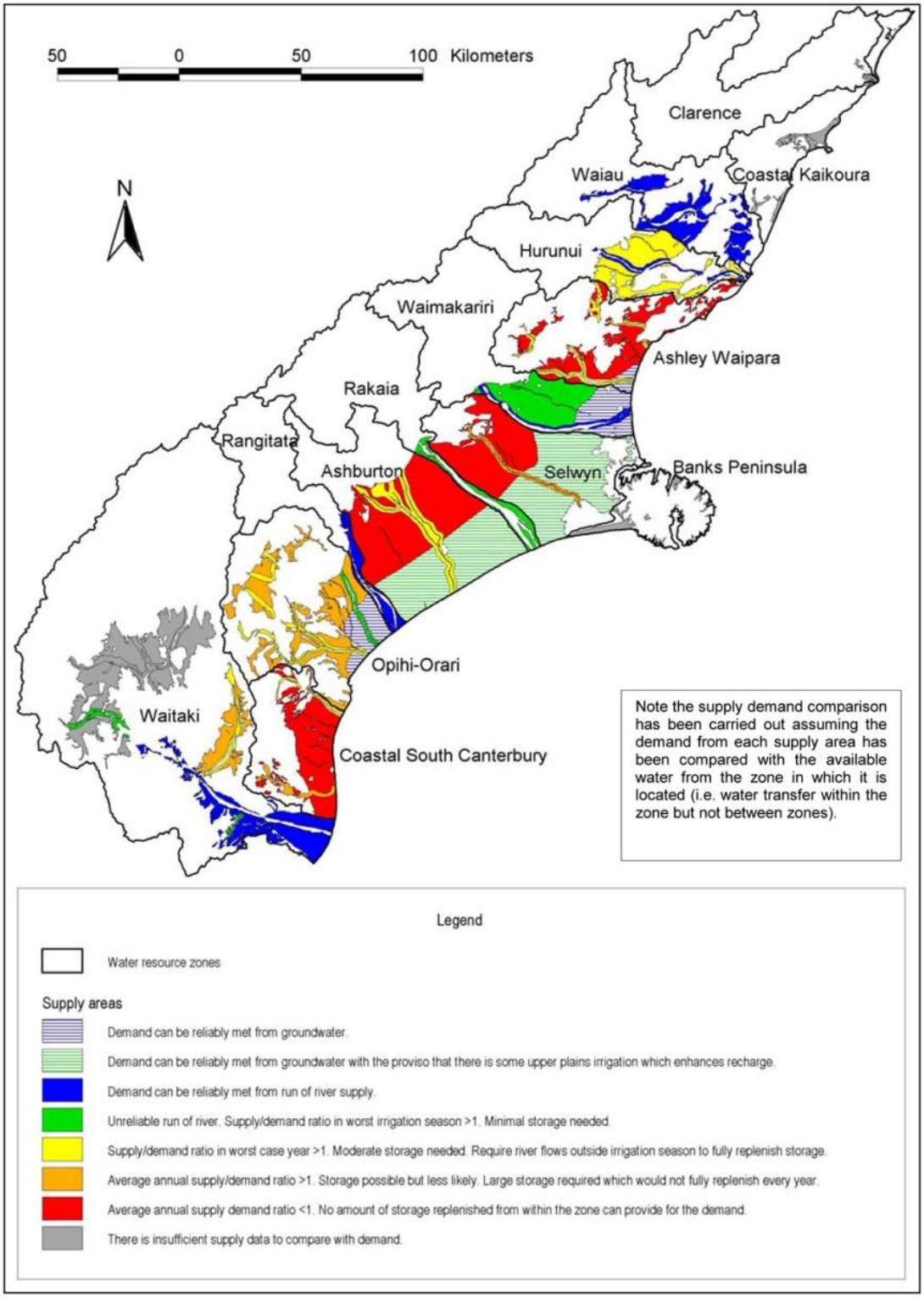

Fig. 2.3 Summary map of freshwater supply and demand situation for the Canterbury region (extracted from Morgan et al., 2002)

The Environment New Zealand 2007 Report states that 77% of allocated freshwaters are for irrigation purposes (Fig. 2.1), similar to the global average of 70% (MfE, 2007). It acknowledges that there are significant regional variations (Fig. 2.2), with Canterbury and Otago regions accounting for almost 75% of the total national allocation. It also acknowledges that in most cases, consent holders do not use the full volume of water allowed under consent, and usage typically ranges between 20 and 80% of allocated volumes (MfE, 2007). However, as consents become harder to acquire and regions like Canterbury move toward water trading, unused allocated water could be traded to others resulting in an unsustainable demand. Figure 2.3 indicates regions in the Canterbury area where allocation amounts do not meet demand during peak demand periods.

As demand increases, the likelihood of water restrictions being placed on irrigators during times of peak usage also increases. These likely restrictions demand improved irrigation scheduling, which is also essential for energy efficiency gains (Chen & Baillie, 2009). This demand will be addressed by practices such as:

- matching irrigation amount and scheduling to soil moisture deficit and crop E_t
- variable row and plant spacing – to match yield potential of different soils
- deferred irrigation practice – withholding water at times of less critical plant growth stages
- variable rate irrigation – using precision agriculture practice to apply water at variable rates to different parts of the crop.

The ability of policy and land users to work toward sustainable irrigation practices in New Zealand requires better measurement techniques, preferably remote, enhancing our ability to predict crop water use and to assess the need for irrigation (Wesseling & Feddes, 2006). An improved understanding of spatial and temporal variations of soil water supply to the crop (Hedley et al., 2008a; 2008b) as well as the biophysical processes of root-water uptake in soil, and transpiration from plant canopies (Green et al., 2006) are also required. Green et al. (2006) showed that if row spacing on

Marlborough vineyards was reduced from 3 m to 2.4 m this would demand twice as much irrigation.

Such efficiency gains combined with water harvesting provides a potential opportunity to at least maintain our present demands for irrigation in New Zealand. Winter rainfall in high country can be stored and fed into waterways during peak demand periods in summer months. For example, three drought years in the 1980s in South Canterbury (1982, 1985, 1988) drove the community to devise and fund a water harvesting project (Hyslop & Scott, 2008). The Opuha Dam is 50 m high, 330 m long, and stores 91 million m^3 of water, creating a 700-ha lake. Stored winter rainfall and runoff is fed into the Opihi River as its level drops during peak irrigation demand period. The Dam was designed (i) to improve environmental flows, (ii) to provide more irrigation water, (iii) for power generation, and (iv) as a lake habitat for improved biodiversity. Residents have noted that the river mouth of the Opihi River only stops flowing 4–5 days per year instead of the pre-storage scheme 100 days per year. This is an example of the potential benefits of New Zealand's high rainfall high country regions adjacent to drought-prone floodplains. Decision tools to optimise irrigation scheduling are required to improve water use and energy efficiencies; while new storage schemes will help provide this water to drought-prone areas of New Zealand in periods of peak demand.

2.1.3. Freshwater Allocation – The Global Situation

Irrigated land area in the world increased from 100 Mha in 1950 to 275 Mha in 2000 (Lal, 2009). The second Green Revolution, needed to feed a global population of 6.7 billion in 2008 that is projected to be 9.2 billion by 2050, must be based on sustainable management of soil and water resources (Lal, 2009).

Meeting this future food demand will be significantly more challenging than the one faced before the first Green Revolution in the 1960s when agricultural efficiency was low everywhere (Jury & Vaux 2007; Rosegrant et al., 2002).

One third of global rivers are intercepted by dams and reservoirs, up from 5% in 1950 (Postel, 2005). 26% of global wetlands have been drained and converted for

agricultural production, with about 60% of wetlands drained in Europe and North America. Global groundwater over-drafting (rate of extraction > rate of recharge) is calculated to be as much as 163 km^3 $year^{-1}$, with about 80% of this occurring in India and China (Postel, 1999). The implications of this are that close to 500 million people are being fed by a water supply that could disappear in the future. Seckler et al. (1999) estimate that as much as 25% of India's grain harvest could be in jeopardy. China is increasingly facing water shortage and food security challenges, with the area of irrigated land in 2003 having increased by 3.5 times the size in 1949. 75% of its grain crop is dependent on irrigation, compared with 15% in the US (Williams, 2006), and over 90% of China's cash crops are produced under irrigation (Mu et al., 2009). In New Zealand, 35% of horticultural land is irrigated, 27% of arable land is irrigated, and about 10% of grazing land is irrigated, 8% of which is for dairying (Statistics New Zealand Agricultural Production Census, 2002).

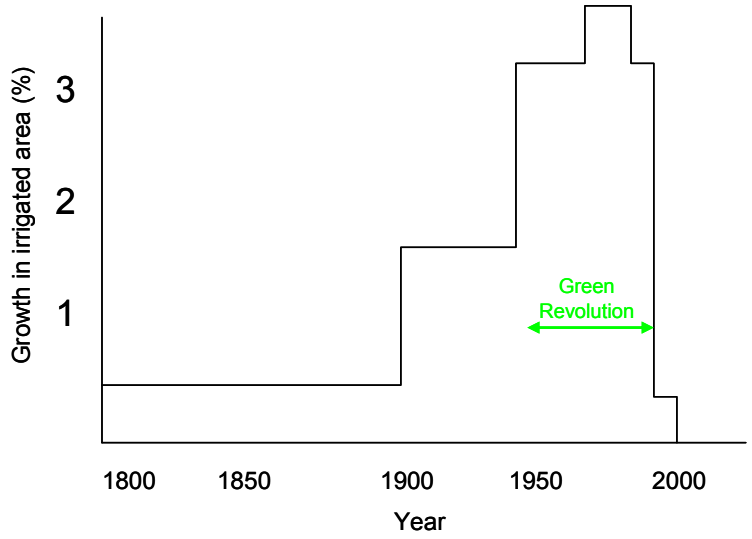

Fig. 2.4 Rate of growth of irrigated area over the last 200 years (FAOSTAT data, Jury & Vaux, 2007)

As stated, irrigated agriculture is the dominant consumptive user of water. Therefore, increases in productivity of irrigation water through changes in management and improvements in efficiency offer the greatest potential for global water savings (e.g., Sadler et al., 2005). However, it seems unlikely that increasing food demand can be

met by increased area of land irrigated plus improved efficiency of use, alone. Constraints on expansion of irrigation are: insufficient land, insufficient water, or excessive cost, which no doubt explains the slower rates of expansion of irrigated land between 2000 and 2003 (Fig. 2.4) compared to the previous 50 years (Jury & Vaux, 2007).

Seckler et al. (1998) estimated the average irrigation efficiency (water required for 100% yield divided by irrigation withdrawals) for 118 countries of the world in 1990 as 43%, and showed that increasing irrigation effectiveness to 70% reduces the need for development of further water supplies for all sectors in 2025 by roughly 50%, with a total water saving of 944 km^3 $year^{-1}$.

2.2. Addressing the Issue

There are a number of measures that can be adopted globally to improve irrigation water use efficiency. Technical improvements include:

- applying water more uniformly (Burt et al., 1997)
- reducing evaporation or runoff losses (Burt et al., 1997)
- improving sprinklers by lowering the spray to reduce air losses and kinetic energy of impact (Jury & Vaux 2007)
- improving irrigation scheduling and water delivery timing to reduce water losses, as well as addressing crop sensitivity at certain development stages (Jury & Vaux, 2007)
- using soil monitoring and E_t estimates to ensure correct amounts of water are applied at the correct time (Jury & Vaux, 2007)
- correct tillage and field preparation to enhance infiltration and reduce evaporative losses (Wallace & Batchelor, 1997)
- improving canal linings and other repair measures to improve the efficiency of water supply from source to the field, which is estimated to average about 70% globally (Bos, 1985).

Table 2.2 Comparison of water productivity of full and deficit irrigation levels for wheat and maize (Zhang, 2003)

	Wheat, Texas, United States		Wheat, Syria		Maize, Texas, United States	
Irrigation level	Yield (t/ha)	PAW* (kg/m3)	Yield (t/ha)	PAW (kg/m3)	Yield (t/ha)	PAW (kg/m3)
Full	4.76	0.64	5.79	0.93	13.95	1.42
67% of full	4.74	0.76	5.24	1.19	11.36	1.53
33% of full	3.88	0.80	5.15	0.99	6.62	1.21
Rainfed	2.19	0.61	3.27	0.93	1.36	0.43

** PAW: water productivity*

Agronomic efficiencies can be made with proper crop selection, crop breeding and crop sequencing. Institutional efficiencies include setting up water user organizations, reducing irrigation water subsidies, establishing conservation incentives, enhancing a legal market for water trading, and offsetting infrastructures for disseminating efficient technologies, better training and extension efforts (Jury & Vaux, 2007).

Other measures to reduce and improve use of irrigation waters globally include deficit irrigation, i.e. strategic application only at critical growth periods, which greatly improves productivity of water (yield per water applied) although overall yields are below potential yields obtained with unlimited irrigation (Table 2.2).

On-farm water harvesting is an ancient practice now being revived to augment existing water supplies (Fleskens et al. 2007; Patrick et al., 2007). Another ancient practice also being revived is flood recession farming – the practice of growing crops on annually flooded land during the recession period (e.g., Kgathi et al. 2005, 2006), which brings more land into production and capitalizes on the natural fertility of the sediment deposited.

Improved water management is required in virtually all areas – and agricultural irrigation, the dominant user, provides the most important option for water savings. The three most significant unsustainable practices that exist worldwide are (i) persistent groundwater over-drafting, which is self-terminating and will threaten 500 million people, (ii) continuing contamination and pollution of groundwater and surface waters, and (iii) inappropriate management of watersheds (Jury & Vaux, 2007).

Pollution of global freshwaters needs to be reduced and eliminated where possible. Water-quality issues are most serious in developing countries where excessive pollution poses both significant health threats and the loss of needed water supply. About 21% of irrigated land worldwide has been degraded by salinity, with the likelihood of this percentage significantly increasing in the next few decades (Postel, 1999). In fact the main cause of failure of new irrigation projects has historically been due to water-logging and salinization of the soil (McNeill, 1992). Much irrigated land is in arid and semi-arid regions where movement of solutes upward in the soil profile, with evaporation at the surface, is greater than downward movement through drainage. Salinization has been exacerbated in these climates where deeper rooting native vegetation (e.g., long-rooted native grasses in the North American Great Plains; deep rooting scrub and Eucalyptus in Australian) have been replaced with shallower rooting grain crops and pasture. Failure to deal with increasing levels of salinization will greatly increase global difficulties in meeting future food demands.

Inappropriate management of watersheds can lead to unsustainable practices on upland areas causing degradation downstream. Integrated catchment management strategies have worked well in some places, but much remains to be done in the developing world. When residents of upland watersheds are poverty stricken, the pressure for mere survival precludes any efforts to manage and care for watershed sustainably (e.g., Rijsdijk et al., 2007).

Future global planning for best use of our freshwaters must involve improved infrastructures, conservation practices making existing systems more efficient, and investment in new improved technologies. Several prototypes for variable rate irrigation systems have been developed but their potential can only be realized with the development of new, improved systems of real-time monitoring, decision, and control systems (de Jonge et al., 2007).

Most importantly, the ultimate goal is always to increase crop productivity per unit of water and land area by improving water management and directed research and policy decisions (Rosegrant et al., 2002).

At the farm-scale in New Zealand, there is a need to develop farm-scale technologies for assessing soil variation and its relation to water use efficiency. In a heterogeneous field in which soil water properties vary, crop yield may differ from point to point by more than 100% (Russo, 1986). The advent of ground-based sensor systems enables soil variability to be mapped and quantified. This review investigates a wide range of ground-based sensor systems becoming available for soil characterization, and assesses those most suited to the present study, i.e. for mapping and quantifying soil variability with respect to its ability to supply water to the crop. It also reviews complementary technological advances, including GPS and GIS, which have allowed ground-based sensor data to be transformed into landscape-scale maps, with some real-time capability. Section 2.2.1 introduces these system components, and Section 2.3 reviews the capabilities of a number of ground-based sensors.

2.2.1. Introduction to ground-based sensors and advances in landscape-scale soils research

2.2.1.1 Sensors

The recent advent of a range of affordable ground-based sensors with accurate GPS for rapid soil mapping has provided the potential for a major technological advance in agricultural practice – perhaps unmatched since John Deere invented the steel plough in 1837.

Ground-based sensors provide high density data, commonly the equivalent of grid sampling at 10-m spacing or better, across an area of perhaps 50–80 ha in one day. There is a current impetus to develop these sensors for on-the-go measurement and mapping of soil properties, with potential benefits from the increased density of measurements taken at a relatively low cost (Jaynes 1996). Although a limited number of ground-based sensors are commercially available, there is an on-going effort to develop new prototypes (Adamchuk, 2008).

In 1998, Viscarra Rossel and McBratney (1998) provided a list of some possible sensors for a range of soil properties, which have important agronomic implications (Table 2.3). Table 2.3 illustrates the potential for the development of invasive and non-

invasive real-time soil sensors and scanners that operate in bands throughout the electromagnetic spectrum, and Figure 2.5 illustrates their position within this spectrum.

Table 2.3 A list of available sensors for assessing a range of soil properties (Viscarra Rossel & McBratney, 1998)

Some possible sensors for a range of soil properties

Soil property	Sensor/scanner (Ref.)	Type
Water	near infra-red (Bowers and Hanks, 1965; Skidmore et al., 1975)	Invasive/ non-invasive
	ground penetrating radar (GPR) (Whalley et al., 1992)	Non-invasive
	microwave reflectance (Whalley, 1991)	Non-invasive
	electrical resistance (Bowers and Bowen, 1975)	Invasive
	capacitance (Dean et al., 1987)	Invasive
Clay content	near infra-red (Ben-Dor and Banin, 1995)	Invasive
Organic matter	660-nm single wavelength sensor (Shonk et al., 1991)	Invasive
	Multiple NIR wavelength sensor (Sudduth and Hummel, 1991)	Invasive
Nitrogen	near infra-red (Ehsani et al., 1997)	Invasive
	ion-selective electrode (Adsett and Zoerb, 1991)	Invasive
	ISFET[a] (Birrell and Hummel, 1997)	Invasive
pH	ion selective electrode	Invasive
	ISFET (Viscarra Rossel and McBratney, 1997)	Invasive
CEC[b]	near infra-red sensor (Ben-Dor and Banin, 1995)	Non-invasive
K	gamma radiometry (Billings, unpublished)	Non-invasive
Electrical conductivity	electromagnetic induction (e.g., Eigenberg and Nienaber, 1997; Mankin et al., 1997)	Non-invasive
Strength	penetrometer (Alihamsyah and Humphries, 1991)	Invasive
Structure	acoustical sensor (Sabatier et al., 1990)	Invasive/ non-invasive
Soil air composition	odour sensing system (Persaud and Talou, 1996)	Non-invasive

[a]ISFET, Ion-sensitive field-effect transistor.[b]CEC, Cation exchange capacity.

The high sampling density obtained by these sensors allows, for the first time, a realization of spatial variability of soil properties across the landscape. The concept that there is considerable spatial variability of soil properties across many landscapes is not new (Smith 1938), but our ability to measure this variability has been limited within the confines of standard experimental methodology. The advent of proximal sensing, commonly employing a global positioning system (GPS) with a selected ground-based sensor provides high density mapping of sensor parameters, providing a quantitative assessment of soil variability. This soil variability was largely ignored prior to the 1980s (Cook & Bramley, 1998). However, the last decade has seen a shift away

from a traditional focus on static soil properties to a focus on describing dynamic soil changes across a landscape, made possible by these new tools and new insights (Pennock & Veldkamp, 2006).

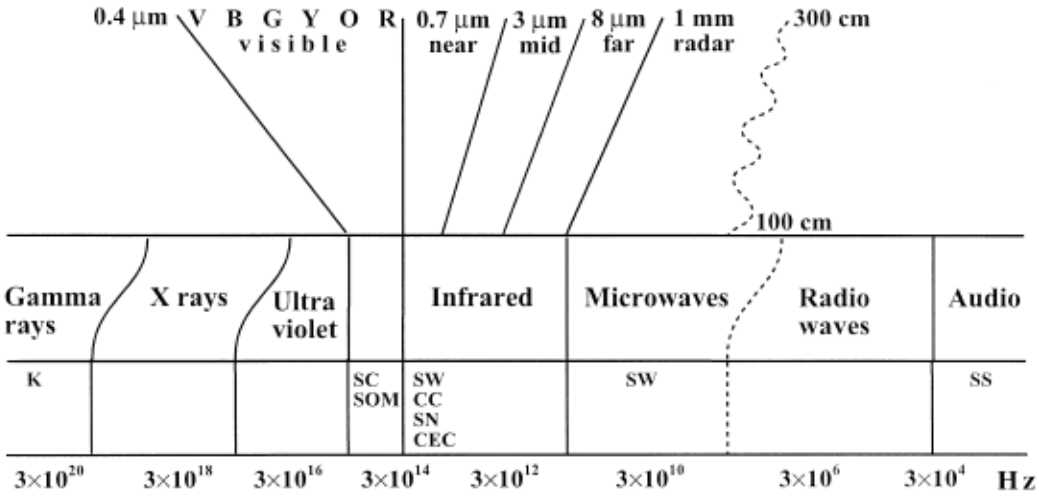

Fig. 2.5 Some possible proximal sensors for potassium (K), soil colour (SC), soil organic matter (SOM), soil water (SW), clay content (CC), soil nitrogen (SN), cation exchange capacity (CEC) and soil structure (SS) occur throughout the electromagnetic spectrum (Viscarra Rossel & McBratney, 1998)

Viscarra Rossel and McBratney (1998) discussed the potential use of these sensors for real-time, simultaneous estimation of several soil properties, e.g., clay, organic matter and water. They examined the potential of these sensing and scanning technologies for the more efficient and economic description of extent and variability of those soil attributes that affect crop growth and yield. A combination of a ground-based sensor with a global positioning system (GPS) allows detailed mapping of soil resources and crop yield variability that may therefore be an important input for site-specific decision making. This detailed information is a prerequisite of precision agriculture practice, which has “ridden on the back” of rapid developments of soil attribute mapping, as well as crop yield mapping and vastly improved GPS systems and their critically useful digital elevation maps.

2.2.1.2. Computing aids

Precision agriculture practice has been aided by complementary advances in computer capability, software development and geostatistics (e.g., Triantafilis et al., 2001a, 2001b; Sommer et al., 2003; Bishop & Lark, 2006). The development of Geographical Information Systems (GIS) has enabled access to spatial soil information, to readily examine the spatial context of soils, and to apply process models to spatially distributed data (Pennock & Veldkamp, 2006). Pennock and Veldkamp also stated that parallel advances in physical and biogeochemical modelling and in computing power has allowed the simulation of complex processes in space and time.

2.2.1.3. Geostatistics

Recent advances in geostatistical analysis mean we no longer have to regard a treatment response as a fixed effect (Bishop & Lark, 2006). The traditional statistical approach to soil and agronomic research, since the definitive work of Sir Ronald Fisher in the 1920s and ’30s, enabled researchers to remove site variation from field experiments, despite a realization that it existed (Cook & Bramley, 1998). However, Bishop and Lark (2006) have described how we now have the ability to design and analysis our experiments at the landscape scale. We are now able to estimate the response to different treatments and treatment contrasts for any target site, using, e.g., kriging, a method that assesses the autocorrelation of data points (their spatial relationships) and models a prediction surface. A defining difference between geostatistics and classical statistics is that the former accepts the existence of spatial autocorrelation, while classical statistics assumes observations are independent variables and spatially uncorrelated (Webster & Oliver, 2007).

2.2.1.4. On-the-go proximal sensing

In their review of remote and ground-based sensor techniques for mapping soil properties, Barnes et al. (2003) envisioned a combination of multispectral imagery, ground-based sensor data, and other ancillary information integrated through appropriate models that could some day provide accurate and detailed soil maps with

a greatly reduced need for direct sampling. The advent of powerful public domain software, such as Google Earth, will help the realization of this vision.

Godwin and Miller (2003) reviewed technologies for mapping within-field variability that include non-invasive electromagnetic induction (EMI), aerial photography, and radiometry. They also discussed sensors available for measuring soil compaction (penetrometers), draught (extended octagonal ring force transducers), clod size (visual sensors) and surface roughness (laser profile meter, ultrasonic displacement transducer) – controllable soil factors influencing crop yield. These authors agreed with Barnes et al. (2003) that a major benefit of such technologies is that they make possible targeted sampling, which takes account of maximum variability within the study area.

The most recent review by Adamchuk (2008) provides a very useful summary chart of systems (Fig. 2.6). Adamchuk states that the major benefit of on-the-go soil sensor systems has been the ability to quantify the heterogeneity of soil within a field and to guide other data collection and field management strategies accordingly. He concludes that as new on-the-go soil sensors are developed, different real-time and map-based differentiated soil treatments may become economically feasible.

Adamchuk discusses the major role of this benefit in the development of precision agriculture technologies. Knowledge of spatial soil variability helps the site-specific management of agricultural inputs, such as seed rate, fertilizer, agrochemicals and irrigation. This, in turn, helps increase profitability of crop production, improve product quality and protect the environment. Knowledge of soil spatial variability helps direct variable rate application of agricultural inputs, aiding best use of natural resources such as freshwater.

2.3. Ground-based sensors for on-the-go soil mapping

2.3.1. Global Navigation Satellite Systems (GNSS)

GNSS receivers act as positional sensors and are now readily accessible to the private user, with a start-up cost of about NZ$250. They have become the most common

sensor in precision agriculture, being used to locate and navigate agricultural vehicles within a field (Adamchuk, 2008), for example during yield mapping. They are also a critical part of on-the-go soil sensing systems.

2.3.1.1. Global Positioning System (GPS)

At present, the United States NAVSTAR Global Positioning System (GPS), shown in Figure 2.7, is the only fully operational GNSS. It is employed worldwide, as part of GNSS-1, with the Russian system GLONASS, plus local augmentation systems. In New Zealand the local area augmentation system is WAAS (Wide Area Augmentation System), (www.garmin.com 2008). The second generation system, GNSS-2, when fully employed, will be a stand-alone fully independent civilian system, exemplified by the European Galileo positioning system,
(www.ifen.unibw-muenchen.de/research/index.htm).

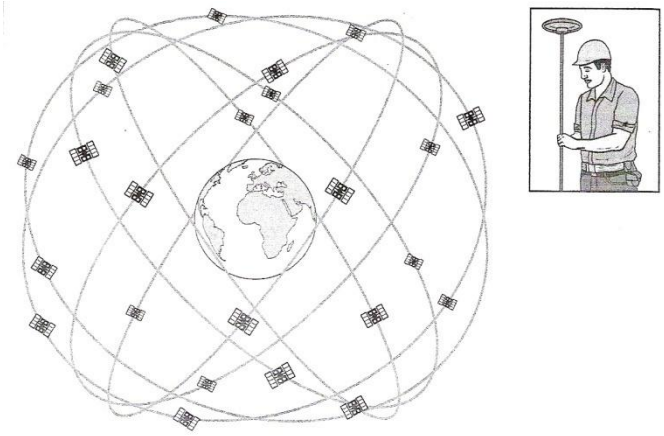

Fig. 2.7 GPS receiver and satellite configuration (Heywood et al., 2006)

When a GNSS receiver is linked to a datalogger it can be used to produce a digital elevation map. The precision of co-ordinates (latitude, longitude, elevation) depends on the type of receiver. The simplest hand-held receivers are only accurate to within 15 m, 95% of the time.

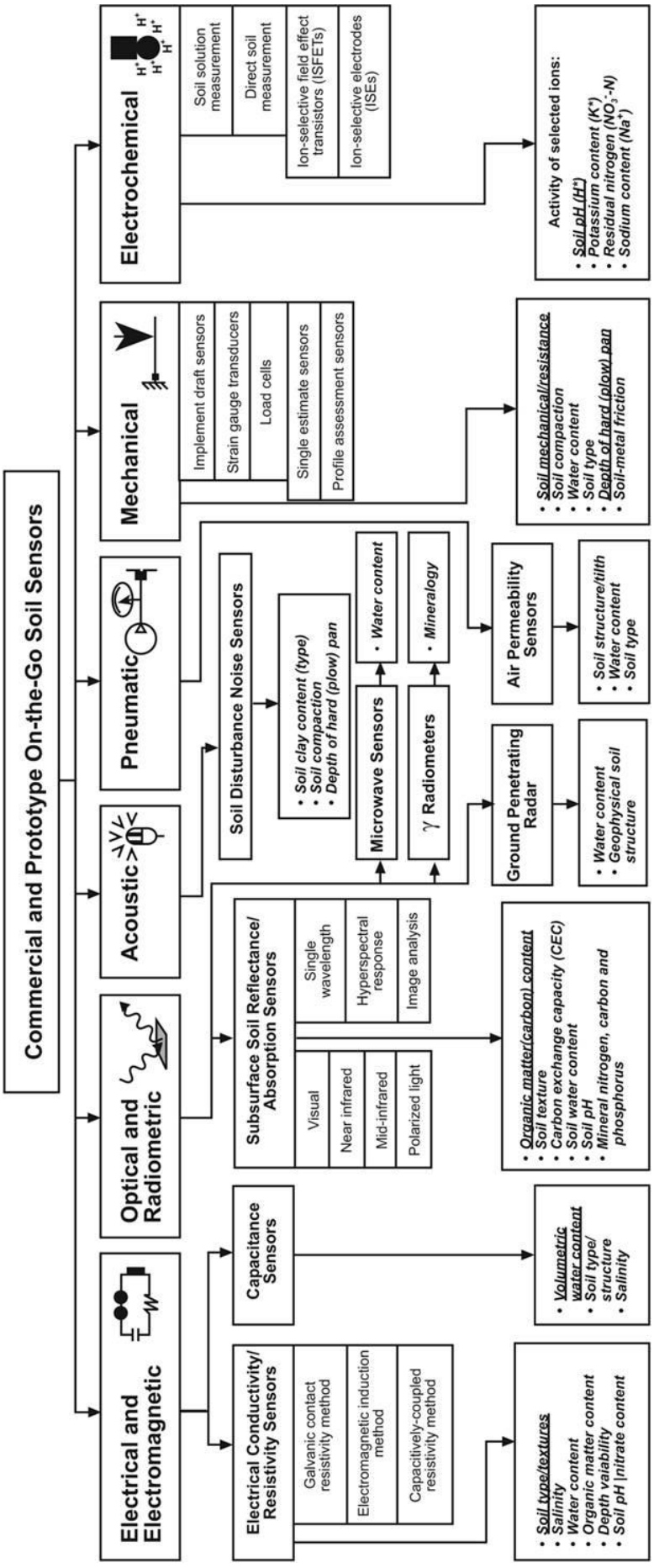

Fig. 2.6 General classification of on-the-go soil sensing systems (underlined soil properties are the most likely analytes) (Adamchuk, 2008)

2.3.1.2. Differential Global Positioning System (DGPS)

DGPS improves the accuracy of estimated position by correcting for natural and introduced errors common to normal GPS observations (e.g., Grunwald, 2006). DGPS corrections are applied in two ways:

- Post-processing – a technique that requires the GPS user to collect GPS data and then, using specialized software, process the GPS data with DGPS data, collected at the same time, from a known location like a base station or permanent reference station.
- Real-time kinematic DGPS – allows the GPS user to immediately take advantage of differential corrections that are broadcast in real-time from DGPS services. It uses a GPS receiver and another receiver (base station) in a fixed position. RTK-GPS systems are the most desirable systems, providing real-time capability for accurate mobile mapping, with centimeter accuracy in each plane (e.g., Godwin, 2003; Trimble, 2009).

2.3.1.3. Application to soil sensing and mapping

A precise digital elevation map (DEM) with centimeter accuracy provides scope for soil property mapping based solely on DEM data (e.g., Sommer et al., 2003). It also provides essential positional data for on-the-go soil sensing systems. Lavado Contador et al. (2006) predicted near-surface soil moisture for a 99.5 ha watershed solely from the DEM data (Pearson's R coefficient 0.71; RMSE 4.56% v/v). They extracted three topographic variables: Kv (vertical curvature), Kh (horizontal curvature) and TI (topographic wetness index) to predict soil moisture. Vitharana et al. (2008) extracted a wetness index (WI) as well as a stream power index (SPI) from a DEM to predict management zones for variable land management. WI was used to predict zones of water saturation, and SPI was used to measure erosive power of flowing water, combining the effect of upstream area and slope angle. Kaleita et al. (2007) used slope, aspect, plan curvature (the curvature along a contour line perpendicular to the slope), profile curvature (the curvature in the direction of the slope), and tangential curvature (the curvature along a vertical plane tangential to a contour line) to define topographic indices for their landscape. Significant relationships were developed between these indices and soil moisture (to 7.5 cm soil depth).

2.3.2. Electrical and Electromagnetic Soil Sensors

Electrical and electromagnetic sensors use electric circuits to measure the capability of soil particles to conduct and/or accumulate electrical charge. The soil becomes part of an electromagnetic circuit and immediately affects the signal recorded by the data logger. Several such sensors have become commercially available (Adamchuk, 2008).

2.3.2.1. Electromagnetic sensors

The two most commonly used, commercially available, electromagnetic sensors for soil mapping are the Geonics© EM range sensors, with an exploratory depth of up to 1.5 m, and the Veris© range sensors, with exploratory depth to 0.9 m. These sensors assess electrical conductivity (EC) of a volume of soil below the sensor. Sudduth et al. (2003) compared these two instruments and found that data were highly correlated (R^2 0.74-0.88). Differences between the EC sensors were more pronounced on layered Missouri soils due to differences in the depth-weighted response curves. However, data obtained with both types of EC sensors were similar and exhibited similar relationships to soil physical and chemical properties. The great advantage of the Geonics EM38 in our New Zealand studies is that it is non-contact and can be pulled across a bare soil or pasture sward – being easily pulled behind an ATV farm bike it is ideally suited to on-the-go mapping of cultivated or pastoral soils. The Geonics EM38 measures apparent electrical conductivity (EC_a).

2.3.2.1.1. The Geonics EM38 sensor

The Geonics EM38 is the most commonly used EM sensor. Other Geonics EM sensors include the EM31, with exploratory depth to 6 m, and the newly released EM38 Mark 2, which simultaneously provides a soil EC_a value to 0.38, 0.75 m and 1.5 m.

The Geonics EM38 sensor measures apparent soil electrical conductivity (EC_a) and magnetic susceptibility, the latter being used to compensate for differences that could affect soil EC_a readings. The sensor was originally designed in the late 1970s at the request of J D Rhoades by Geonics Ltd, Canada, to measure soil salinity (McNeill 1980; Rhoades 1993). Rhoades (1981) saw a need for an improved rapid field method for assessing soil salinity, because about one third of irrigated land in Canada and the US

has been seriously salt-affected, which impacted on crop yield, sometimes causing crop failure.

A small transmitter coil in the sensor is energized with an alternating current (Fig. 2.8). This current generates a primary time-varying magnetic field in the ground, which, in turn, induces small currents that generate their own secondary magnetic field. A receiver coil responds to both primary and secondary magnetic field components. The secondary field detected at the receiver coils is a linear function of soil EC_a (McNeill 1992). Conductance of the electric currents through the soil is via three main pathways:

- Alternating layers of soil particles and their bound soil solution,
- Continuous soil solution,
- Through and along the surfaces of soil particles in direct contact with each other.

(Rhoades and Corwin, 1990)

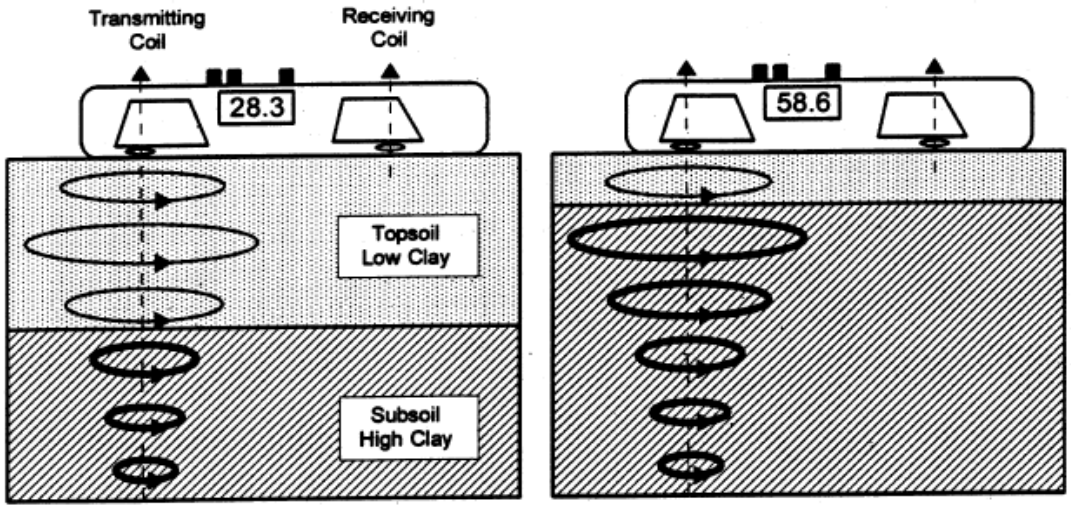

Fig. 2.8 Schematic diagram showing operation of the Geonics EM38 soil conductivity sensor in vertical dipole mode over deep topsoil (left) and shallow topsoil (right) (Sudduth, 2001)

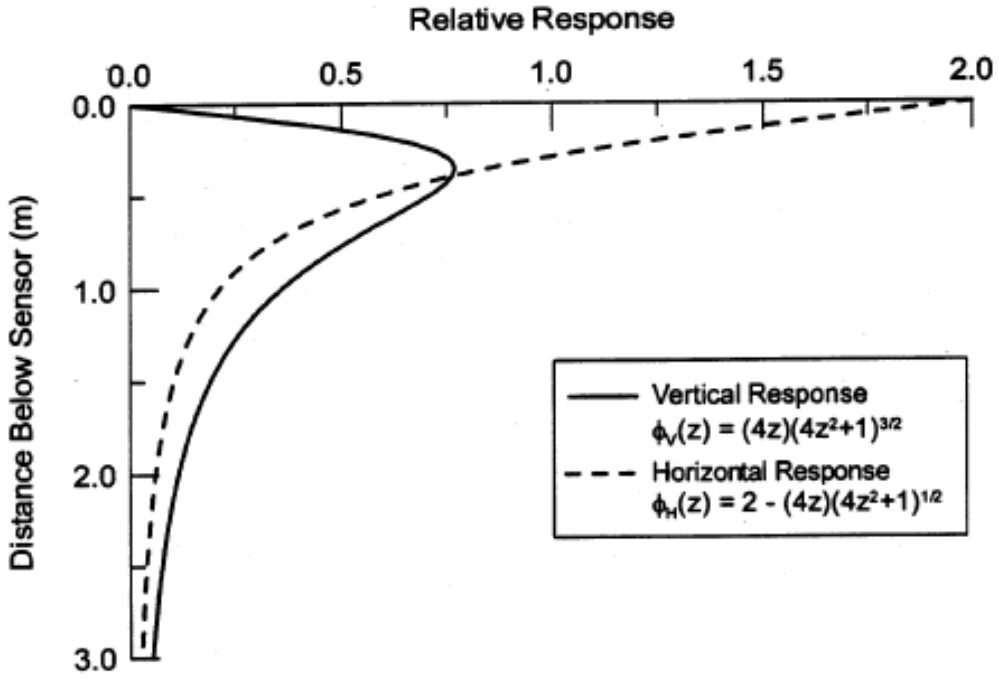

Fig. 2.9 Relative response of EM38 sensor as a function of distance (adapted from McNeill, 1992) (Sudduth, 2001)

The EM38 can be used in two modes. The vertical dipole mode (upright) provides an effective measurement depth of about 1.5m. The horizontal dipole mode (laid on its side) provides effective measurement depth of about 0.75m. Instrument response to soil electrical conductivity varies as a nonlinear function of depth (Fig. 2.9).The sensor is ideally designed for on-the-go operation when used in combination with GPS, datalogger, field computer, and all-terrain vehicle (Fig. 2.10).

Fig. 2.10 **On-the-go EM mapping system, employing a Geonics EM38, RTK-GPS, datalogger, on-board field computer and ATV**

2.11	2.12
	

Fig. 2.11 **Geonics EM38 – 1980s model**

Fig. 2.12 **Geonics EM38 Mark 2 – 2008 model**

2.3.2.1.2. The Veris EC Surveyor

The Veris instrument uses a direct contact method for assessing soil EC. As the EC Surveyor is pulled through the field, one pair of coulter-electrodes injects a known voltage into the soil, while the other coulter-electrodes measure the drop in that voltage (www.veristech.com).

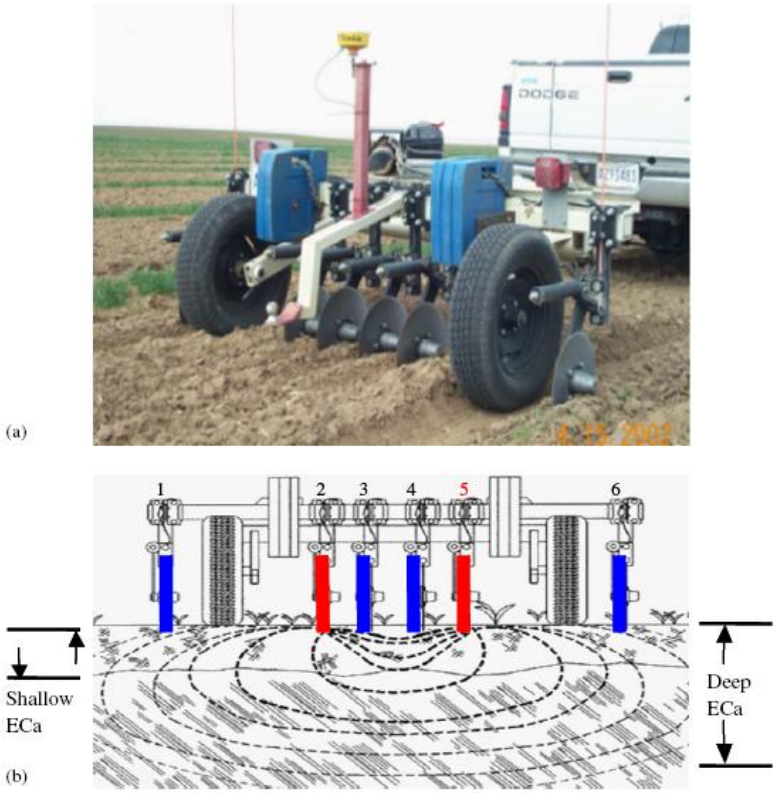

Fig. 2.13 (a) The Veris 3100 Mapping System mounted behind truck or tractor, equipped with Trimble geographic information system. (b) Schematic of coulter electrode configuration with coulters 2 and 5 inducing current while coulters 3 and 4 measure shallow (0–0.3 m depth) and coulters 1 and 6 measure deep (0–0.9 m depth) apparent electrical conductivity (EC_a) (McCutcheon et al., 2006)

2.3.2.1.3. Applications of EM soil mapping

Researchers soon discovered that in non-saline soils the EM sensors were usefully showing other soil differences, for example soil type boundaries (Doolittle et al. 1995, 1996; Jaynes 1996). Jaynes found that EM mapping can be used both as a reconnaissance soil mapping tool and to improve boundary accuracy on existing soil maps. EM sensors primarily respond to soil clay content and moisture in non-saline

soils (e.g., Sudduth, 2001). In the 1980–1990s these sensors were also used to assess depth to claypan (Doolittle et al., 1994; Brus et al., 1992; Bork et al., 1998), soil water content (Kachanowski et al., 1988), cation exchange capacity, and exchangeable calcium and magnesium (McBride et al., 1990). Initially, researchers used the EM sensors for point readings, then they started logging positional co-ordinates of each site with GPS (e.g., Doolittle et al., 1995), and finally the system was mobilized by attaching it to an all terrain vehicle (ATV) (Kitchen et al., 1996). Kitchen et al. (1996) found a strong relationship between EM readings and depth of sand deposition (R^2 = 0.73–0.94) in recent flood deposits from the 1993 mid-west floods along the Missouri and Mississippi Rivers.

Lund et al.'s (1998) defining work described the potential for EM maps to be used for site-specific management of soils at the field scale. By this stage, farmers in the US had started to yield map crops, and it was realized that yield maps could be interpreted on a basis of soil differences. There was a need to map soil variability and the EM sensors met this need. Lund et al. introduced the concept of managements zones, and prescription maps derived from EM data and provided the link between EM mapping and precision agriculture, site-specific management and variable rate application. Their paper provided the direction for much of the subsequent EM mapping research and development around the world (e.g., Johnson et al., 2003; Hedley et al., 2004; Corwin et al., 2006; Taylor et al., 2007).

The development of these on-the-go EM mapping systems was concurrent with major developments in computer capability, GIS software, and geostatistical concepts. Much of the earlier research related soil EC_a to soil properties by simple regression modelling, normally linear or stepwise. In 2001, Triantafilis et al. (2001a, 2001b) used linear regression and kriging to improve predictions. They explained how geostatistics uses spatial data correlation to improve predictions, which contrasts with classical statistical methods (see Sections 2.2.1.2 and 2.2.1.3). The spatial relationship of all data is investigated by the initial calculation of a variogram, which acts as a quantified summary of all the available structural information of one or more random function. Kriging can be thought of as a two-step process: (a) production of a variogram to quantify spatial relationships, and (b) development of a prediction model, including

spatially defined relationships and a quantified error term. The term 'kriging' recognizes the geologist, DG Krige, who in the early 1950s used and developed the method to estimate the gold content of ores from drill cores in the South African goldfields (Webster & Oliver, 2006).

Triantafilis (2001a) compared five geostatistical models – ordinary kriging, regression kriging, three-dimensional kriging, co-kriging and multi-linear regression – to predict soil salinity from electromagnetic induction data. Finding that regression kriging gave the best prediction, they suggested this was the result of the incorporation of regression residuals within the kriging system.

EM mapping systems continue to be refined, with EC_a data being used to define soil mapping units (Anderson-Cook et al., 2002; James et al., 2003) as well as a surrogate measure of a range of soil properties, e.g., soil pH (R^2 = 0.66–0.80, Dunn & Beecher, 2007), soil available N (R^2 = 0.47, Korsaeth, 2005; R^2 = 0.79–0.98, Eigenberg et al., 2002, 2006), clay content (R^2 = 0.85, Weller et al., 2007), soil water content ($R^2 \geq 0.7$, Sherlock & McDonnell, 2003; $R^2 \geq 0.7$, Brevik et al., 2006; R^2 = 0.93, Huth & Poulton, 2007), and available soil water-holding capacity (Waine et al., 2000; Reedy & Scanlon, 2003; Wong & Asseng, 2006; Jiang et al., 2007; Hezarjaribi & Sourell, 2007; Kitchen et al., 2008).

Wong et al. (2006), Jiang et al. (2007) and Kitchen et al. (2008) assume that water is the most limiting factor in dryland grain farming, and regress field AWC estimates against EC_a. Hezarjaribi and Sourell (2007) also calibrated EC_a data with AWC, but used 29 laboratory-assessed values for AWC, based on air-dried 2 mm sieved soil samples, which would not give a good estimate of field capacity. Waine et al. (2000) developed relationships between EC_a, soil texture and field-assessed AWC, to produce AWC maps. This method measures soil texture and moisture, enabling the prediction model to define more clearly the individual effects of soil texture and moisture on EC_a.

These studies used localized EC_a-prediction models, which can be usefully employed for site-specific land management, for example, Johnson et al. (2003) used EC_a-defined management zones in a wheat crop to: (i) soil sample to assess residual nutrients and soil attributes affecting herbicide efficiency, (ii) yield goal determination and (iii)

prescription maps for metering site-specific inputs. Little progress has been made toward global EC_a- prediction models.

Carroll and Oliver (2005) used point readings of EC_a (15 m apart) to predict soil properties across two 23-ha sites with contrasting soils (a shallow Calcisol, less than 0.2 m deep in places, and a Luvisol soil) and concluded that EC_a predictions were not consistent across the two study areas. EC_a best predicted sand, silt and water content ($R^2 \geq 0.8$) at the Calcisol site, and sand and clay ($R^2 \geq 0.8$) at the Luvisol site. Carroll and Oliver concluded that the EC_a map did not reliably describe any one soil property, but did describe soil variability, which could be used to define management zones and for targeted soil sampling. There was no discussion of the fact that EC_a will correspond to the soil variable that has the greatest influence on soil EC at any one point. If soil moisture varies significantly across a landscape with uniform texture, perhaps due to topographic differences, then EC_a would be expected to relate most closely to soil water. If, however, soil texture is varying significantly, in non-saline soils – this will in most cases have an overriding control on EC_a values, (Fig. 2.14).

Sudduth et al. (2005) also investigated the ability of EC_a data to predict soil properties across sites – and their study included a much wider range of soil and land resource areas, including different management practices and climatic conditions. They found that it might be feasible to develop relationships between EC_a and (i) clay and (ii) CEC that are applicable across a wide range of soil and climatic conditions. Correlations with other soil properties (soil moisture, silt, sand, organic C and paste EC) were not as strong. They also investigated whether there was any advantage in collecting data simultaneously with two EM sensors (Veris 3100 and Geonics EM38), for better prediction of soil properties (Fig. 2.14).

Sudduth et al. (2005) concluded that although some predictions were slightly improved by the combination of data from the two EM sensors, the added effort and expense are probably justifiable only in limited circumstances. They do, however, emphasise the need to check for drift when using the Geonics EM38, by returning to the same swath on an hourly basis. They also concluded that it was not necessary to apply temperature corrections to their data.

As EM mapping has become a commercial reality in the US and Australia, standard guidelines have been produced to guide quality control of commercial EM mapping companies (e.g., O'Leary & Peters, 2004).

Soil Property	State	Best single-ECa model			Veris shallow + deep		Veris + EM38	
		ECa data	r^2	S.E.[a]	r^2	S.E.	r^2	S.E.
Soil moisture	MO	N.S.[d]			N.S.		N.S.	
	IL	–[b]	–	–	–	–	–	–
	MI	N.S.			N.S.		0.49	34
	WI	$EC_{a\text{-sh}}$	0.38	27	0.71	19	0.75	18
	SD	$EC_{a\text{-dp}}$, q[c]	0.68	28	0.73	26	0.68	28
	IA	$EC_{a\text{-sm}}$	0.40	36	0.34	38	0.58	31
	All	$EC_{a\text{-dp}}$	0.15	45	0.15	45	0.24	42
Clay	MO	$EC_{a\text{-sm}}$	0.26	49	0.60	39	0.60	38
	IL	$EC_{a\text{-sm}}$	0.48	28	0.43	30	0.51	28
	MI	$EC_{a\text{-dp}}$, q	0.42	30	0.42	30	0.42	30
	WI	$EC_{a\text{-sm}}$	0.29	20	0.54	16	0.54	16
	SD	$EC_{a\text{-sm}}$	0.22	35	0.25	35	0.22	35
	IA	$EC_{a\text{-sm}}$	0.47	49	0.52	47	0.68	39
	All	$EC_{a\text{-sm}}$, q	0.61	48	0.34	63	0.72	42
Silt	MO	$EC_{a\text{-sm}}$	0.29	46	0.38	44	0.44	42
	IL	N.S.			0.22	54	0.36	50
	MI	N.S.			N.S.		0.40	107
	WI	$EC_{a\text{-sh}}$	0.55	66	0.81	45	0.81	45
	SD	$EC_{a\text{-dp}}$, q	0.26	91	0.35	85	0.35	85
	IA	$EC_{a\text{-sm}}$	0.37	73	0.33	77	0.50	66
	All	$EC_{a\text{-sm}}$, q	0.18	143	0.12	148	0.28	136
CEC	MO	$EC_{a\text{-sm}}$	0.40	3.4	0.47	3.3	0.70	2.5
	IL	$EC_{a\text{-sm}}$	0.57	3.5	0.59	3.5	0.79	2.6
	MI	$EC_{a\text{-sm}}$, q	0.21	3.9	N.S.		0.65	2.7
	WI	$EC_{a\text{-sm}}$	0.14	2.0	0.66	1.3	0.66	1.3
	SD	$EC_{a\text{-sm}}$, q	0.44	3.6	0.44	3.6	0.51	3.4
	IA	$EC_{a\text{-sm}}$	0.55	4.5	0.54	4.6	0.66	4.0
	All	$EC_{a\text{-sm}}$	0.66	3.8	0.49	4.7	0.70	3.6

[a] Standard errors (S.E.) are in units of g kg^{-1} (soil moisture, clay, silt) and cmol kg^{-1} (CEC).
[b] No soil moisture data available for Illinois fields.
[c] The letter "q" denotes a quadratic regression, all others are linear.
[d] N.S. denotes no significant ($P \leq 0.05$) regression.

Fig. 2.14 Regression statistics for the estimation of profile-average soil properties as a function of EC_a using individual and multiple datasets (Sudduth et al., 2005)

2.3.2.2. Electrical sensors for soil water content mapping

The fact that the dielectric constant of water is an order of magnitude greater than that of soil makes measurement of capacitance, or dielectric constant, a very attractive technique to determine soil moisture content (Starr, 2005; Adamchuk et al., 2004).

Since the defining work of Topp et al. (1980), time-domain reflectometry (TDR) has become an established method for accurate in situ soil water content assessment, with a proven accuracy of ±0.02 m^3 m^{-3} for many soils (Evett & Parkin, 2005). The method involves the installation of wave-guides into the soil to a certain depth. However, Topp et al.'s famous calibration relating soil water content to dielectric constant has been adopted too widely, and does not always provide the same accuracy for other sensors, for example, FDR (frequency domain reflectometry) instruments (Evett & Parkin, 2005). Evett and Parkin (2005) explained that this is partly because FDR instruments operate at frequencies well below the range of TDR instruments where the dielectric constant is insensitive to frequency changes.

Trials showed that an FDR instrument, the Streats Instrument Aquaflex, underestimated water content by 0.15 m^3 m^{-3} (Evett & Parkin, 2005). Such instruments therefore need to be calibrated on a site-by-site basis.

Several researchers have used a tine-shaped capacitance sensor for on-the-go measurement of soil moisture (e.g., Lammers et al., 2008; Richard et al., 2008; Whelan et al., 2008). Richard et al. (2008) concluded that the capacitance probe was strongly influenced by tillage history and did not report a relationship to soil water content. However, the capacitance sensor was usefully employed simultaneously with a microwave ground-based radar sensor and a laser profilemeter to interpret physical condition of the soil, on a basis of mechanical resistance, surface roughness and clod size – a measure of seed-bed preparation. Lammers et al. (2008), using a combined capacitance moisture sensor and penetrometer to assess soil resistance and water content, concluded that the vertical penetrometer had limited value for evaluation of soil trafficability, which was its original purpose, and that the soil water content profile was not characterized very well by the capacitance sensor in the field trials.

Whelan et al. (2008) also used a tine-based force/capacitance soil sensing system to measure draught resistance and soil moisture content across a 113-ha paddock (Fig. 2.15). A simple correlation between mean measured values and estimated moisture content (R^2 = 0.28) was poor, but when combined with force measurements (R^2 = 0.77, 0.85) provided a useful estimate of soil resistance, which these workers were able to relate to certain yield differences.

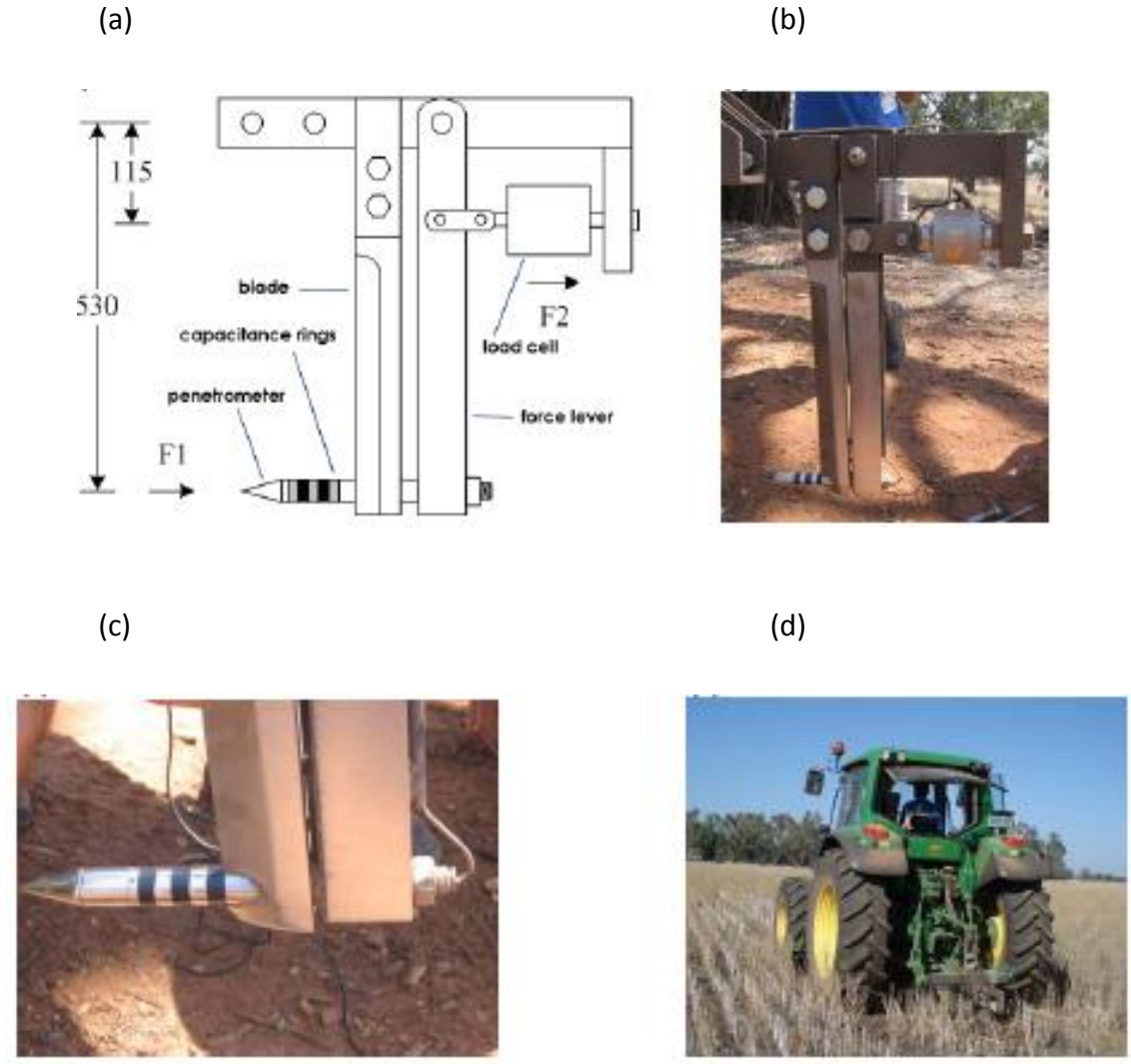

Fig. 2.15 (a) Schematic of the soil sensing system, (b) actual instrument, (c) combined force and moisture penetrometer, and (d) in-field operation (Whelan et al., 2008)

These three groups of researchers, therefore, have not been able to assess soil water content accurately using an on-the-go capacitance sensor system.

2.3.3. Optical and radiometric sensors

Optical and radiometric sensors collect light reflectance or another electromagnetic wave signal (ground penetrating radar or gamma-radiometer) and interpret this signal on a basis of soil differences (Adamchuk, 2008), (see Fig. 2.5).

Optical sensors measure intensity of visible and near-infrared energy and can be vehicle-mounted and used in the same way as remote sensing. Also, optical sensors have recently been adapted for subsurface on-the-go mapping, in a similar way to electrical and electromagnetic sensors (Section 2.3.2). Since reflectance can be easily measured simultaneously in more than one portion of the spectrum at a time these sensors have the ability to provide more comprehensive information about individual data points (Adamchuk, 2008).

Visible and Near Infrared Spectroscopy (Vis-NIR) and Laser-induced Breakdown spectroscopy (LIBS) are two methods used for field characterization of soil properties (Bricklemeyer et al., 2008); the former has been recently developed for on-the-go soil mapping (Lund et al., 2008).

Ground-penetrating radar (GPR) is also used for non-invasive surface feature mapping, with a potential to be developed for measuring soil spatial structure (De Benedetto et al., 2008).

Also, portable gamma (γ) radiometers have recently been trialed for soil characterisation, and some units are now available commercially for on-the-go soil mapping (van Egmond, 2008).

2.3.3.1. Vis-NIR Sensors

Visible and near infrared diffuse reflectance spectroscopy (Vis-NIR DRS), using either all or part of the 350–2500 nm range of the electromagnetic spectrum, is becoming the preferred laboratory method for rapid, non-destructive simultaneous assessment of a suite of soil properties (Brown et al., 2006; McBratney et al., 2006; Brown, 2007; Awiti et al., 2008) by scanning air-dried, sieved samples, normally placed in a petri dish. This is despite research showing that mid-infrared (MIR) spectroscopy is more accurate

than Vis-NIR DRS (McCarty et al., 2002; Pirie et al., 2005; Viscarra Rossel et al., 2006; Reeves et al., 2008). However, Vis-NIR DRS requires less sample preparation and allows measurement on field-moist soils. Moisture could prevent effective MIRS, because of excessive optical absorbance (Lund et al., 2008).

Brown et al. (2006) examined the precision and accuracy of empirical Vis-NIR soil characterization modelling when applied to a diverse, "global" set of independent soil samples from five continents and a wide range of climatic regions (3768 soil samples from Africa, Asia, the Americas, and Europe). Best predictions were for percent clay, mineralogy (smectite, kaolinite), organic carbon, inorganic carbon, extractable iron, and cation exchange capacity. Brown et al. concluded that Vis-NIR DRS soil characterization has the potential to replace or augment standard soil characterization techniques where rapid and inexpensive analysis is required. Although Brown (2007) applied the global calibration to a watershed in Uganda and was able to predict clay mineralogy (smectite) remarkably well, without including any local soil samples, it had insufficient accuracy for soil organic matter estimation.

Other researchers have developed Vis-NIR DRS for on-the-go soil mapping (Lund et al. 2008; Mouazen et al. 2005, 2007; Sudduth et al. 2008). Mouazen developed a system attached to a subsoiler, mounted to a 3-point tractor hitch (Fig. 2.16). Fibre optic cables connect a light source (mounted in a protective case attached to the base of the subsoiler) to a GaAs diode-array for measurement in the NIR region (944.5–1710.0 nm), and a Si array for the visible and SWIR region (306.5–1135.5 nm). As the tractor moves, light from the light source is reflected from the soil, along the cable to the detectors.

Estimations for soil moisture are good (R = 0.75, RMSEP = 0.025 kg kg^{-1}), and soil carbon, pH and phosphorous have also been estimated successfully (R^2 > 0.69) (Mouazen et al., 2007). The system has also been used with a single beam load cell and transducer to estimate bulk density and draught (Mouazen et al., 2006). Draught, or soil mechanical resistance, is a measure of soil compaction.

Fig. 2.16 Subsoiler-optical unit for on-line Vis-NIR DRS field measurement (Mouazen et al., 2005)

Lund et al. (2008) developed two modules: an on-the-go shank for collecting Vis-NIR DRS measurements at a discrete depth as it traverses the field (similar to Mouazen's system), and a probe for collecting Vis-NIR DRS measurements of the soil profile to a depth of 1 m (Fig. 2.17).

Fig. 2.17 Vis-NIR DRS shank module (left) and Vis-NIR DRS probe module (right) (Lund et al., 2008)

This system, commercially produced by Veris©, is controlled by a PC-based operating system. Its primary perceived function is for soil carbon mapping (R^2 > 0.4, 0.9, 0.7, 0.8 for 24 fields in each of four states: Maryland, Illinois, Iowa, Kansas, respectively), necessitated by a global interest in soil carbon sequestration to mitigate greenhouse gas emissions. It has also been related to nitrogen, moisture, mineralogy and other soil properties (R^2 = 0.2–0.9).

Some of the initial research leading to these current successes was undertaken by Shonk et al. (1991) and Sudduth (1993). Kaleita et al. (2005) also used a hand-held spectrometer (331–1069 nm) to assess soil moisture (R^2 = 0.71). Maleki et al. (2007) have also used the on-the-go system of Mouazen et al. (2005) to assess soil phosphorus for variable rate application.

Kusumo et al. (2008) developed a portable Vis-NIR spectrophotometer with a prototype soil probe to assess soil carbon, soil nitrogen and root density (R^2 > 0.75) on soil cores in the field, and Hedley et al. (2008a) have used the same portable system to assess soil moisture of an in situ soil surface (R^2 = 0.71) in the field. This system has the advantage of being able to be used in non-arable situations, where a vehicle mounted on-the-go system would be impractical, for example, steep pastoral hill country.

2.3.3.2. Laser induced breakdown spectroscopy (LIBS)

This instrument is laboratory-based but a field-portable instrument is being developed, once again driven by the challenge to map soil carbon effectively (Gehl & Rice, 2007). However, its affordability will put it out of the range of most researchers. The method is based on atomic emission spectroscopy, where an intense laser pulse is focused onto the soil surface, forming a microplasma that emits light characteristics of the compositional elements of the sample. While its greatest potential would be for in situ elemental analysis of soils, recent advances in statistical handing of output for soil carbon analysis (Martin et al., 2007) make it a potential new, but expensive, method for field soil analysis.

Bricklemeyer et al. (2008) used a LIBS system concurrently with a Vis-NIR system to investigate any potential benefits of combining the data. Scanning intact cores to eight

depths, they found that the combined data were the best predictors of total carbon (R^2 = 0.69), while LIBS was the best predictor of inorganic carbon ((R^2 = 0.7) and Vis-NIR was the best predictor of soil organic carbon (R^2 = 0.51).

2.3.3.3. Ground penetrating radar (GPR)

GPR is a widely accepted method for shallow subsurface feature mapping (Grunwald, 2006), and can be adapted for on-the-go soil mapping (Doolittle & Collins, 1998). It distinguishes subsurface features on a basis of dielectric constant, and therefore has potential use for assessing soil moisture content.

A GPR antenna is pulled along the ground by hand or vehicle, propagating radio waves in distinct pulses, these are then reflected off subsurface features and detected back at the source by a receiving antenna (Grunwald, 2006). The travel time of these wave pulses is determined by the dielectric constant of the soil, similar to the operation of TDR.

Huisman et al. (2003), in a review of GPR methods for soil water content assessment, commented that the new generation of GPR instruments provide improved estimates of soil moisture compared with earlier versions, and this has revived an interest in the use of GPR for on-the-go water content determination.

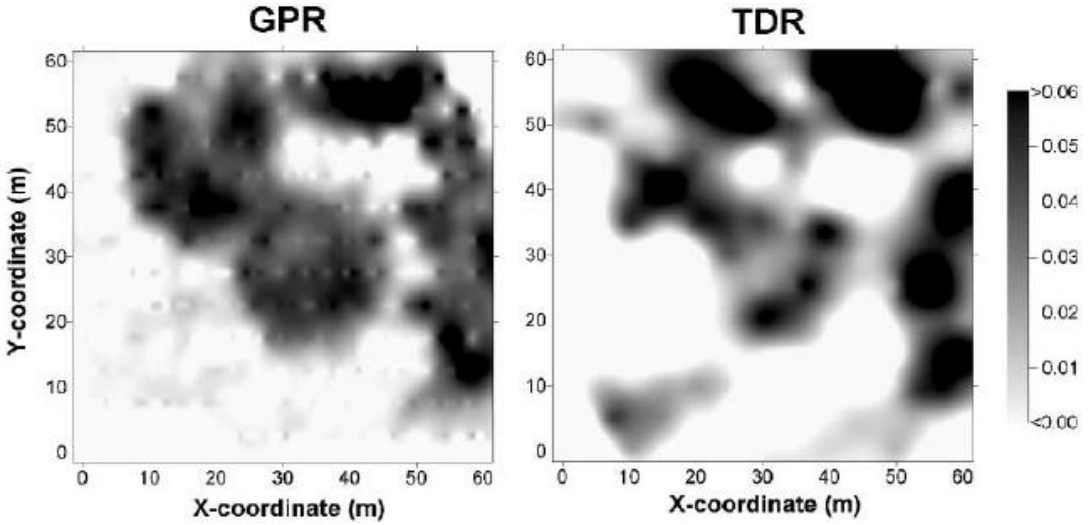

Fig. 2.18 GPR and TDR assessed soil water (m^3 m^{-3}), interpolated from the difference between soil water content data points obtained before and after an irrigation event (Huisman et al., 2003)

In Figure 2.18 the GPR-generated map is of higher resolution than the TDR-generated map, due to a much higher density of sample points. While the two maps clearly show good agreement, the GPR tended to underestimate water content, and the measurement volume over which the ground wave averages was still unresolved (Huisman, 2003). Researchers also acknowledge that the robust relationship between TDR and dielectric constant does not apply to the lower frequency GPR antennae (Huisman, 2003).

Alumbaugh et al. (2002) derived soil moisture content estimates from cross-borehole GPR (XBGPR), and Huisman et al. (2003) have suggested this is the most likely GPR method to be continued as an important research tool.

(a) EC_a derived % clay

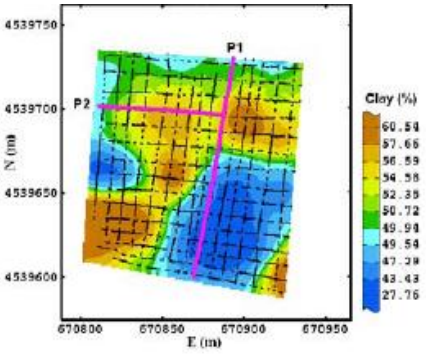

(b) EC_a derived % stoniness/gravels

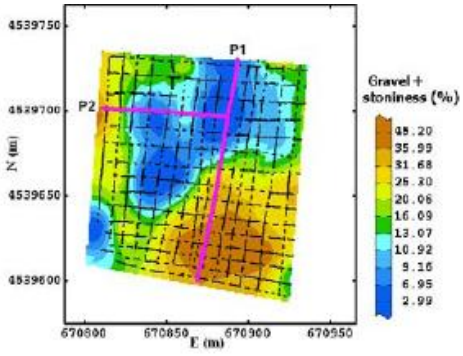

(c) 3D GPR profile (600MHz)

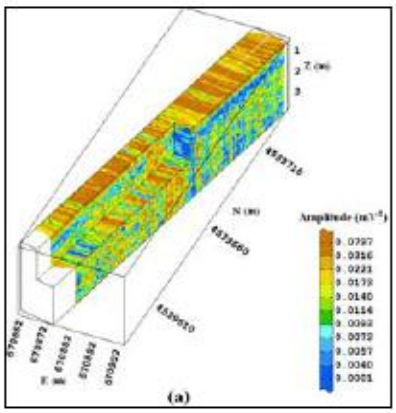

(d) 3D GPR profile (1600 MHz)

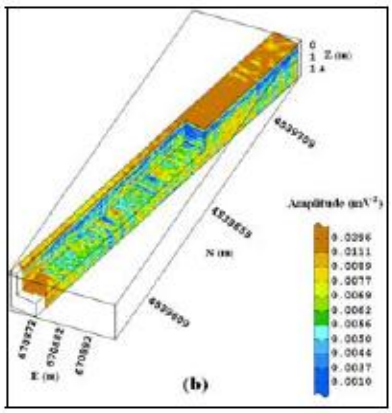

Fig. 2.19 Maps of (a) EC_a derived % clay, (b) EC_a derived % stoniness/gravels compared with 3D GPR profiles (P2 transect) obtained with (c) 600 MHz antenna and (d) 1600 MHz antenna (De Benedetto et al., 2008)

De Benedetto et al. (2008), investigated the potential to combine GPR and EM for soil mapping, using the system for on-the-go mapping of shallow calcareous vineyard soils, over gravels, in Italy. They reported that when the propagating GPR wave encounters any change in electrical properties down the soil profile, it is reflected or scattered back toward the surface.

Figure 2.19 shows the 3D GPR transect (c) and (d) for P2 transect marked in (a) and (b). The figure illustrates the low attenuation of the GPR wave in the areas of highest EC, corresponding to high clay content, and low content of gravels and stoniness. De Benedetto et al. concluded that EMI and GPR can be used for rapid reconnaissance mapping of subsurface features in agricultural fields. Differences observed by both techniques were largely determined by textural differences, which is a controlling feature of subsurface water flow. Therefore, at present, GPR provides a useful qualitative assessment of soil water content.

2.3.3.4. Gamma sensors

Gamma-ray spectrometry is a relatively new soil property sensing technique that shows promise in high resolution soil property mapping (Wong et al., 2008). Originally airborne, sensors can now be vehicle-mounted, for example, the SAIC Exploranium GRS portable gamma-radiometer (Wong & Harper, 1999; Taylor et al., 2008) and “The Mole” system of The Soil Company, Groningen, Netherlands (van Egmond et al. 2008). The vehicle-mounted sensor, with an effective exploration depth of about 30–45 cm, has been used for on-the-go soil mapping over wheat stubble (Wong et al., 2008) and 5 cm of fresh snow (Söderström et al., 2008).

The basis for gamma-ray spectrometry is that γ-ray photons have discrete energies, characteristic of the radioactive isotopes from which they originate, and the photon’s source can be determined by measuring its energy (Viscarra Rossel et al., 2007). While many naturally occurring elements have radioactive isotopes, only ^{40}K and the decay series of uranium (U) and thorium (Th) have long half-lifes, are abundant in the environment, and produce γ-rays of sufficient energy and intensity to be measured

(Viscarra Rossel et al., 2007). Signal attenuation increases by approximately 1% for each 1% increase in volumetric water content (Cook et al., 1996) Different rock types contain varying amounts of radioisotopes of K, Th and U, as do the soil profiles to which they weather (Viscarra Rossel et al., 1997).

Viscarra Rossel et al. (2007) used bagging-PLSR of gamma sensor data to give robust predictions of clay, coarse sand, pH and iron contents. Bagging-PLSR randomly draws "bags" of data from the dataset, which are then used to test the fit of the remaining data. This method can lead to improved accuracy of prediction. It uses an aggregated mean with 95% confidence intervals to provide a more robust predictor. Viscarra Rossel et al. commented that proximally sensed γ-ray spectrometry proved to be a useful tool for predicting certain soil properties in different soil landscapes. Although Taylor et al. (2008) were unable to predict pH by γ-ray spectrometry on wet Scottish soils, the sensor was used simultaneously with an EMI sensor, and results showed that data from the two sensors could be combined to improve fits for topsoil data (clay, pH, CEC, P) but not for subsoil. EMI predictions for topsoil clay (R^2 = 0.50) were improved by the addition of gamma ray data (R^2 = 0.66) giving an R^2 of 0.79.

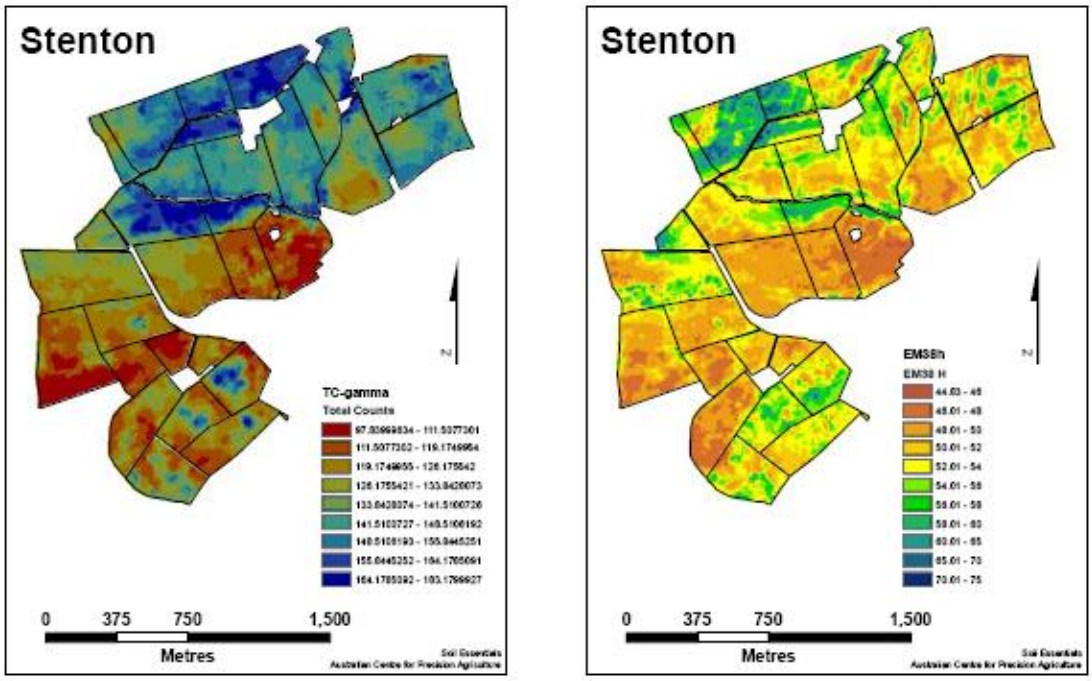

Fig. 2.20 Maps of gamma sensor output (left) and EMI output (right) (Taylor et al., 2008)

Wong et al. (2008) also used dual EM38-gamma-radiometric sensors to improve soil predictions. Previously Wong et al. (1999) were able to predict total K and plant-available K with great accuracy (R^2 = 0.9).

The method has been developed commercially in The Netherlands (van Egmond et al., 2008). The gamma sensor system, “The Mole”, is placed on a tractor and carried over the field. The system has been calibrated for a number of soil properties, and is used to map soil properties where R^2 predicted is > 0.65. Soil parameter maps are supplied to the farmer to guide crop management. Four types of maps are presented: regionally calibrated maps of soil physical properties (e.g., clay content maps); field-calibrated maps of chemical soil properties (e.g., potassium maps); calculated maps based on pedo-transfer functions (e.g., water retention maps); and calculated risk maps (e.g., compaction risk, nematode risk). Water retention maps are presumably estimated from physical property and percent clay maps, and are then used as a management tool for variable planting distance. Nematode risk maps are presumably based on soil textural differences (e.g., Ortiz et al. 2007). Soil properties estimated include:

- Clay content
- Sand content
- Grain size
- Soil type
- Organic matter
- pH
- phosphates
- potassium
- magnesium
- bulk density
- water retention (plant available moisture)
- saturated hydraulic conductivity
- risk for compaction
- nematode risk (www.soilcompany.com)(Van Egmond, 2008)

2.3.4. Mechanical sensors

Mechanical sensors are used to estimate mechanical resistance of soils, and some have been discussed in Section 2.3.2.2, because they are often used simultaneously with a capacitance sensor for soil water content estimation. Load cells or strain gauges record force as they penetrate or cut into the soil, and results aim to benefit variable tillage of soils, although uptake of these methods is very limited so far (Adamchuk, 2008).

Yule et al. (1999) used a fully instrumented tractor with GPS to map field performance and demonstrated that the effects of compaction almost doubled tillage costs at the headlands and gateways. Noticing the relatively low average engine power utilization (47%) in their first test field, they subsequently operated the tractor in the highest gear possible at less than the rated engine speed in a second field and increased the engine power utilization to 56%, saving US $7/ha in cultivation costs (Godwin, 2001).

A prototype system incorporating mechanical impedance sensors with electrical and optical sensors has been developed at Lincoln, Nebraska (Adamchuk, 2008). A vertical blade detects soil mechanical resistance between 5 and 30 cm. Simultaneously, a capacitor-type sensor detects variability in soil moisture, and two sets of photo-diodes and light emitting diodes protected with a sapphire window detect soil reflectance in the red and blue portions of the electromagnetic spectrum. The system has the potential to delineate field areas with potential compaction, excessive moisture and/or low organic matter levels. (See Section 2.3.2.2 for more examples).

2.3.5. Acoustic and pneumatic sensors

Acoustic sensors have been investigated for determining soil texture and/or bulk density by measuring change in noise level caused by the interaction of the tool with soil particles (Liu et al., 1993). They have also been used for detecting insect infestations, for example, grass grub in turf grass (Zhang et al., 2003).

Pneumatic sensors have been used to measure soil permeability on-the-go, although the relationship between sensor output and physical soil state is poorly understood, and additional research is required (Adamchuk, 2008).

2.3.6. Electrochemical sensors

These ion-specific sensors have an advantage of being soil property specific and also provide valuable information about soil fertility. An on-the-go pH and lime requirement sensing system is commercially available from Veris© (www.veristech.com) that uses two ion-selective electrodes to directly determine pH of naturally moist soils (Fig. 2.21).

More recently, Adamchuk et al. (2005) have developed a system for on-the-go simultaneous measurement of soil pH, available potassium, nitrate-nitrogen and sodium contents, using ion-selective electrodes. Coefficients of determination (R^2) of regression of direct soil measurement against a corresponding reference set were equal to 0.93–0.96 (soil pH), 0.61–0.62 (potassium), 0.41–0.51 (nitrate-nitrogen), and 0.11 (sodium).

As an example, soil pH is determined as the vehicle travels across the field. A sampling mechanism obtains a horizontal core soil sample from an approximate depth of 10 cm (Fig. 2.21). The sample is then brought into firm contact with the sensitive membranes and reference junctions of two combination pH ion-selective electrodes. As soon as the output stabilizes (approximately 10 s) the electrode surfaces are rinsed with water and a new sample is obtained. Location of the soil sample is determined with GPS and logged with the corresponding pH reading.

Fig. 2.21 Veris on-the-go pH and soil EC mapping system (left) and sampled soil for in-field pH determination (right)

Accurate on-the-go soil pH measurement is a reality (Adamchuk, 2008). Potassium and nitrate electrodes can already be used to distinguish between very low and very high levels of soluble potassium and residual nitrate; research is continuing to improve their accuracy. Application of sodium electrodes, however, remains questionable.

2.4 Discussion and Conclusions

Section 2.3 provided a review of ground-based soil sensors, appropriate for on-the-go soil mapping, with most emphasis placed on those relevant to the present water use efficiency study. Other sensors exist that have not been discussed, e.g., microwave (surface roughness) (Richard et al., 2008) and magnetics (iron content) (Maier et al., 2006) sensors.

In reviewing the literature, the electromagnetic sensors stand out as the most popular and useful sensors for general soil characterization, to this point in time. For this reason the EM sensor will be used in the present study to quantify and map soil variability at the farm-scale. EM data can successfully be interpreted on a basis of soil texture and soil type (e.g., Sudduth et al., 2005), and extrapolated to estimate available water-holding capacity (e.g., Kitchen et al. 2008). Soil moisture sensors, e.g., time domain (TDR) and frequency domain (e.g., capacitance sensors) have been successfully employed for accurate on-the-spot estimation of soil moisture (e.g., Evett et al., 2006). However, on-the-go applications of capacitance sensors for soil moisture assessment have been less successful (e.g., Whelan et al., 2008; Lammer et al., 2008).

Optical and radiometric on-the-go sensors have also been used for accurate soil moisture assessment (e.g., Mouazen et al., 2005). A Vis-NIR DRS sensor will be trialled in the present study for field soil analysis of soil moisture. One advantage of Vis-NIR DRS sensors is that soil spectral data can be interpreted for a number of soil properties at the same time (e.g., soil moisture, carbon and nitrogen) (Viscarra Rossel & McBratney, 1998). Vis-NIR DRS has also been employed to assess a wide range of other soil properties, including soil pH, cation exchange capacity, clay, sand and phosphorus (Adamchuk, 2008). In addition on-the-go ion-specific electrodes have been used for

soil pH and K status (Adamchuk et al., 2005), although there are some operational difficulties to be overcome (Lobsey et al., 2008).

Ground-based gamma spectrometers have recently become available to soil researchers, and collected data have been widely interpreted. For example, the gamma sensor trade-named The Mole is used to produce a wide range of soil parameter maps. Such maps are used for precision agriculture strategies, which could include irrigation scheduling.

A number of examples have been given of the simultaneous use of more than one sensor, e.g., EM and gamma sensors (Doolittle & Collins, 1998; Wong et al., 2008; Taylor et al., 2008). Dual sensors commonly improve soil property predictions (e.g., Taylor et al., 2008), because they respond to more than one variable (Adamchuk, 2008). Dual sensors have the increased potential, compared with a single sensor, to compensate sparsely sampled field measurements and estimate their spatial distribution at high resolution in complex field situations without the need for expensive and extensive direct sampling and measurements (Wong et al., 2008). Given that one of the most critical aspects of soil testing is actually obtaining representative soil samples (Adamchuk et al., 2004), the ability of on-the-go soil sensing to map soil variability, for (i) guided soil sampling and (ii) guidance for installation of on-the-spot soil monitoring, e.g., installation of embedded soil moisture sensors for guiding irrigation scheduling, is a significant advance in soil parameter mapping.

Taylor et al. (2008) employed GPS, EM and gamma radiometry to acquire seven data layers at a Scottish farm (elevation, $EC_{vertical.}$, $EC_{horizontal.}$, $Gamma_{total\ counts}$, $Gamma_{K\ counts}$, $Gamma_{Ucounts}$, $Gamma_{Th\ counts}$). These datasets were collated into one file, and k-means cluster analysis was performed to generate 6 classes, which were then targeted for soil sampling. The six classes can also be used as management zones for variable rate application of, for example, seed, fertilizer or irrigation water, and also targeted for installation of sensors, for example, for on-the-spot monitoring of soil moisture.

Future challenges for development of new soil sensors include deciding on the correct sensor combinations that may be region-specific, as well as more automated sensor data processing techniques that require less subjective expert input (Adamchuk, 2008).

On-the-go soil sensing and mapping is used for real-time and map-based variable rate application. Richard et al. (2008) employed microwave and laser sensors for surface roughness, a load cell for soil resistance, and a capacitance probe for soil moisture, all attached to the rear of a tractor. They discussed the feasibility of real-time manipulation of tillage depth and speed, as well as seed rate, based on real-time sensor data. Map-based variable rate application has been adopted widely over the last decade, with a prescription map concept for variable rate applications (e.g., Godwin, 2003).

Thompson et al. (2007) and Blonquist et al. (2006) used on-the-spot soil moisture sensors to guide irrigation scheduling. Thompson et al. (2007) monitored soil moisture every 30 minutes in a greenhouse replicated plot trial, using capacitance sensors. Actual commencement of crop water stress was indicated by the first statistically significant difference in midday leaf water potential (LWP), measured by sampling a leaf at midday and assessing soil water potential (Soil Moisture Co Model 3005, Santa Barbara, CA, USA). This was matched to soil moisture conditions, “apparent daily crop water uptake” (ADCWU) and “daily soil water loss” (DSWL). DSWL is calculated over 24 hours and ADCWU over day-light hours. As the leaf goes into stress ADCWU becomes smaller.

Blonquist et al. (2006) monitored soil moisture with one Acclima Digital TDT transmission line sensor in a trial plot, and the sensor was used to directly control the irrigator, switching on the irrigator when soil moisture dropped below a threshold value. While they examined the potential water savings of such a system, there was no discussion of how to cope with spatial variability when such a system is scaled up to field and farm scale. The map-based concept, made possible by on-the-go soil sensor systems, and discussed by Adamchuk (2008), addresses the issue of spatial variability that will occur at some sites.

Currently soil property maps, developed from soil sensing systems, are largely site-specific. Obviously a universal sensor calibration for one soil property is ideal – but rarely achieved. Some advances have been made in this direction for laboratory-based Vis-NIR soil sensing by Brown et al. (2006) based on a dataset of 3768 samples

collected from four continents; and by Viscarra Rossel et al. (2008) based on >7000 spectra contributed from 23 countries.

The potential use and application of these new high resolution proximal soil sensing methods is exemplified by an international collaborative effort DIGISOIL in the European Union (DIGISOIL, http://eusoils.jrc.ec.europa.eu/projects/DIGISOIL/; 2009). DIGISOIL is a consortium of European scientists who are developing new in situ and proximal sensing technologies to assess soil properties and degradation indicators that can be used for the production of high quality geo-referenced soil maps (Grandjean et al., 2008). DIGISOIL intends to improve in situ and proximal measurement technologies with integration into digital soil mapping (DSM), because of the obvious need for high resolution and accurate maps of soil properties. The stated core objective is to explore and exploit these technologies to answer societal demand to address soil degradation issues and to benefit from ecological and economic functions of soils. DIGISOIL will specifically develop and test the most relevant geophysical technologies for mapping soil properties using GPR, EMI, seismic, magnetic and airborne hyperspectral methods.

This project and its stated aims exemplify an obvious need for high resolution and accurate maps of soil properties to address soil degradation issues noted around the world (e.g., Lal., 2009; Mu et al., 2009; Basset-Mens et al., 2009; Williams, 2004; Grandjean et al., 2008; Adamchuk, 2008), as well as the need for sustainable use of natural resources (Williams, 2004; Jury & Vaux, 2007; Swaminathan, 2007).

This literature review has listed available proximal sensing technologies and has outlined how they can be used at the farm-scale for site-specific management, allowing more precise application of inputs with more efficient use of natural resources, e.g., freshwater for irrigation. It has identified the relevant sensors to be used in the present research project. Opportunities also exist to establish correlations between sensor measurements and environmental issues such as erosion, compaction, organic matter decline, and salinisation.

These new methods for in situ soil analysis and mapping will provide new information for interpretation and management of soil and landscape performance. For example, a soil reflectance spectra obtained by a radiometric sensor in the field is a unique

signature for that soil, and advances in its analysis will be accompanied by new opportunities to assess soil properties and suites of properties in a completely new way, making it possible to monitor and compare performance and sustainability of soils and landscapes under existing and projected practice.

CHAPTER THREE

Proximal Sensing of Soil and Pasture at Forest-to-Farm Land Use Change Sites

The rationale for the research reported in this chapter was to investigate the potential of two proximal sensing methods: on-the-go soil EM mapping, and backpack Vis-NIR field spectroscopy for (i) quantitative mapping of soil variability and (ii) rapid field analysis of selected soil and plant properties, respectively. Seven sites were selected in the Taupo-Rotorua region of North Island, New Zealand, where recent conversion of plantation forest to pastoral farming provided an opportunity for assessing soil changes and pasture development during the initial years after tree removal. The conversion of forest to pasture involves major disturbance of the soil profile during tree clearing and stump removal frequently resulting in highly variable soils for pasture establishment. This was therefore a suitable case study to investigate proximal sensing methods for assessing soil variability at the farm-scale. The central concept of geostatistics – the variogram and kriging – for analysis of the spatial structure of soil properties is discussed in this chapter.

Some of the research reported in this chapter has been presented at two conferences and accepted as one journal paper:

Hedley CB, BH Kusumo, ID Sanchez, M Hawke, MJ Hedley and MP Tuohy. 2006. Forest to Farm Conversions – a Field Characterization of Soil Heterogeneity relating to Pasture Production. p 42. In New Zealand Soil Science Society 2006 Conference Proceedings "Soils and Society". 72pp.

Hedley CB, BH Kusumo, ID Sanchez, MJ Hedley M P Tuohy and M Hawke. 2007. Proximal sensing of soil and pasture development under "forest to farm" land use change. p 158-169. *In* Designing Sustainable Farms: Critical aspects of soil and water management. (Eds. L.D. Currie and L.J Yates). Occasional Report No.20. Fertilizer and Lime Research Centre, Massey University, Palmerston North, New Zealand. 527pp.

Hedley CB, Kusumo, BH, Hedley MJ, Tuohy M and G Arnold. 2009. Soil C and N sequestration and fertility development under land recently converted from plantation forest to pastoral farming. New Zealand Journal of Agricultural Research 52: 443–453.

Abstract

Current forest-to-farm land-use changes are causing concern for (i) reduced forest sinks for carbon (C) sequestration, (ii) water quality, and (iii) increased pressure on water resources for irrigation. The challenge is to design new pastoral farms within the limitations of their environs. However, for this process to be achieved, the impacts of land-use change on soils and their environment must first be measured.

Sites were selected under recently converted pastures (1-yr, 3-yr, 5-yr conversions) and permanent pasture at three farms in the Taupo-Rotorua Volcanic Zone. Two proximal sensing techniques: (i) on-the-go soil electromagnetic (EM) mapping, and (ii) backpack Vis-NIR field diffuse reflectance spectroscopy, were trialed for (i) simultaneously mapping soil apparent electrical conductivity (EC_a) and elevation as a measure of soil variability and (ii) rapid in situ field analysis of soil carbon (C), soil nitrogen (N), soil moisture content (θ) and herbage N.

Soil fertility results (0–7.5 cm soil depth) show rapid increase in Olsen P, with soils reaching their optimum agronomic range within 3–5 years after conversion, at two of the three farms. Results suggest a soil C sequestration rate (0–15 cm soil depth) of 6.0 T ha^{-1} yr^{-1}, and a soil N sequestration rate of 0.48 T ha^{-1} yr^{-1} for the first five years after conversion at two of the farms. Decreasing C:N ratios with time since conversion reflect improved fertility status, and imply that in initial years of pasture establishment, N leaching to freshwater is reduced due to its immobilization into soil organic matter.

EC_a sensor data were used to investigate soil variability using variogram analysis and kriging. The resulting soil EC_a maps are available for defining soil management zones to allow site-specific management, e.g., variable rate fertilizer application and precision irrigation. Analysis of zones defined on a basis of soil variability relating to slope and aspect differences at two of these hill country sites, showed that north-facing slopes had highest C:N ratios, lowest Olsen P and lowest herbage N, suggesting less soil development, lower fertility and a reason to reduce fertilizer input to this zone. Diffuse reflectance spectra were used successfully to predict soil C, N and θ (R^2 predicted = 0.75; 0.86 and 0.70 respectively), and herbage N (R^2 predicted = 0.67).

Our research suggests forest-to-farm land-use change, with inputs of N, P, K and S to soils, allows significant soil C and N sequestration for at least 5 years after conversion. Further research is therefore required using control sites monitored over a number of years to confirm this preliminary study. The design of these new pastoral farms can be facilitated by proximal sensing tools, which allow real-time mapping of soil properties across the landscape.

3.1. Introduction

Plantation forest covers 7% of New Zealand, and the Kaingaroa Forest, on the Pumice soils of the Central Plateau, North Island, is one of the largest planted forests in the world. Here *Pinus radiata* growth rates (for 25-year-old trees) vary between 22 and 39 m^3 ha^{-1} yr^{-1} (Kimberley et al., 2005), and are therefore some of the highest growth rates globally (Carle et al., 2002). This outstanding production performance is largely attributed to deep rooting (up to 5 m) in these soils, plus a suitable climate (Molloy, 1998). Despite this success, recent trends are deforestation of plantation forests and conversion to pastoral farming. In the Taupo-Rotorua area, 18% of the forest harvested in 2005 has been converted to pasture, with a proposed conversion area of approximately 60 000 ha (Brodnax, 2007). This trend is mirrored on the Canterbury Plains where almost 1000 ha have been converted.

The likely implications of this land-use change include detrimental effects on air and water quality, due to increased nitrous oxide emissions and nitrates leaching through the soil, primarily due to dung and urine excreted by introduced grazing ruminants, and to a much lesser extent to increased use of nitrogen fertilizers (e.g. de Klein and Ledgard, 2005). In addition there is increased pressure on freshwaters as resource consents are sought for irrigation. This land-use change has impacted on New Zealand's greenhouse gas accounting because forests planted since 1990 can be included as "forest sinks", i.e. net consumers of carbon dioxide. The impacts of forest-to-farm land-use change on N and C budgets are therefore currently based on the consequences of tree removal, and few studies have documented changes in the larger soil C and N pools.

Significant disruption of the soil profile occurs as trees are ripped out to be replaced by pasture. Pasture has then to be established in soil profiles that can be highly variable over a distance of only a few metres. Significant inputs of N and phosphorus (P) fertilizers are required to build soil fertility in these soils, which have been under forest for several decades (Wheadon and Adam 2006). However, case studies report that pasture establishes very rapidly in these volcanic soils, with newly converted land achieving production levels of over 1100 kg milk solids ha^{-1} (Wheadon & Adam, 2006).

It is important to monitor soil property changes accurately to improve accuracy of C accounting, allow soil fertility management of new pastures, and schedule efficient water use. The variable nature, both spatially and temporally, of these newly converted soils is ideally assessed by methods that can map variability of soil properties across the landscape. Emerging technologies for this purpose include the use of proximal sensors with GPS (Godwin & Miller, 2003; Adamchuk et al., 2004), and subsequent handling of logged data using GIS software.

Adamchuk et al., (2004) discuss the wide use of electromagnetic (EM) sensors for rapid field acquisition of soil-related information, which enable a high sampling density at relatively low cost. The Geonics© EM38 sensor measures a mean weighted value for apparent induced electrical conductivity (EC_a in mS m^{-1}) for a volume of soil below the sensor to approximately 1.5m depth which primarily relates to soil texture and moisture differences in non-saline soils (Godwin & Miller, 2003; Hedley et al., 2004; Huth & Poulton, 2007). Vis-NIR spectroradiometers can also be used to measure reflectance, absorption or transmittance characteristics of any material such as soil or pasture, providing a rapid technique to evaluate specific properties (Adamchuk et al., 2004). The amount of energy reflected from a surface at a particular spectral wavelength range is dependent on the properties of that material, so that spectra can be pre-processed and then calibrated with a standard sample set to predict properties such as total soil carbon, nitrogen and moisture content in unknown samples, potentially real-time, in the field. Scattering of electromagnetic waves from rough surfaces is defined as specular (direct) or diffuse (indirect) and diffuse reflectance spectra have been used successfully for characterizing air-dried 2-mm sieved soil

samples (Shepherd & Walsh, 2002; McCarty et al., 2002)) in the laboratory, but fewer studies have used it for real-time field analysis.

Our research aims to assess the impacts of forest-to-farm land-use change on soils and soil fertility and to relate these to pasture development. It also uses proximal sensing techniques to assess (i) soil and pasture variability and (ii) whether variable management (e.g. variable rate fertilizer and irrigation) of these disturbed soils is desirable, with the ultimate goal of more sustainable use of resources and reduced detrimental environmental effects.

3.2. Methodology

3.2.1. Site Selection

Three farms on a range of soils were selected in the Taupo-Rotorua Volcanic Zone to assess soil changes and pasture development during the first 5 years after conversion of forest to pasture. At each farm, a permanent pasture site was sampled as well as one or two conversion sites on comparable soil types. At each site three transects were chosen, and along each transect five positions were sampled in May 2006. Reflectance spectra of pasture and soil were collected using an ASD FieldSpec Pro FR spectroradiometer (350–2500 nm). Then soils were sampled for subsequent soil fertility analysis; and pasture samples were clipped for further laboratory analysis.

The three farms were:

Atiamuri (38° 19.9 S, 176° 2.7 E)

- 1-yr conversion *Pinus radiata* to pasture
- 5-yr conversion *Pinus radiata* to pasture
- Permanent pasture

Manawahe (37° 59.8 S, 176° 41.6 E)

- 1-yr conversion *Eucalyptus nitens* to pasture
- 5-yr conversion *Pinus radiata* to pasture
- Permanent pasture

Tokoroa (38° 9.9 S, 175° 47.8 E)

3-yr conversion *Pinus radiata* to pasture

Permanent pasture

The conversion sites had previously been forested for 23 years at Atiamuri; 26 years (*Pinus radiata*) and 10 years (*Eucalyptus nitens*) at Manawahe; and 63 years at Tokoroa. Pumice Soils (Hewitt 1998) at Atiamuri are mapped as Taupo sandy silts (Vucetich and Wells, 1978), consisting typically of 15 cm of topsoil over a yellow-brown raw pumice subsoil (Orthic Pumice soils; Hewitt, 1998). Tephric Recent soils (Hewitt, 1998) at Manawahe have formed in Kaharoa Ash, with little profile differentiation in the dark sandy raw pumice parent material. At Tokoroa, the soils are older more weathered deep fertile ash soils, probably intergrade Allophanic soils (Hewitt, 1998), with some pumice present in the profile.

Table 3.1 Typical annual fertilizer form and rate applied after land conversion from plantation forest to pasture

Site	Time	Fertiliser Form	Rate	N	P	K	S	Trace
				(kg ha^{-1})			(kg ha^{-1})	
Atiamuri	Autumn	DAP*	400	72	80	-	-	
	Spring	SSP:KCl:SOA* mix [42:35:23]	330	16	13.4	58	32	Co, Se
Manawahe	Autumn	Sustain/Clover King/Potash	260	40	18	10	36	
	Spring	Sustain/Clover King/Potash	260	40	18	10	36	
Tokoroa	Initial (2003)	Super 10:DAP mix [83:17]**	1200	36	137	-	2	
	Spring (2004-05)	Cropzeal 15P	300	40	45	37	2	
	Autumn (2004-05)	DAP*	200	36	40			
	Spring (2005-06)	Super 10K + urea + calmag mix [85:7:8]	1150	37	76	98	82	
	Autumn (2005-06)	DAP:KCl mix [60:40]	350	37	42	70		

*DAP = diammonium phosphate; SSP = single superphosphate; KCl = potassium chloride; SOA = ammonium sulphate; ** cultivated in first year for swedes

During pasture seedbed preparation at the Atiamuri and Tokoroa farms, capital dressings of DAP were added supplying up to 137 kg ha^{-1} P, with additions of Mg, trace elements and lime. After the initial year, conversion pastures at all three properties typically receive two N dressing annually (autumn and spring) of between 74 and 88 kg N ha^{-1} yr^{-1} (Table 3.1).

3.2.2. Proximal Sensing Methods for Field Mapping and Analysis

3.2.2.1. On-the-go EM mapping

A Geonics EM 38 sensor was used with on-board datalogger, RTK-DGPS and Trimble field computer on an all-terrain vehicle (ATV), for simultaneous collection of positional and topographically located EC_a (mS m^{-1}) data. Survey data points were collected as 1-s intervals along parallel 10-m swaths, where possible, with an average ATV speed of 15 kph, at these hill country sites. This allowed a measurement to be taken approximately every 4 m along each swath. All sites were EM mapped except for the Manawahe 1-yr and permanent pasture site. The spatially defined EC_a dataset was kriged using Geostatistical Analyst in ArcGIS (ESRI© 1999) to produce a map of soil EC_a, with map classes determined by Jenks' natural breaks classification. This classification determines the best arrangement of values into classes by iteratively comparing sums of the squared difference between observed values within each class and class means.

3.2.2.2. Collection of Reflectance Spectra using a Backpack Vis-NIR Spectrometer

Ten replicate soil reflectance spectra were collected at each position along each transect (50 per transect) using an ASD FieldSpec Pro FR spectroradiometer (Analytical Spectral Devices), and the method described by Kusumo et al., (2006, 2008a, 2008b) at the three Atiamuri sites and at the Manawahe 5-yr and permanent pasture sites. Kusumo *et* al., (2006, 2008a, 2008b) have developed a prototype soil probe, that contains an internal light source, thus removing dependence on sunlight, and based on the plant probe supplied by ASD. Reflectance spectra were collected (350–2500 nm) from a freshly cut soil surface, using the prototype probe attached via a fibre optic cable to the ASD FieldSpec Pro FR spectroradiometer. These hyperspectral data are

recorded at bandwidths of 1.4–2 nm intervals. Ten replicate pasture reflectance spectra were also collected at these sites, using the method described by Sanches et al., (2006). Sanches et al., (2006) have developed a canopy probe that is placed onto the pasture surface to record pasture reflectance spectra using an ASD FieldSpec Pro FR spectroradiometer.

3.2.3. Soil and Pasture Sampling

Soils were sampled to 7.5 cm depth (five cores bulked per position, five positions per transect) for chemical analysis to assess soil fertility status; and to 15 cm depth for total carbon and nitrogen analysis. Pasture was sampled from a fixed area under exclusion cages (3 replicates per site) to estimate pasture production. In addition, pasture samples were clipped for subsequent herbage analysis of total N, after pasture reflectance spectra had been collected.

3.2.4. Laboratory Analysis

Soils were air-dried and 2 mm sieved before chemical analysis. These air-dried soils were then analyzed for Olsen P, P retention, pH, cation exchange capacity (CEC), total C and total N. Herbage was oven-dried at 70°C, ground and then analysed for total N. Standard laboratory analytical procedures were used (Blakemore et al., 1987). http://www.landcareresearch.co.nz/services/laboratories/eclab/eclabtest_list.asp

3.2.5. Statistical analysis of the EC_a sensor data

The EC_a sensor datasets were investigated with some classical statistics, which is, however, only of limited use for spatial data processing, being based on the premise of normal distribution and independency, rarely seen in practice in natural system data; and taking no account of scale (Taylor, 2004; Rossi et al., 1992). Rossi et al (1992) proposed that the assumption of spatial dependence is more practical and realistic, and geostatistics has now been adopted by a wide range of ecological disciplines, originating in mining and spreading to hydrogeology, soil science, agriculture, and environmental protection (Webster and Oliver, 2007).

In this study the mean, median, standard deviation, and percent coefficient of variation around the mean (%CV) were estimated for each EC_a dataset. The %CV statistic is perhaps the most commonly used statistic in precision agriculture. It is however important to realize that it does not take scale into account (Beckett & Webster, 1971). Classical statistics are non-spatial and do not differentiate field sizes (Taylor, 2004).

3.2.6. Geostatistical analysis of EC_a sensor data

EC_a data were pre-processed to remove (i) low accuracy data and (ii) outlying EC_a values. The pre-processed EC_a data were then analyzed using Vesper software v1.6, developed by the Australian Centre for Precision Agriculture (Minasny et al., 2006), to investigate its spatial structure by variogram analysis. Variogram analysis is the cornerstone of geostatistics (Webster and Oliver, 2007), and plots the variance between any 2 values against lag distance, where lag distance is the separation distance between these 2 values.

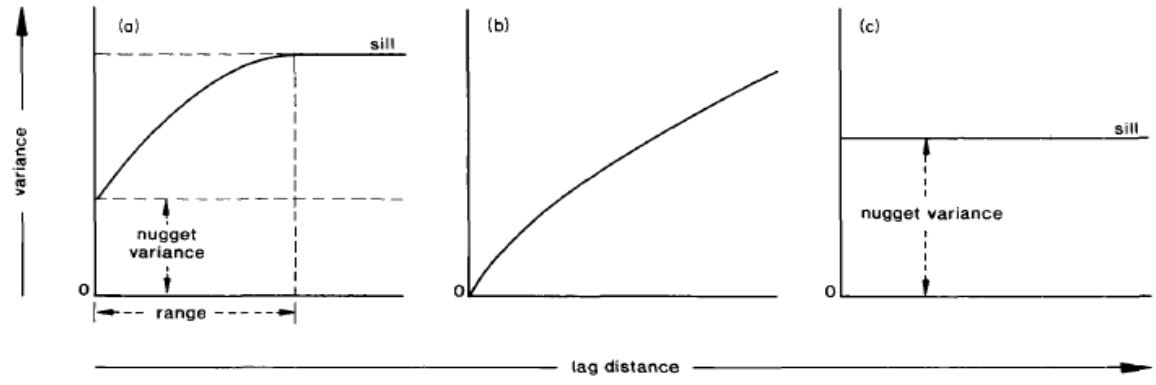

Fig. 3.1 Three theoretical functions for spatial correlation: (a) bounded variogram; (b) unbounded variogram and (c) pure nugget variogram (from Oliver & Webster, 1991)

The variogram expresses mathematically the way in which the variance of a property changes as the distance and direction separating any two points varies (Oliver & Webster, 1991), (Fig. 3.1). It is described mathematically as:

$$\gamma(h) = \frac{1}{2N(h)} \sum_{i=1}^{N(h)} [A_i(x_i) - A_i(x_i + h)^2]$$

where γ(h) is the semivariance between a pair of points N; A_i is the value of a given property at location x_i and h is the lag distance in metres, (Oliver & Webster, 2007).

The underlying theory in geostatistics is that the variogram can be extrapolated to the surrounding region on the assumption that the variance depends only on the difference between places and not on their absolute position. The importance of correct variogram model selection is vital before the next step when the variogram model parameters are used to interpolate a prediction surface, a process known as kriging. Figure 3.1 shows three variogram models. In most cases variance will increase with increasing lag distance, as in Figure 3.1a and 3.1b. These variograms are interpreted as showing strong correlation or spatial dependence (low variance) at the shortest distances, which weakens as the separation increases. This intuitively expresses what we should expect: places near each other are more similar than places further apart. The variogram in Figure 3.1a increases and then flattens when it reaches a maximum variance known as the sill variance and it is described as bounded. The lag distance at which the sill is reached is the range, which marks the limit of spatial dependence. Alternatively the variogram might increase indefinitely as in Figure 3.1b, which is termed unbounded. Frequently the variogram has a positive intercept on the ordinate, the nugget, which corresponds to random variation, as described in classical statistics. A completely flat variogram, termed pure nugget (Fig. 3.1c) shows that there is no spatial dependence in the data, the classical solution, but frequently not observed in practice. A pure nugget variogram from survey data suggests that the scale of variability has not been captured and defined by the sampling strategy, because soil scientists know that soil is a continuum where there is spatial dependence at some scale. For more information on geostatistical analysis of environmental data the reader is referred to Webster and Oliver (2007) or McBratney and Webster (1986).

Variogram processing of the EC_a data precedes interpolation of the data into a prediction surface, i.e. kriging. The best variogram model is determined by the lowest

RMSE (root mean square error). Variogram analysis was also conducted in Geostatistical Analyst in ArcMap 9.2 (ESRI© 1999-2006 ESRI Inc.) for kriging these data. The Ordinary Kriging option in Geostatistical Analyst uses circular, spherical, exponential, Gaussian, rational quadratic, and linear type models, using the mathematical function specified with the variogram type to fit a line or curve to the semivariance data on the variogram. Ordinary Kriging assumes that the variation in values is free of any drift. The models are provided to ensure that the necessary conditions of the variogram model are satisfied, as discussed by McBratney and Webster (1986). The variance for each cell size is calculated based on the average variance of all point pairs within the cell. The variogram is then fitted to the variance points using a nonlinear least squares approximation. By increasing the cell size, the number of sample points per cell size interval increases, thereby providing enough data points to estimate the variogram. Once the variogram is estimated, a smaller cell size can be used to create the actual output raster (ArcGIS, ESRI, 2009); the prediction surface, i.e. map of EC_a values.

3.2.7. Spectral pre-processing

Hyperspectral data collected with the ASD FieldSpec Pro FR were pre-processed using SpectraProc software (Hueni and Tuohy, 2006). This software allows input of the ASD binary file format and outputs processed spectral data as CSV (Comma Separated Values) files for further spread sheeting and statistical analysis. SpectraProc holds the raw spectral data on a dedicated file server (MySQL AB, 2005) and uses metadata to link the reflectance files via a path name to the spectral database. The hyperspectral data, essentially multivariate data consisting of thousands of variables, must be pre-processed before statistical correlations with measured data can be made. Data pre-processing includes waveband filtering, smoothing, synthesizing/down sampling, derivative calculation and finally averaging of the ten replicate reflectance spectra (Kusumo et al., 2008a, 2008b). The pre-processed data were imported into Minitab (© 2006 Minitab Inc.) and calibration models for prediction of soil total C, N, moisture and pasture N were developed using Partial Least Square Regression (PLSR).

The ability of the PLSR model to predict soil properties was assessed using the following statistics: (1) RMSE (root mean square error), which is the standard deviation of the difference between the measured and predicted values of soil properties; (2) RMSEP (root mean square error of prediction) which is calculated from the validation data (Esbensen et al., 2006):

$$RMSEP = \sqrt{\frac{\sum (y_m - y_v)^2}{N}}$$

where y_m is the measured laboratory value, and y_v is the predicted value from the PLSR model, and N is the number of samples; (3) r^2 which is the proportion of variance in y_m accounted for by the PLSR model predicted values (y_v); (4) RPD (ratio of prediction to deviation) which is the ratio of the standard deviation of measured values of soil properties to the RMSE; and (5) RER (ratio error range) which is the ratio of the range of measured values of soil properties to the RMSE:

$$RPD = \frac{STDEV(y_m)}{RMSEP},\ RER = \frac{Max(y_m) - Min(y_m)}{RMSEP}$$

The best prediction model is shown by the highest RPD, RER, r^2 and the lowest RMSEP (Kusumo et al., 2008a).

3.3. Results

3.3.1. Soil fertility analyses

The mean Olsen P values at the Atiamuri 1-yr and 5-yr conversion sites were 16 mg P L^{-1} and 38 mg P L^{-1} soil respectively (Fig. 3.2a; Table 3.2). At the Tokoroa farm the 3-yr conversion site had an Olsen P of 18 mg P L^{-1} soil and the permanent pasture site had an Olsen P value of 56 mg P L^{-1}. This range in Olsen P values reflects the interactions between differences in fertilizer application rates and soil P retention; the Tokoroa soils receiving much higher rates of P (Table 3.1) but also having higher % P retention values (Fig. 3.2b; Table 3.2). The Manawahe 1-yr, 5-yr conversion and permanent pasture sites have Olsen P values of 26, 12 and 30 mg P L^{-1} soil respectively. The higher

Olsen P of the 1-year compared with the 5-year conversion site reflects the recent autumn fertilizer application that has been applied (Table 3.1).

Higher P retention of the Tokoroa soils (Fig. 3.2b; Table 3.2) reflects the greater allophane content of these soils. P retention and pH values (Fig. 3.2c; Table 3.2) tend to be lower, and CEC (Fig. 3.2d; Table 3.2) tends to be higher with time since conversion (Fig. 3.2). It is likely that these changes reflect accumulation of organic matter due to pasture root establishment, plant litter and frequent dung and urine deposition by grazing ruminants in these newly established pastoral soils.

As time since conversion increases, total soil C and N values increase in the top 7.5 cm of these soils (Fig. 3.3a; Fig. 3.3b; Table 3.2). These trends suggest total C is accumulating at a rate of approximately 0.67 % per year, and total N is accumulating at a rate of approximately 0.05% per year, in the Atiamuri and Manawahe soils for the first 5 years after conversion, in the top 7.5 cm of the soil profile. C:N ratio decreases from 15–18 in newly converted soils to 14–15 in 5-yr conversion soils to 11–12 in permanent pastures, reflecting the proportionally greater accumulation of N compared with C in these soils, as the ryegrass-clover sward establishes with accompanying N fixation, as well as N inputs from dung, urine and fertilizer (Table 3.1). Soils were further sampled to 15 cm (Table 3.2) to investigate sequestration rates to this greater depth. The results suggest that total C is accumulating at 0.50 % per year, and total N is accumulating at 0.04 % per year, for the first 5 years after conversion, in the Atiamuri and Manawahe soils to 15 cm depth.

Pasture yields in the converted sites were 78–100 % compared with the permanent pasture sites (Fig. 3.2d, Table 3.2). In the first year after conversion, 81% and 95% of permanent pasture yield was achieved at Manawahe and Atiamuri, respectively.

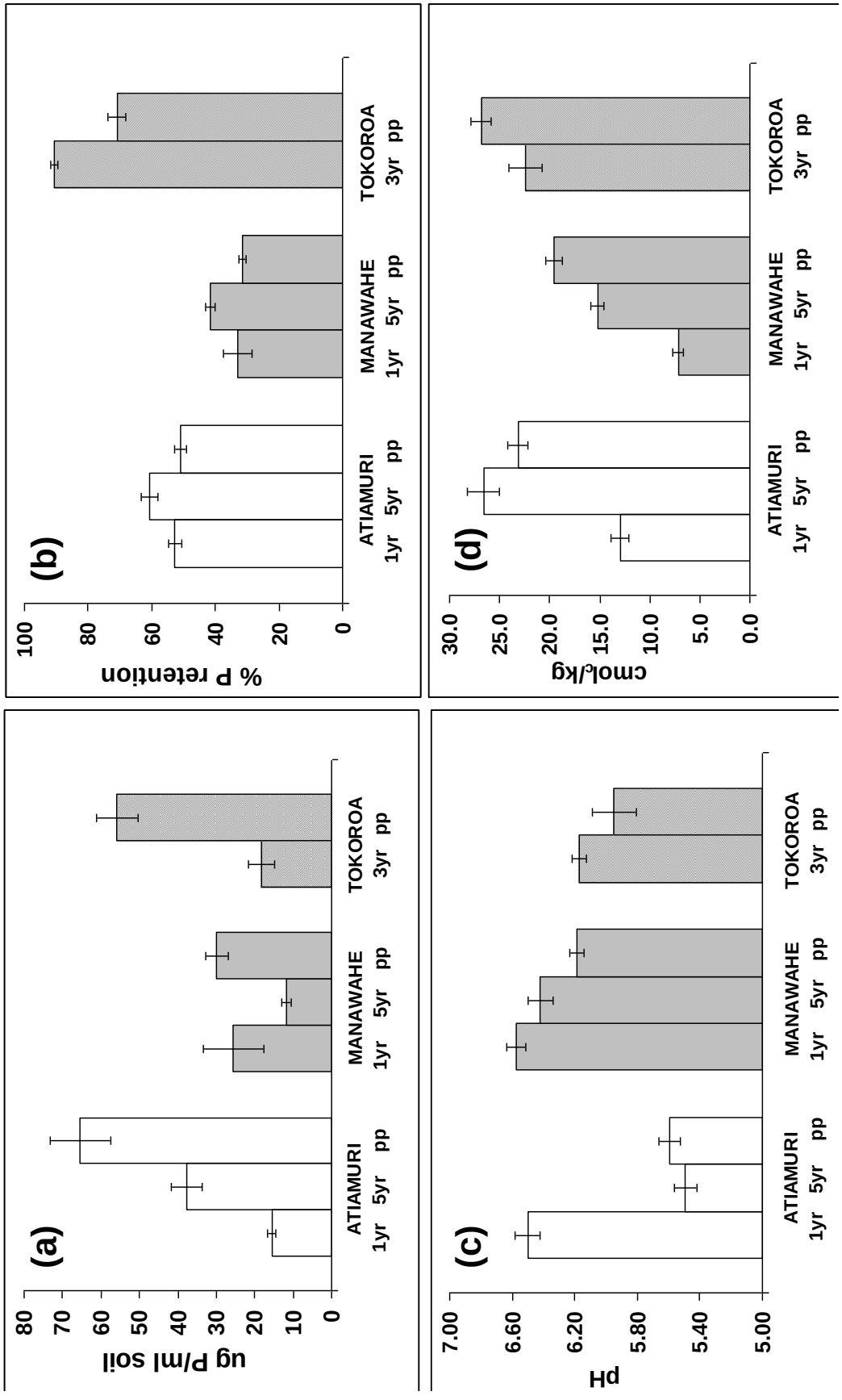

Fig. 3.2 **(a) Olsen P, (b) P retention, (c) pH and (d) CEC of 0–7.5 cm soil samples (mean of 15 bulked replicates) taken from permanent pasture (pp) and pastures recently converted from forest (1-yr, 3-yr, 5-yr)**

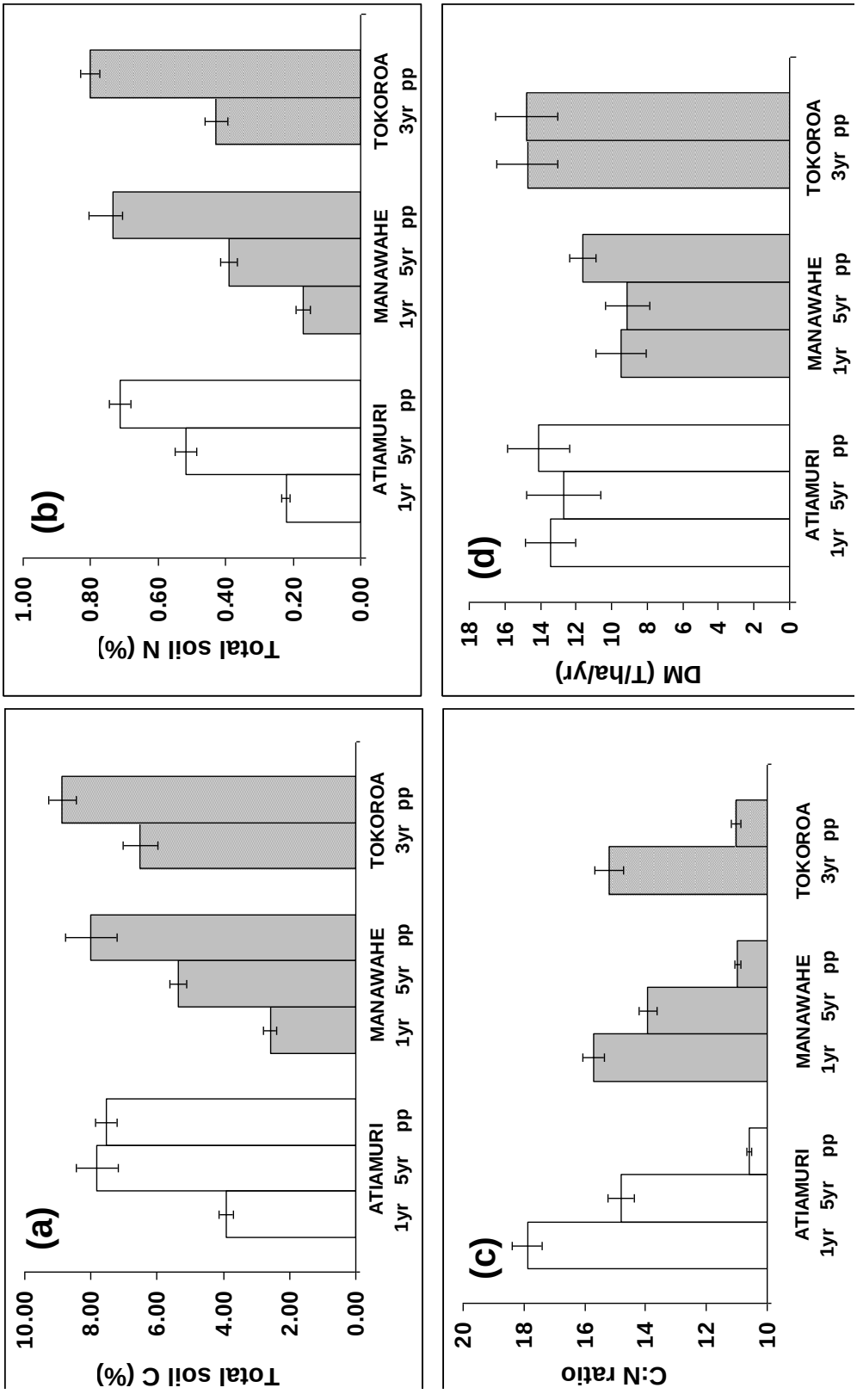

Fig. 3.3 **(a) Total C, (b) total N and (c) C:N ratio of 0–7.5 cm soil samples (mean of 15 bulked replicates) taken from permanent pastrure (pp) and pastures recently converted from forest (1-yr, 3-yr, 5-yr); and (d) pasture production data**

Table 3.2 Soil fertility (0–7.5 cm), pasture production, and moisture, C, N and C:N ratio (0–15 cm) for soil samples at study sites

Site	Land Use	Olsen P		pH		Moisture content	
		ugP ml^{-1}	*s.e.*		*s.e.*	m^3 m^{-3}	*s.e.*
Atiamuri	1-yr conversion	15.6	*1.2*	6.50	*0.08*	0.61	*0.10*
	5-yr conversion	37.7	4.1	5.49	0.07	0.75	0.29
	Permanent Pasture	65.4	*7.9*	5.59	*0.07*	0.74	*0.17*
Manawahe	1-yr conversion	25.6	*7.9*	6.57	*0.06*	-	-
	5-yr conversion	11.7	*1.2*	6.42	*0.08*	0.39	*0.07*
	Permanent Pasture	29.9	*2.9*	6.19	*0.05*	0.41	*0.16*
Tokoroa	3-yr conversion	18.3	*3.5*	6.17	*0.05*	0.82	*0.12*
	Permanent Pasture	55.8	*5.3*	5.95	*0.14*	0.82	*0.16*
Site	**Land Use**	**CEC**		**P retention**		**Pasture Production**	
		meq $100g^{-1}$	*s.e.*	**%**	*s.e.*	T DM ha^{-1} y^{-1}	*s.e.*
Atiamuri	1-yr conversion	12.9	*0.9*	52.7	*2.0*	13.5	*1.4*
	5-yr conversion	26.6	*1.6*	60.6	*2.7*	12.7	*2.1*
	Permanent Pasture	23.2	*1.1*	51.0	*1.9*	14.1	*1.8*
Manawahe	1-yr conversion	7.2	*0.5*	33.0	*4.4*	9.5	*1.4*
	5-yr conversion	15.2	*0.6*	41.7	*1.5*	9.1	*1.3*
	Permanent Pasture	19.5	*0.8*	31.4	*1.2*	11.6	*0.7*
Tokoroa	3-yr conversion	22.5	*1.7*	90.7	*1.1*	14.7	*1.7*
	Permanent Pasture	26.8	*1.0*	70.9	*2.9*	14.8	*1.8*
Site	**Land Use**	**Total N**		**Total C**		**C:N Ratio**	
		%	*s.e.*	**%**	*s.e.*		
Atiamuri	1-yr conversion	0.21	*0.02*	3.62	*0.34*	17.5	
	5-yr conversion	0.40	*0.04*	6.35	*0.80*	15.7	
	Permanent Pasture	0.52	*0.03*	5.66	*0.32*	10.9	
Manawahe	1-yr conversion	0.15	*0.02*	2.42	*0.21*	15.7	
	5-yr conversion	0.33	*0.02*	4.73	*0.26*	14.5	
	Permanent Pasture	0.47	*0.03*	5.51	*0.38*	11.7	
Tokoroa	3-yr conversion	0.37	*0.03*	6.02	*0.55*	16.2	
	Permanent Pasture	0.62	*0.03*	7.24	*0.44*	11.7	

3.3.2. Soil and pasture spectral reflectance

The total soil C, N and moisture content datasets were used as a calibration set for the spectral data. Reflectance spectra were pre-processed using waveband filtering, smoothing, data reduction, derivative calculation and averaging. The pre-processed multivariate data were then regressed against the calibration data using PLSR (R^2 = 0.95 for C and N; R^2 = 0.96 for θ, n = 90).

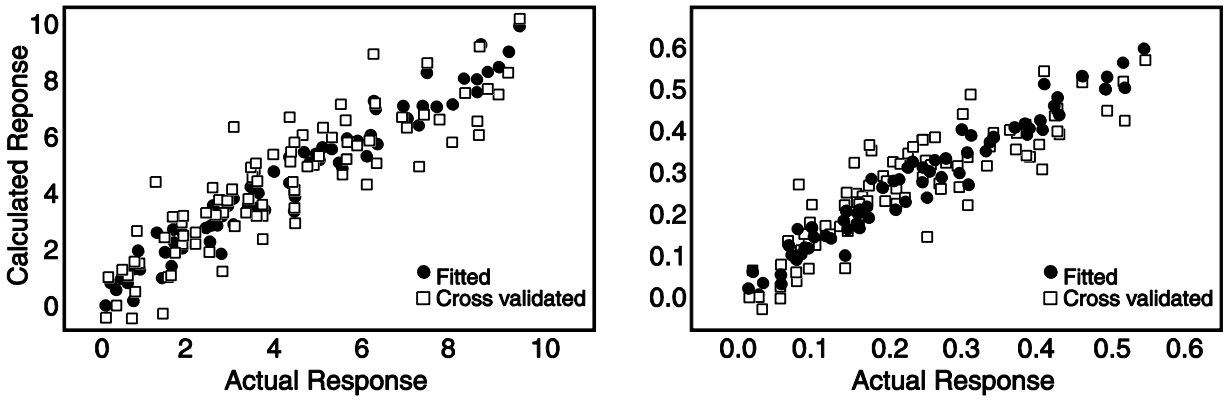

(a) R^2 = 0.95; R^2 (predicted) = 0.75
9 components

(b) R^2 = 0.95; R^2 (predicted) = 0.86
9 components

Fig. 3.4 Partial least square response plot of measured and predicted total soil (a) carbon and (b) nitrogen in soil samples

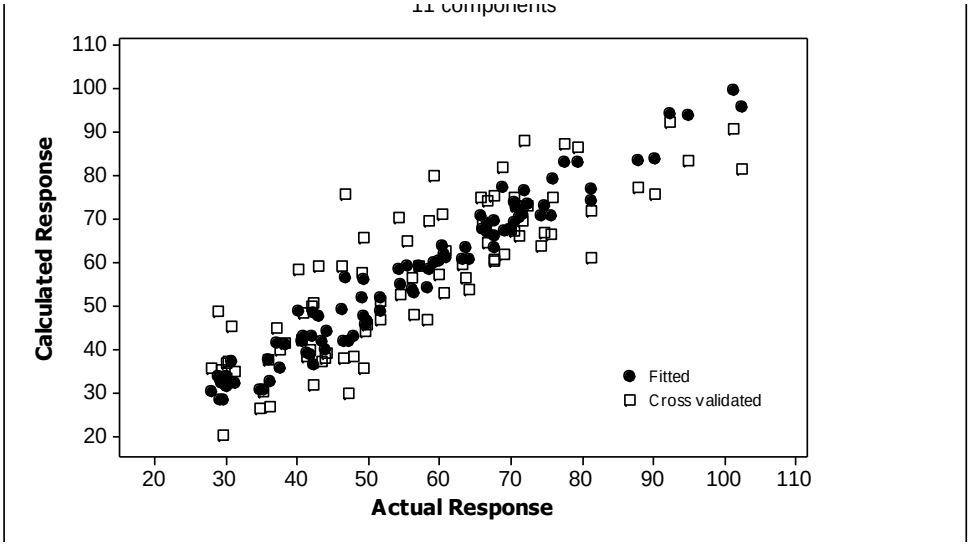

(a) R^2 = 0.96; R^2 (predicted) = 0.70, 11 components

Fig. 3.5 Partial least square response plot of measured and predicted soil moisture content in soil samples

The derived relationships were used to predict total soil C (R^2 = 0.75; RPD=2.01; RER=9.07; RMSEP 1.21%), total soil N (R^2 = 0.86; RPD=2.66; RER=11.15; RMSEP=0.07%) and soil moisture content (R^2 = 0.70) using leave-one-out cross-validation (Figs. 3.4 and 3.5).

Partial least square regression of pre-processed spectral data (n=48) for herbage N against the calibration samples (R^2 = 0.97), gave predictions of measured herbage N using leave-one-out validation (R^2 = 0.67) (Fig. 3.5).

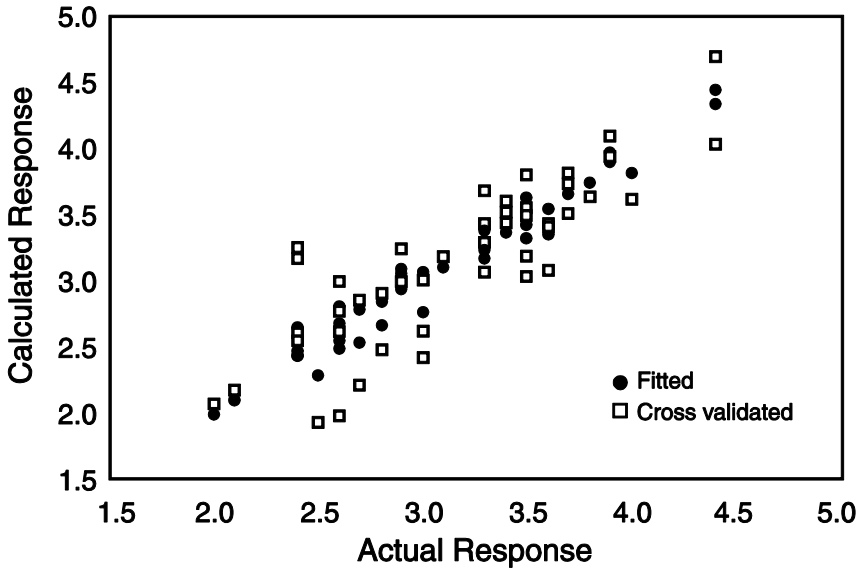

R^2 = 0.97; R^2 (predicted) = 0.67

Fig. 3.6 Partial least square response plot of measured and predicted herbage nitrogen for a range of pastures on volcanic soils

These results suggest that this method for collecting Vis-NIR reflectance spectra in the field has great potential as a new, rapid, cost-effective method for field analysis of soil C, N and θ, and herbage N, enabling sampling to be conducted at a greater density than previously practically possible, so that the spatial variability of the soil property can be investigated.

3.3.3. Electromagnetic Induction (EMI) Survey results

Table 3.3 provides classical statistics of the pre-processed EC_a datasets for each site, showing that values were similar at the Atiamuri and Tokoroa farms, suggesting that weighted mean soil textures to 1.5 m depth were similar within each farm, and confirming site selection within each farm on a basis of similar soils. The slightly lower mean EC_a recorded at the 5-yr Manawahe conversion site is consistent with the slightly coarser, younger Pumice soils located here (Table 3.3).

Table 3.3 Statistical analysis of EC_a datasets collected during EMI survey

Site	Land use	N	Mean	Standard deviation	Median	% CV
Atiamuri	1-yr conversion	808	22.2	3.86	22.5	17.1
	5-yr conversion	1213	23.1	3.33	23.6	14.1
	Permanent pasture	628	23.9	3.61	24.2	14.9
Manawahe	5-yr conversion	598	20.4	2.24	20.3	11.0
Tokoroa	3-yr conversion	892	23.7	4.10	23.9	17.3
	Permanent pasture	692	22.4	3.40	22.6	15.2

The % CVs are slightly higher for the 1-yr conversion site at Atiamuri compared with the other 2 Atiamuri sites. Likewise at Tokoroa the 3-yr conversion site has a higher %CV than the permanent pasture site. These results suggest greater soil variability at these conversion sites, which was further investigated using geostatistics.

The spatial structure of the EMI survey data was explained by bounded exponential and spherical variogram models (Fig. 3.7). The variograms exhibit periodicity to differing extents, which could be due to sampling patterns (all sites) or perhaps lines where trees pre-existed (conversion sites). There was evidence of buried windrows at the Atiamuri 5-yr conversion site. Total soil EC_a variability, expressed by sill value, is

similar at all Atiamuri sites, and smallest for the Manawahe site, where mean EC_a values were lowest (Table 3.3). Also the spatial structure (shown by the magnitude of difference between sill and nugget) was similar at the Atiamuri sites, and smaller at the Manawahe 3-yr conversion site. At Tokoroa there is more spatial structure at the permanent pasture site compared with the conversion site and the distance that this exists over (the range) is also greater. The range of spatial dependence increases from the Atiamuri 1-yr site to 5-yr site, and from the Tokoroa 3-yr site to permanent pasture. This supports the %CV results.

Table 3.4 Variograms Model Parameters for EC_a datasets of 6 sites (models produced using Vesper 1.6 software, ACPA)

Site Name	Description	Model	RMSE	Co	C	A (m)
Atiamuri	1-yr conversion	**Exponential**	**0.692**	**2.897**	**9.980**	**3.949**
		Spherical	0.732	3.241	9.550	8.730
Atiamuri	5-yr conversion	**Exponential**	**1.219**	**2.886**	**9.960**	**13.170**
		Spherical	1.263	2.982	9.190	25.210
Atiamuri	Permanent pasture	**Exponential**	**1.595**	**4.867**	**9.510**	**2.448**
		Spherical	1.603	4.890	9.420	4.017
Manawahe	5-yr conversion	Exponential	0.512	0.000	5.048	1.846
		Spherical	**0.486**	**0.070**	**4.971**	**5.527**
Tokoroa	3-yr conversion	**Exponential**	**0.390**	**6.991**	**4.365**	**5.341**
		Spherical	0.493	8.874	2.480	22.080
Tokoroa	Permanent pasture	**Exponential**	**0.944**	**2.072**	**13.670**	**10.000**
		Spherical	1.334	2.864	12.420	24.250

RMSE: root mean square error; Co: nugget; C: sill-nugget; A(m): range

The variograms indicate that the optimum sampling distance to fully explore soil EC_a variability at all sites is ≤ 6m, i.e. less than half the range of spatial dependence (Kerry and Oliver, 2008). This confirms the need for an improved cost effective method for rapid, accurate analysis of samples in the field, with the ultimate goal of real-time high resolution parameter mapping.

(1) Atiamuri 1-yr conversion

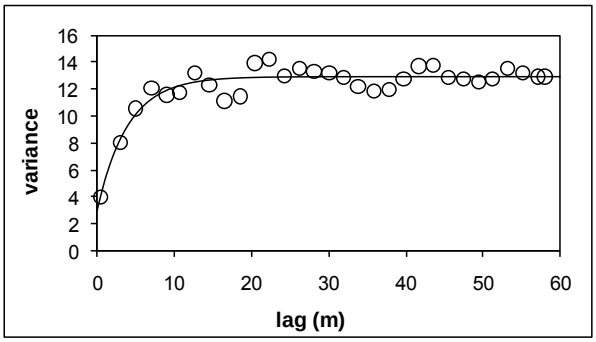

(2) Atiamuri 5-yr conversion

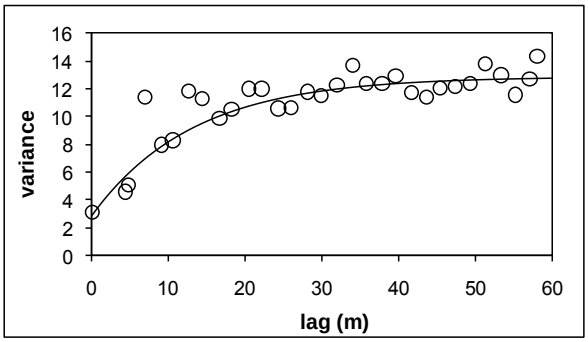

(3) Atiamuri permanent pasture

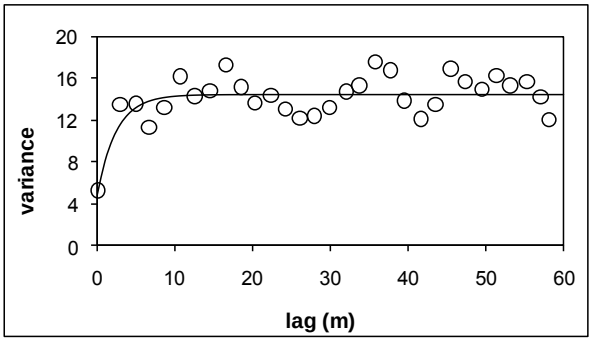

(4) Manawahe 5-yr conversion

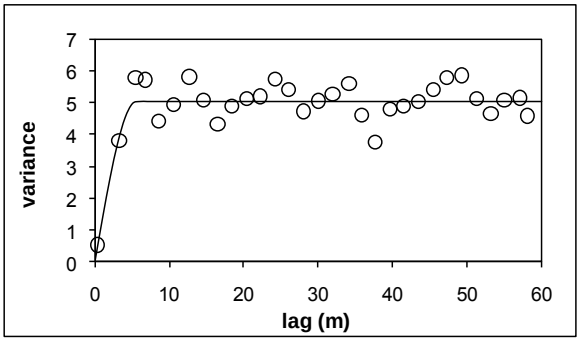

(5) Tokoroa 3-yr conversion

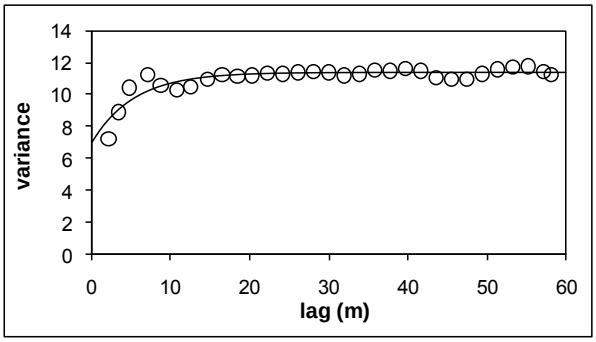

(6) Tokoroa permanent pasture

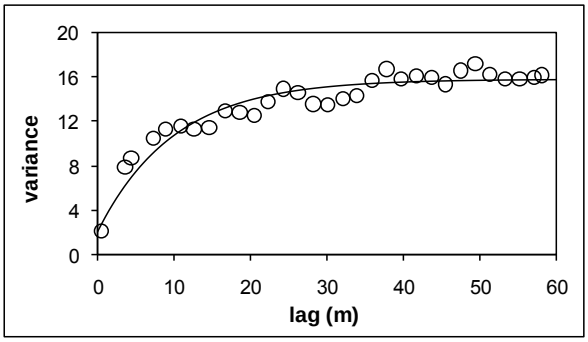

Fig. 3.7 Experimental and Variogram Models of EC_a datasets from 6 sites

In general the soil EC_a patterns shown in Figures 3.8, 3.9 and 3.10 reflect the local topography, with higher EC_a soils (wetter, finer textured) occurring in lower lying zones. In addition the Atiamuri 1-yr conversion EC_a map (Fig. 3.8) shows a zone of

lower EC_a in the south part of the site, where trees have been ripped out and topsoils disturbed.

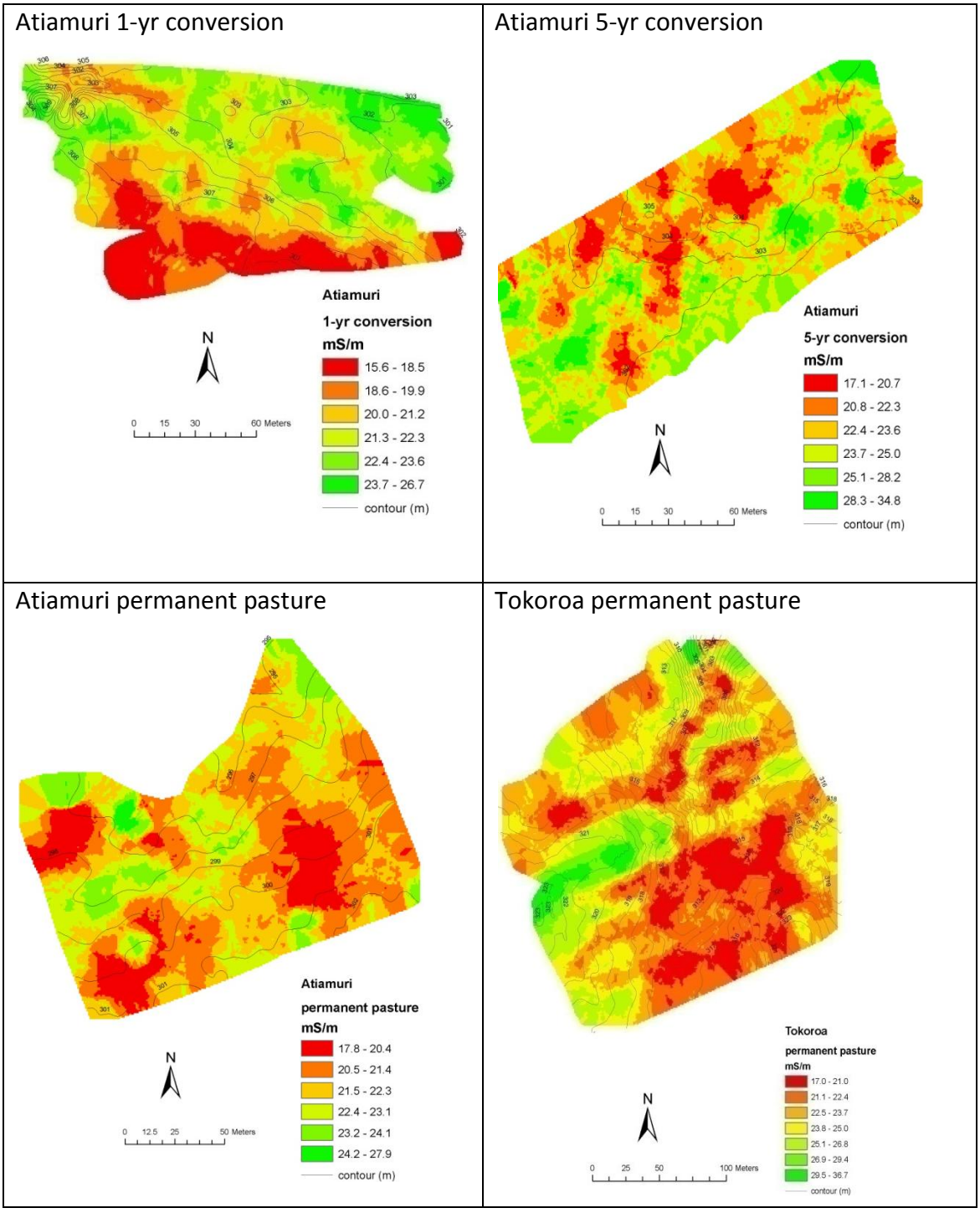

Fig. 3.8 EC_a maps for Atiamuri 1-yr conversion, 5-yr conversion and permanent pastures sites and Tokoroa permanent pasture site

At Tokoroa 3-yr (Fig. 3.9) and Manawahe 5-yr (Fig. 3.10) conversion sites the 3 soil transects were selected to sample different topographic units of slope and aspect, obtaining soil and plant analyses from the widest range of observed soils at each site. This provides the opportunity to compare the soil and plant analyses of these different topographic units. The three transects were selected to compare (i) lower, flatter areas with (ii) north-facing slopes and (iii) south-facing slopes. The lower flatter areas are characterized by higher EC_a soil zones (Figs. 3.9 and 3.10), suggesting soils are finer textured and/or wetter than other land units. Higher EC_a values on flatter land were associated with lower C:N ratios (13.7-15.5) and higher Olsen P compared with lower EC_a values on the north-facing slopes and associated higher C:N ratios (15.8–17.9). This suggests that soil development by incorporation of organic matter is more rapid in the flatter areas. This zone is also most likely preferred as a stock campsite enhancing soil fertility and organic matter accumulation. Herbage N content reflects the short term soil N status and has intermediate values on the south-facing slopes.

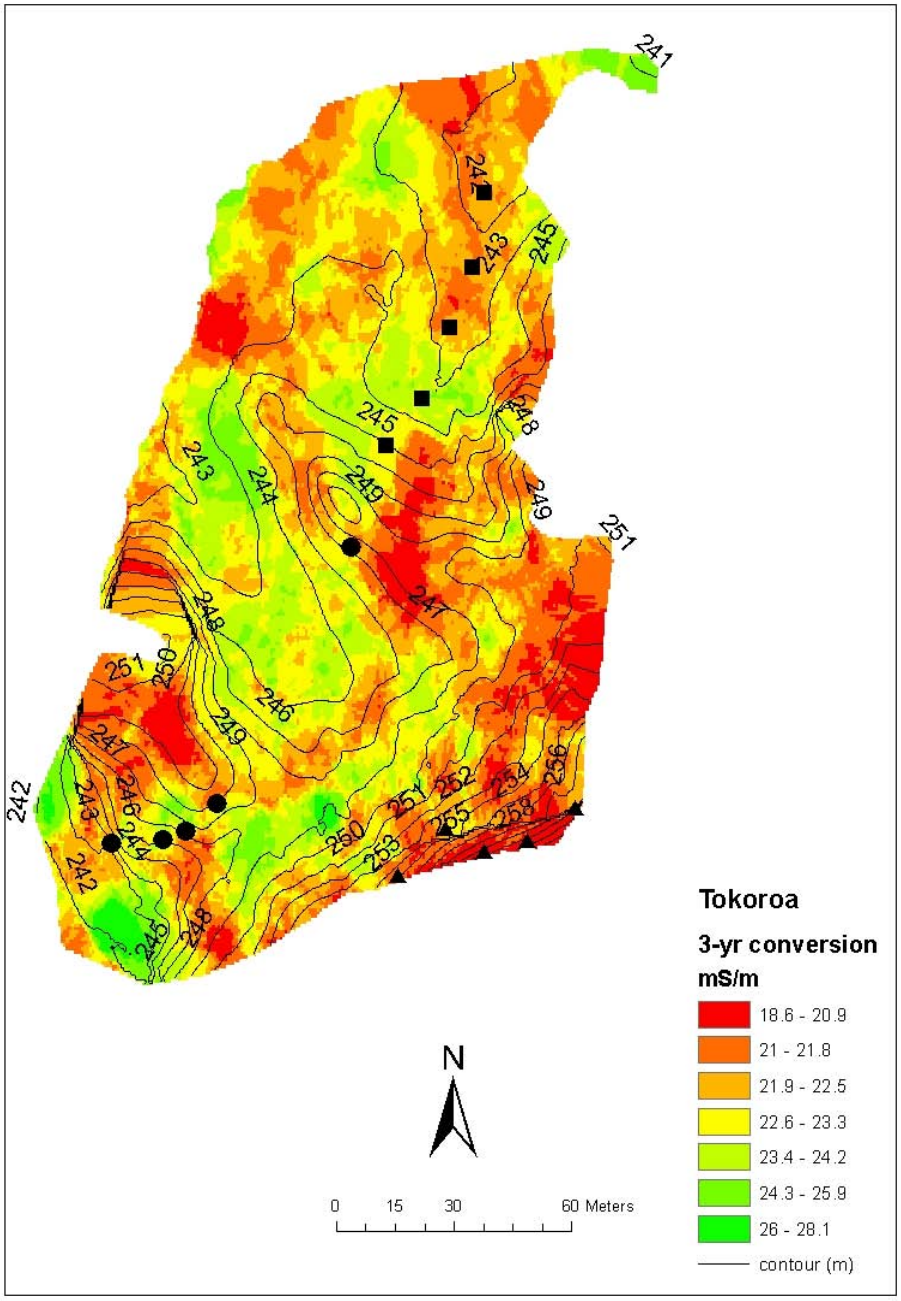

Land Unit	Map symbol	Soil C (%)	Soil N (%)	Soil C:N	Olsen P (ugP ml^{-1})	Herbage N (%)
N-facing slope	▲	5.93 (0.630	0.33 (0.02)	17.2	7.3 (1.7)	2.17 (0.13)
S-facing slope	●	4.34 (0.68)	0.29 (0.06)	14.9	20.2 (3.0)	3.33 (0.48)
Flat	■	7.78 (0.89)	0.50 (0.04)	15.5	45.3 (5.7)	not measured

Fig. 3.9 **EC_a map for Tokoroa 3-yr conversion site (showing soil sampling positions) for soil C, soil N, Olsen P and herbage N on contrasting land units**

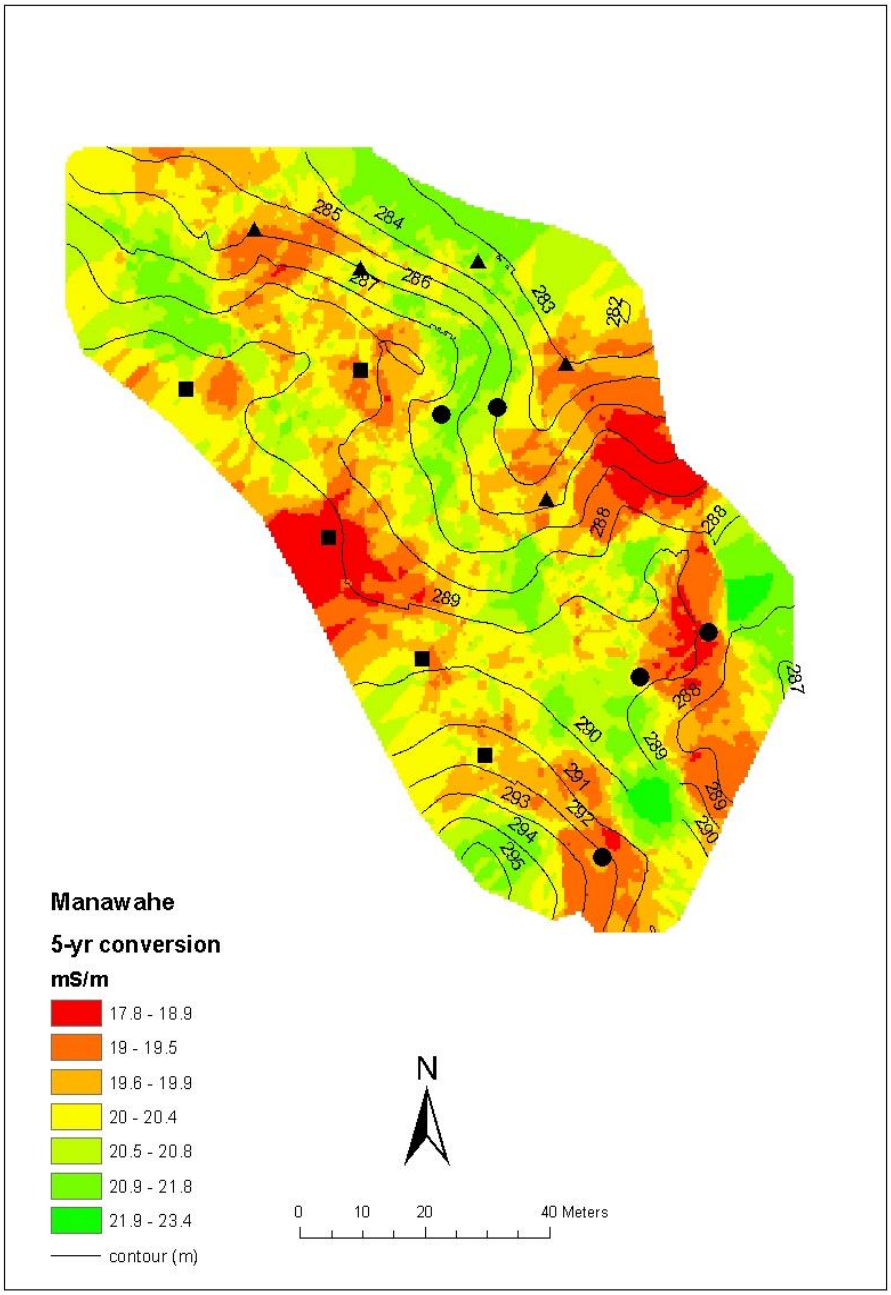

Land Unit	Map symbol	Soil C (%)	Soil N (%)	Soil C:N	Olsen P (ug P ml^{-1})	Herbage N (%)
N facing slope	▲	3.79 (0.29)	0.24 (0.02)	15.8 (0.2)	7.4 (0.7)	2.87 (0.13)
S facing slope	●	5.38 (0.30)	0.37 (0.02)	14.5 (0.4)	14.6 (1.8)	3.33 (0.32)
Flat	■	5.03 (0.43)	0.37 (0.04)	13.7 (0.2)	14.6 (2.2)	3.70 (0.20)

Fig. 3.10 **EC_a maps for Manawahe 5-yr conversion site showing soil sampling positions) for soil C, soil N, Olsen P and herbage N on contrasting land units**

3.4. Discussion

The capital dressings of P applied in the first 2 years after conversion resulted in optimum or near optimum Olsen P test values for pasture establishment, within the first 5 years at the Atiamuri and Tokoroa farms (Fig. 3.1a). These allophanic soils require a lower optimum Olsen P range (20–30) than pumice soils (35–45) (Morton & Roberts, 1999). At the Manawahe site, where pumiceous soils occur, Olsen P values remain sub-optimal even in the permanent pasture site, presumably due to lower inputs of fertilizer.

It is assumed that the marked increases in soil P status are partly responsible for improved pasture yields, improved N fixation, and therefore greater return of plant litter and dung to soil resulting in increases in soil C. These soil C increases were 0.67 % per year in the top 7.5 cm of soil, and 0.50 % per year in the top 15 cm of soil, for the first 5 years since conversion at the two farms where 1-yr and 5-yr conversion sites were available. Soil C (in the top 7.5 cm of soil) in the Taupo sandy silt soil at Atiamuri increased from 3.90 % (first year conversion) to 7.53 % (permanent pasture); a similar increase to that found in the same soil type (0–10 cm soil depth) converted from scrub to pasture in the late 1950s where soil C increased from 4.2 % C (1.5 years conversion) to 6.2 % C after 15 years under pasture (Walker, 1968). Walker measured soil C increases of 3.62 % to 5.66 % to 15 cm soil depth.

Similarly, as time from conversion increases, soil N increases at about 0.05 % per year (0–7.5 cm soil depth), with an overall narrowing of C:N ratio with time. This narrowing of C:N ratio was also noted by Walker (1968), and reflects the process of added N to the soil being immobilized into soil organic matter, until a point where C:N ratio stabilizes at about 10–11. These data also indicate that sequestration of C and N by these soils, in the 0–7.5 cm soil depth, is about 4 T ha^{-1} yr^{-1} and 0.3 T ha^{-1} yr^{-1} respectively, and in the 0–15 cm soil depth are about 6 T ha^{-1} yr^{-1} and 0.48 T ha^{-1} yr^{-1} respectively. Thus, soil C sequestration in the initial years after conversion partially offsets the forest sink capacity which has been lost. Reported growth rates of *Pinus radiata* in this region are between 22 and 39 m^3 ha^{-1} yr^{-1} (Kimberley et al., 2005). Assuming 25% fresh weight is C, these forests would then accumulate between 5.2 and

9.7 T C ha^{-1} yr^{-1}, so the recorded soil C sequestration rate is a significant offset. Scott *et al*. (2006) also estimated greater inputs of C under steady-state pasture (9 T ha^{-1} yr^{-1} to 50 cm soil depth) compared with established (>12 years) forest (1.53 T ha^{-1} yr^{-1}), using the Roth-C model.

The ability of these newly converted soils to sequester nitrogen suggests a large proportion of the N fertilizer applications (between 76 and 88 kg N ha^{-1} yr^{-1}) and biologically fixed N is being immobilized into soil organic matter. This suggests that N leaching losses are low in initial years after pasture establishment, which warrants further investigation.

Soil and herbage analyses provided a calibration set for regressing against reflectance spectra obtained from soil and herbage. Algorithms of multivariate data derived from the soil spectra were successfully regressed against these calibration data using partial least squares regression (R^2 > 0.9), and then used to predict soil C (R^2 = 0.95; R^2 predicted = 0.75), soil N (R^2 = 0.96; R^2 predicted = 0.86 and soil moisture content (R^2 = 0.96; R^2 predicted = 0.70) using leave-one-out cross validation. In addition pasture reflectance spectra have been related to herbage N (R^2 = 0.97) and predicted values using cross-validation (R^2 = 0.67). These preliminary results illustrate the potential use of this method for rapid field assessment of C, N and moisture in soils and N in pastures. Portable field spectroradiometers have the potential to greatly facilitate the process of rapid soil carbon monitoring, which would be necessary if soil carbon accounting becomes an integral part of greenhouse gas accounting in future Kyoto Protocol commitment periods beyond the present one of 2008–2012.

EC_a soil zones reflect soil and topographic differences so that they could be used for site-specific management decisions (Yule et al., 2005). For example, north-facing slopes showed lower productivity and therefore fertilizer rates could possibly be reduced to these zones saving cost without reducing productivity.

3.5. Conclusions

At all forest to clover-based pasture conversion sites in this study, applications of phosphatic and nitrogen fertilizer are associated with increasing topsoil phosphate status and differential increases in topsoil soil C and N contents causing decreases in the C:N ratio of the topsoil organic matter, with time since conversion.

Changes in soil organic matter (reflected by C and N content plus C:N ratio) caused by conversion are spatially variable, reflecting soil disturbance during conversion but also reflecting differences in soil physical conditions and pasture vigour. Spectral reflectance has been used successfully to predict soil C, N, moisture content and herbage N content.

This preliminary study has indicated that soil EMI surveys and soil and pasture reflectance surveys have the potential to provide maps of soil and pasture changes across the landscape that can improve the accuracy of, for example, soil C accounting, and depict zones for site-specific application.

CHAPTER FOUR

Development of proximal sensing methods for mapping soil water status in an irrigated maize field

This chapter develops methodology for linking soil EC_a datasets to soil available water-holding capacity (AWC). The high resolution digital elevation map (DEM) obtained during the EMI survey is co-kriged with TDR-derived volumetric soil moisture surveys (n = 50) to produce a soil moisture map (2D and 3D spatial depiction). The potential of the back-pack field Vis-NIR spectral reflectance method for rapid field analysis of soil moisture patterns is further explored, after the initial trial described in Chapter 3.

The research detailed in this chapter was presented orally at the 1st Global Workshop on High Resolution Digital Soil Sensing and Mapping Conference, convened by the International Union of Soil Sciences, and held in Sydney, Australia in February 2008. It has also been accepted for publication as an invited book chapter in an International Union of Soil Sciences publication, based on research papers presented at the Sydney workshop.

Publications emanating from this chapter:

Hedley CB, Yule IJ, Tuohy MP, Kusumo BH (2008) Development of Proximal Sensing Methods for Mapping Soil Water Status in an Irrigated Maize Field. In Proceedings of the 1st Global Workshop on High Resolution Digital Soil Sensing and Mapping, 5–8 February, Sydney, Australia. CD-ROM.

Hedley CB, Yule IJ, Tuohy MP, Kusumo BH (2008) Development of Proximal Sensing Methods for Mapping Soil Water Status in an Irrigated Maize Field. Chapter accepted for Book 'Proximal Soil Sensing for High Resolution Soil Mapping', to be published late 2009, based on papers presented at the 1st Global Workshop on High Resolution Digital Soil Sensing and Mapping, 5–8 February, Sydney, Australia. In Press.

Abstract

Approximately 80% of allocated freshwater in New Zealand is used for irrigation, and the area irrigated has increased by 55% every decade since 1965. The research described in this chapter is therefore developing new techniques to map and monitor soil attributes relevant to irrigation water-use efficiency. The apparent electrical conductivity (EC_a) of soils under a 33 ha irrigated maize crop was mapped using a mobile electromagnetic induction (EM) and RTK-DGPS system, and this map was used to select three contrasting zones. Within each zone, further EC_a values were recorded at a range of volumetric soil water contents (θ) to develop a relationship between EC_a, soil texture, soil moisture and available water-holding capacity (AWC), (R^2 = 0.8). This allowed spatial prediction of AWC, showing that these sandy and silty soils had similar AWCs (*c.*160 mm m^{-1}). High resolution digital elevation data obtained in the EM survey were also co-kriged with TDR-derived θ to produce soil moisture prediction surfaces, indicating drying patterns and their relationship to topography and soil texture. There was a 12.5–13.1% difference in soil moisture to 45 cm soil depth between the wettest and driest sites at any one time (n = 47). Spatial and temporal variability of soil moisture, indicated by these co-kriged prediction surfaces, highlights the need for a rapid high resolution method to assess in situ soil moisture. The potential of soil spectral reflectance (350–2500 nm range; 1.4–2 nm resolution) for rapid field estimation of soil moisture was therefore investigated. Soil spectra were pre-processed and regressed against known soil moisture values using partial least squares regression (R^2 *calibration* = 0.79; R^2 *prediction* using leave-one-out cross validation = 0.71). These proximal sensing methods facilitate spatial prediction of soil moisture; information which could then be uploaded to a variable rate irrigator.

4.1. Introduction

New Zealand reflects a global trend in which increasing gains in agricultural productivity are supported by increasing use and reliance on irrigation. This has led to over-allocation of freshwater for irrigation in parts of the country, mirroring the global situation. In addition, efficiency of water use is very low in some systems, for example,

up to 50% of water can be wasted in flood irrigation systems (Jury & Vaux, 2007). Centre-pivot irrigators, however, have the ability to apply exact depths of water accurately to a crop, and recent advances have been made towards individual nozzle control for variable rate irrigation (Bradbury 2009; Hedley 2008b). However, adequate decision-support systems for variable rate irrigators are not available, and there is a need for real-time monitoring, decision and control systems to be developed (De Jonge et al., 2007).

This decision-support system would ideally provide real-time information to the irrigator about daily spatial soil water status, where soil water status is defined as the amount of water available to the crop. As crop yield is directly related to water stress, this not only addresses the need for sustainable freshwater use but also introduces cost efficiencies to the producer.

The total amount of water a soil can supply to a crop is usually measured by the volume it can hold between field capacity and wilting point, which can be assessed in the field (Hedley et al., 2005). Water status is the amount of this total available water that is available to a crop on any one day; and is commonly expressed as mm water per mm rooting depth in soil. However, the spatial variability of this status, as indeed is the case for many soil properties, will vary across the landscape, a fact largely ignored before the 1980s (Cook & Bramley, 1998).

EM mapping is a proximal sensing method that maps soil variability on a basis of soil texture and moisture in non-saline conditions (Hedley et al., 2004). The EM sensor records one weighted mean value for apparent soil electrical conductivity (EC_a) to 1.5 m depth, and this can be related directly to soil moisture (e.g. Huth & Poulton, 2007), if soil moisture is the major variable affecting EC_a. EC_a has also been used to predict AWC (Waine et al., 2000; Hedley et al., 2005; Hezarjaribi & Sourell, 2007); AWC being the amount of water held by the soil between field capacity and wilting point. Field capacity is defined as the point where all macro-pores have drained, and is measured in the field two days after a heavy rain (i.e. two days after an event which brings the soil to saturation). Wilting point is the lower limit of available water, the soil moisture content reached when a plant will permanently wilt.

In comparison, direct soil moisture mapping has traditionally been accomplished by exhaustive point measurements – both time-consuming and costly. Embedded sensors such as time domain reflectometry (TDR) are improvements but require considerable time and effort for installation and measurement, and the data cannot be easily logged (Kaleita et al., 2005). A method of determination that does not require exhaustive manual measurements is therefore desirable for robust precision irrigation soil information support systems. Proximal sensing with a Vis-NIR spectroradiometer allows rapid field collection of soil reflectance spectra, which can then be related to a calibration set of soils for gravimetric soil moisture estimation (*w*) (Mouazen et al., 2005; Kaleita et al., 2005). Mouazen et al. (2005) use a tractor-drawn subsoiler chisel to carry an optical unit through the soil. This unit carries reflected light to a spectrophotometer (wavelength range 306–1710 nm) attached to the tractor. A prediction correlation of 0.75 (root mean square error of prediction, RMSEP of 0.0250 kg kg^{-1}) was obtained for in-line field measurements compared with a prediction correlation of 0.98 (root mean square error of cross validation, RMSECV of 0.0175 kg kg^{-1}) under laboratory conditions. Kaleita et al. (2005) used an HR2000 spectrometer (spectral resolution: 0.065 nm; wavelength range 331–1069 nm) to estimate *w*. Their results returned a lower R^2 validation of 0.63 for all soils, and an improved 0.71 when only the light coloured soils were included.

This chapter reports on our progress in the development of proximal sensing methods to assess daily spatial soil moisture status for precision irrigation. It uses high resolution EC_a data to predict AWC, and high resolution DEM to co-krige TDR values. TDR values are used to investigate spatial and temporal variability of soil moisture at the research site. The potential of backpack Vis-NIR spectroradiometry for rapid, real-time mapping and monitoring of soil moisture is also discussed.

4.2. Material and Methods

4.2.1. Study site

A 33 ha irrigated maize crop was selected at a farm near Bulls, approximately 30 km north-west of Palmerston North, in the Rangitikei River Catchment, New Zealand. A

600 m centre-pivot irrigator is used at this site during periods of seasonal drought. The soils occur on a terrace surface and are mapped as Ohakea silt loams (Mottled, Immature Pallic soil; New Zealand Soil Classification; Endoaquepts; USDA NRCS classification; Stagnic Cambisol, FAO-WRB soil classification), characterized by silt loam topsoils and mottled subsoils to about 0.6 to >1.0 m above heterogeneous layers of sands and gravels. In some places sand has blown onto this terrace soil from an adjacent sand dune forming the Ohakea loamy sand (Mottled, Immature Pallic soil; Endoaquepts; USDA NRCS classification; Stagnic Cambisol, FAO-WRB soil classification). This soil is characterized by loamy sand topsoil over mottled silt loam subsoil over sands and gravels.

4.2.2. Electromagnetic induction mapping and soil AWC

A Geonics EM38 electrical conductivity sensor with Trimble RTK-DGPS and Trimble Ag170 field computer on-board an ATV was used to map soil variability. The Geonics EM38 measured apparent soil electrical conductivity (EC_a) to 1.5 m depth, providing one mean weighted value that is primarily influenced by soil texture and moisture in non-saline soils (e.g. Hedley et al., 2004). Survey data points were collected at 1 s intervals, at an average ATV speed of 15 kph, with a measurement recorded approximately every 4 m along transects 10 m apart. The EC_a map was produced using ordinary kriging in Geostatistical Analyst, (ArcMAP).

A method was then developed, based on that of Waine et al. (2000), to relate EC_a values to AWC. Three zones with low, intermediate and high EC_a values were selected on the EC_a map, and AWC estimated for each zone. AWC was estimated in the field by sampling three replicate soils in each zone for volumetric soil moisture content (θ) on days when the soils were at field capacity (soil moisture deficit, SMD, 0 mm), an intermediate moisture content (SMD 40 mm), and very dry (close to wilting point; SMD 130 mm). At a SMD of 130 mm the very dry soil was losing water at no more than one mm per day, and was assumed to be close to wilting point. Soils were cored to 600 mm (0–150 mm; 150–300 mm; 300–450 mm and 450–600 mm) and soil moisture was determined gravimetrically on the known volumes of soil. Hand-held EC_a values were also recorded.

Soil samples were also collected for particle size analysis (0–150 mm; 150–300 mm; 300–450 mm and 450–600 mm). Percent sand, silt and clay was determined by wet sieving the > 2 mm soil fraction and by a standard pipette method for the < 2 mm soil fraction; and one mean value for percent sand, silt and clay to 600 mm was calculated for three replicates in each zone. This was then converted to a single number, using the fineness class developed by Waine et al. (2000) for UK soils. This fineness class provides a numeric ranking of soils (1-6 in 0.5 intervals for the 11 classes on a soil texture triangle) on a basis of increasing fineness of texture, and provides a single numeric value for soil texture.

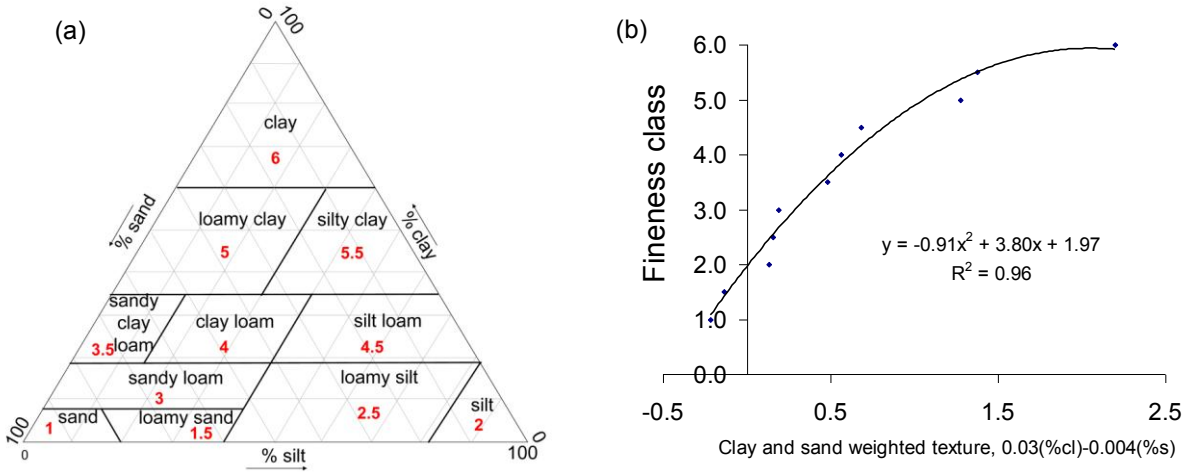

Fig. 4.1a **New Zealand soil texture triangle (Milne et al., 1995) defines 11 soil texture classes on a basis of percent sand, silt and clay (fineness class indicated in red)**

Fig. 4.1b **Fineness class developed for UK soils (Waine et al., 2000) applied to New Zealand soil texture classes**

To check the applicability of this fineness class for New Zealand soils, a centroid value of percent sand, silt and clay was obtained for each of the 11 classes in the New Zealand soil texture triangle (Fig. 4.1a), which is used for standard soil descriptions (Milne et al., 1995). Both UK and New Zealand soil particle classifications classify soil particle sizes as 0.06–2 mm (sand), 0.002–0.06 mm (silt) and < 0.002 (clay).

The texture weighting equation developed by Waine et al. (2000) to produce a line of best fit for UK soils was then applied to the New Zealand soil data giving an R^2 of 0.96

(Fig. 4.1b), confirming its suitability for New Zealand soils. The texture weighting equation developed for UK soils can therefore be used for New Zealand soils to define a numeric value (fineness class) for New Zealand soil textural classes:

$$\text{Fineness class} = -0.8981\ (T_w)^2 + 3.8704(T_w) + 1.9686$$

and

$$\text{Texture weighting } (T_w) = 0.03\ (\%\ \text{clay}) - 0.004\ (\%\ \text{sand}) \qquad \text{(Waine et al., 2000)}$$

The fineness class determined for soils in this study was then plotted as a single value on the abscissa against θ on the y coordinate to produce a texture-moisture graph. The texture-moisture graph displays curves of θ against soil texture for a range of soil moistures between field capacity and very dry (near wilting point) providing a field estimate of AWC. It can be used to predict AWC for other soils of known texture within this range. EC_a was measured each time field θ was measured and these EC_a values were plotted against the derived AWC value.

4.2.3. Soil moisture measurement

4.2.3.1. Time domain reflectometry (TDR)

Volumetric soil moisture, θ, was measured by TDR (n = 47) monthly between December and March to assess spatial and temporal variability of soil moisture.

4.2.3.2. Collection of Vis-NIR soil reflectance spectra

A Vis-NIR spectroradiometer was trialed for rapid field estimation of soil moisture. Ten replicate soil reflectance spectra were collected at 90 positions using an ASD FieldSpec Pro FR spectroradiometer (Analytical Spectral Devices). A prototype soil probe was used, by replacing an internal light source with the higher intensity halogen lamp, and based on the ASD plant probe. Using the prototype probe attached via a fibre optic cable to the ASD FieldSpec Pro FR spectroradiometer in a backpack, reflectance spectra were collected (350–2500 nm) from a freshly cut soil surface at 20 mm soil depth. These hyperspectral data are recorded at bandwidths of 1.4–2 nm intervals. After

spectra had been obtained, soil samples were collected (20–50 mm) at each position to determine soil moisture.

4.2.3.3. Spectral data preprocessing

The hyperspectral data were pre-processed before partial least squares regression was used for prediction and statistical correlations made. Data pre-processing included waveband filtering, smoothing, downsampling, derivative calculation, and finally averaging of the ten replicate reflectance spectra using SpectraProc v1.1 software (Hueni & Tuohy, 2006). The pre-processed data were then imported into Minitab 14 (© 2006 Minitab Inc.) and a calibration model for prediction of soil moisture was developed using partial least squares regression.

4.3. Results and Discussion

4.3.1. Electromagnetic induction mapping and soil AWC

The EC_a map delineates soil differences on a basis of texture and moisture, confirmed by soil pit examination, particle size analysis and soil moisture measurements (Table 4.1). Three zones, representing areas of low, medium and high EC_a values (Zones A, B and C respectively, Fig. 4.2, Table 4.1), were then defined as three classes (using Jenks natural breaks) of a prediction surface produced using a spherical semivariogram and ordinary kriging (Geostatistical Analyst, ARCMap). These zones were ground-truthed as Ohakea loamy sands in the orange-red zones (Zone A); Ohakea silt loams in the yellow-green zones (Zone B) and a natural low-lying ponding area where subsoils are more intensely mottled and soils are generally wetter (Zone C), (Fig. 4.2).

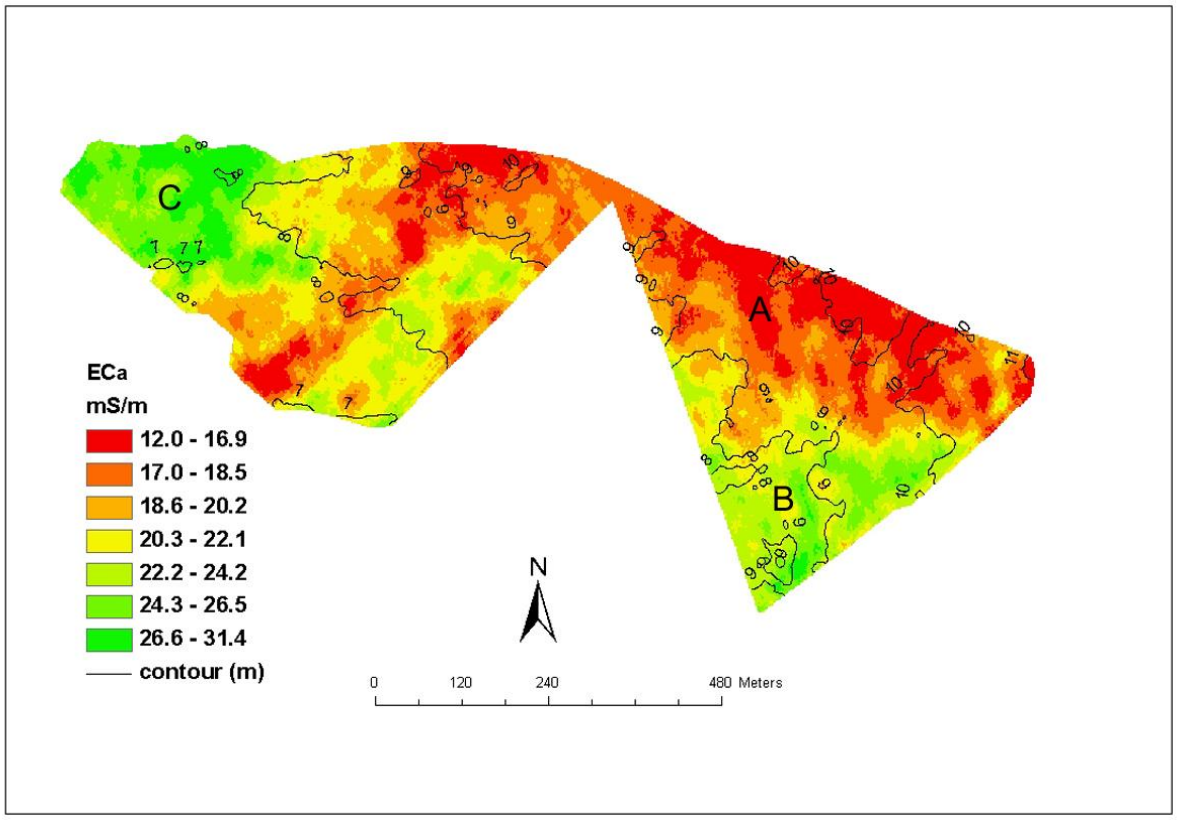

Fig. 4.2 **EC_a map of the study area showing Zone A, B and C**

Table 4.1 **EC_a (20 August 2006 survey) zone characteristics.**

Zone	EC_a range (mS m^{-1})	Clay (%)*	Soil moisture (m^3 m^{-3}) 12/12/06	5/1/07	12/2/07	27/3/07
			Pre-irrigation		During irrigation	
Zone A	12.0–18.5	11	0.276	0.253	0.241	0.258
Zone B	18.5–26.0	23	0.297	0.276	0.258	0.285
Zone C	22.0–31.4	14	0.359	0.320	0.306	0.295

** weighted mean value for 0–600 mm soil depth*

Texture-moisture graphs (Fig. 4.3a) and a derived relationship between EC_a and AWC (Fig. 4.3b) were used to produce the AWC map (Fig. 4.4). In Figure 4.3a the top curve represents θ at field capacity and the lower curve represents θ when the soils were very dry (close to wilting point), for the textural range of sampled soils.

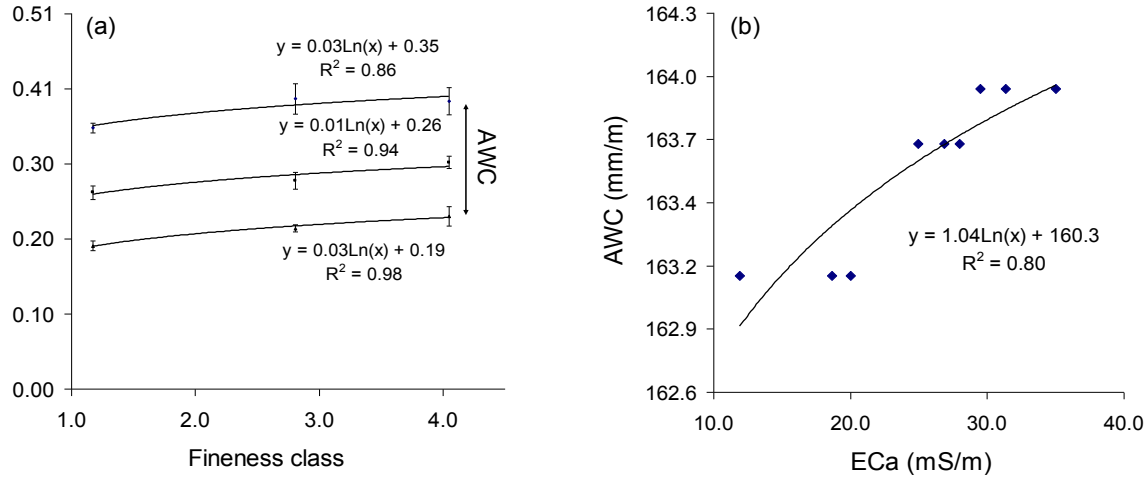

Fig. 4.3a Texture-moisture graph showing θ at field capacity (top curve), an intermediate moisture (middle curve) and when soils were near wilting point (lower curve) for a range of soil textures

Fig. 4.3b Relation of AWC to EC_a for the study area

Therefore the difference between these two curves is a field estimate of AWC. AWC is then plotted against EC_a (Fig. 4.3b), using the hand-held EC_a values which were recorded for each replicate at each time of sampling for soil moisture. This provides a relationship between AWC and EC_a (R^2 = 0.8), allowing spatial prediction of AWC using the EC_a data.

These sandy and silty soils have very similar AWCs (161–164 mm m^{-1}), i.e. these soils hold similar amounts of crop-available water at field capacity, as shown in Figure 4.4.

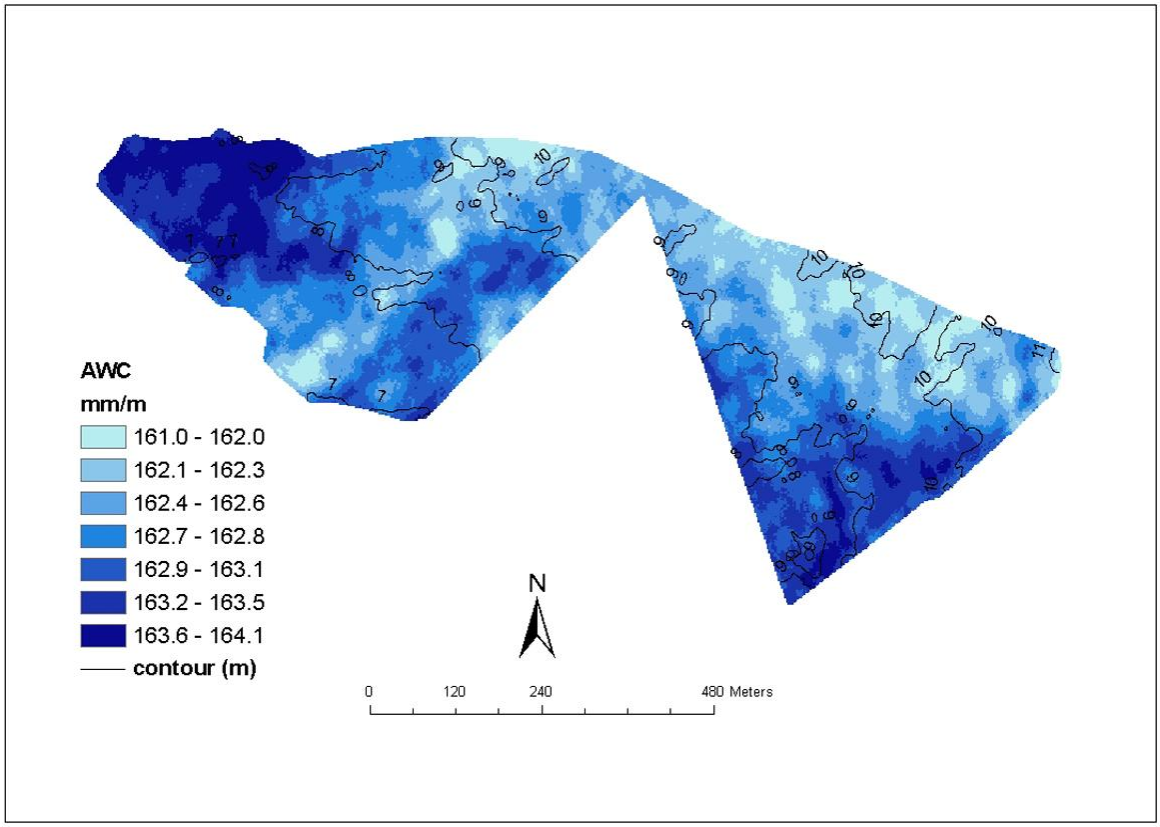

Fig. 4.4 AWC map of the study area

4.3.2. Soil moisture measurements

The TDR survey shows, however, that at any one time soil moisture varied by 0.12–0.13 $m^3 m^{-3}$ across this 33 ha maize field. It is suggested that this is accounted for by (i) soil profile differences in texture, structure and depth to gravels, and (ii) topographic position.

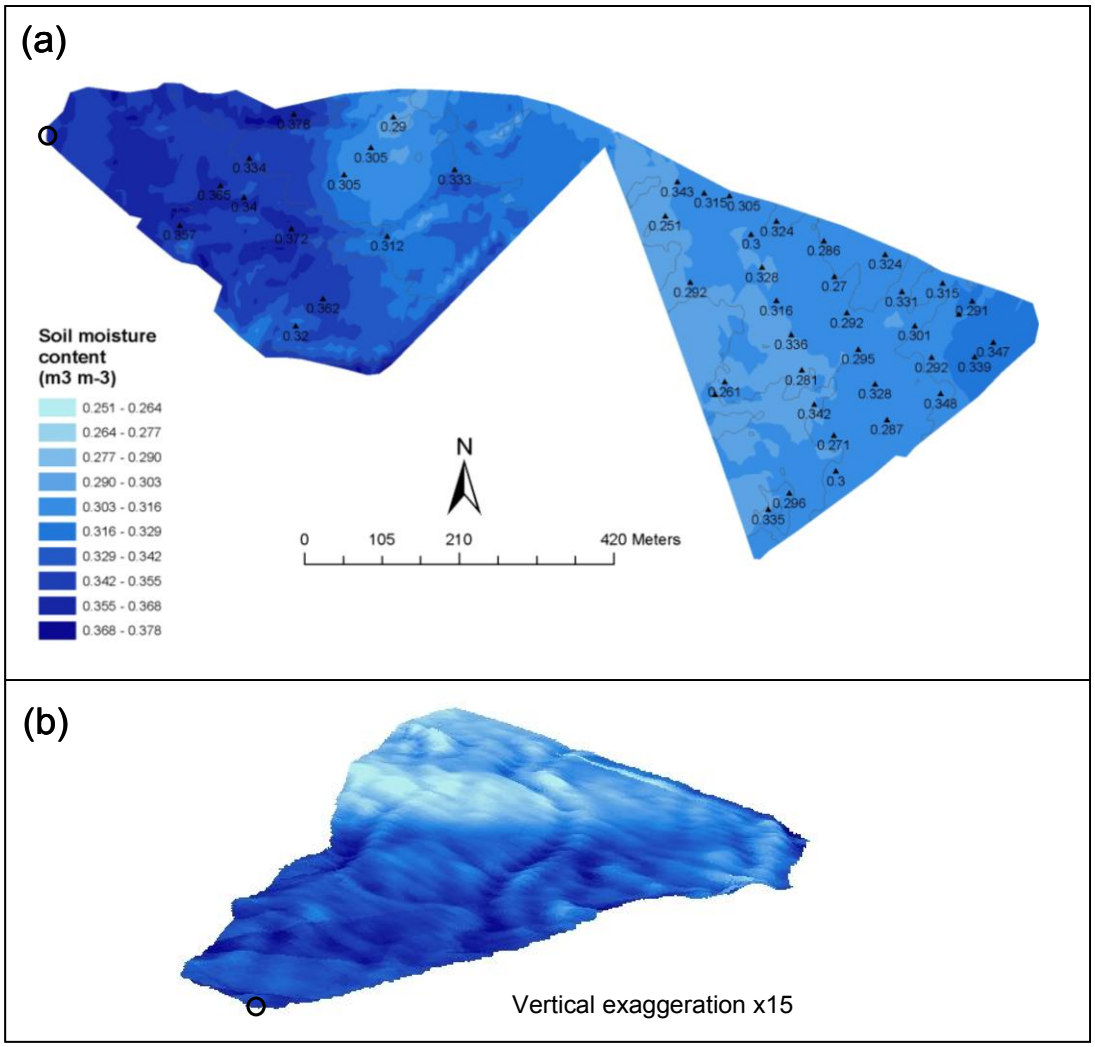

Fig. 4.5a **Soil moisture prediction surface (13 Dec 06) obtained by co-kriging TDR (n=47) with high resolution digital elevation data (n=9350). Point TDR values are shown**

Fig. 4.5b **3D soil moisture prediction surface (NW end) showing wetter soils in hollows and a drier area where sandy soils with low EC_a values exist (Zone A). The black circle, o, shows the corresponding point on prediction surfaces in Figs. 4.5a and 4.5b**

Sandy soils tend to have a greater proportion of larger pores which will drain faster than smaller pores. Topographic position is also a controlling factor for drainage – some soils in low-lying areas typically remaining wetter for longer.

TDR values, co-kriged with high resolution digital elevation data from the EC_a survey, had a slightly smaller root mean square error of prediction (2.78) compared with ordinary kriged TDR values (2.84).

4.3.3. Vis-NIR soil reflectance spectra

Soil reflectance spectra were collected in the spring when the soils were close to field capacity and soil surfaces exposed for collection of the spectra were very wet and in some cases smeared. Ten replicate spectra were obtained at each position. The collected spectra were then pre-processed and imported into Minitab 14 (MINITAB Inc., 2003) for principal component analysis (PCA) and partial least squares regression analysis (PLSR) against the measured data. A PCA score plot was used to observe the pattern of sample scattering. During PLSR processing 12 samples which had standardized residuals ≥ 2.0 were removed as outliers. An R^2 (calibration) of 0.79 and R^2 (prediction using leave-one out cross validation) of 0.71 was obtained, with a RMSECV of 0.019 kg kg^{-1} and RPD (standard deviation over RMSECV) of 1.85, the latter providing a measure of how large the error (RMSECV) is with respect to the range of soil moisture encountered during calibration. In comparison, Kaleita (2005) obtained an R^2 (calibration) of 0.71 or lower when predicting field moisture from field collected spectra, and commented that one prediction model did not fit different soil types. Mouazen et al., (2005) used a calibration developed in the laboratory (cross validation correlation 0.98, R^2 = 0.96), by adding known amounts of water to one soil, therefore minimising any other soil differences. However, if this method is to be successfully used in the field it should be robust enough to predict soil moisture in soils where several soil properties vary as well as soil moisture (for example, organic matter content, surface roughness, texture). Mouazen et al., (2005) used the laboratory-developed calibration to predict in-line subsoiler chisel field reflectance measurements and report a prediction correlation of 0.75 (RMSEP = 0.025 kg kg^{-1}; RPD = 3.376) in the field compared with 0.98 (RMSEP = 0.016; RPD = 5.115) in the laboratory. Our results suggest field-collected spectra can be successfully used for calibration with a prediction correlation of 0.84 and prediction error (RMSECV) of 0.019 kg kg^{-1} for this field site.

4.4. Conclusions

EC_a was used to spatially predict AWC (R^2 of 0.80), which shows that these soils store very similar amounts of plant available water. TDR (n=47), however, indicates that the spatial and temporal variability of soil moisture is significant, showing that drying patterns vary, which is most likely due to topography and soil profile differences. Ideally, therefore, the site should be characterized on a number of occasions during one drying cycle. Vis-NIR reflectance spectra are easily collected in the field and this method shows promise for rapid, accurate sensing of in situ soil moisture. Best practice precision irrigation scheduling decisions can then be made for utilization of water stored in the soil profile, accounting for high resolution spatial and temporal differences in soil water status.

CHAPTER FIVE

Proximal Sensing Soil Water and Assessing Irrigator Performance as Decision Tools for Precision Irrigation

Chapter Five acknowledges that any assessment of irrigation water-use efficiency must account for accuracy of delivery by the irrigation system. In New Zealand over the last decade the replacement of traditional irrigation systems (e.g. border dyke gravity flood) with accurate sprinkler systems (e.g. Valley, Zimmatic, Reinke centre-pivot and lateral sprinker systems) has created new opportunities for accurate, uniform delivery of irrigation water. This chapter uses the irrigated maize grain research site of Chapter 4 [Manawatu maize 1] and describes a method for evaluating irrigator performance. It also introduces the concept of using a soil water balance to estimate how much plant available soil water is in the soil profile on any one day. The soil water balance uses climate and crop-specific factors (crop type, crop stage) to estimate rate of daily evapotranspiration, and is adjusted for site-specific soil AWC. The limitations of using one modelled value for soil available water in irrigation scheduling are discussed; developing concepts introduced in Chapter 4 about the influence of micro-topography on soil wetting and drying patterns.

This research was presented at an international conference on water resources, held in Adelaide:

Hedley CB, Yule IJ, Tuohy MP (2008) Proximal sensing of soil water and assessing irrigator performance as decision tools for precision irrigation. Oral presentation and reviewed paper in Proceedings Joint 31st Hydrology and Water Resources Symposium and 4th International Conference on Water Resources and Environmental Research, 14–17 April, 2008, Adelaide, Australia

Abstract

Increasing demand by agriculture on global freshwater supplies is seen as the main factor behind increasing global freshwater scarcity. This is being reflected in New

Zealand where the area of irrigated land has increased by 55% every decade since 1965. It is therefore important to assess and improve irrigation system efficiencies, both irrigator performance and crop water use.

Irrigator efficiency is largely assessed by its ability to deliver water uniformly. The lower quartile distribution uniformity coefficient (DU_{lq}) was used to measure uniformity of water applied by a 600 m centre-pivot irrigator to a 33 ha maize crop. Two rows of 40 catch-cans collected water during one pass. Collected volumes were used to calculate DU_{lq} of the system, which was 79% excluding and 68% including the end-gun.

In addition to water delivery by the irrigation system, water supply by the soil to the crop was estimated using a simple water balance approach. The accuracy of this one value for site-specific management was then assessed by mapping soil variability using a mobile system with a Geonics EM38 electromagnetic induction (EM) sensor with RTK-GPS, and relating this to available water-holding capacity (AWC). A soil water-texture graph was developed and used to estimate AWC values that were then regressed against EM values. Volumetric soil water content (θ) and hand-held EM values were measured in the field, for soils of known texture, between field capacity and when the soil was very dry. In addition, time domain reflectometry was used at 47 sites, to assess θ range at any one time (12.5–13.1% to 45 cm soil depth). Results show that soils had similar AWCs but significantly different drying patterns, due to topographic position in the landscape.

Improvements in irrigator efficiency are possible by regular checks and maintenance. Variability of water supply to the crop by soils can be addressed by variable rate irrigation used together with a suitable decision support tool for spatial soil water status.

5.1 Introduction

The world's consumption of water is doubling every 20 years, at twice the rate of global population increase (Bazza & Najib, 2003). Intensification of land use worldwide

has been highly successful in feeding the world's population, despite dire warnings in the 1960s of future food shortages. This intensification of land use has relied on increased use of irrigation and 70% of global freshwater extractions are for irrigation (UN/WWAP, 2003).

In New Zealand, irrigation accounts for about 80% of allocated freshwaters, and, while grazing land is by far the biggest user (78%), arable land and horticulture are also significant users – and more dependant on irrigation: 35% of horticultural land is irrigated, 27% of arable land is irrigated and about 10% of grazing land is irrigated of which 8% is for dairying (Statistics New Zealand Agricultural Production Census, 2002).

Green et al. (2006) discuss the significant challenges facing irrigation to ensure its sustainable future. For precise application of water to soils, spatially variable models are needed that will include monitoring devices, interrogated remotely and in real-time, to provide decision support information for irrigation scheduling (Green et al., 2006). De Jonge et al. (2007) also acknowledge the need for better decision support systems for variable rate irrigation.

Existing decision tools for irrigation scheduling include mechanistic modelling and/or measurement of soil moisture at a few locations in the area under irrigation. However, technological advances and economic availability of sensors, GPS, GIS and wireless transmission of data provide the potential for real-time mapping and monitoring of soil properties, such as soil moisture, across the whole landscape.

We no longer need rely on conventional field experiments where inherent variability is managed by design; researchers are now beginning to use geostatistical approaches for the design and analysis of landscape-scale experiments (Bishop & Lark, 2006; Bramley & Panten, 2007). Conventional research regarded a treatment response as a fixed effect, but GIS tools such as kriging and co-kriging allow it to be handled as a random variable within the landscape (Bishop & Lark, 2006). Inspiring words – and the driving force behind the research presented here.

Apparent soil electrical conductivity (EC_a) is a proven useful soil survey tool (Brevik et al., 2006) controlled by a combination of soluble salts, clay content and mineralogy,

soil water content and soil temperature (McNeill, 1980; Sudduth et al., 2001). It can be used as a surrogate measure of soil moisture content. Brevik et al. (2006) compared soil EC_a readings with soil water content ($r^2 \geq 0.70$) at fixed sites over a 5 month period for 2 years; and Huth and Poulton (2007) developed a calibration method to predict soil water content ($r^2 = 0.93$) using EC_a and also a seasonal temperature correction factor so that the calibration developed in one year could be applied to another year. Both studies confirm that although EC_a is influenced by a suite of soil properties it can usefully be used to predict soil moisture content where this is the major variable. In non-saline soils, EC_a reflects the relatively stable soil textural pattern of a landscape (Hedley et al., 2004) and its magnitude at any one time is strongly influenced by dynamic changes in soil moisture content (Hedley et al., 2005).

Whole system sustainable irrigation considers the efficiencies of the irrigator as well as soil water supply and plant water use. Bloomer (2006) has played a significant role in developing best practice protocols for irrigator evaluation in New Zealand. The New Zealand Code of Practice for Irrigator Evaluation includes a system survey and assesses system operation, environmental measures (wind, evaporation topography), field observations (e.g., soil appearance, wheel ruts, ponding, runoff), system checks, flow and pressure measurement, sprinkler performance, and a uniformity test of water applied.

This research aims to develop decision tools to improve the efficiency of water used by an irrigated maize crop. It investigates the use of a proximal sensor, the Geonics EM38 electromagnetic sensor, GPS and GIS for assessing spatial variability of soils and their supply of water to the crop. It co-kriges field soil moisture values with high resolution elevation data to produce a soil moisture map, and it also assesses irrigator performance.

5.2 Methodology

5.2.1. Selection of Field Site

A 33 ha irrigated maize crop was selected at a farm near Bulls, approximately 30 km north-west of Palmerston North, in the Rangitikei River Catchment, New Zealand. A 600 m centre-pivot irrigator is used at this site during periods of seasonal drought. The soils have formed in fine textured alluvium deposited by the Rangitikei River onto a gravel terrace surface, and border a sand dune–sand plain system where a chronosequence of soils has developed in four dune systems aligned by the prevailing wind and of increasing age away from the coast (Molloy, 1988).

Soils on the terrace surface are mapped as Ohakea silt loams (Mottled, Immature Pallic soil; Hewitt, 1998). They are characterized by silt loam topsoils and mottled subsoils to about 0.6 m to >1.0 m above heterogenous layers of sands and gravels. In some places sand has blown onto this terrace soil from an adjacent sand dune forming the Ohakea loamy sand (Mottled, Immature Pallic soil). The Ohakea loamy sand is characterized by loamy sand topsoil over mottled silt loam subsoil over sands and gravels. It is likely that the distinctive loamy sand topsoil of the Ohakea loamy sand is formed in aeolian deposits that blew onto the silt loam terrace soils at a later date than the main period of alluvial deposition.

5.2.2. Crop water requirement

A simple daily soil water balance was modelled using regional climatic data, daily site-specific rainfall measurements and a field-estimated value for soil available water-holding capacity (AWC), providing information about the amount of soil water available to the crop on a daily basis. Change in water storage in the soil profile was calculated:

$$\Delta S = R - Et - Ro \qquad (1)$$

Where ΔS is the change in water storage in the soil profile, R is rainfall (plus irrigation), Et is evapotranspiration and Ro is runoff or drainage from the profile, and each term

has units of mm day^{-1} (Scotter et al., 1979), with soil storage at a maximum at field capacity. Site-specific evapotranspiration for the maize crop was calculated by multiplying the regional reference Et (calculated for a hypothetical well watered grass cover) by a crop factor (Kc), using standard coefficients (Allen et al., 1998).

5.2.3. Soil properties

5.2.3.1. EM mapping for soil variability

A Geonics EM38 electrical conductivity sensor with RTK-GPS and Trimble Ag170 field computer on board an ATV was used to map soil variability on a basis of soil texture and moisture. The Geonics EM38 measured apparent soil electrical conductivity (EC_a) to 1.5 m depth providing one mean weighted value which is primarily determined by soil texture and moisture in non-saline soils (e.g., Sudduth et al., 2001; Hedley et al., 2004). Survey data points were collected at 1-s intervals, at an average ATV speed of 15 kph, with a measurement recorded approximately every 4 m along transects 10 m apart. The EM map was produced using ordinary kriging in Spatial Analyst in ArcGIS. The map was subsequently used to select three zones representing the greatest range of soils at this site (on a basis of their soil texture and moisture to 1.5 m depth) for a field estimation of the range of soil AWC.

5.2.3.2. Field estimation of soil available water-holding capacity (AWC)

Three zones with high, intermediate and low EC_a values were selected from the EM map representing the greatest range of soils on a basis of their texture and moisture. Volumetric soil moisture content was then determined on three replicates in each zone on days when the soils were at field capacity, an intermediate moisture content and very dry. Soils were cored to 60 cm (0–15 cm; 15–30 cm; 30–45 cm and 45–60 cm) and soil moisture was determined gravimetrically on the known volumes of soil. A depth of 60 cm was selected to encompass the portion of soil exploited by the majority of maize roots (Aslam 2005). Aslam (2005) used a profile wall technique to count root numbers of maize plants, 100 days after sowing, in a similarly textured alluvial soil under similar climatic conditions. Other workers have reported maize root depths to 1 m or greater (e.g., Pellerin & Pages, 1996); however, in the present study where soils

were at or close to field capacity for the first 100 days of growth and subsoils are mottled dense silt loams there is no need for roots to penetrate deeply searching for water, and it is likely that root pattern and penetration depth is similar to that found by Aslam in a similarly textured soil under similar climatic conditions. Therefore the sampling depth of 60 cm was used in this study to assess AWC.

Percent sand, silt and clay was determined on these soil samples by wet sieving the > 2 mm soil fraction and by the pipette method for the < 2 mm soil fraction (USDA, 1996). A mean weighted value for soil texture to 60 cm was then calculated for each replicate using a fineness class developed by Waine et al. (2000), where:

$$\text{Fineness class} = -0.8981\,(\text{Tw})^2 + 3.8704(\text{Tw}) + 1.9686 \quad (2)$$

$$\text{Texture weighting (Tw)} = 0.03\,(\%\text{clay}) - 0.004(\%\text{sand}) \quad (3)$$

(Waine et al., 2000)

These data were then used to develop soil texture-moisture graphs from which AWC was determined for the different textured soils. Hand-held EC_a values were also measured for each replicate at each time. AWC values were regressed against EC_a, as described in Hedley et al. (2005) to develop a relationship between EC_a and AWC, so that EC_a could be used as a spatial predictor of AWC.

5.2.4. Soil water content

The spatial and temporal variability of the soil moisture pattern was investigated using time domain reflectometry (TDR). TDR is a preferred accurate method for in situ field measurements of volumetric soil water content (e.g., Green et al., 2006).

47 sets of TDR waveguides were installed in the soil at GPS-located sites (15 cm, 30 cm and 45 cm depth) to assess the range and spatial pattern of soil moisture at any one time across the 33 ha research area. Monthly measurements were made before, during and after the period of irrigation.

In addition, these GPS-located TDR values were co-kriged with high-resolution digital elevation data obtained during the EM survey to predict a soil moisture map of the field site.

5.2.5. Irrigator performance

Performance of the 600 m centre-pivot irrigator was assessed following the Irrigation New Zealand Code of Practice (Bloomer, 2006), which has been developed from protocols used by the USDA (ASCE, 1978; ASAE, 1993). The key measure of uniformity used is the lower quartile distribution uniformity coefficient, DU_{lq}, defined as the ratio of the smallest accumulated depths of distribution to the average depths of the whole distribution. It uses a commonly used fraction – the lowest quarter – which has been used by the USDA since the 1940s (Ascough & Kiker, 2002). DU_{lq} expresses the evenness of water application to a crop over a specified area and implies that all irrigation systems incur some non-uniformity, and that it is most useful to compare the mean of the lowest quarter of values to the mean value. The drier areas are where water stress will occur first during a drying phase, with consequent reduced yields.

DU_{lq} was determined by arranging two rows of 40 catch-cans either side of a radial line starting about 20% of the way along the lateral from the pivot and extending to just inside the wetted radius of the end-gun, which collected water during one pass of the irrigator (Fig. 5.1).

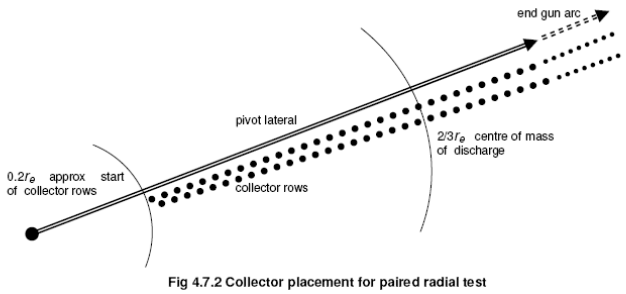

Fig. 5.1 Collector placement for paired centre-pivot radial uniformity test (Bloomer, 2006)

The lower quartile distribution uniformity ratio (DU_{lq}) was then calculated (Bloomer, 2006), using irrigation evaluation software, Irrig8 v1.1.1 (© Page Bloomer Associates Ltd and PinkHouse Software Ltd) and equation (4):

$$DU_{lq} = \frac{\overline{V}_{lq}}{\overline{V}} \quad (4)$$

where DU_{lq} is the lowest quarter distribution uniformity coefficient

$\overline{V}_{lq}$ is the average volume of water collected in the lowest quarter of the field

$\overline{V}$ is the average volume of water collected by all collectors in the data analysis

Another important evaluation of irrigator performance is the precision of application, which was measured as the difference between the mean depths of water delivered compared with the target depth set on the irrigator control unit. In addition, operating pressures of individual nozzles were assessed at the beginning, middle and end of the centre-pivot to ensure they were working at the optimum design pressure. A visual check of irrigator movement and leaks was also conducted.

5.3 Results and discussion

5.3.1. Supply of water to the maize

The amount of water stored in the soil on any one day was calculated by modelling a daily soil water balance (Fig. 5.2c). The rate of evapotranspiration (Et) ranged from 0.3 to 7 mm/day during the maize growing season (Fig. 5.2a); monthly mean air temperature ranged from 8.8°C to 14.6°C. Rainfall was well distributed through the growing season apart from a period of moisture deficit between mid-January and late March when irrigation water was applied (Fig. 5.2b). The period from sowing in October to the end of December 2006 was particularly wet and cold. Regional Manawatu climatic data (NIWA, 2007) shows that the months October–December

2006 were the second wettest on record (325 mm compared with a mean average of 146 mm) and recorded the second lowest sunshine hours (318 hours, 72 hours below normal). The mean December temperature of 13.8°C was the lowest recorded (2.3°C below normal), (NIWA, 2007).

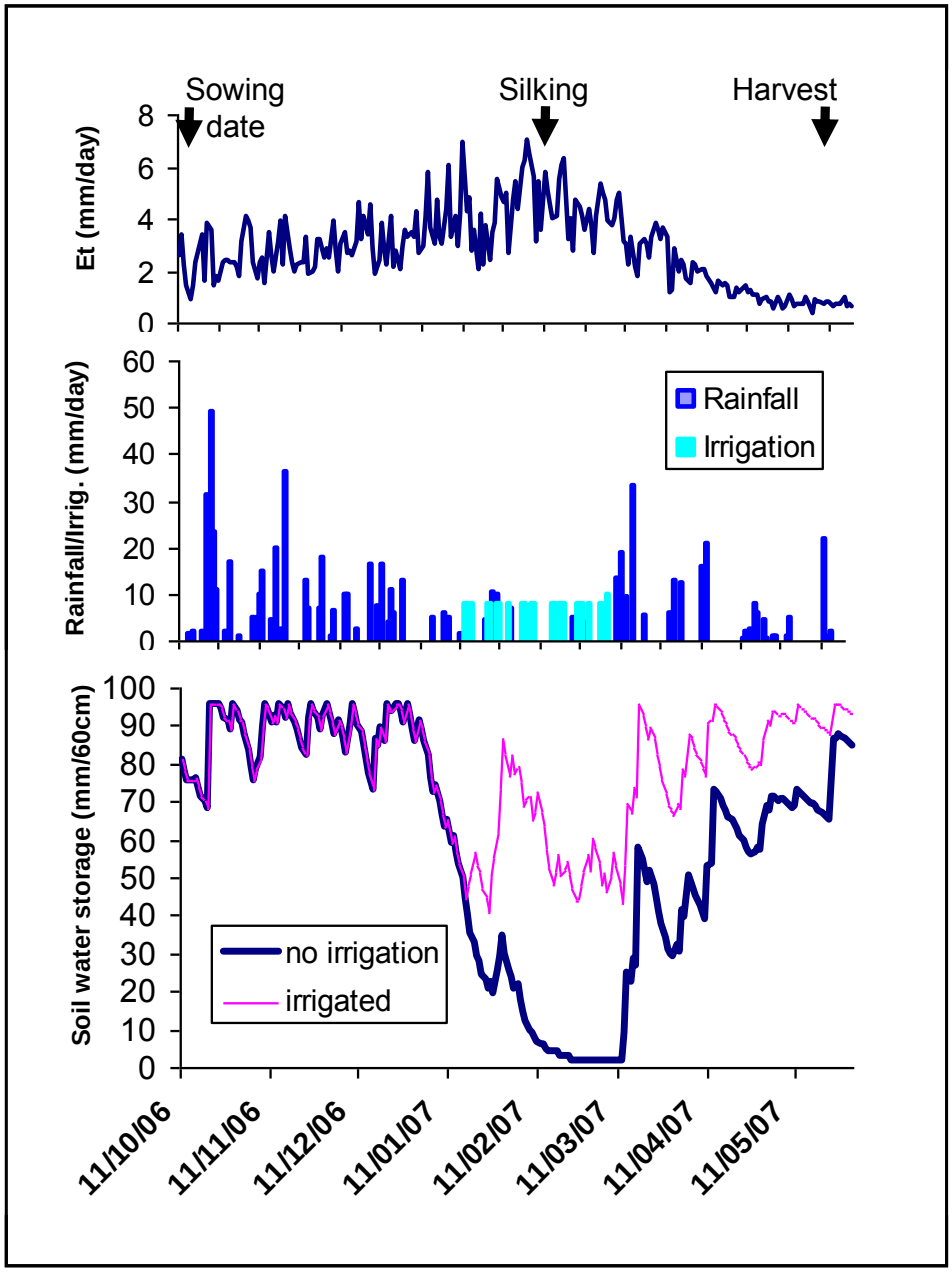

Fig. 5.2 **E_t, rainfall, irrigation and soil water storage during the maize growing season**

A mean AWC value of 16% v/v was used in the soil water balance spreadsheet which was based on field measurements (results presented below).

A 0.55 fraction of the AWC is readily available to the maize crop (Allen et al., 1998). Therefore for the top 60 cm of soil where the majority of roots exist the AWC is 96 mm 60 cm^{-1}, and 53 mm of this is readily available to the crop. The daily water balance predicts that the trigger point for irrigation is 15 January (Fig. 2c). In practice the farmer started to irrigate on 18 January as the soil dried noticeably (Fig. 5.2c). This period of irrigation included the maize silking stage in mid-February when water deficits are most detrimental to yield. Drought stress during early tassel development causes stunted growth and poor tassel development (Aslam, 2005). The water balance approach is therefore a useful decision tool for irrigation commencement.

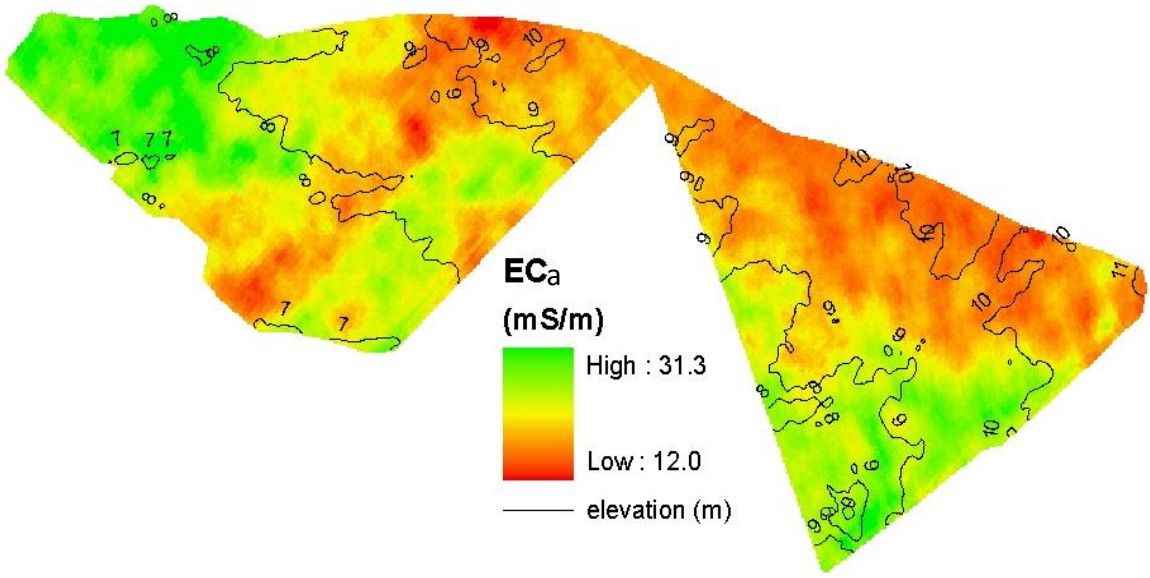

Fig. 5.3 Soil apparent electrical conductivity (EC_a) map of the Manawatu maize grain on alluvial soils research site [Manawatu maize 1]. EC_a reflects soil textural differences.

This approach, however, does not consider the spatial variability of soil water supply. Soils across a landscape may have different AWCs as well as different drying and wetting patterns. Different AWCs are largely controlled by the soil texture, structure and depth. The EC_a map (Fig. 5.3) shows areas of coarser textured sandy soils (orange colours, lower EC_a values) and finer textured silty soils (green colours, higher EC_a values), which was confirmed by field observations.

Measurements show that AWCs of these soils, estimated as the difference between field capacity (0.35–0.39 $m^3 m^{-3}$) and volumetric water content when the soils were very dry (0.20–0.22 $m^3 m^{-3}$) were very similar (Fig. 5.4).

AWC, predicted from the texture-moisture graph is regressed against soil EC_a, so that soil EC_a can be used to map AWC (Fig. 5.4). AWC of these soils ranged between 97 and 99 mm per 60 cm soil depth and they therefore have the potential to supply similar amounts of water to all parts of the field.

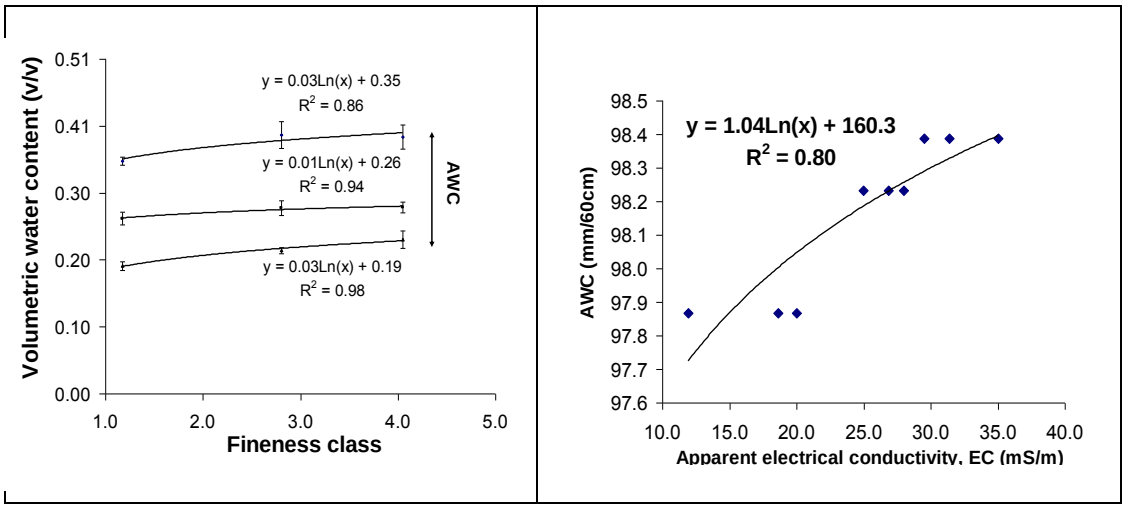

Fig. 5.4 Texture-moisture graph (left), showing volumetric soil moisture at field capacity (top curve), an intermediate moisture (middle curve) and near wilting point (lower curve) for a range of soil textures, used to estimate AWC; and relationship between AWC and EC_a (right)

Our TDR survey, which directly compared moisture content at 47 sites at any one time, provides a comprehensive survey of soil moisture differences and shows some significant differences in soil moisture between sites (Table 5.1). These differences relate to different drying patterns due to position in the landscape, with small hollows being wetter and higher knoll areas being drier. Some low lying areas of soils remained saturated and above field capacity for several days during wet periods, as water drained into them from surrounding slopes. The largest range between maximum and minimum soil moisture values measured at any one time was 24.7% (0–15 cm soil depth), 16.1% (0–30 cm soil depth), and 13.1% (0–45 cm soil depth). Each set of 47

data points was normally distributed (Anderson-Darling Normality test, all p-values > 0.05, n = 47), and each position was GPS-located.

Therefore, if irrigation water usage is to be optimised, the drying and wetting patterns of local topography must be considered and characterised spatially and temporally at this site.

Kaleita et al. (2007) state that "understanding variability patterns in soil moisture is critical for determining an optimal sampling scheme both in space and in time, as well as for determining optimal management zones for agricultural applications that involve moisture status". This is important information required for designing precision farming operations, such as precision irrigation. At this site the drying and wetting patterns have a greater influence on soil moisture pattern than AWC.

Table 5.1 Spatial and temporal variability of soil moisture at 47 sites in a 33 ha maize crop on alluvial soils, assessed by TDR

Soil depth (cm)	0–15	0–30	0–45	0–15	0–30	0–45	0–15	0–30	0–45	0–15	0–30	0–45
Date	13/12/06			5/01/07			12/02/07			26/03/07		
	Soil volumetric moisture content (%)											
max	45.0	39.1	37.8	36.4	35.2	34.9	33.4	32.8	30.9	37.2	34.9	35.6
min	20.3	25.7	25.1	19.7	21.3	21.9	16.4	16.7	18.4	21.3	20.5	22.5
mean	30.5	32.0	31.5	26.5	27.7	28.7	23.8	24.8	25.2	27.2	28.4	28.4
st dev	*5.2*	*3.6*	*2.9*	*3.4*	*3.2*	*2.7*	*4.3*	*3.7*	*2.7*	*3.4*	*3.2*	*2.5*
% CV	*17.1*	*11.2*	*9.2*	*12.9*	*11.7*	*9.5*	*18.0*	*15.9*	*10.9*	*12.4*	*11.1*	*8.6*
range	*24.7*	*13.4*	*12.7*	*16.6*	*13.9*	*13.0*	*17.0*	*16.1*	*12.5*	*15.9*	*14.1*	*13.1*

The TDR soil moisture dataset was co-kriged with high-resolution digital elevation data obtained during the EM survey. Co-kriging uses more than one variable to krige a GIS prediction surface, and is particularly useful where the primary variable is undersampled with respect to a secondary variable that is assumed to correlate with the primary variable (Goovaerts, 1997). In this case, as the soil moisture dataset (n=47) is correlated with the surface topographic features of the landscape, the high resolution digital elevation dataset (n=10709) was obtained during the EM survey by using an RTK-GPS system and used to co-krige these data.

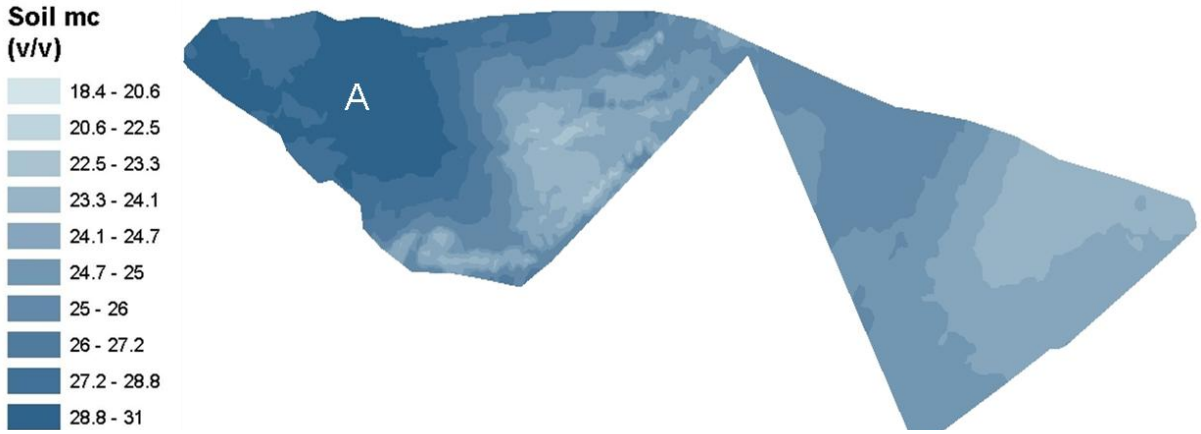

Fig. 5.5 Soil moisture map (0-45 cm depth), 12 Feb 2007, obtained by co-kriging θ and high resolution digital elevation data

Figure 5.5 shows the spatial pattern of soil moisture on 12 February 2007, during the period of irrigation.

A low lying natural ponding area (designated "A") is clearly depicted in the soil moisture map (Fig. 5.5) as an area of wetter soils. Such information is a useful decision tool for variable rate irrigation if the pattern is temporally stable. Temporal stability was assessed by regressing these GPS-located data points against sets recorded at the other TDR survey times, as done by other workers (e.g., Pires da Silva et al., 2001). Our results show that the soil moisture pattern was relatively stable over time during the period with no irrigation (R^2 = 0.8), but was less stable with time during the period of irrigation (R^2 = 0.3). This suggests that the irrigation system introduces another source of variation, and/or additional water was supplied to some areas e.g. lateral flow from adjacent sand dunes, during this period.

Irrigation scheduling should account for variability of soil water supply to the crop – some areas will dry out faster and reach the trigger point for irrigation sooner. Assuming soil moisture differs by 6% from the mean value used in the daily water balance (based on our TDR results), this equates to a difference of 20 mm of available water in the top 60 cm. Jamieson et al. (1995) found that yield was suppressed by about 40 kg per mm of soil water deficit. Therefore, a 20 mm deficit would stress the

plant and cause yield reductions of about 0.8 T/ha. Where soils are 6% wetter than the predicted soil moisture, unwanted drainage of irrigation water past the root zone may occur, resulting in wasted irrigation water and potential leaching of nutrients into groundwater pathways. An irrigation system is therefore required that will deliver different amounts of water to different parts of the crop at different times. This is enabled by individual nozzle control on the irrigator system.

While this digital information could ideally be uploaded to an automated irrigation system with variable rate nozzle control for precision irrigation, it is acknowledged that at this field site the scale of site-specific management is a challenge with significant soil moisture changes over distances of a few metres. However a goal of this research is to develop a suitable decision support system for variable rate irrigation. At other sites the AWC map will potentially be a useful tool for irrigation scheduling, for example, where thin stony soils exist beside deeper, finer textured soils. However, at this site, the local topographic control has an overriding influence on soil moisture patterns.

De Jonge et al. (2007) noted that there is an increased focus on variable rate irrigation systems and several prototypes have been developed, but adequate decision support systems have not (De Jonge et al., 2007). They comment that there is a need for more research to develop real-time monitoring, decision and control systems to be used with variable rate irrigators.

5.3.2. Irrigator performance

One of the most important measures of the accuracy of an irrigation system is its ability to apply a known amount of water uniformly to the crop. Another important measure is the precision with which it can supply a target amount of water. Uniformity of water delivery is usually defined by a radial distribution uniformity test for a centre-pivot irrigator. The results of the test conducted at this site showed that the distribution uniformity, DU_{lq}, of the irrigator was 0.79 (0.68 including the end-gun). This is similar to that found by McIndoe (1999) in a study of some centre-pivot systems in New Zealand where the uniformity test gave results between 34 and 100%, averaging at 78%; although McIndoe (1999) was able to improve this to 96% with

improved irrigation management in the subsequent year. In comparison, Stronge (2001) evaluated border strip irrigation systems at more than 175 sites throughout Canterbury, New Zealand, and found an average application efficiency of 56%. Edkins (2006) points out that although DU_{lq} is a very useful measure of irrigator performance it does not consider other factors such as drainage, evaporation and application rate. The DU_{lq} test adjusts the volume of water collected to account for increasing field areas represented by collectors placed further away from the pivot centre. It is also weighted more heavily on the driest quarter of the field, implying that best management would leave 1/8 of the field under-watered and 7/8 over-watered (Bloomer, 2006). Best management therefore assumes: (i) that complete uniformity of water application is an unrealistic expectation, and (ii) that it is better to aim at under-watering (which causes yield reduction) a small part of the field rather than over-watering (which causes wasted water; nutrient leaching, ponding, anaerobic soils, pugging and compaction).

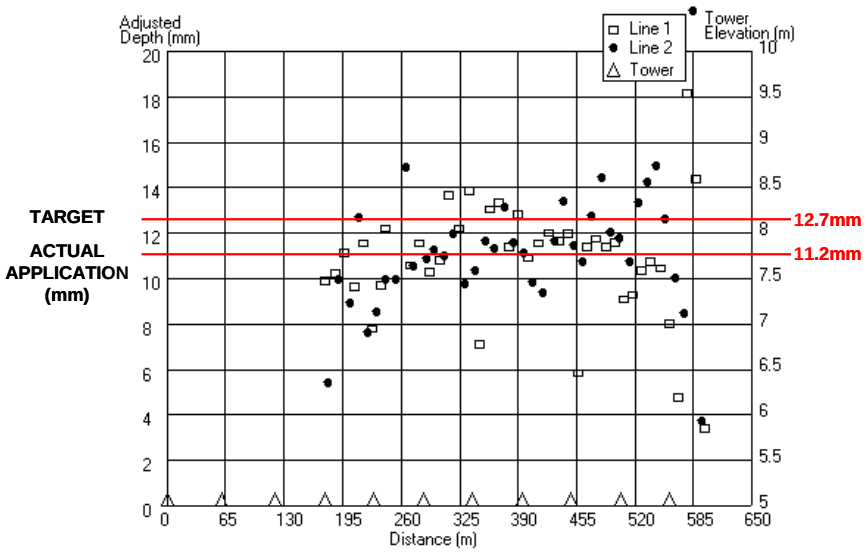

Fig. 5.6 Centre-pivot radial uniformity test showing actual depths of water applied along the 600 m boom compared to the target depth

The end-gun applied water less uniformly than the remainder of the centre-pivot. When the end-gun was included in calculations, the mean actual application rate was

1.5 mm less than the target application rate of 12.7 mm, a precision of 88%; however, this was improved to 1.2 mm (precision of 91%) when the end-gun measurements were omitted from calculations (Fig. 5.6).

5.4 CONCLUSIONS

Existing best practice decision tools for irrigation scheduling include use of climatic data to model a daily water balance, producing a single soil water deficit value on any one day. However, our results show that, at this research site, soil moisture content (to 45 cm depth) at any one time varied significantly by 12.7–13.1%. The use of one single value obtained from a daily water balance does not account for this within-field variability, and a soil at this site which is, for example, 6% drier than its trigger point for irrigation, has a 20 mm soil water deficit to 60 cm, potentially reducing yield by about 0.8 T/ha. This variability could be assessed by mapping soil water deficit. In addition, the amount supplied by the irrigator will vary spatially, and this research has found that the distribution uniformity of the irrigator, estimated using DU_{lq}, was 68% (including the end-gun), while precision of application was 88%. Therefore, at this site, the actual amount of water available to the crop varies considerably from the one mean value generated by existing best practice.

Improved use of irrigation water would be possible if the irrigator was adapted to apply different amounts of water to different parts of the field at different times. High resolution digital elevation data collected during EM mapping was co-kriged with TDR values to produce a prediction surface of soil water content, useful information to be uploaded to an automated irrigator system, if it is temporally stable. Research is ongoing to develop real-time monitoring and mapping tools for assessing soil water status with the aim of developing a decision support tool for variable rate irrigation systems.

CHAPTER SIX

A method for spatial prediction of daily soil water status for precise irrigation scheduling

This chapter reports on the second year of field research and introduces and discusses the concept of variable rate irrigation. The method established in previous chapters for the development of AWC maps is extended to develop a field capacity (FC) map and from here to predict daily soil water status, by the addition of a daily time step. Soil water balance modeling and soil moisture monitoring are used to predict and measure volumetric soil moisture respectively. Soil moisture monitoring is shown to be more appropriate for predicting daily soil water status at this 35 ha irrigated maize field on alluvial soils. Soil drying and wetting patterns are not predicted well by the soil water balance model because it does not account for the influence of a rising water table and lateral flow of water from adjacent sand dunes. The spatial and temporal stability of soil wetting and drying patterns is investigated using TDR (n = 50). A wireless sensor network is installed on site to monitor soil wetting and drying patterns in EC_a-defined management zones. The study site uses half of Manawatu Maize 1 (Chapters 4 and 5) plus a new adjacent field, used for wheat production in the previous year but under irrigated maize cultivation for the year of investigation [Manawatu maize 2].

This research has been accepted for publication in the Journal of Agricultural Water Management:

Hedley CB and IJ Yule (2009) A method for spatial prediction of daily soil water status for precise irrigation scheduling. Journal of Agricultural Water Management 96: 1737–1745, submitted 21/01/09; reviewers' comments received 10/06/09; revised manuscript submitted 11/07/09; accepted for publication 16/07/09.

Abstract

Available water-holding capacity (AWC) and field capacity (FC) maps have been produced using regression models of high resolution apparent electrical conductivity

(EC_a) data against AWC (adj. R^2 = 0.76) and FC (adj. R^2 = 0.77). A daily time step has been added to field capacity maps to spatially predict soil water status on any day using data obtained from a wireless soil moisture sensing network which transmitted hourly logged data from embedded time domain transmission (TDT) sensors in EC_a-defined management zones. In addition, regular time domain reflectometry (TDR) monitoring of 50 positions in the study area was used to assess spatial variability within each zone and overall temporal stability of soil moisture patterns. Spatial variability of soil moisture within each zone at any one time was significant (coefficient of variation [% CV] of volumetric soil moisture content (θ) is 3–16%), whilst temporal stability of this pattern was moderate to strong (bivariate correlation, R = 0.52–0.95), suggesting an intrinsic soil and topographic control. Therefore, predictive ability of this method for spatial characterisation of soil water status, at this site, was limited by the ability of the sensor network to account for the spatial variability of the soil moisture pattern within each zone. Significant variability of soil moisture within each EC_a-defined zone is thought to be due to the variable nature of the young alluvial soils at this site, as well as micro-topographic effects on water movement, such as low-lying ponding areas and lateral flow from adjacent sand dunes. In summary, this paper develops a method for predicting daily soil water status in EC_a-defined zones; digital information available for uploading to a software-controlled automated variable rate irrigation system with the aim of improved water use efficiency. Accuracy of prediction is determined by the extent to which spatial variability is predicted within as well as between EC_a-defined zones.

6.1 Introduction

Spatial decision support tools for precise irrigation scheduling are needed to address unprecedented demands on global freshwaters by irrigation schemes (Sadler et al., 2005; Green et al., 2006; De Jonge et al., 2007). These decision support tools would ideally address the spatial and temporal variability of crop demand and soil supply and be compatible with recent advances in full automation of accurate sprinkler irrigation systems, such as centre-pivot and lateral move irrigators (e.g. Peters & Evett, 2007, 2008; Kim et al., 2008). Centre-pivot systems typically have high irrigation application

efficiencies of 75–90% (Martin et al., 1990). In New Zealand, centre-pivots have been found to have a field uniformity averaging 78% (McIndoe, 1999). Other systems, such as border-check irrigation, are generally less efficient, as the irrigator has limited control over the amount of infiltration during an irrigation event, and large losses are likely on permeable soils, or where runoff cannot be captured and reused for irrigation (Wood et al., 2007).

Simultaneous to technological developments enabling more accurate delivery of irrigation water there has been an increasing awareness that in many situations it is best to vary the amount of water applied spatially, due to, for example: (i) variable crop demands, (ii) soil variability, and (iii) non-irrigation zones such as tracks, buildings and small water bodies over which the irrigator passes. Variable rate irrigation (VRI), recently dismissed as uneconomic (e.g. Lu et al., 2005), is receiving renewed interest as pressure on freshwater resources increases and technological improvements to hardware are made (Sadler et al., 2005). VRI addresses the need for improved water use efficiency of existing irrigation systems which use about 80% of allocated freshwaters world-wide (Jury and Vaux, 2007).

Most variable rate systems concentrate on centre-pivot technology, due to the potential to employ real-time sensing equipment, vary application rates and cover the entire field (De Jonge et al., 2007). Dukes and Perry (2006) report 93% coefficient of uniformity for a variable rate system, when tested in uniform rate mode.

Several prototype systems for variable rate irrigation application have been developed, but adequate decision support systems have not (Sadler et al., 2005). In order to increase practical functionality of precision irrigation; real-time monitoring, decision and control systems must be developed.

Existing irrigation decision support systems include the modelling approach (regional or site-specific) (e.g. De Jonge et al., 2007; Humphreys et al., 2008), direct crop stress measurement (Green et al., 2006; Peters & Evett., 2008), soil moisture measurements (Blonquist et al., 2006; Kim et al., 2008; Velladis et al., 2008) or a combination of these methods (e.g. Thompson et al., 2007).

Modelling approaches use climatic data and a soil water balance to predict availability of water to a crop, with an inherent weakness of reliance on the quality of its data input which may or may not incorporate any real-time site-specific measurements. Rainfall data can vary significantly from regional data being used in the water balance component. Both Humphreys et al. (2008) and De Jonge et al. (2007) also acknowledge the importance of quality site-specific soil water hydraulic data for crop modelling. Modelling has useful predictive ability for yield, but there are limitations for real-time irrigation scheduling, where quality data which include the effects of site-specific rainfall, rooting depth and compaction zones are essential.

Thompson et al. (2007) use a novel method for determining time for irrigation from crop stress assessed indirectly through soil moisture measurements. Onset of crop stress is indicated by a reduced apparent daily crop water uptake. Peters & Evett (2008) use a "temperature-time-threshold method". Crop leaf temperature is used as an indicator of crop stress which is measured on a fully automated centre-pivot irrigation system, where infrared thermocouple thermometers are attached to the trusses of the pivot. A field datalogger is polled once a day at midnight to assess whether canopy temperature was above a threshold level. Peters & Evett compared this novel decision tool for irrigation onset with manual irrigation scheduling and found that there was no significant difference between the two methods. They conclude that the fully automated "temperature-time-threshold method" has the potential to simplify management, while maintaining the yields of intensely managed irrigation.

Soil moisture monitoring decision tools for irrigation onset are perhaps the most widely used. Practically a farmer will walk over soils to assess visible signs of drying, or perhaps have some soil moisture monitoring sites. Recent advances have been made to automatically link soil moisture monitoring sites to software decision tools linked to irrigation systems (Blonquist et al., 2006; Velladis et al., 2008; Kim et al., 2008).

Blonquist et al. (2006) installed one TDT (time domain transmission) sensor in a 280 m^2 field plot connected to a CS3500 Controller. The controller logged volumetric soil water content (ϑ) which it compared to an irrigation threshold, and was connected to the solenoid valve on the irrigation line supplying water to the irrigation system. This

system applied 53% less water than the conventional method. Velladis et al. (2008) extended this approach to a smart sensor array for measuring soil moisture and scheduling irrigation in a 2.3 ha cotton field. The sensor array consisted of nodes placed into four irrigation management zones based on soil type, soil apparent electrical conductivity (EC_a) and historic yield maps. Similarly, Kim et al (2008) used a wireless sensor network to link soil moisture monitoring sites to software control of a site-specific precision linear-move irrigation system. This system provides an excellent example of what is now possible for full automated control of an irrigation system using a distributed wireless sensor network.

These previous three examples use "on-the-spot" EC_a targeted soil moisture monitoring sites to direct irrigation.

However further research is desirable to fully address spatial variability of soil water supply to the crop. EC_a mapping, when employing a real-time kinematic differential global positioning system (RTK-DGPS), easily defines soil spatial variability at resolutions of less than a metre. Therefore the opportunity exists to not only use the EC_a map to target soil moisture monitoring sites, as illustrated above, but also to calibrate the EC_a map against soil water-holding properties, so that a soil water status map can be produced, for spatial irrigation scheduling, available for upload to a fully automated variable rate irrigation system.

EC_a variations are primarily a function of soil texture, moisture content and cation exchange capacity (e.g. Hedley et al., 2004; Sudduth et al., 2005) in non-saline soils, and relationships can be developed between EC_a, soil texture and moisture content to predict soil available water-holding capacity (AWC) (Waine et al., 2000; Godwin & Miller, 2003; Hedley et al., 2008a [Chapter 4]; Hedley & Yule, 2009). Alternatively EC_a has been directly related to laboratory-assessed AWC (R^2 = 0.35–0.77) (Hezarjaribi & Sourell, 2007) and field-assessed AWC (R^2 = 0.67–0.87) (Jiang et al., 2007), where field capacity (FC) and wilting point (WP) were assessed in the field. Hezarjaribi and Sourell (2007) discuss that there are three options to delineate different AWC zones in the field: (1) grid soil sampling, (2) remote sensing reflectance and (3) a ground-based sensor method; and that the third method is preferable being fast, affordable, non-

destructive and with high spatial resolution. They used EC_a mapping to define zones for targeted soil sampling – and FC and WP were then assessed in the laboratory on air-dried, crushed and 2-mm sieved samples, with AWC estimated as the difference. As unprecedented demand on global freshwaters for irrigation continues it is increasingly important to develop a practicable, affordable method suitable for commercial uptake which significantly improves water-use efficiency and simplifies management.

Research presented in this chapter therefore aims to produce daily soil water status maps available for upload as shapefiles to an automated variable rate centre-pivot with the goal of simplified management of irrigation systems and greater water use efficiency. The method is developed to be appropriate for uptake by practitioners, and this chapter describes our method development. It:

(i) uses high resolution EC_a sensor data and soil characterisation of EC_a-defined zones to develop a relationship between EC_a and soil AWC and FC for map development,

(ii) adds a daily time step to the FC map producing daily soil water status maps, and

(iii) assesses the accuracy of these maps by defining spatial and temporal variability of the soil moisture pattern within and between each EC_a-defined management zone.

6.2. Materials and methods

6.2.1. Trial Site

Our trial site is a 35.2 ha irrigated maize (*Zea mays* L.) field, near Bulls, in the Rangitikei River Catchment, Manawatu District, New Zealand (site position: S40º13´22.1´´ E175 º17´46.4´´). The region experiences a temperate climate with rainfall between 900 and 1000 mm and approximately 1800 sunshine hours per annum. Seasonal dry periods vary from year to year, but commonly irrigation would be used between the months of December and March. A 600-m Valley centre-pivot is employed here. Three years of

yield mapping shows that yields vary greatly within this 35.2 ha field in any one year, making it an appropriate site for assessing whether site-specific management is desirable.

The soils have formed in fine textured alluvium deposited by the River onto a gravel terrace surface, and the site borders a sand dune-sand plain system. The soils are mapped as Ohakea silt loams (Mottled, Immature Pallic soils; Hewitt, 1998). They are characterised by silt loam topsoils and mottled silt loam subsoils, which are between 0.6 to more than 1.0 m thick, above heterogeneous layers of sand and gravel. In places, sand has blown onto the terrace surface from an adjacent sand dune forming the Ohakea loamy sand (Mottled, Immature Pallic soil). The Ohakea loamy sand is characterised by loamy sand topsoil over mottled silt loam subsoil over sands and gravels.

There is moderate topographic variation, with an average slope of 0.92% and elevation difference of 4.6m.

6.2.2 EC_a soil survey

An on-the-go electromagnetic induction (EMI) mapping system was employed to map soil EC_a (Hedley et al., 2004). Soil EMI surveys provide a quantitative spatial assessment of soil EC_a variability, which is used to define soil management zones for site-specific management (e.g. Velladis et al., 2008). In addition, soil EC_a is controlled by soil textural and moisture differences in non-saline soils, and therefore, as discussed in Section 6.1, there is potential to relate soil EC_a to soil water-holding characteristics. The system consists of a Geonics EM38© electromagnetic sensor, Trimble RTK-DGPS, on-board datalogger and Trimble Ag170 field computer for simultaneous acquisition of high resolution positional and EC_a data. The sensor was towed, in vertical mode, on a rubber mat behind an all-terrain farm vehicle at an average speed of 10–15 kph, and sensor data was logged at 1-s intervals, equating to a measurement recorded approximately every 4 m. Swath widths were 12 m apart. The RTK-DGPS system, in high accuracy mode, has a horizontal accuracy of $\pm$ 10 mm and a vertical accuracy of $\pm$ 20 mm. The survey was conducted on 29 August 2007.

Filtered data comprising latitude, longitude, height above mean sea level and EC_a (mSm^{-1}) were then imported into ArcGIS (Environmental Systems Research Institute, ESRI© 1999). Points were kriged in Geostatistical Analyst (ESRI © 1999) using a spherical semivariogram and ordinary kriging to produce a soil EC_a prediction surface map. Three management zones were defined on this map (using Jenks natural breaks) for further soil sampling.

6.2.3 Characterisation of EC_a-defined soil zones

6.2.3.1 Hydraulic characterisation

The soil hydraulic properties in each of the three zones were investigated by soil sampling at three representative sites in each zone. Intact soil cores, 100 mm diameter and 80 mm in height, were taken from the middle of three sample depths (0–200 mm, 200–400 mm, 400–600 mm) for laboratory characterisation of bulk density and soil moisture release characteristics (5 kPa and 10 kPa); smaller cores (50 mm diameter and 20 mm in height) were taken for soil moisture release at 100 kPa. A bag of loose soil was also collected (0-200 mm, 200-400 mm, 400-600 mm soil depth) for lab estimation of permanent wilting point (1500 kPa) (Burt, 2004; Gradwell, 1972) and particle size distribution. Total available water-holding capacity (AWC) was estimated as $\theta_{1500kPa}$ - θ_{10kPa} where θ_{10kPa} is taken as field capacity and $\theta_{1500kPa}$ is wilting point. Readily available water-holding capacity (RAWC) was estimated as θ_{100kPa} - θ_{10kPa}. Soil EC_a was determined at the time of sampling at each position, as the mean of six hand-held measurements.

6.2.3.2 Particle size distribution

Percent sand, silt and clay was determined on these soil samples by organic matter removal, clay dispersion and wet sieving the >2-mm soil fraction and then by a standard pipette method for the <2-mm soil fraction (Claydon, 1989).

6.2.4 Soil moisture modelling and monitoring

6.2.4.1 Daily soil water balance modelling

A meteorological station was installed on-site to collect hourly rainfall, wind speed, solar radiation, and air temperature data. These data were used to calculate a daily evapotranspiration rate, using the FAO Penman-Monteith equation (Allen et al., 1998). Vapour pressure was estimated from the minimum daily temperature. A water balance model was developed which included a dual crop coefficient (Allen et al., 1998) to predict the effects of intermittent irrigation wetting events on basal crop transpiration and soil evaporation separately. Daily adjustments were made for crop height and development stage for the maize grain crop; and all daily irrigation events were logged. The water balance model was used to calculate a daily soil moisture deficit (SMD), using zone-specific AWC values, but does not account for available water sourced via capillary rise from a high water table, or lateral flow. Any effects of capillary rise and lateral flow on plant-available water storage were assessed by noting depth to water table and distance from sand dunes. Scotter (1989) reports that the equivalent depth of plant-available water increases substantially from 26 to 183 mm as the water table rises from 1.2 to 0.4 m in sandy soils adjacent to the present study site. The effects of lateral flow from higher to adjacent lower areas is shown to be important over distances of 400m, and can provide further plant-available water (Scotter, 1989).

TDT soil moisture measurements were used to monitor soil moisture changes to include any contribution of available water due to capillary rise (from a high water table) and lateral flow (from adjacent sand dunes) to each zone.

6.2.4.2 TDT soil moisture monitoring of EC_a-defined soil zones

Soil moisture was logged hourly during the growing season by a TDT Aquaflex© soil moisture sensor network, with one sensor installed into representative positions in each of the three zones (low, intermediate, high EC_a) defined from the EC_a map. The three metre long sensors were installed diagonally from a depth of 50 mm to 600 mm to provide a mean value for θ (0–600 mm) for an equivalent soil volume of 6 L. This

depth was selected to include the majority of the maize root zone, estimated by previous researchers on a similar soil type in the same climatic region (Aslam, 2005) and confirmed by visual pit inspections at this trial site. A radio aerial mounted on a 3.5 metre mast wirelessly transmitted hourly soil moisture data to a remote PC in the farm office.

6.2.4.3. TDR assessment of spatial and temporal variability of soil moisture within and between zones

TDR wave-guides were installed, to 450 mm soil depth, at 50 sites in the 35.2 ha maize field (Fig. 6.1). The positions were ≥ 50 m apart on a grid pattern (See Fig. 6.1). Measurements were taken six times during the growing season between November, when the soils were at field capacity (FC), and the end of March towards the end of grain drying, to assess (i) spatial variability of θ within and between zones, and (ii) temporal stability of the soil moisture pattern.

6.2.4.4. Daily time step for soil water status mapping

The high resolution (< 1 m) soil EC_a dataset was used to produce a soil EC_a map with three soil zones (Section 6.2.2). AWC and FC was determined for each of these 3 zones (Section 6.2.3.1); and soil moisture changes were modelled (Section 6.2.4.1) and measured (Section 6.2.4.2) on a daily basis for each zone.

Soil sampling at 9 positions (3 replicates in each of 3 zones) provided 9 values for soil AWC and FC (Section 6.2.3.1), each with a corresponding soil EC_a value. These data were used to investigate relationships between (i) EC_a and AWC, and (ii) EC_a and FC.

A relationship between soil EC_a and FC was used to produce a soil FC map, and the AWC data was used to determine an irrigation trigger point ($\theta_{trigger)}$ for each FC value, based on a known crop-specific depletion factor of 0.55AWC for maize grain (Allen et al., 1998).

The modelled daily soil moisture values for each position (Section 6.2.4.1) or zone (Section 6.2.4.2) were then investigated for use to modify the sensor data on a daily basis so that the day on which irrigation is required could be predicted spatially.

6.3. Results

6.3.1. Soil EC_a map and zone characteristics

The soil EC_a map reflects soil and topographic differences observed at this site (Fig. 6.1; Table 6.1), which are classified into three zones (low, medium, high EC_a), with a 33 m range of spatial dependence of EC_a values, indicated by variogram analysis (Table 6.2).

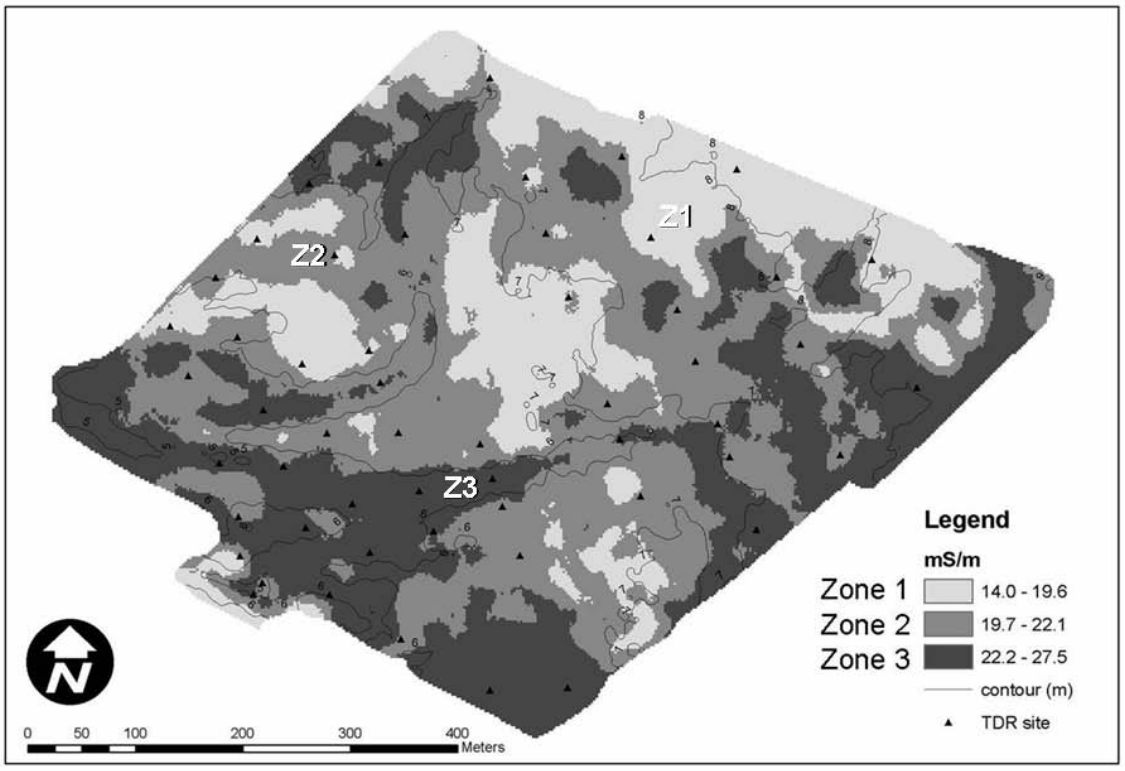

Fig. 6.1 Soil EC_a map of the study area (Z1, Z2 and Z3 = Aquaflex positions in Zone 1, Zone 2 and Zone 3 respectively)

A band of low EC_a soils (14.0–19.6 mS m^{-1}) along the NE side of the field borders a sand dune and delineates a region where soil profiles are characterised by about 200 mm of black sand overlying silt loam subsoil. These Zone 1 soils have higher sand content (61.0%) compared with the other two zones (Zone 2 = 35%; Zone 3 = 12%), (Table 6.1). Clay content increases from 8.3% in Zone 1 to 13.0% in Zone 2 and 26.8% in Zone 3 (Table 6.1). Finer textured soils in Zone 2 occur on flatter surfaces, and the finest textured silt loam soils in Zone 3 typically occur in wet hollows and channels where

water will preferentially flow to and settle in during wet periods, increasing the susceptibility of these zones to soil compaction.

Table 6.1 Soil characteristics of the three EC_a-defined soil zones (one mean value reported for 0–600 mm soil depth)

Zone	EC_a(Oct 07)	Sand	Silt	Clay	FC	WP	AWC	RAWC	Irrigation Trigger
	mSm^{-1}	%			m^3m^{-3}				
1	14.0–19.6	61.0	30.8	8.3	0.30	0.11	0.19	0.09	0.20
2	19.7–22.1	35.0	52.3	13.0	0.32	0.14	0.18	0.08	0.22
3	22.2–27.5	12.0	61.3	26.8	0.36	0.26	0.10	0.04	0.30

FC = field capacity; WP = wilting point; AWC = total available water-holding capacity; RAWC = readily available water-holding capacity

Zone 1 soils have lowest FC (0.30 m^3m^{-3}) but largest AWC (0.19 m^3m^{-3}) and RAWC (0.09 m^3m^{-3}) compared with the other two zones, reflecting a greater proportion of pores at the size range required to hold available water for plant use (0.0002–0.03 mm).

Table 6.2 Variogram parameters for the EC_a survey data ($mS\ m^{-1}$)

Parameter	Co	C1	a (m)
EC_a (mSm^{-1})	1.09	5.38	33

Co: nugget variance; Co + C1: sill; a: apparent range of spatial dependence; for n=14152

Zone 3 soils retain a greater proportion of their water at lower matric potentials, with a relatively high θ of 0.26 m^3m^{-3} at wilting point (WP), compared with 0.14 m^3m^{-3} (Zone 2) and 0.11 m^3m^{-3} (Zone 1). This is illustrated by the graph of soil water retentivity data (Fig. 6.2), relating soil matric potential (the energy that the water is held by the soil) to volumetric water content (θ), and reflects the finer textured soils in Zone 3.

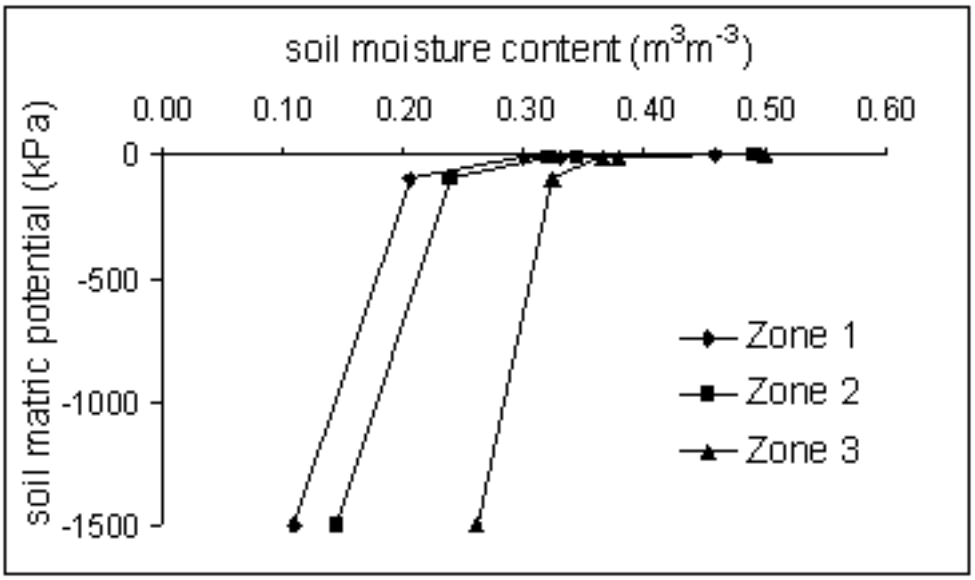

Fig. 6.2 Soil retentivity data for the 3 EC_a-defined soil zones (one mean value reported for 0 – 600 mm soil depth)

Soil EC_a is related to measured AWC (R^2=0.76) and FC (R^2=0.77) (Fig. 6.3); so that the regression equations are available to predict soil AWC and FC for each soil EC_a value.

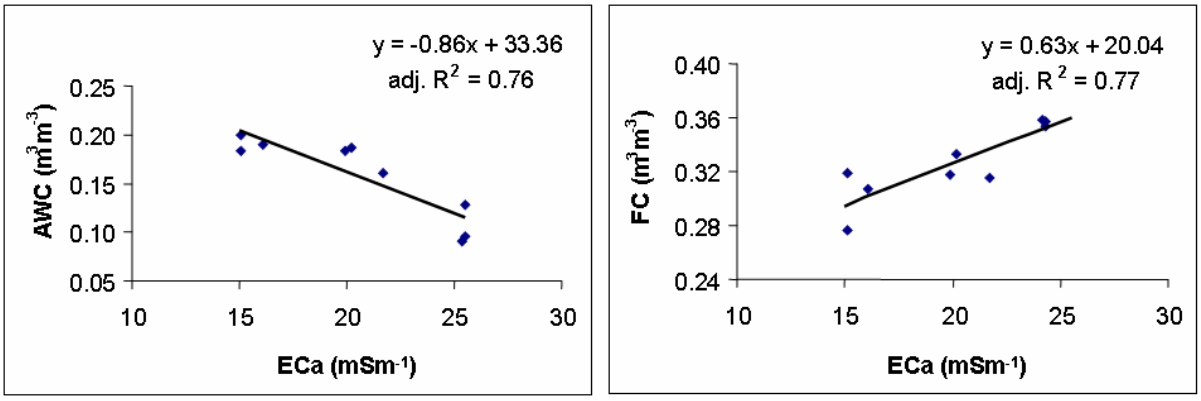

Fig. 6.3 Relation of EC_a to soil AWC and FC at the study site

The relationship of soil EC_a to soil water-holding properties reflects the major influence of soil texture and moisture on soil EC_a (Hedley et al., 2004; Sudduth et al., 2005); the soil providing more conducting pathways for the electric current induced by the EM38 sensor as texture becomes finer and soil moisture content increases.

6.3.2 Soil moisture modelling and monitoring

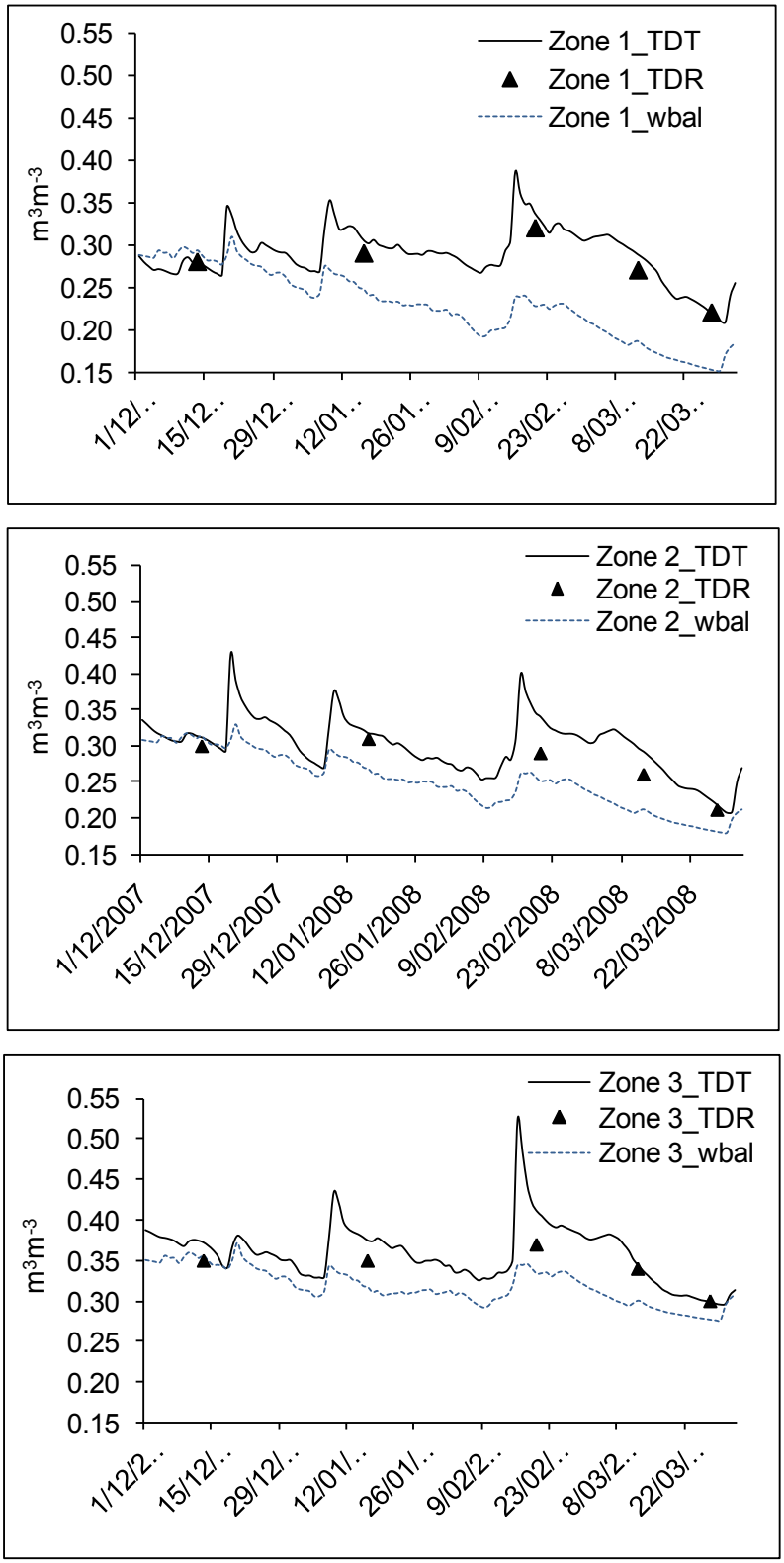

Fig. 6.4 **Soil wetting and drying patterns in the three EC_a-defined soil zones measured by TDT (0–600mm) and TDR (0–450mm) and modelled by water balance (wbal)**

Figure 6.4 plots the soil water balance-predicted soil moisture for each zone and compares it with TDT measured values (one mean value to 600 mm). It clearly shows that the soil water balance is underestimating soil θ, providing evidence for additional supply of water from a high water table and/or lateral flow from adjacent sand dunes. Therefore, for this study, the measured TDT values (θ_{tdt}) provide more accurate prediction of daily soil moisture changes in each zone than modelled values (θ_{wbal}).

Figure 6.4 also shows that TDR determined mean values (θ_{tdr}) (mean value to 450 mm) for each zone fall between θ_{wbal} and $\theta_{tdt.}$ This suggests that a component of water contributed via capillary rise or lateral flow is from depths below 450 mm. In Zone 1, θ_{tdr} and θ_{tdt} show closer agreement suggesting that a greater proportion of the water supplied to this zone (above that predicted by the soil water balance) is in the 0–450 mm soil depth. This zone is the most likely zone to benefit from lateral movement of soil water being adjacent to sand dunes.

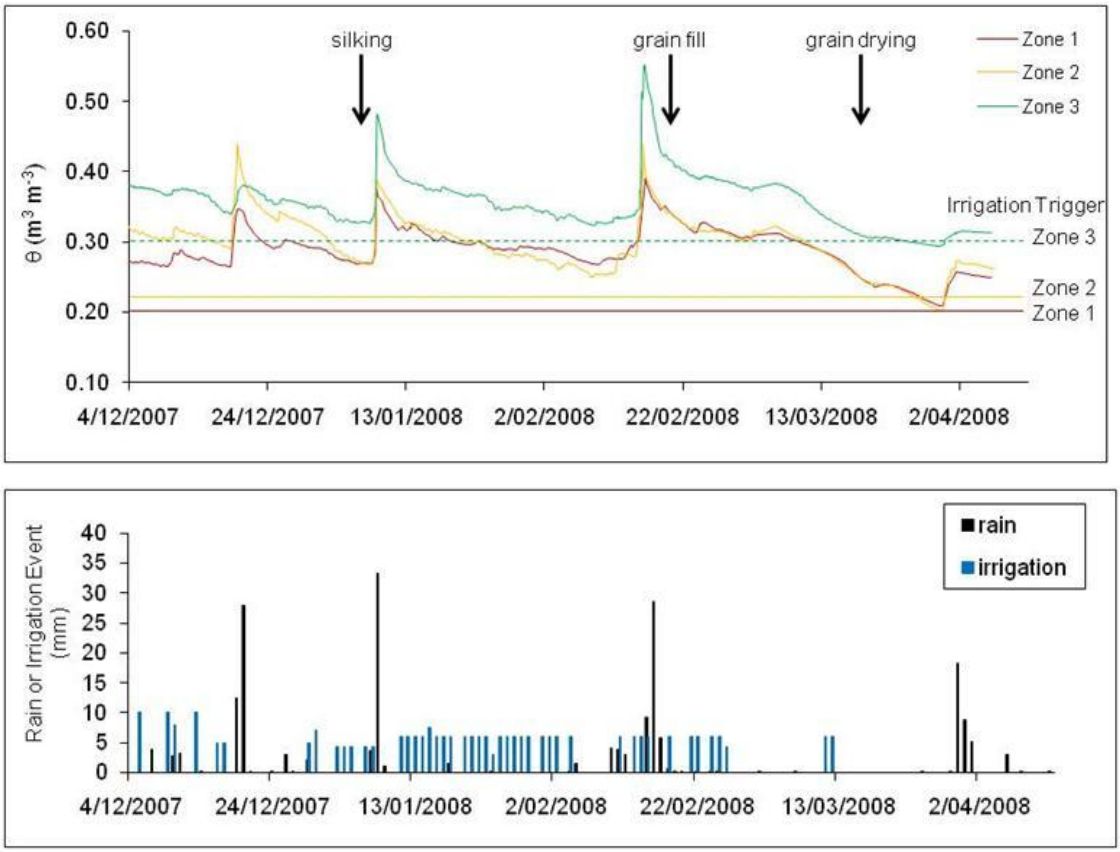

Fig. 6.5 Measured θ_{tdt}, rainfall and irrigation events during the maize growing season

Figure 6.5 shows θ_{tdt} and $\theta_{trigger}$ plotted for the period of irrigation (21/11/07 to 12/03/08), and during this period 290 mm of irrigation was applied, and there was 154 mm rainfall. This data was used to predict daily soil water status in each soil zone and compare it with zone specific $\theta_{trigger}$.

Figure 6.5 shows that Zone 3 remains wetter than the other two zones, reflecting its hydraulic properties described in Section 3.1.

6.3.3 TDR assessment of spatial and temporal variability of soil moisture within and between soil EC_a zones

Site mean θ_{tdr} (n=50) to 450 mm soil depth had a % coefficient of variation (%CV) ranging between 9 and 14 % for the 6 TDR survey dates (Table 6.3). The 14/11/07 mean θ_{tdr} (n=50) for this 35.2 ha field, when soils were at FC, had the smallest % CV of 9% compared with the other survey dates. After this date soil moisture spatial variability increased as soils drained at different rates, depending on their pore size distribution and position in the landscape.

Table 6.3 also shows the spatial variability of soil moisture within the 3 EC_a-defined zones. This information can be used to assess how accurately one predicted soil θ value for each zone represents the whole zone. It indicates that, for this case study, the small differences observed between each zone θ at any one time, explained by soil textural and structural differences (Table 6.2), are not significantly different. Spatial variability within each zone is considerable and this is most likely controlled by local topographic features which control soil water movement, such as hollows and ridges (Lavado Contador et al., 2006; Kaleita et al., 2007). In addition our results suggest contributions via lateral flow from adjacent sand dunes (Zone 1) and capillary rise from a seasonally high water table in low-lying areas. The water table was observed to rise to 0.8 m below the soil surface in low-lying areas during the winter months.

Table 6.3 Site and zone soil moisture (θ) statistics from TDR data for the irrigated 35.2 ha maize field

		14 Nov 07	13 Dec 07	16 Jan 08	20 Feb 08	12 Mar 08	27 Mar 08
Site (n=50)	mean	0.33	0.29	0.30	0.32	0.28	0.24
	sd	0.03	0.03	0.04	0.03	0.03	0.03
	%CV	9	10	13	10	12	14
Zone 1 (n=6)	mean	0.32	0.31	0.30	0.32	0.28	0.23
	sd	0.03	0.02	0.01	0.03	0.01	0.02
	%CV	8	8	3	5	6	10
Zone 2 (n=17)	mean	0.33	0.29	0.30	0.32	0.27	0.23
	sd	0.03	0.03	0.04	0.03	0.03	0.04
	%CV	9	12	14	11	13	16
Zone 3 (n=27)	mean	0.33	0.29	0.31	0.33	0.29	0.25
	sd	0.03	0.02	0.03	0.03	0.03	0.03
	%CV	9	8	11	10	11	12

θ is reported in $m^3 m^{-3}$

The TDR data (n=50) was also used to assess the temporal stability of the spatial pattern (Fig. 6.6). A scatterplot matrix of TDR surveys against each other (Fig. 6.6) illustrates that there was moderate–significant temporal stability of this soil moisture pattern (bivariate correlations range from 0.52 to 0.95) which was most obvious when the soils were comparatively dry in March, after irrigation had stopped and grain drying was occurring (R>0.9). A 95% bivariate normal density ellipse is imposed on each scatterplot. Site-specific management based on a spatial model prediction of soil water status would be impracticable if soil drying patterns were largely random with time across a landscape. However, these results support data presented by other researchers that spatial variability is far more stable in time than would be expected from random processes (Starr, 2005; Kaleita et al., 2007). Vachaud et al. (1985) suggest that this temporal stability is largely explained by relationships between soil texture and water content; and work by da Silva et al., (2001) supports this hypothesis.

(a) Bivariate correlations

	NOV14	DEC13	JAN16	FEB20	MAR12	MAR27
NOV14	1.00	0.77	0.53	0.69	0.70	0.65
DEC13	0.77	1.00	0.70	0.72	0.74	0.68
JAN16	0.53	0.70	1.00	0.83	0.78	0.72
FEB20	0.69	0.72	0.83	1.00	0.94	0.84
MAR12	0.70	0.74	0.78	0.94	1.00	0.95
MAR27	0.65	0.68	0.72	0.84	0.95	1.00

(b) Scatterplot matrix

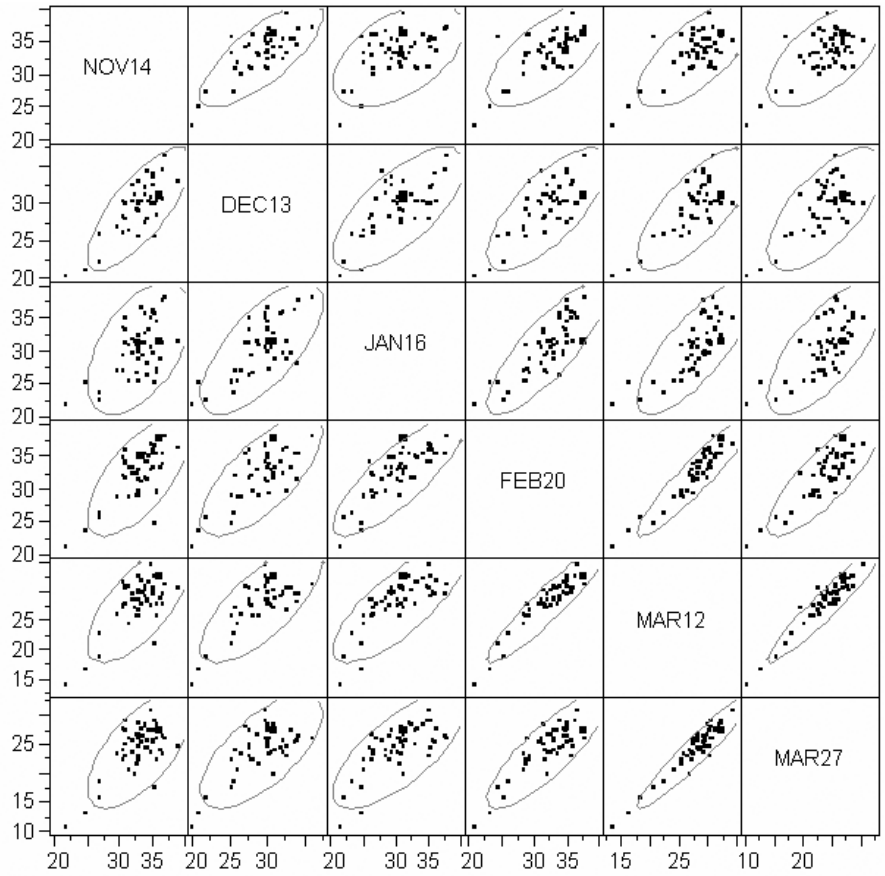

Fig. 6.6 (a) Bivariate correlations and (b) Scatterplot matrix of soil moisture content values measured by TDR at 50 sites

Therefore although there was significant spatial variability within zones, this variability was temporally stable to some extent, so that, if defined, the spatial variability could be managed. Many more soil moisture sensors would be required at this site to characterise the spatial variability for variable rate irrigation scheduling.

6.3.4 Soil water status mapping

Regression equations developed between EC_a (mean of 6 hand-held measurements) and lab-estimated AWC (adj. R^2 = 0.76, n = 9) and FC (adj. R^2 = 0.77, n = 9) (Fig. 6.3; Section 3.1), were used to predict AWC and FC from sensor data. $\theta_{trigger}$ was then also predicted for each EC_a value.

Table 6.4 Time step calculation on day *x* for prediction of daily soil water status

X	Y	EC_a	Zone	AWC	FC	$\theta_{trigger}$	$\theta_{tdt\_day\ x}$
2705372	6107081	17.83	1	0.18	0.31	0.21	0.29
2705377	6107081	18.22	1	0.17	0.31	0.22	0.29
2705382	610781	18.29	1	0.17	0.31	0.22	0.29
2705367	6107076	17.59	1	0.18	0.31	0.21	0.29
2705372	6107076	17.78	1	0.18	0.31	0.21	0.29

Where:

X,Y	high resolution positional co-ordinates (m) (NZMG 1949 datum)
EC_a	EC_a value (E) at this position (mSm^{-1})
Zone	defined by class range on the EC_a map
AWC	= -0.86E + 33.36 (Fig. 6.3a)
FC	= 0.63E + 20.04 (Fig. 6.3b)
$\theta_{trigger}$	determined as 0.55 AWC
$\theta_{tdt\_day\ x}$	measured in each zone on day *x*

The 0.55 AWC depletion factor suggested by Allen et al. (1998) was used in this study as a trigger for irrigation scheduling. Other workers use an allowable depletion of 0.50 (De Jonge et al., 2007) and 0.60 (flood irrigation) and 0.70 (sprinkler irrigation) (Humphrey et al., 2008), although Humphrey et al. (2008) report that using these thresholds the maize crop was under-irrigated.

A zone identification code was also added to each EC_a data point (Table 6.4).

The sensor dataset was updated each day by updating θ_{tdt} for each zone, so that the sensor dataset can be used for spatially defined irrigation scheduling. Irrigation is scheduled for any unique position when $\theta_{tdt\_day\,x} < \theta_{trigger}$.

This spatially defined digital data is available to drive a software alert system to an automated variable rate irrigation system, so that sprinklers can be switched on for each spatially defined zone.

6.4. Discussion

A method has been described for spatial prediction of daily soil water status, using a FC map derived from the relationship of EC_a to FC, with the addition of a daily time step by continuous monitoring of soil moisture wetting and drying patterns in each zone. Daily TDT soil moisture data were used in preference to water balance modelling to more accurately assess additional inputs of water as lateral flow and capillary rise. The spatial variability of soil moisture measurements within each EC_a-defined zone at any one time is large (%CV=3.21–16.09) which limits the accuracy of the soil water status maps at this site.

Whelan and McBratney (2000) explain that spatial variability must be correctly characterised for effective site-specific management. If this is not possible, then the "null hypothesis" of precision agriculture applies, i.e. uniform rate application is more appropriate than variable rate application. Spatial differences in soil moisture are likely to be one controlling factor influencing yield, but if they cannot be realistically modelled they cannot be addressed. Whelan and McBratney (2000) report a median CV% of 9% for a number of θ values measured over a range of sampling scales from a comprehensive literature review. Median CV%, a measure of spatial variation for θ (at any one time) varies between 3.2 % and 15.9 % for the three EC_a-defined zones at this site, where sampling scales of 50 –100 m were used.

It is preferable to assess the spatial structure of soil moisture measurements using a variogram, and Whelan and McBratney (2000) report a median apparent range of spatial dependence of 22 m, from their review. Kaleita et al. (2007) used variograms to

explore the geospatial structure of soil moisture content of a 3.3 ha research site, and found that 10 m was an appropriate cell size for precision agriculture operations at this site. Sadler et al. (2002) also discuss the importance of management zone size. Variogram analysis of θ was not conducted at this site due to insufficient soil moisture data points (n = 50). Kerry and Oliver (2008) suggest that a minimum of 100 data points is required to compute a reliable variogram to assess spatial structure of this soil attribute.

However EC_a relates well to soil hydraulic properties and variogram analysis of soil EC_a shows that soil variability, on a basis of soil texture and moisture, has a spatial dependence of 33 m (Table 6.2), which indicates the potential density of soil moisture monitoring sites required to characterise the soil hydraulic characteristics influencing soil water status at this site.

The assessment of temporal stability of θ pattern in this study by regressing $\theta_{\text{time } x}$ against $\theta_{\text{time } y}$ showed that ≥ 52% of the observed variability could be explained. 77% of the observed variability was explained between November and December surveys, before irrigation commenced. Least temporal stability was observed between the last non-irrigated survey and first irrigated survey, suggesting that the irrigation system has an effect on the soil moisture pattern. The pattern was most temporally stable as the soils dried out at the end of the growing season, with 84–95% explained between February and March surveys. The temporal stability of soil moisture patterns is attributed to dependence on relatively stable properties such as topography and soil particle class (Starr, 2005). Tomer and Anderson (1995) found that 51–77% of spatial variability in soil water content was explained by elevation, slope, and hillside curvature, in a sandy hill slope; while da Silva et al. (2001) found that clay content and C content and to a lesser extent tillage method influenced soil water storage patterns over time.

This research shows that a greater number of monitored soil moisture zones would be required for effective spatial irrigation scheduling in these highly variable, young alluvial soils. Recent technological advances in distributed wireless sensor networks (e.g. Kim et al., 2008) are facilitating low energy, high density monitoring of soil

moisture. Micro-sensors are being developed with on-board power supply, computational capability and ability to detect and communicate with other sensors in a network, thus providing affordable opportunities for larger numbers of sensors to be included into spatial irrigation scheduling decision support tools in the near future.

6.5. Conclusions

A high resolution EC_a datalayer has been used to target zones for characterising soil hydraulic properties, which relate well to EC_a. A method has been developed for interpolation of AWC and FC prediction surfaces, and real-time soil moisture monitoring has been used to predict soil water status within each zone. The accuracy of this prediction is limited by significant spatial variability of the soil moisture pattern within EC_a-defined zones which was larger than differences between zones. To improve the accuracy of prediction, and facilitate variable rate irrigation scheduling, a larger number of EC_a-defined zones would need to be characterised and monitored at this site.

CHAPTER SEVEN

Soil water status mapping and variable rate irrigation scenarios for two Manawatu farms

This chapter develops the concept of variable rate irrigation (VRI), introduced in Chapter 6. It uses two case studies to investigate the potential water savings of VRI compared with uniform rate irrigation (URI) for (i) pasture and (ii) a maize grain crop. At both sites EM mapping is employed to produce a soil EC_a map, which is then interpreted on a basis of the measured soil differences, field capacity (FC), available water-holding capacity (AWC), % sand and % clay. AWC maps are developed from the EC_a maps. At the pastoral site [Manawatu pasture], VRI saves water by irrigating to the stress point of delineated EC_a-defined soil management zones with different AWCs. At the maize grain cropping site [Manawatu maize 1], VRI saves water by shutting off irrigation water to one zone where real-time soil moisture monitoring shows that the soils have impeded drainage and do not dry out to their trigger point for irrigation. Research findings reported in this chapter were presented at four meetings and have been published in the Precision Agriculture Journal:

Hedley CB, Yule IJ (2008) Soil EM mapping for advanced irrigation scheduling. *In Proceedings* "Advanced Farming Systems" LandWise Conference, 14–15 May, Gisborne, NZ.

Hedley CB (2008) Precision Agriculture – providing the competitive edge for primary industry. Presentation at New Zealand Institute of Primary Industry Management, 5–7 June 2008, Queenstown, NZ.

Hedley CB, Yule IJ (2008) A high resolution soil water status mapping method for irrigation scheduling and two variable rate scenarios for pasture and maize irrigation. In Proceedings of 9th International Precision Agriculture Conference, 20–23 July 2008, Denver, USA.

Bradbury S, Hedley CB (2008) Opportunities in New Zealand for Variable rate Irrigation. Invited Presentation to FAR (Foundation for Arable Research) Workshop, 21 July 2008, Ashburton, NZ.

Hedley CB, Yule IJ (2009) Soil water status mapping and two variable-rate irrigation scenarios. Journal of Precision Agriculture 10:342–355.

Abstract

Irrigation is the major user of allocated global freshwaters, and scarcity of freshwater threatens to limit global food supply and ecosystem function – hence the need for decision tools to optimize use of irrigation water. This research shows that variable alluvial soil ideally requires variable placement of water to make the best use of irrigation water during crop growth. Further savings can be made by withholding irrigation during certain growth stages. The spatial variation of soil water supplied to (i) pasture and (ii) a maize crop was modelled and mapped by relating high resolution apparent electrical conductivity (EC_a) maps to soil available water-holding capacity (AWC) at two contrasting field sites. One field site, a 156-ha pastoral farm, has soil with wide ranging AWCs (116–230 mm m^{-1}); the second field site, a 53-ha maize field, has soil with similar AWCs (161–164 mm m^{-1}). The derived AWC maps were adjusted on a daily basis using a soil water balance prediction model. In addition, real-time hourly logging of soil moisture in the maize field showed a zone where poorly drained soil remained wetter than predicted. Variable rate irrigation (VRI) scenarios are presented and compared with uniform-rate irrigation (URI) scenarios for 3 years of climate data at these 2 sites. The results show that implementation of VRI would enable significant potential mean annual water saving (21.8 % at Site 1; 26.3 % at Site 2). Daily soil water status mapping could be used to control a variable rate irrigator.

7.1. Introduction

An unprecedented demand by agriculture on global freshwater supplies is seen as the main cause of increasing global freshwater scarcity (Jury & Vaux, 2007). Intensification of land-use and complementary developments, such as plant breeding, have maintained global food production during the period since the 1960s commonly referred to as the Green Revolution (Swaminathan, 2007). This intensification of land-use has relied on increased use of irrigation, and irrigation is now the major user of global freshwater, taking 70% of all extractions (UN/WWAP, 2003). Some of the

freshwater taken for irrigation is used ineffectively, and there is a need for research and technological advances to improve water use efficiency. In New Zealand, where irrigation uses 77% of allocated freshwaters (NZ Ministry for the Environment, 2007), the area of irrigated land has roughly doubled every decade since the 1960s. There are now some 500 000 ha under irrigation, which supports the increases in agricultural productivity over recent decades.

Water has traditionally been a readily available resource for all users; but concepts of water metering, water trading and water footprints (Hoekstra & Chapagain, 2008) are now a reality. Improved use aims for better conversion of each millimetre of applied water to dry matter production, minimizing runoff, drainage and evaporation, and maximizing yield. The link between water applied and yield is well established; potential yield requires transpiration to proceed at its potential rate (Allen et al., 1998; Hanks, 1974). A variable rate irrigation (VRI) system can vary water application rates spatially. It improves water-use efficiency by maintaining readily available water in the soil for the plant to transpire at its potential rate, and by withholding irrigation when the soil is at field capacity (FC). Some recent studies have concluded that such systems are uneconomic (e.g. Lu et al., 2005). However, with increased attention being given to conserving freshwater during drought, and to municipal and industrial demands, and with awareness of recreational and environmental needs, conclusions regarding profitability and desirability of VRI may change (Sadler et al., 2005). Variable rate irrigation has obvious potential opportunities for conserving water by simply turning off sprinklers over farm tracks, drains, etc., as well as by varying the rate of water applied to different crop and soil types. Although prototype systems for VRI have been developed (e.g. King and Kincaid, 2004) with performance testing (Dukes and Perry, 2006), soil-related decision support systems have not (Sadler et al., 2005; Green et al., 2006; De Jonge et al., 2007). Decision support systems for a variable rate irrigator require information about how much plant available water is present in the soil on any one day and how it varies spatially, as well as information about crop water requirement. The portion of plant available water (defined as the volumetric soil water content between FC and wilting point) present in a soil on any one day can be modelled using a water balance approach, or measured directly by real-time logging

using a soil moisture sensor; and weather station data can be used to estimate potential evapotranspiration (E_t) (Sadler et al. 2005). Blonquist et al. (2006) used a time domain transmission (TDT) electromagnetic sensor linked directly to an irrigator, for real-time logging of soil moisture and control of applied irrigation. Irrigation is initiated by the sensor signal when a threshold soil water content is reached. These researchers found that their system applied 16% less water than when irrigation scheduling was based on a numeric model for estimating soil moisture content and weather station-derived E_t, and 53% less water than when using a fixed irrigation depth of 50 mm per week. An accurate site-specific measurement is preferable to one predicted from a model, but it is unclear how representative the soil moisture status at the sensor site is of the whole field. Sadler et al. (2002) discuss the need for farm-scale soil maps to address this issue, emphasising the role that soil variation plays in significant differences in crop response to uniform irrigation application.

Russo (1986) also found that spatially variable soil responds differently under uniform irrigation, with some combinations of irrigation depth and salinity resulting in relative differences between crop yields in one field exceeding 100%. Russo (1986) concluded that, due to their inherent spatial variability, it is important to analyse the spatial distribution of soil in a field to direct improved irrigation management schemes.

Deficit irrigation (DI) is a complementary method to VRI for conserving irrigation water, and is much easier to enforce. It withholds irrigation water at strategic times of less critical growth. Kang et al. (2000) recommended a DI strategy by reducing irrigation at the seedling and stem-elongation stages, in the semi-arid loess plateau of northwest China where a rapid decline of water resources has led to an urgent need to reduce irrigation.

To summarize, freshwater for irrigation is often limited and better use of this valuable natural resource can be achieved by: (i) VRI that facilitates improved placement of irrigation water onto variable soil and (ii) DI that further conserves water by strategic timing of irrigation.

This paper presents a method for assessing soil variability and linking it to daily soil water status. Daily soil water status maps are produced using a relationship between

available water-holding capacity (AWC) and soil apparent electrical conductivity (EC_a). Previous research has linked EC_a to soil water content (Brevik et al., 2006) and AWC (Waine et al., 2000). This research adds a daily time-step to the AWC map using a water balance model to produce a file that could be uploaded daily to a computer-controlled variable rate irrigator. Two variable rate irrigation scenarios are described to illustrate the potential water savings of this method

7.2. Methods

7.2.1. Site selection

The study was undertaken at two sites. The first site is a 156-ha field site near Palmerston North, New Zealand, at Massey University No. 1 Dairy Unit and part of No. 4 Dairy Unit (S40°22′57.4″ E175°35′38.2″), where summer-induced water stress occurs in some years that necessitates irrigation (see Fig. 7.1). Ryegrass (*Lolium perenne L*.) and white clover (*Trifolium repens L*.) pasture predominate. The soil types are mapped as Fluvial Recent and Fragic Pallic soils (Hewitt, 1998). The Fluvial Recent soil has formed in greywacke alluvium and the Fragic Pallic soil (Fragiaqualfs, USDA NRCS classification) has formed in Pleistocene greywacke loess, with small tephric contributions. Average annual rainfall is approximately 1000 mm, and the mean winter temperature is 8.5°C and mean summer temperature is 17.9°C.

Table 7.1 Annual rainfall and evapotranspiration data for the 2 sites (1/1/05–1/1/08)

Site	Land Use	Parameter		2005	2006	2007
Site 1	Pasture	Rainfall	(mm yr^{-1})	1093	1575	958
		Pasture E_t	(mm yr^{-1})	849	781	853
Site 2	Maize	Rainfall	(mm yr^{-1})	908	1180	821
		Crop E_t	(mm yr^{-1})	1084	1010	1105

The second site, a 53-ha irrigated maize crop, was selected at a farm in the Rangitikei River Catchment, approximately 30 km north-west of Palmerston North, New Zealand (S40°13′22.1″ E175°17′41.8″).

Average annual rainfall at Site 2 is slightly lower (see Table 7.1), and a 600-m centre-pivot irrigator is used during periods of seasonal drought. Site 2 is on a terrace surface and the soil is mapped as Ohakea silt loam (Mottled, Immature Pallic soil, Hewitt, 1998; Endoaquept, USDA NRCS classification). The soil is characterized by a silt loam topsoil over a mottled subsoil to depths of 0.6 to >1.0 m above heterogeneous layers of greywacke sands and gravels. In some places sand has blown onto this terrace soil from an adjacent sand dune, forming the Ohakea loamy sand (Mottled, Immature Pallic soil). This is characterized by loamy sand topsoil over mottled silt loam subsoil over greywacke sands and gravels.

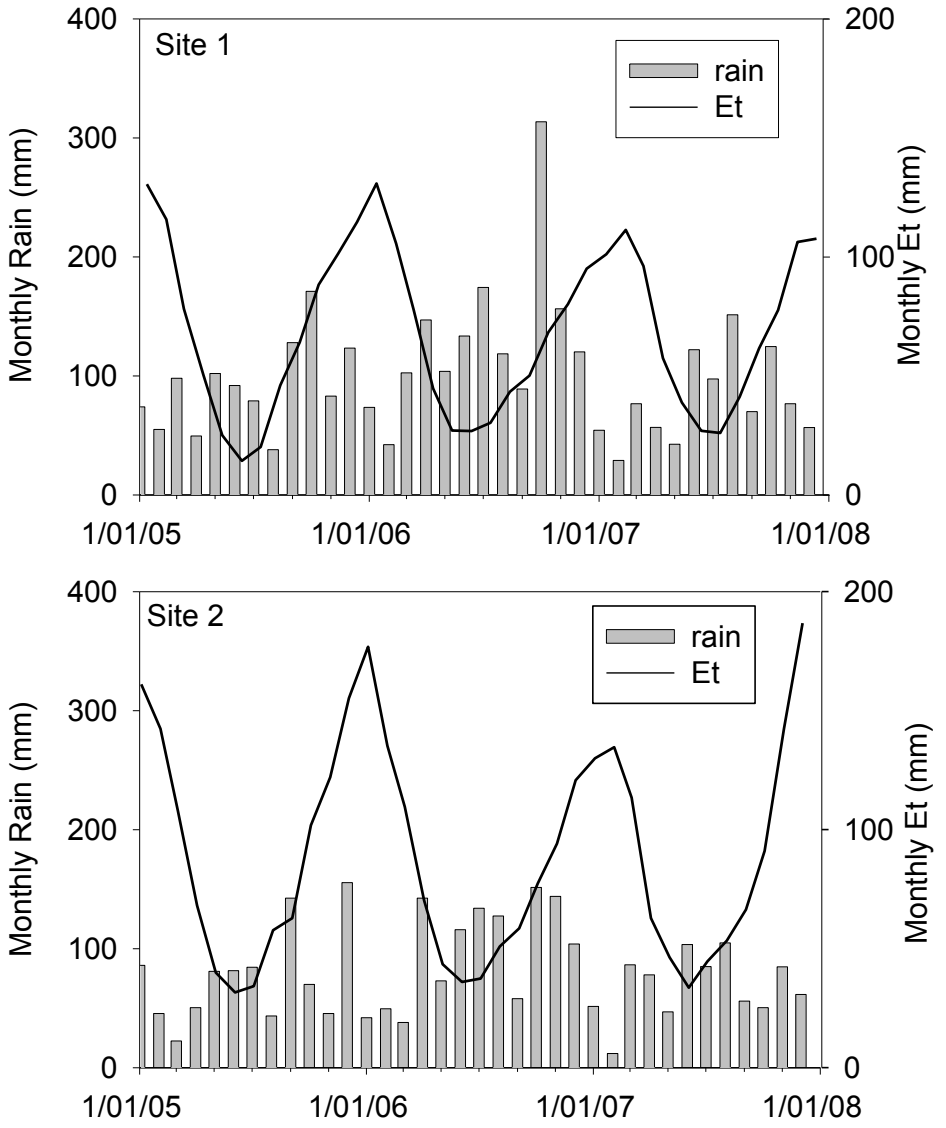

Fig. 7.1 Monthly rainfall and E_t at Site 1 (pasture) and Site 2 (maize) for the period 1/01/05 - 1/01/08

7.2.2. Mapping of EC_a and soil AWC

A Geonics EM38 electrical conductivity sensor (Geonics Ltd., Mississauga, Ontario, Canada) with RTK-DGPS and Trimble Ag170 field computer (Trimble Navigation Ltd., Sunnyvale, California, USA) on board an all-terrain vehicle (ATV) was used to map soil variability. The Geonics EM38 sensor, used in the vertical mode, measured apparent soil electrical conductivity (EC_a) to a depth of 1.5 m, providing one mean weighted value that is influenced primarily by soil texture and moisture in non-saline soil (e.g., Sudduth et al. 2005; Hedley et al. 2004). Data were recorded at 1-s intervals, at an average ATV speed of 15 km h^{-1}, with a measurement recorded approximately every 4 m along transects 10 m apart. The EC_a prediction surface was produced using a spherical variogram model and ordinary kriging in Geostatistical Analyst (ArcGIS, ESRI, Redlands, California, USA). It was classified into seven zones using Jenks' natural breaks classification which determines the best arrangement of values into classes by iteratively comparing sums of the squared difference between observed values within each class and class means. The best classification identifies breaks in the ordered distribution of values that minimizes the within-class sum of squared differences.

An AWC map was then derived from the EC_a map using a method reported previously (Hedley et al., 2008a). The EC_a prediction surface was classified into a smaller number of zones to reflect observed soil differences better, using Jenks' natural breaks classification. A field estimate of zone AWC was then obtained by sampling the soil at three replicate positions within each zone. The replicate positions were 5 m apart within each zone and at least 5 m from a zone boundary. The AWC was estimated as the difference between volumetric soil water content (θ) on a day when the soil was at field capacity (FC) (θ_0, soil moisture deficit [SMD] 0 mm) and on another day when the soil was very dry, close to wilting point (θ_{130}, SMD 130 mm). Soil samples were obtained at depths of 0–150 mm; 150–300 mm; 300–450 mm and 450–600 mm from a core. One mean value was obtained for each replicate position for θ_0, θ_{130}, and particle size distribution, by calculating a mean for the four soil depths. The mean of the three replicate positions was then calculated to provide a mean zone value. The EC_a values were also determined at each position on each sampling day, using the EM38 sensor in vertical hand-held mode, to calculate a mean zone value.

The mean for soil texture was converted to a single number using a numeric index developed by Waine et al. (2000) for UK soil, and found to be appropriate for New Zealand soil textural classes (Hedley et al., 2008a). This index ranks soil (1–6 in intervals of 0.5 for the 11 classes on a soil texture triangle) on the basis of increasing fineness of texture. Soil moisture content curves at FC and very dry were then plotted against soil texture on the abscissa. The difference between the two curves is a field estimate of AWC. This was then plotted against EC_a to derive a relationship between EC_a and AWC, which was used to produce maps of AWC.

7.2.3. Real-time soil moisture logging

Electromagnetic TDT (Aquaflex©, Streat Instruments Ltd., Christchurch, New Zealand) sensors were inserted into each EC_a-defined soil management zone, at Site 2, to log real-time hourly θ. These data were wirelessly transmitted to a remote computer for real-time irrigation scheduling. The TDT sensors are 3 m long and were placed diagonally in a trench from 50 mm depth at one end to 550 mm depth at the other end; the trench was then back-filled. The trench was between and parallel to two rows of maize. The TDT estimates the soil dielectric constant accurately, which is strongly influenced by volumetric soil moisture content. The sensors have a 6-L sphere of influence. They were installed after the maize crop had been planted, and used to log water use during the maize growing season. The sensors were calibrated using gravimetrically determined soil moisture measurements on soil cores of known volume, by sampling to 600 mm at a range of soil moistures at the sensor sites.

7.2.4. Daily water balance model

The amount of plant-available water held in the soil on any one day was calculated using a water balance model (Allen et al., 1998). This model determines soil water content in terms of root zone soil water depletion (*S*) relative to FC, and is expressed as a water depth in the root zone (mm).

$$S_i = S_{i-1} - R_i - I_i - C_i + Et_i + D_i, \quad (1)$$

where S_i is root zone soil water depletion at the end of day i (mm), S_{i-1} is the depletion at the end of the previous day, $i-1$ (mm), R_i is the rainfall on day i (mm), I_i is the irrigation applied on day i (mm), C_i is the capillary rise from groundwater (GW), assumed to be zero when GW>1 m, on day i, Et_i is crop evapotranspiration on day i (mm) and D_i is drainage (runoff plus root zone water loss due to deep percolation) on day i.

Root zone soil water depletion at FC is zero (S = 0), and as soil water is extracted by E_t a critical soil moisture deficit (CSMD) is reached where E_t is limited to less than potential values, and pasture or crop E_t begins to decrease in proportion to the amount of water remaining in the root zone (Allen et al., 1998). The amount of water held in the soil between FC and CSMD is defined as the readily available water (RAW), which was determined using the specific pasture and maize depletion fractions defined by Allen et al. (1998). Site-specific R and I were measured, and E_t was estimated from site-specific climate data and adjusted for crop stage at the irrigated maize site. Capillary rise, C, was assumed to be zero at both sites. A value for D, which includes runoff and deep percolation below the root zone, was calculated as the excess water above FC by the soil water balance model.

The water balance, calculated for each soil zone AWC, assesses mm of available water present in each soil zone on any one day, indicating the day when the CSMD is reached and irrigation should commence.

7.3. Results

7.3.1. Maps of EC_a and AWC

The EC_a maps for both sites (Figs. 7.2a and 7.3a) identify soil zones of contrasting texture, which were confirmed by visual soil profile investigation and soil sampling (Table 7.2).

At Site 1 (Fig. 7.2, Table 7.2), Manawatu loamy gravel soils are identified by the smallest EC_a values (<20 mS m^{-1}). Manawatu sandy loam soil has EC_a values of 20–25-mS m^{-1}, Turitea silt loam soil is in the 25–50 mS m^{-1} range and the finest textured Tokomaru silt loam soil has EC_a values > 50 mS m^{-1}. Percentage clay, FC and AWC increase with increasing EC_a (Table 7.2).

At Site 2, the zone with smallest EC_a values (<18 mS m^{-1} in Fig. 7.3a) is characterized by Ohakea loamy sands, and has smallest mean percentage clay (Table 7.2). The remaining two zones are characterized by Ohakea silt loam soil, with the high EC_a zone delineating an area of poorly drained mottled Ohakea silt loams in the north-west corner of the field, confined by sand dunes. There was little difference between AWC for these three zones (Table 7.2).

Moisture-texture curves (at θ_0 and θ_{130}) are shown in Figs. 7.2b and 7.3b for Site 1 and Site 2, respectively. The regression equations for the dry soil curves (θ_{130}) were subtracted from those of the FC curves (θ_0) to derive an estimate of AWC (Figs. 7.3b and 7.4b) for each zone. This estimate of AWC was then regressed against the EC_a values measured at each soil sampling time (Figs. 7.2c and 7.3c). The regression equation, predicting AWC from soil EC_a values, was then used to produce the AWC maps (Figs. 7.2d and 7.3d). A direct relation between soil moisture at FC and soil EC_a for Site 1 is also shown in Figure 7.4 (R^2 = 0.6).

The heterogeneous soil at Site 1 has predicted AWCs ranging between 106 and 245 mm m^{-1}, compared with a much smaller predicted range at Site 2 (161–164 mm m^{-1}), reflecting the wider range of soil textural class at Site 1. The implications of this for irrigation scheduling at Site 1 are that the EC_a-defined soil zones will reach their critical soil moisture trigger point at different times.

The CSMD, or irrigation trigger, was calculated using the depletion factors of 0.5 AWC (pasture) and 0.55 AWC (maize) as suggested by Allen et al. (1998) for each soil zone. When soil moisture is maintained above this critical deficit level, E_t can proceed at its potential rate allowing potential plant yield to be achieved, assuming that soil moisture is the major controlling factor of crop yield.

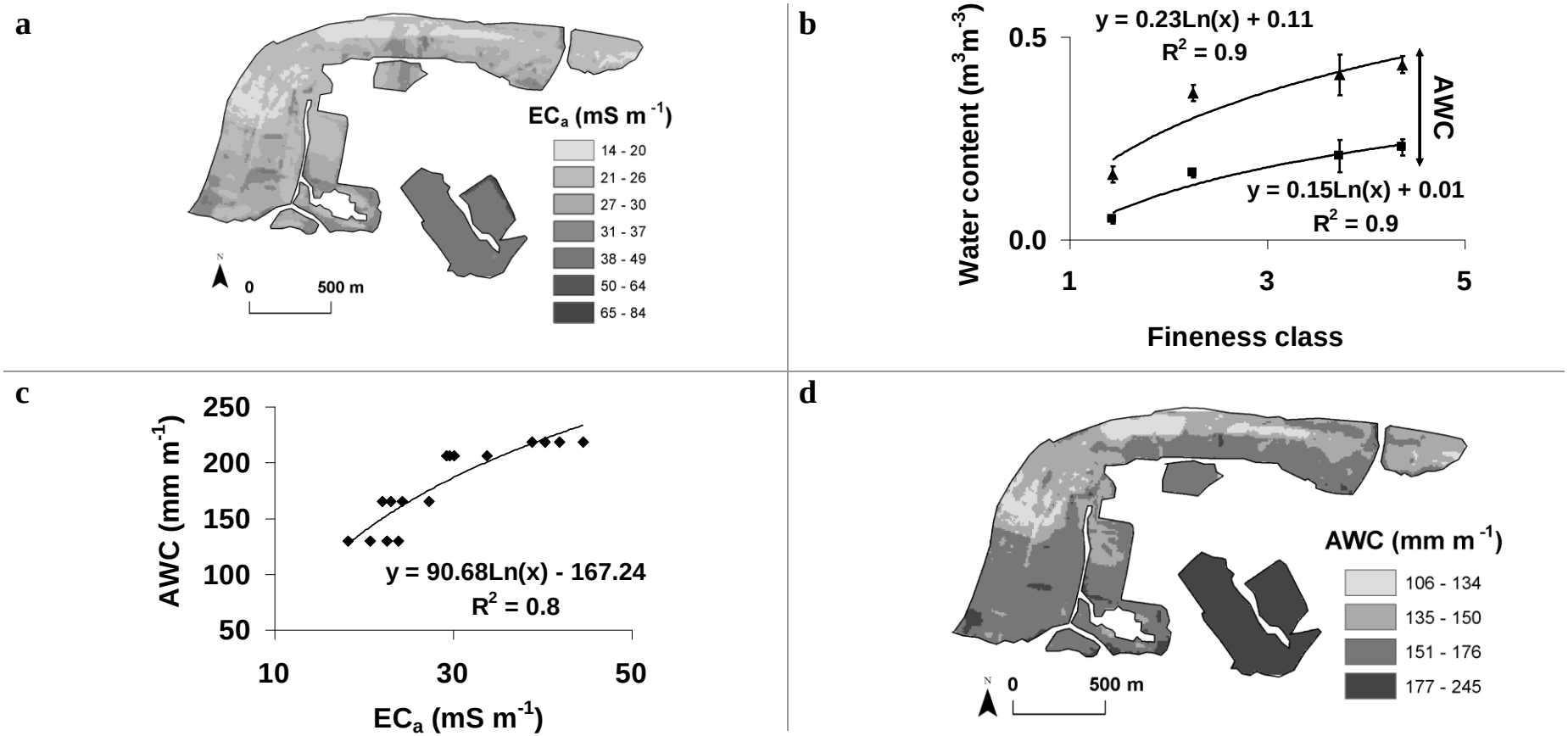

Fig. 7.2 Site 1: (a) EC_a map, (b) water content-soil texture curves, (c) AWC-EC_a regression curve and (d) derived AWC map

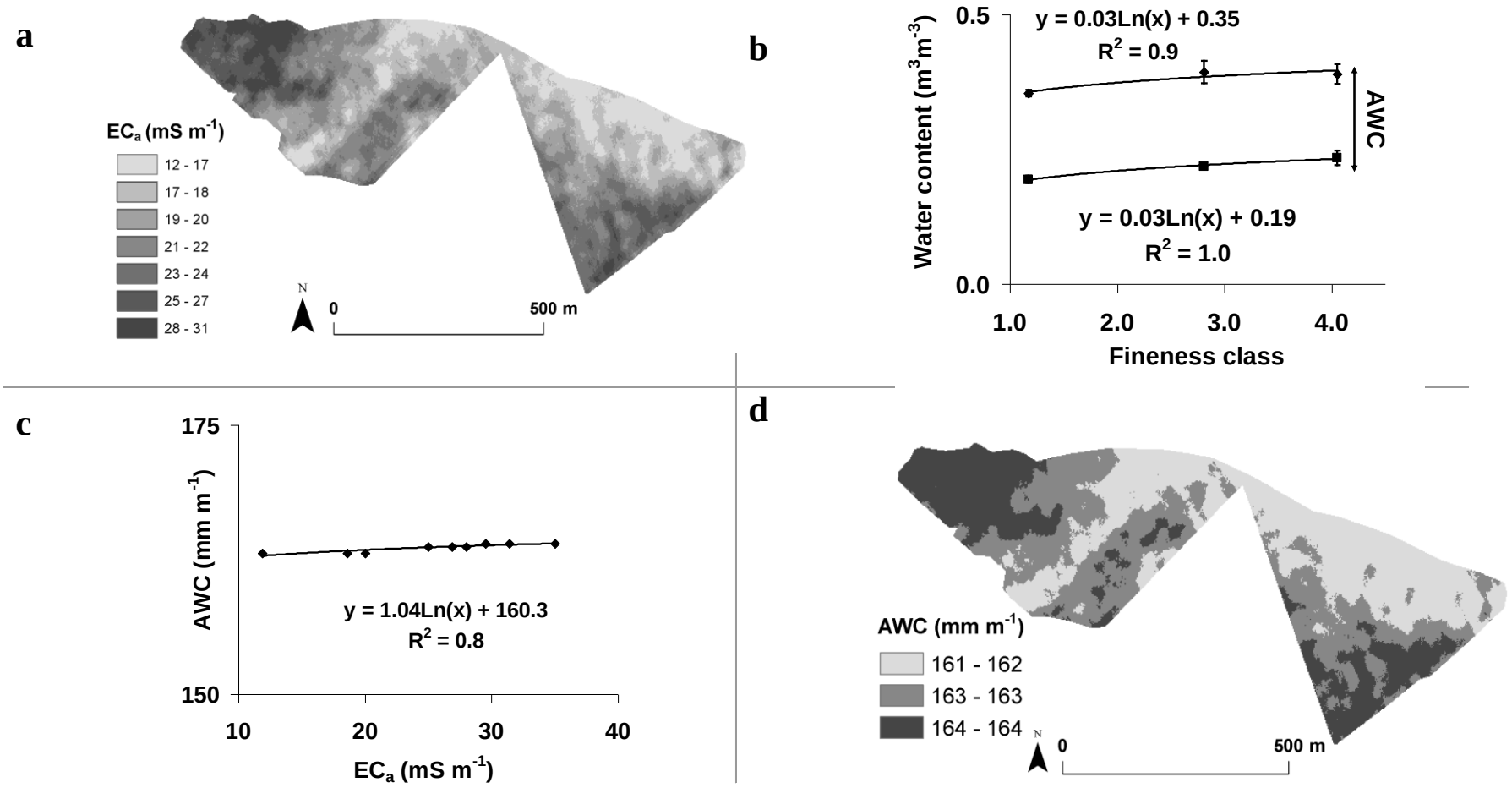

Fig. 7.3 Site 2: (a) EC_a map, (b) water content-soil texture curves, (c) AWC-EC_a regression curve and (d) derived AWC map

Table 7.2 Measured soil zone characteristics at Sites 1 and 2

Site 1. Pastoral Farm

Soil Zone	(1) Manawatu loamy gravel	(2) Manawatu sandy loam	(3) Turitea silt loam	(4) Tokomaru silt loam
Field Capacity (m^3m^{-3})	0.16	0.30	0.41	0.43
AWC (m^3m^{-3})	0.13	0.17	0.21	0.22
Sand (%)	65	53	19	6
Clay (%)	4	10	20	26

Site 2. Maize Field

Soil Zone	(1) Ohakea loamy sand	(2) Ohakea silt loam	(3) Ohakea mottled silt loam
Field Capacity (m^3m^{-3})	0.35	0.39	0.39
AWC (m^3m^{-3})	0.16	0.16	0.16
Sand (%)	63	22	38
Clay (%)	11	24	14

Field Capacity (FC) = soil water content 2 days after saturation

Mean profile sand and clay (%) reported

7.3.2. Water balance calculation

The water balance was used to assess the day that CSMD occurred, so that hypothetical irrigation scheduling could be applied to each soil zone, for three seasons (1/7/04 - 30/6/05; 1/7/05 - 30/6/06; 1/7/06 - 30/707). The hypothetical irrigation events apply 10 mm water every time this trigger point is reached.

An example is given in Figure 7.5. The two plots in each graph illustrate the millimetres of available water on any one day; assuming no irrigation (grey line) and with hypothetical irrigation (black line), for the period 1/1/07 – 1/8/07. Figure 7.5 shows that summer plant

demand for soil moisture depletes the majority of the available water during the summer of 2007 at these two sites, as it does in each of the 3 years studied.

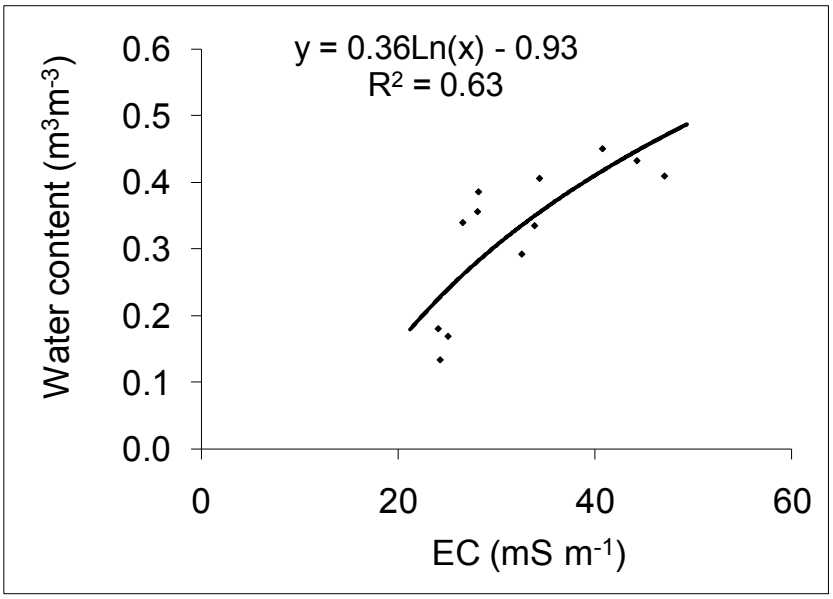

Fig. 7.4 Relation of soil water content (m3 m-3) at FC to soil ECa (Site 1)

7.3.3. Variable rate irrigation scenarios

At both sites a uniform-rate irrigation (URI) schedule was compared with variable rate irrigation (VRI) schedules (Table 7.3; Table 7.4) for each of the three seasons (1/7/04–30/6/05; 1/7/05–30/6/06; 1/7/06–30/707). The URI scheduling added a hypothetical 10 mm irrigation event every time the most droughty soil zone reached its CSMD, in order to maintain potential E_t and therefore potential yield across the whole area. The VRI schedules adjust irrigation according to soil AWC differences, so that irrigation is applied only to the soil zone when its specific CSMD is reached. Our results show that, at Site 1 (Table 7.3), total irrigation applied during the summer dry months (2004/05, 2005/06, 2006/07) using URI was 160 mm, 220 mm and 140 mm, respectively, with an annual demand on irrigation water of 255 ML, 351 ML and 223 ML, respectively (Table 7.3), for this 156-ha pastoral farm.

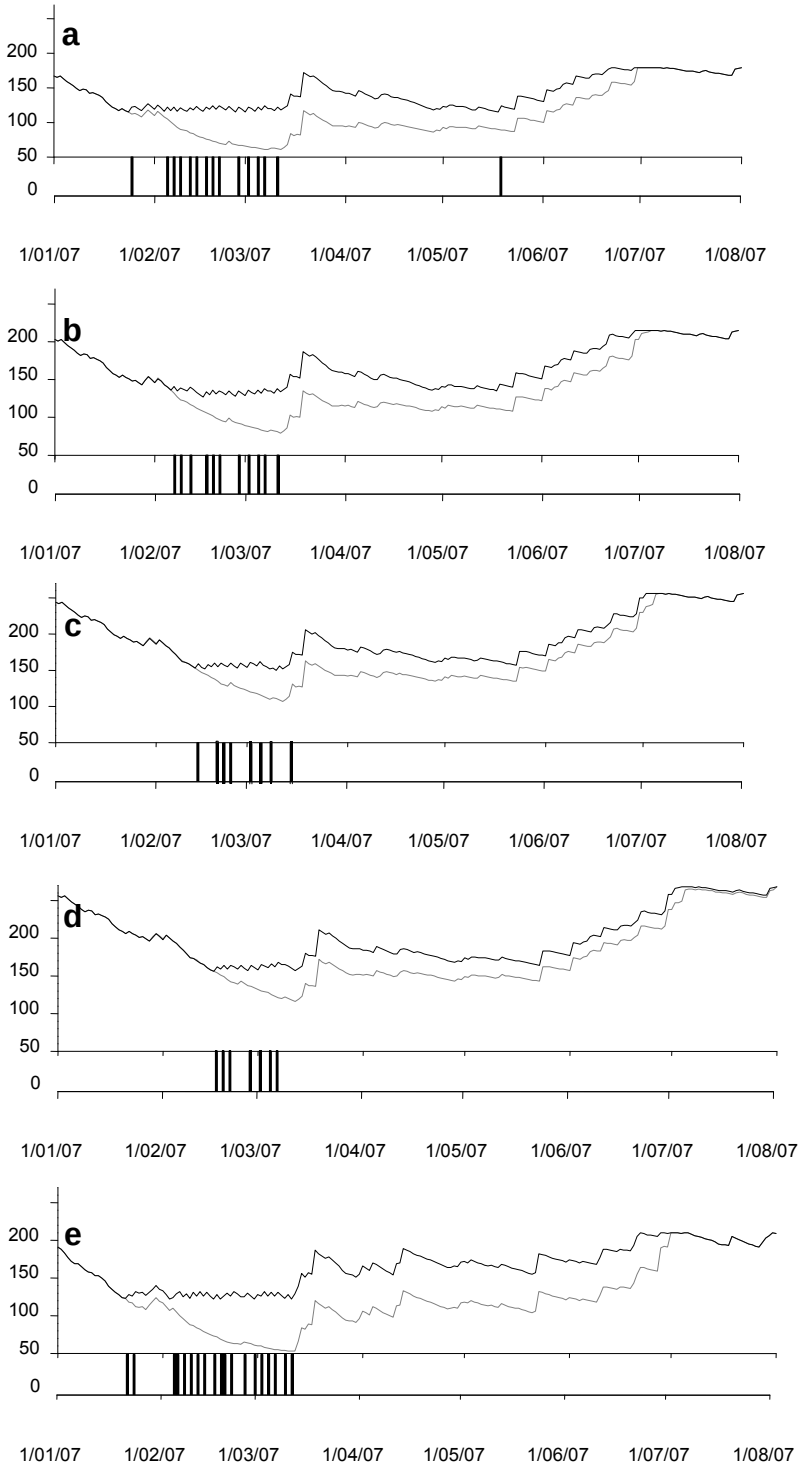

Fig. 7.5 Soil water balance without irrigation (grey plot) and with irrigation (black plot) for: (a) Site 1, Zone 1, (b) Site 1, Zone 2, (c) Site 1, Zone 3, (d) Site 1, Zone 4, (e) Site 2. Hypothetical 10 mm irrigation events (black bars) are shown below these plots for each soil zone

Table 7.3 A comparison of irrigation water use by VRI and URI at Site 1

Year	Area (ha)	Zone	Irrigation (m^3 ha^{-1})*	Zone irrigation water use per season (ML)	Site irrigation water use per season (ML)**
Uniform-rate irrigation (URI) scenario					
2004–05	159.6	All	1600		255
2005–06	159.6	All	2200		351
2006–07	159.6	All	1400		223
Variable rate irrigation (VRI) scenario					
2004–05	30.2	1	1600	48	
	93.9	2	1300	122	
	18.6	3	1000	19	
	16.9	4	900	15	
	159.6				204
2005–06	30.2	1	2200	66	
	93.9	2	1700	160	
	18.6	3	1300	24	
	16.9	4	1300	22	
	159.6				272
2006–07	30.2	1	1400	42	
	93.9	2	1000	103	
	18.6	3	800	15	
	16.9	4	700	12	
	159.6				172
Annual water saving (URI – VRI)					
			(%)	(mm ha^{-1})	(ML)
2004–05			20.2	32	51
2005–06			22.5	49	80
2006–07			22.9	32	51

*1 mm irrigation = 10 m^3 ha^{-1}; **ML = megalitre = 10^6 L

By contrast, only the most drought-prone zone received the maximum level of irrigation with VRI scheduling. At Site 1, VRI scheduling applied between 90–160 mm, 130–220 mm and 70–140 mm for the three growing seasons, respectively. This is an annual water saving of 32 mm ha^{-1} (51 ML), 49 mm ha^{-1} (80 ML) and 32 mm ha^{-1} (51 ML), respectively, as shown in Table 7.3. The VRI saves water by using stored readily available water in the soil profile, and by delaying irrigation until the point where this stored water has been used in

each soil management zone. For example, for the period 1 January 2007 to 1 April 2007 at Site 1(Fig. 7.5), Zone 1 required 14 10-mm irrigation events to maintain soil moisture above the critical deficit. Zone 2 required 11 events, Zone 3 required 8 and Zone 4 required 7 events. Our results show that a VRI system would conserve a mean 21.8% of irrigation applied or 38 mm ha^{-1} (60.4 ML) per year, for the three years assessed.

Table 7.4 A comparison of irrigation water use by VRI and URI at Site 2

Year	Area	Zone	Irrigation	Zone irrigation water use per season	Site irrigation water use per season
	(ha)		(m^3 ha^{-1})*	(ML)	(ML)**
Uniform-rate irrigation (URI) scenario					
2004–05	53.2	All	2900		154
2005–06	53.2	All	3500		186
2006–07	53.2	All	1900		101
Variable rate irrigation (VRI) scenario					
2004–05	15.2	1	2900	44	
	24.0	2	2900	70	
	14.0	3	0	0	114
2005–06	15.2	1	3500	53	
	24.0	2	3500	84	
	14.0	3	0	0	137
2006–07	15.2	1	1900	29	
	24.0	2	1900	46	
	14.0	3	0		74
Annual water saving (URI – VRI)					
			(%)	(mm ha^{-1})	(ML)
2004–05			26.3	76	41
2005–06			26.3	92	49
2006–07			26.3	50	27

*1 mm irrigation = 10 m^3 ha^{-1}; **ML = megalitre = 10^6L

At Site 2 (Table 7.4), the AWCs of soil in the three management zones are very similar, so VRI would not be required on the basis of variable soil AWC. However, the TDT data indicate that the soil in Zone 3 remained wetter than the critical deficit for the duration of the maize growing season (Fig. 7.6). This high EC_a zone contains mottled and poorly drained soil in a natural ponding area between confining topography. Therefore, the TDT

data enabled irrigation scheduling predicted by a water balance model to be adjusted with real-time monitoring to predict CSMD more accurately. In this case VRI is required because the soil has impeded drainage. Variable control would shut off water to this zone where the soil is wetter than predicted by the water balance model. Table 7.4 indicates that at this site, this VRI scenario would give a mean water saving of 26.3% or 73 mm ha $^{-1}$ (38.7 ML) per year for the three years investigated (2005–2007).

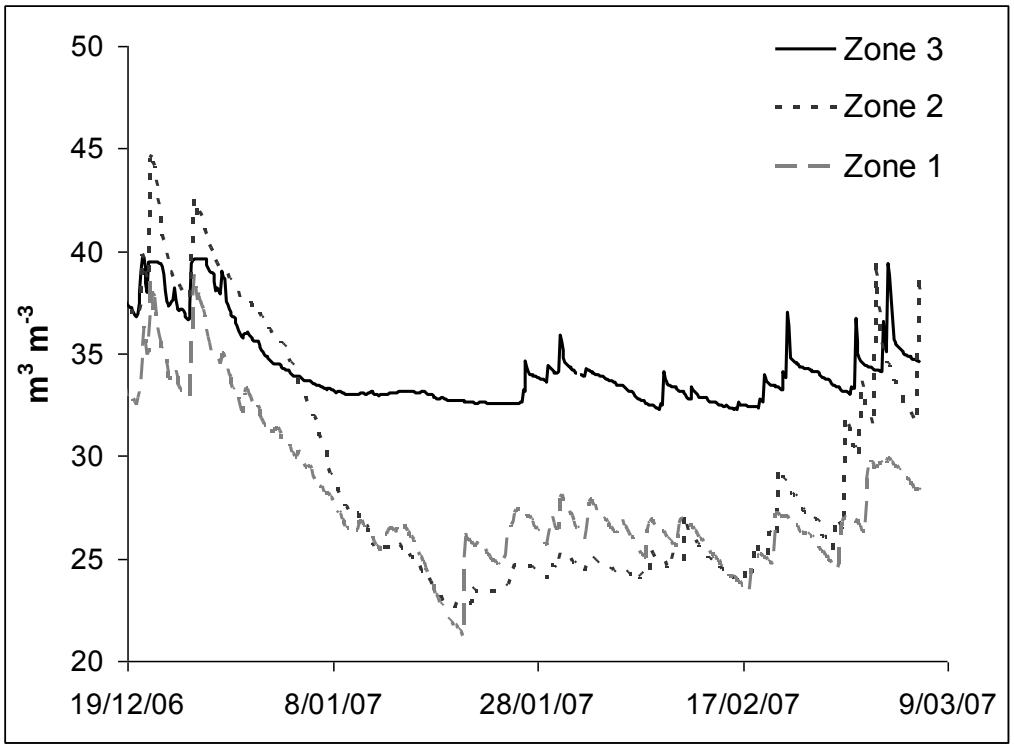

Fig. 7.6 Volumetric soil water content (m^3 m^{-3}) at Site 2 (Dec 2006 – March 2007)

7.4. Discussion

The VRI scenarios presented here show significant potential water savings of 21.8–26.3% when irrigation water is adjusted for variable soil AWCs and site-specific factors, such as poor drainage, to maintain soil water content above the critical deficit where plant growth starts to be limited. Existing machine design may preclude these potential water saving, however VRI systems are becoming available. They deliver prescribed variable irrigation

depths to different management zones using automated individual sprinkler control (Hedley et al., 2008b; Bradbury, 2009).

The cost benefits of using less irrigation water are significant in many parts of the World. For example, users in about 80% of the irrigation districts in California pay volumetric water charges, based on volume of water used per individual field (Burt, 2006). Burt (2006) notes that volumetric pricing is advocated by the World Bank. It is mandatory in many areas in the western U.S., but is still uncommon in the vast majority of irrigated areas in less developed countries. Also, when water becomes scarce, water trading may occur increasing the cost of irrigation water to the user markedly. Water trading in New Zealand is in its infancy in parts of Canterbury, South Island, where water has been over-allocated in certain areas (Morgan et al., 2002). However, in Australia, water trading has existed for about twenty years. Recently a pilot project in Australia has allowed 51 transactions involving 9.5 GL of water between New South Wales, Victoria and South Australia, which Young et al. (2000) estimated to be worth collectively over A$9.9 million; this was presumably to maintain the economic viability of communities.

The significant potential water savings by VRI technologies suggest that they will become more affordable as irrigation costs increase, as discussed by Sadler et al. (2005). In addition to cost benefits associated with water charges and reduced pumping costs, VRI allows better strategic use of allocated freshwaters. This becomes important where allocated freshwaters are limited, because the saved water can be diverted elsewhere. In this case VRI delays other strategies such as DI (Kang et al., 2000), which aim to sustain irrigation systems in a region by conserving water but are accompanied by reduced yields.

7.5. Conclusions

The mapping of EC_a is a valuable method for high resolution quantitative assessment and mapping of soil variation. Soil EC_a has been linked to the soil water-holding properties AWC and FC, enabling spatial variation of soil available water to be delineated. Daily water depletion in these zones can then be modelled using a water-balance approach enabling

VRI scheduling. Site- specific information supplied by embedded soil moisture sensors in the soil root zone at Site 2 showed that the high EC_a-defined zone was an area of poorly drained soil that remained wetter than predicted by the water balance model. Therefore, soil water balance modelling plus real-time monitoring of zone θ is desirable for reliable site-specific irrigation scheduling. The method outlined provides a powerful decision tool for VRI scheduling, and the information can be uploaded as a file that can be updated daily to a computer controlled variable rate irrigator with individual sprinkler control.

Decision tools that improve water use efficiency, such as VRI, are not only becoming cost effective in some parts of the world, but will also facilitate a more sustainable use of freshwaters.

CHAPTER EIGHT

Soil water status maps for variable rate irrigation of Waimakariri soils, Canterbury, New Zealand

This Chapter further develops the methodology for AWC map production previously used in Chapters 4, 5, 6 and 7 and also estimates potential water savings of a VRI system for a new case study area, as a further comparison to the savings established at the two sites in Chapter 7. The new case study area is a dairy pastoral soil [Canterbury pasture] in the Canterbury Plains of the South Island, New Zealand, where the majority of New Zealand's irrigation expansion has occurred over the last decade; Canterbury using two-thirds of the national allocation of freshwaters for irrigation. The chapter also develops some additional key performance indicators for comparing VRI and URI. It was written as an invited book chapter for the "GIS Applications in Agriculture" series published by CRC Press. It presents a simplified soil water balance Excel spreadsheet on CD-ROM, which readers can use to investigate different irrigation schedules for different soil AWCs. Results presented in this chapter were also presented at the 1st Irrigation New Zealand Conference in Christchurch, Canterbury, South Island, NZ in October 2008; and in the public press (SPAA Precision Ag News), and Groundbreaker magazine. In addition, they contribute to an invited article for www.precisionag.com:

Hedley CB and Yule IJ (2009) Soil water status maps for variable rate irrigation. Invited book chapter in "GIS Applications in Agriculture– Nutrient management for improved energy efficiency" 3rd book in CRC GIS in Agriculture Series (Eds. David Clay, John Shanahan, Fran Pierce) Accepted for book publication in 2010.

Hedley CB, Yule IJ, Bradbury S (2008) Spatial irrigation scheduling with soil EM mapping. In Irrigation New Zealand (Ed.), Handbook of 1st Irrigation New Zealand Conference, 14–15 October 2008, Abstract CS5:02. 56 p. Christchurch: Caxton Press.

New Zealand: Focus on Water Management. www.precisionag.com (Global Information Centre for High Technology Agriculture), uploaded December 2008

Popular articles:

Sensing for precision irrigation. In SPAA Precision Agriculture News. Volume 4 Issue 2 Autumn/Winter 2008, p15. Published by Southern Precision Agriculture Association (SPAA), South Australia ISSN1449-3705.

More efficient water use through variable rate irrigation. In Groundbreaker – the professional guide to cultivation and crop establishment. Issue 106: 22–25. Rural Contractor and Large Scale Farmer publications.

Abstract

Energy requirements and security of food production will be improved by increasing the water use efficiency of existing irrigation systems.

Agriculture uses 70–80% of allocated global freshwaters for irrigation, and in recent years increased dependence on irrigation to sustain food production for the global community is depleting freshwater resources in many part of the world below sustainable limits. These pressures can be reduced by optimising irrigation scheduling. Technological advances in irrigation, mainly in automated and semi-automated sprinkler irrigation systems, allow application of water with millimetre precision at a fixed position. In addition, variable rate sprinkler systems can apply different depths of water to different positions. This chapter presents and demonstrates a GIS soil-based decision support tool for an automated variable rate irrigation sprinkler system.

The case study presented illustrates how (i) soil total available water-holding capacity (AWC) maps can be derived from soil apparent electrical conductivity (EC_a) maps, and (ii) a daily time step can be added to the AWC map to produce a soil water status map, updated daily, available for uploading to a variable rate irrigation (VRI) system. Soil water status is defined as the millimetres of plant available water stored in the soil on any one day. This

chapter also discusses some advantages of a VRI system, including benefits for nutrient management, water savings, and energy savings.

The accuracy of these soil water status maps is dependent on how well each EC_a-defined zone can be hydrologically characterised. VRI is desirable where highly variable soils exist under one irrigation system, and has further applications for irrigating different crops under one irrigator, shutting off or reducing irrigation over exclusion areas such as raceways, gateways and low-lying and/or compacted poorly draining areas, as well as for chemigation and fertigation.

8.1 Introduction

The case study for this chapter is a 40-hectare irrigated dairy pasture near Christchurch, on the Canterbury Plains of South Island, New Zealand.

The Canterbury Plains are the largest alluvial plains in New Zealand covering 750 000 ha. Here highly variable young alluvial soils have developed in different depths of fine materials (sands and silts) over outwash gravels. Recent alluvial soils (<3000 years old) occur on low terraces that can be highly variable in depth and stoniness. A recent trend has been the conversion of these stony terrace soils, traditionally used for dry-land extensive grazing, to dairy pastures. This is accomplished by augmentation of natural annual rainfall (500–600 mm) with irrigation using centre-pivot and lateral sprinkler irrigation schemes (Fig. 8.1). This significant land-use change has occurred since 1990 when sheep farming predominated (Fig. 8.2), so that in 2006 Canterbury had become a national leader in dairy production.

One irrigation system typically irrigates an area of more than 300 ha so that where the depth of fine material to gravels is highly variable so will be the ability of the soil to hold and retain water available for plant use. A frequent consequence is over-watering of very stony soils, and in this case variable rate irrigation becomes desirable. The 2008 Environment Report of the Canterbury Regional Council recognised the significant

pressure being put onto Canterbury's lakes and rivers due to intensification of land use, allocation of freshwaters, changing climatic factors and changes arising from nutrient inputs and sedimentation. Surface water takes have doubled from about 100 $m^3 s^{-1}$ to 200 $m^3 s^{-1}$ and groundwater takes have trebled from about 50 $m^3 s^{-1}$ to 150 $m^3 s^{-1}$ since 1990. In New Zealand, irrigation demands 77% of all allocated freshwaters, and 66% of this irrigation water is used in the Canterbury region. The amount of consented irrigated land in New Zealand increased by 52% over the period 1999 to 2006, an annual rate of increase of 7% (MfE, 2007). This national increase is also largely explained by demand for irrigation by growth in the dairy industry.

Fig. 8.1 The introduction of centre-pivot irrigation systems into Canterbury, New Zealand, provides opportunities for variable rate irrigation technology to be used (photo: Google Earth, 2009)

In Canterbury, river flows have dropped from the long-term mean at nearly all monitored sites, and in some cases flows are 10–25% below the long-term mean. One of the largest recorded drops is on the Selwyn River just south of Christchurch (37% decrease), while the Rakaia River south of the Selwyn has drops of 10%. The case study for this chapter is

situated between the Rakaia and Selwyn Rivers, where a centre-pivot sprinkler system is used to irrigate dairy pastures, on Waimakariri soils.

The Waimakariri soils are widespread in this region and are relatively young alluvial soils on low terraces. The single most important factor determining their properties, like many other soils in the Canterbury Plains, is the depth of fine material over the outwash gravels. The variable nature of these soils and the need to increase irrigation and energy efficiency makes this area an excellent site for a precision irrigation management case study.

In this study an on-the-go electromagnetic (EM) mapping system was used to collect high resolution (<10 m) GPS located EC_a data, which was then kriged into EC_a maps using the Geostatistical Analyst extension tool in ArcGIS. Soil EM surveys are very useful for investigating soil salinity issues (e.g., Rhoades et al., 1993; Cassel, 2007); however, EC_a information can also be used to characterize soil texture and moisture variability (Kitchen et al., 1996; Hedley et al., 2004; Sudduth et al., 2005). The approach used to determine the available water-holding properties of soil management zones from the EC_a information is discussed and demonstrated.

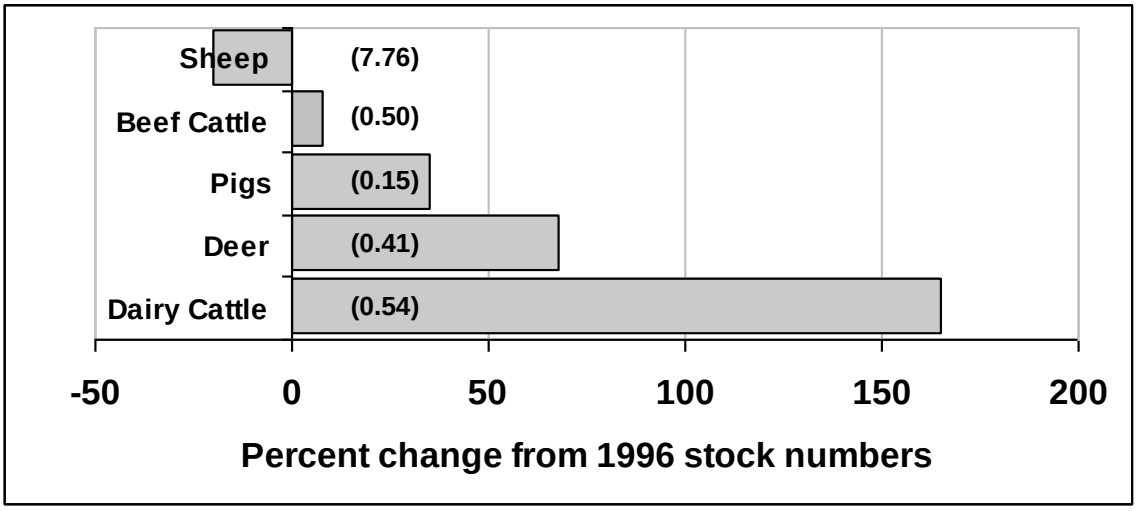

Fig. 8.2 Relative change in stock numbers in Canterbury, New Zealand, between 1996 and 2006, with estimated 2002 population totals (millions) in brackets (Statistics NZ) (ECan, 2009)

Variable rate irrigation (VRI) scheduling requires knowledge of plant demand as well as soil supply of available water at any position on any day (Hedley & Yule, 2009). Two methods for monitoring the drying and wetting patterns are (i) a daily water balance model and (ii) in situ soil moisture monitoring. AWC can then be adjusted on a daily basis to produce soil water status maps for spatial irrigation scheduling. The map is available to upload to an automated PC-controlled variable rate sprinkler system. Sprinkler systems with VRI control of individual sprinklers are being developed with varying degrees of automation (Kim et al., 2008; Bradbury, 2009), to address the need for improved water use efficiency.

Precision irrigation decisions can be crop-based or soil-based. The emphasis of this chapter is the development of a soil-based decision support tool, so that precision irrigation can be applied on a basis of soil differences. This is particularly important in regions where highly variable, young, alluvial soils exist, such as in many parts of New Zealand.

8.2 Methods

8.2.1 Site selection

The dairy farm lies 50 km WSW of Christchurch. Here a 600-m centre-pivot sprinkler irrigation system was installed to irrigate dairy pastures for the seasonally dry part of the year, typically November through to March. A 40-ha portion of the irrigated zone was selected for this study. Regional statistics suggest that irrigation can increase pasture dry matter production from 6.4 T DM ha^{-1} yr^{-1} to at least 11.1 T DM ha^{-1} yr^{-1}. Stocking rates are 3.3 cows ha^{-1} with irrigation. To minimize feed deficits, 200 kg N ha^{-1} yr^{-1} are typically applied.

The soils at this site are mapped as Waimakariri soils (Weathered Fluvial Recent soils), characterised by varying depths of fine sandy material with wide-ranging stoniness, over outwash gravels which occur at varying depths.

8.2.2 Apparent Electrical Conductivity (EC_a) Mapping

A Geonics electromagnetic EM38 sensor (Geonics Ltd, Mississauga, Ontario, Canada) and real-time kinematic-differential global positioning system (RTK-DGPS) with Trimble Ag170 field computer (Trimble Navigation Ltd, Sunnyvale, California, USA) on-board an all-terrain vehicle (ATV) were used for on-the-go soil EC_a mapping. The ATV was driven at 12 km h^{-1} at swath widths of 10 metres. Soil apparent electrical conductivity (EC_a), measured by the EM38 sensor, was logged simultaneously with high resolution positional data every second. The EC_a and positional data were collected on a data memory card in the Ag170 field computer.

8.2.3 GIS Manipulation of the EM data

Data were extracted from the data memory card, and manipulated into a suitable file format in an Excel spreadsheet for interpolation and map production in ArcGIS. The process for importing data into ArcGIS, transforming the WGS84 coordinates to local coordinates (in this case NZMG'49), setting a field boundary, and raster interpolation for EC_a map development, followed the method detailed by Cassel (2007) in Chapter 8, in the first book of this series, "GIS Applications in Agriculture" (Pierce & Clay, 2007). Cassel (2007) provides a step-by-step account of a procedure similar to the one which is summarised below.

- Positional and sensor data was imported into ArcMap as a csv file. This data was then displayed and converted into a shapefile.
- A new polygon shapefile was created in Arc Catalogue and moved into the map document. This file was used to define the outline shape of the sensor data using Editor.
- Ordinary kriging was used in Geostatistical Analyst to develop the EC_a prediction map. Variogram models of the sensor data were compared to assess which one best characterised the data, and in this case a spherical variogram was used. The kriged surface was exported as a raster file.

- The raster surface was clipped to the shape of the polygon outline file using Spatial Analyst/Extraction/Extract by Mask.
- The clipped raster was then classified into three zones, by right clicking on the file and selecting Symbology in Properties. Colour coding was also set in Symbology.

The three soil EC_a classification zones were targeted for soil sampling for AWC estimation.

8.2.4 Estimation of Soil AWC in EC_a-defined Management Zones

The soil total available water-holding capacity (AWC) of each EC_a-defined management zone (high EC_a zone, intermediate EC_a zone, low EC_a zone) was estimated by soil sampling at three replicate sites within each zone.

AWC is defined as the difference between the equivalent depths of water that the effective root zone (or a sampling depth within that root zone) contains at field capacity (FC) and at permanent wilting point (WP). It is preferable to determine FC in situ, i.e. in the field, to account for interactions between horizons in the soil profile. It is estimated here as the equivalent water depth held after 2 days of free drainage following a heavy rain (or irrigation) event. WP is also best estimated in the field using the crop of interest, although this was not possible at this irrigated site.

The soil was sampled to 60 cm depth to include the majority of roots, which extract the soil water for plant use. Soil samples (0–15 cm, 15–30 cm, 30–45 cm, 45–60 cm) were collected when the soils were at FC in August 2008, for estimation of field moist soil water content (i.e. FC), bulk density, percent stones, and a laboratory estimation of WP. Small intact soil cores (55 mm × 25 mm) were collected, where possible, to assess bulk density. In cases where the soils were too stony to enable intact soil cores to be collected for bulk density estimation, the bulk density of a neighbouring sample was extrapolated to this sample depth. Percent stones was determined by collecting bagged samples to a defined depth. Larger stones were sieved out and weighed in the field and the remaining samples

were taken back to the lab for calculation of the remaining percent stones. WP was assessed from the gravimetric soil water content of repacked 2-mm sieved soil samples equilibrated at a tension of 1500 kPa, on a 15-bar pressure plate extractor (Soilmoisture Equipment Corp. 1500, Santa Barbara, CA, USA).

8.2.5 Soil Water Balance

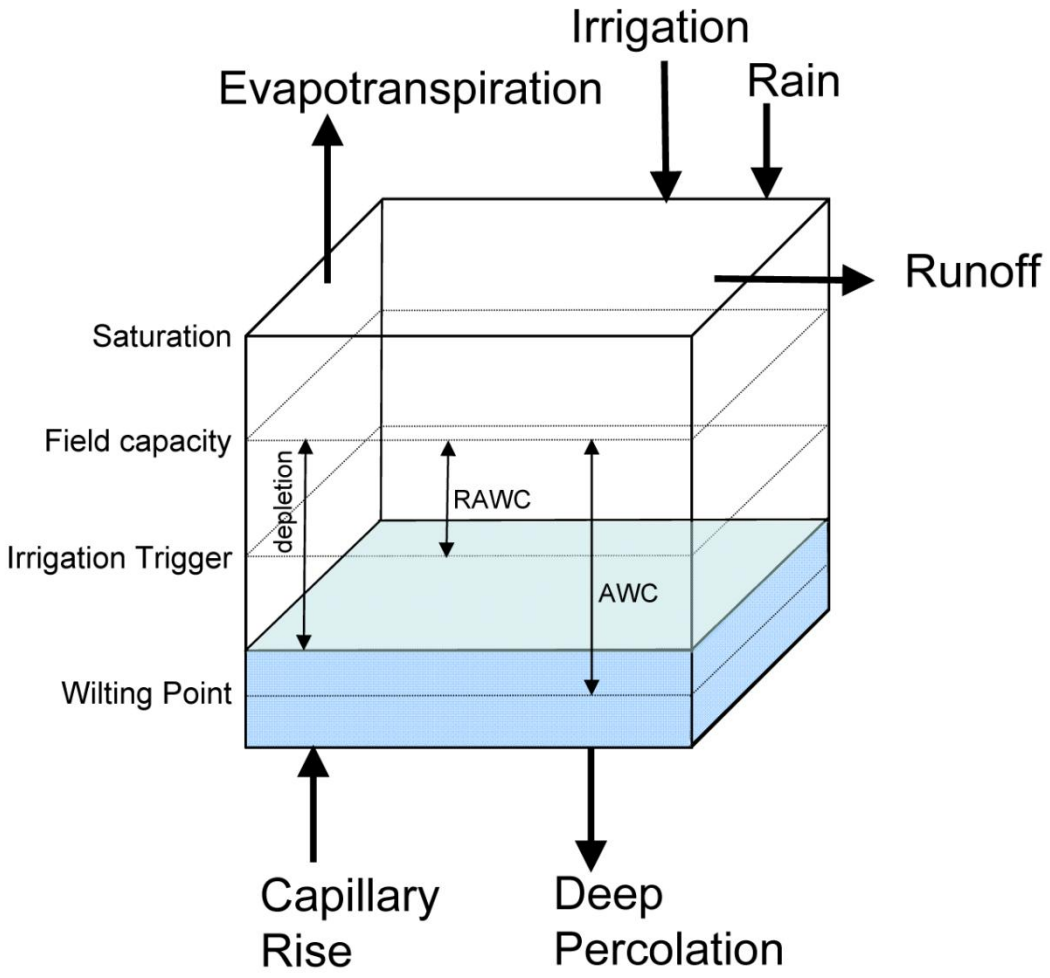

Fig. 8.3 Diagram to represent the soil water balance of a root zone (adapted from Allen et al., 1998). RAWC = readily available water-holding capacity; AWC = total available water-holding capacity (AWC)

A soil water balance was used to estimate the soil water deficit on any one day. Model inputs are (i) soil AWC value; (ii) daily rainfall; (iii) daily regional calculation for potential evapotranspiration (PET); and (iv) irrigation events. Model outputs are (i) soil moisture deficit on any one day, and (ii) expected runoff and deep percolation (estimated as the excess water when soils reach FC) (Fig. 8.3).

The soil water balance was initiated on 3 August 2007, a day when the soils were expected to be at FC, after a cool, wet winter period and large winter rainfall event (34 mm). Capillary rise was assumed to be zero in these soils, as the depth of water table was sufficient to maintain the capillary fringe below the lower level of the root zone.

The Excel spreadsheet (Fig. 8.4) was used to calculate the daily soil moisture deficit (SMD) for each EC_a-defined zone. A simplified version of the soil water balance spreadsheet used in this study is provided on the CD which accompanies this book, and step-by-step details for its use are given in the Appendix to this chapter. It uses climatic data obtained from a nearby meteorological station, which is freely accessed from a website (http://cliflo.niwa.co.nz/). The first worksheet in this Excel file provides the data specific to this case study. The second worksheet provides a soil water balance template for the user to enter their own site-specific data. Required inputs are site-specific daily rainfall and PET data, soil AWC (≤250 mm) and trigger point for irrigation. The worksheet automatically calculates the optimal irrigation schedule. The depth of irrigation can be changed (≤50mm).

				WITH IRRIGATION					NO IRRIGATION			
Year	INPUT Rain (mm)	Irrigation (mm)	INPUT Er (mm)	E (mm)	D (mm)	S (mm)	SMD (mm)	IRRIGATION EVENT (IE) (mm)	E (mm)	D (mm)	S (mm)	SMD (mm)
3/08/2007	**0**	0	**1**	1	0	101	-3	0	1	0	101	-3
4/08/2007	**34**	0	**1**	1	33	101	0	0	1	33	101	0
5/08/2007	**0**	0	**1**	1	0	100	-1	0	1	0	100	-1
6/08/2007	**0**	0	**0**	1	0	99	-2	0	1	0	99	-2
7/08/2007	**0**	0	**1**	0	0	99	-2	0	0	0	99	-2
8/08/2007	**0**	0	**1**	1	0	98	-3	0	1	0	98	-3
9/08/2007	**0**	0	**2**	1	0	97	-4	0	1	0	97	-4
10/08/2007	**0**	0	**2**	2	0	95	-6	0	2	0	95	-6
11/08/2007	**0**	0	**2**	2	0	93	-8	0	2	0	93	-8
12/08/2007	**6**	0	**1**	2	0	97	-4	0	2	0	97	-4

Fig. 8.4 Part of the Excel spreadsheet used to predict daily soil moisture deficit and irrigation events for each soil zone (see Appendix) [Er = reference E_t; E = actual E_t; D = drainage; S = available water stored in the soil; SMD = soil moisture deficit]

As a rule-of-thumb irrigation should commence when approximately half the plant-available water (AWC) has been used up. Specific depletion factors and methods for determining this "irrigation trigger", "critical deficit" or "stress point" (SP) are given in Allen et al. (1998). The trigger point marks the point where the available water in the soil is no longer readily available to the plant, and evapotranspiration (E_t) from that plant falls below its potential rate. The transpiration (T) component of E_t is directly related to plant yield. If the plant transpires at its potential rate it will usually achieve potential yield, assuming no other limiting factors. If the plant transpires below its potential rate, due to inadequate supply of readily available water, then yield will usually reduce proportionally (Allen et al., 1998).

8.3 Results and Discussion

8.3.1 EC_a Map and Soil Water-holding Properties

The EC_a map separates the field into three areas with different soil characteristics (Fig. 8.5). Soils in the high EC_a zone are deep sandy soils with no stones, characterised by 20 cm

deep topsoils over 10–30 cm sandy loam subsoils. Below this a transition BC horizon extended to a depth varying between 45 cm and > 1 m over outwash gravels. In contrast, the low EC_a zone is characterised by stony–very stony topsoils and subsoils, each typically about 15 cm in depth, overlying a transition BC horizon, with outwash gravel parent materials occurring at 45-cm depth (Table 8.1).

Table 8.1 Soil AWC, FC, Wilting Point and Percent Stones for each EC_a–defined zone. AWC, FC, and WP are expressed as a depth of water (mm) in each sampling depth, and in the site mean depth (60 cm)

Soil	EC_a range	Sample depth	AWC	Field Capacity	Wilting Point	Percent Stones
	mS m^{-1}	cm	mm	mm	mm	%
Waimakariri sandy loam	14.7–16.7	0–15	46	58	12	0
		15–30	21	28	7	0
		30–45	17	20	4	0
		45–60	17	20	3	0
Site mean		*0–60*	*101*	*126*	*26*	*0*
Wamakariri stony sandy loam	13.7–14.6	0–15	32	39	7	43
		15–30	20	23	3	68
		30–45	11	13	2	23
		45–60	11	13	2	23
Site mean		*0–60*	*74*	*88*	*14*	*39*
Waimakariri very stony sandy loam	12.5–13.6	0–15	12	20	7	42
		15–30	18	21	3	75
		30–45	7	9	1	81
		45–60	7	9	1	81
Site mean		*0–60*	*44*	*59*	*12*	*70*

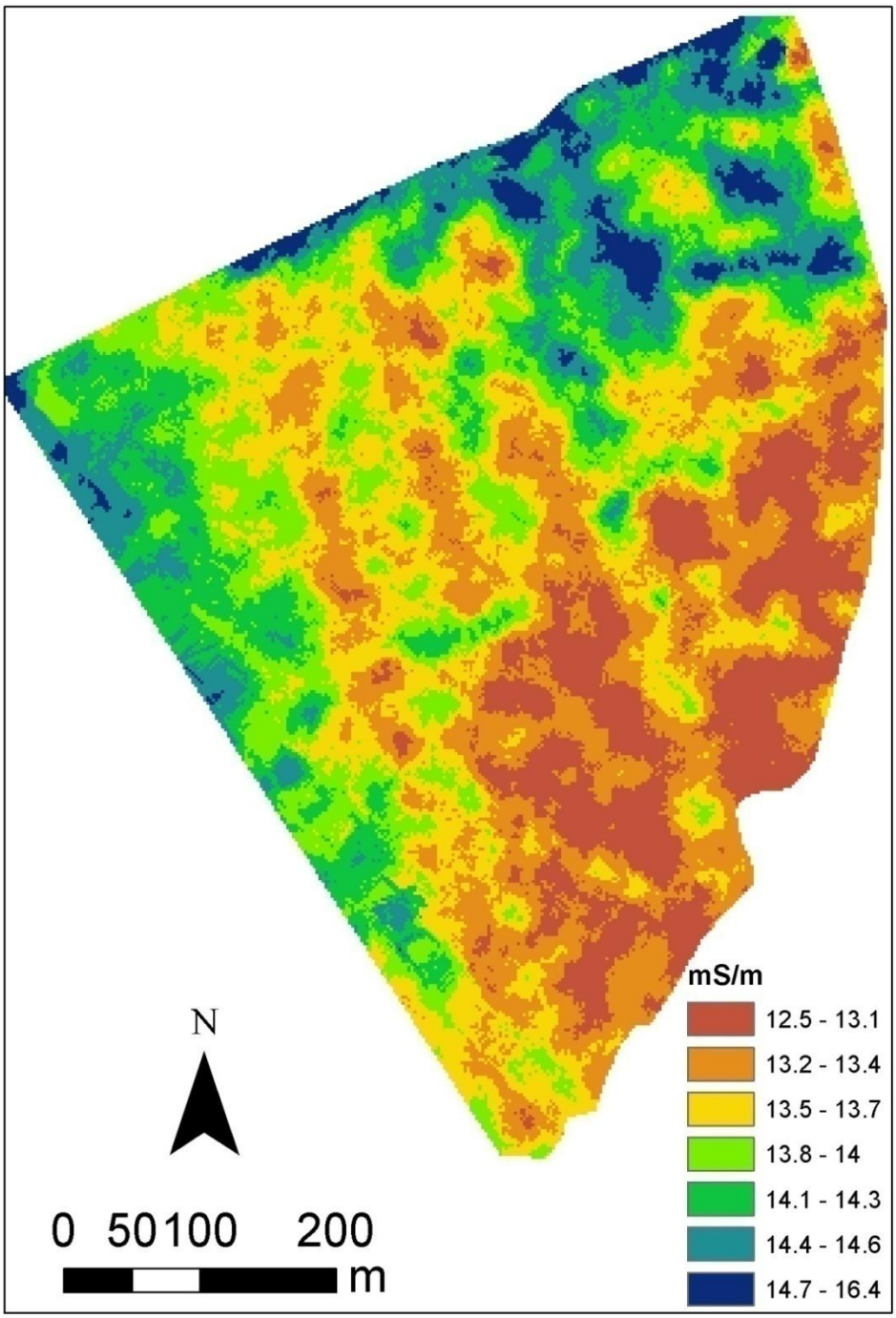

Fig. 8.5 **EC_a map of the 40-ha Canterbury dairy pasture on Waimakariri soils, irrigated by a centre-pivot sprinkler irrigation system**

Data from Table 8.1 were used to develop a relationship between soil EC_a and AWC (Fig. 8.6).

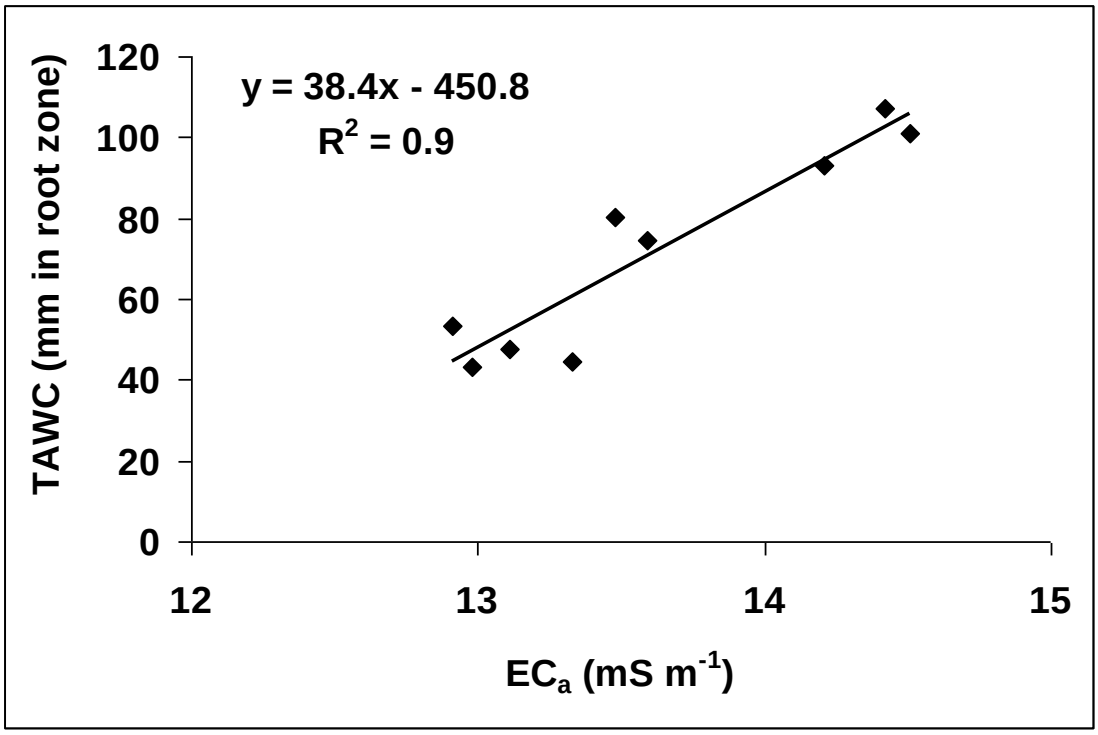

Fig. 8.6 Relation of soil EC_a to AWC for Waimakariri soils, at the study site

The relationship shown in Figure 8.6 was used to predict soil AWC from the high density EC_a dataset, and the resulting AWC map is shown in Figure 8.7.

The soil AWC varies considerably at this site, ranging from 36 to 144 mm. Assuming a mean evapotranspiration rate of 4 mm for the hottest months of November to February, the most stony soils, with lowest AWC will reach the irrigation trigger point (0.5 AWC) after just 4–5 days of drying from FC; while the stone-free sandy soils are able to store enough readily available water for about 18 days.

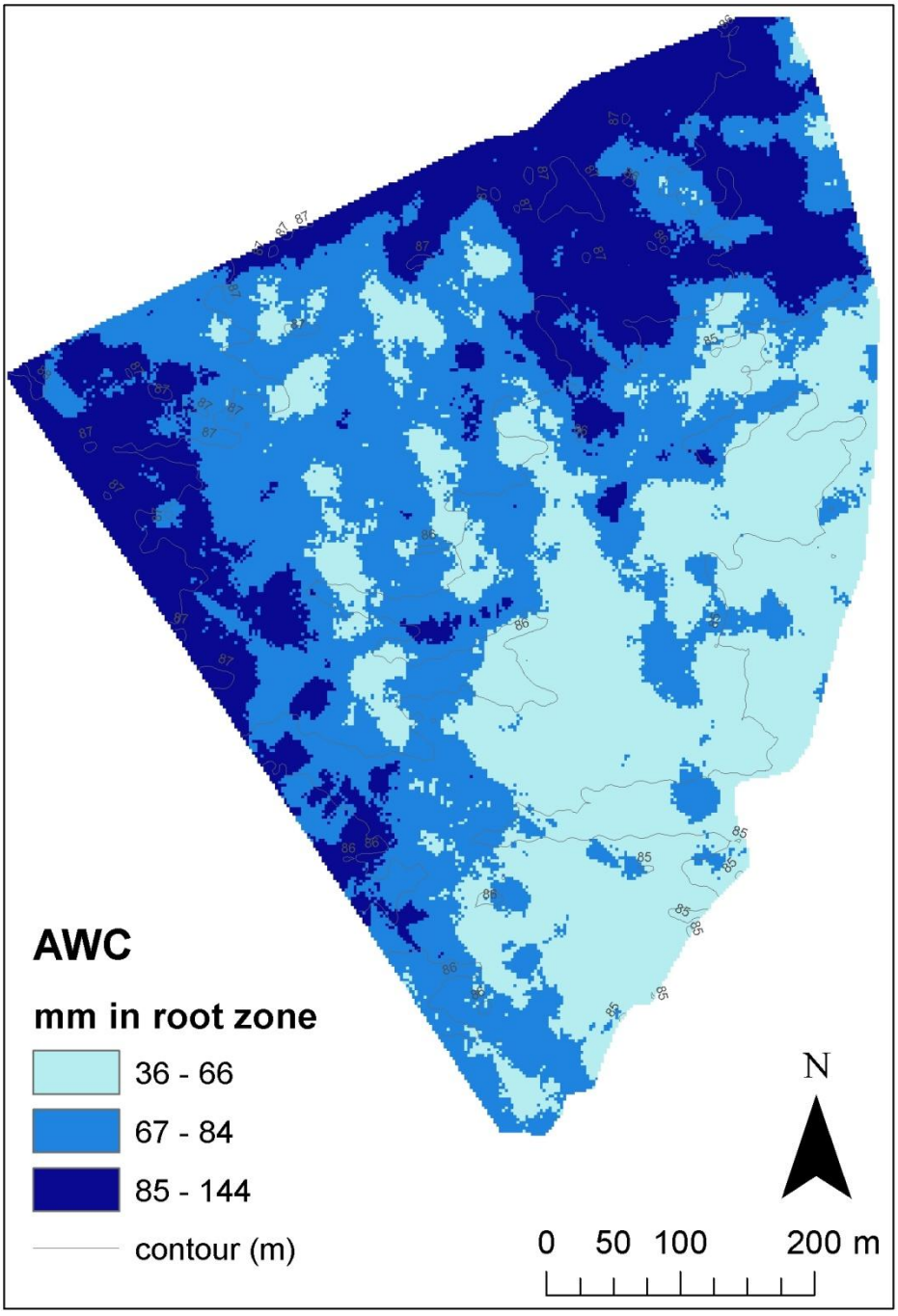

Fig. 8.7 **AWC map (maximum mm available water in the root zone) of the 40 ha dairy pasture, irrigated by a centre-pivot sprinkler irrigation system**

8.3.2 Soil Water Balance and Irrigation Scheduling

A soil water balance was used to track the wetting and drying patterns of soils in the three management zones. Daily rainfall and E_t data were obtained from the closest meteorological station, and soil AWC was adjusted for each soil zone. The soil water balance was updated daily to provide a real-time irrigation scheduling tool.

The water balance predicts the day on which the soil trigger point is reached, and irrigation should commence. Hypothetical variable rate irrigation scheduling applies 10 mm of irrigation to Zone 3 (AWC 44 mm) on 1 September, 2007. The first irrigation event scheduled to Zone 2 (AWC 73 mm) for the 2007/08 summer season is on 30 September, and Zone 1 (AWC 101 mm) soil water storage is sufficient to readily supply water to pasture until its first scheduled irrigation event on 25 October 2007 (Fig. 8.8). The water balance was also used to compare total irrigation water demands under a VRI system compared with a URI (uniform rate irrigation) system. URI assumes that to obtain potential yield the whole site is irrigated to the trigger point of the zone with the smallest AWC, maintaining readily available water in these stony soils and all other zones. In contrast, VRI irrigates each soil zone to its specific trigger point. We have calculated hypothetical 10 mm irrigation events for VRI and URI, and the results for the 2007/2008 season are presented in Figure 8.8. The water savings using VRI are quantified in Table 8.2 for August 2007 to December 2008.

Table 8.2 Potential water savings of VRI compared with URI for Waimakariri soils at the study site

Site	Zone	Area	Irrigation amount		Irrigation events	Total volume	Mean depth
		ha	mm	m^3 ha^{-1}	days	ML	mm
URI							
Total		40	520	5200	52	208	520
VRI							
Waimakariri sandy loam	1	9	440	4400	44	40	
Waimakariri stony sandy loam	2	20	470	4700	47	94	
Waimakariri very stony sandy loam	3	11	520	5200	52	57	
Total		40				191	477
VRI – URI Water Saving							
					%	ML	$mm\ ha^{-1}$
					8	17	43

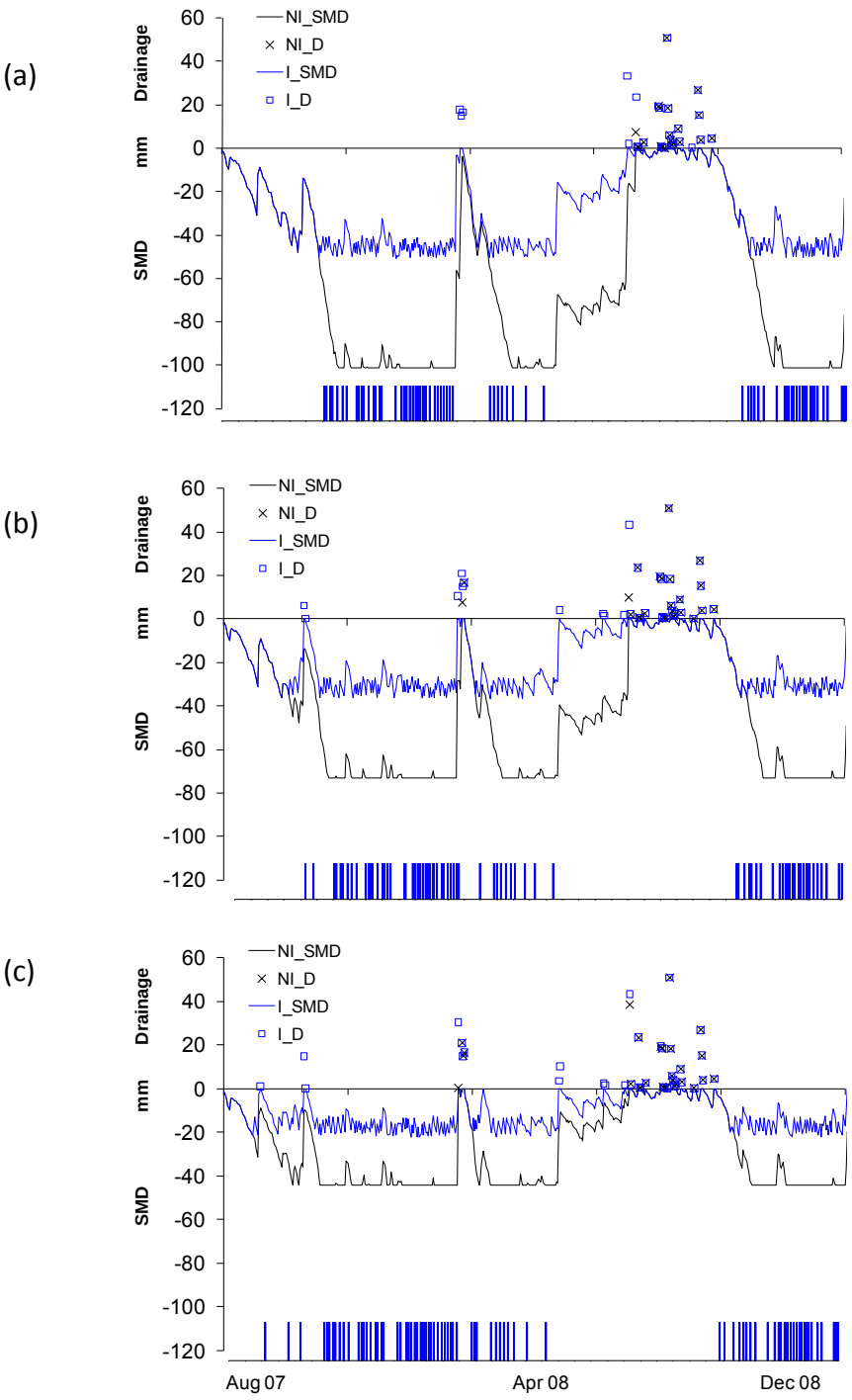

Fig. 8.8 **Soil moisture deficit (SMD, mm), drainage (□ , X, mm) and 10 mm irrigation events (vertical bars at the bottom of each graph) for the 3 soil zones (a = Zone1-AWC 101 mm; b = Zone2-AWC 73mm, c = Zone3-AWC 44 mm) from August 2007, when the soils were at FC, to December 2008. NI = no irrigation; I = irrigation; D = drainage/runoff**

The relationship between soil water storage and EC_a on any day can be determined and used to predict the soil water status map. EC_a values were extracted from the EC_a map, for each sampling site position, as described in the next paragraph.

- A shapefile of the soil sampling GPS positions was imported into the EC_a map document in ArcMap.
- EC_a values were extracted using Spatial Analyst in Arc Toolbox, and selecting the option Extraction/Extract Values to Points. The input point feature file is the GPS position shapefile, the input raster is the EC_a raster, and a new output point features file is created with EC_a values extracted for each GPS co-ordinate.
- The extracted EC_a data point values can be viewed by right-clicking on the new file and viewing the new "raster value" column in the Attribute Table. The attribute table can be exported as a dbf file and opened in Excel.

Figure 8.9 shows the relationship between soil EC_a and predicted soil water storage in the root zone (mm) for 3/08/07 (FC) and 1/09/07, 29/09/07 and 24/10/07 when Zones 1, 2 and 3 received their first spring-time irrigation, respectively, as the soils began to dry out after the wet winter months.

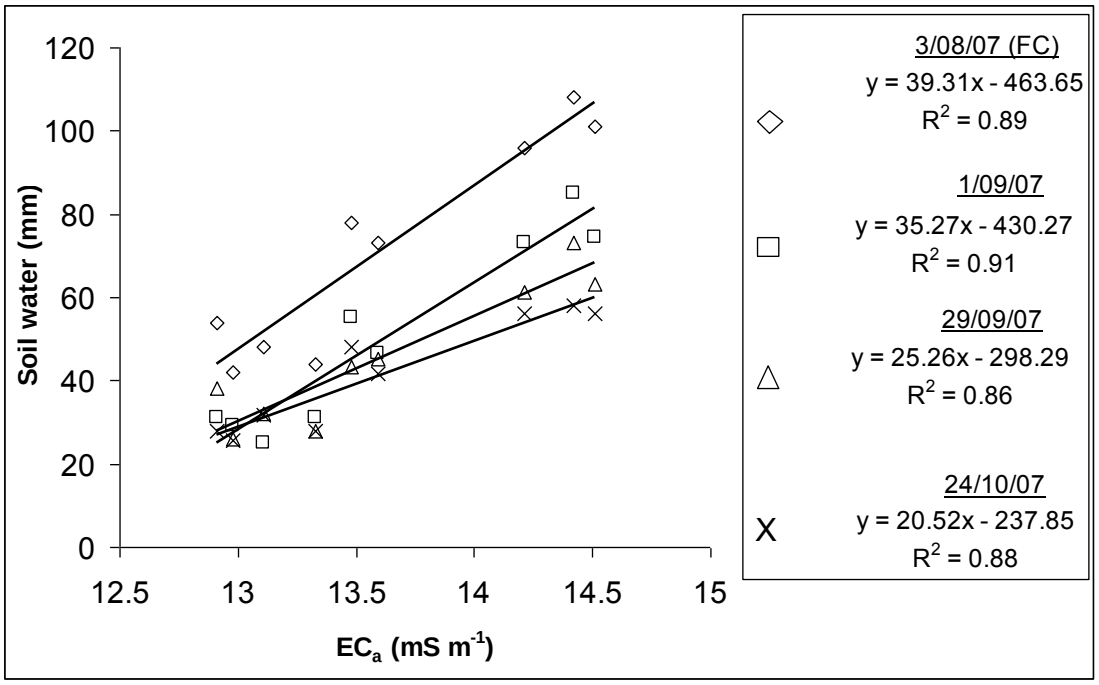

Fig. 8.9 Linear regression models of soil water balance-predicted soil available water status (mm available water in the root zone) against soil EC_a on 3/8/07, 1/9/07, 29/9/07 and 24/10/07 for each soil profile analysed

The linear regression model is used to interpret the high resolution EC_a dataset in terms of soil water status on any one day, and the maps produced are available for uploading to a VRI system to control irrigation scheduling to specified zones on specified days.

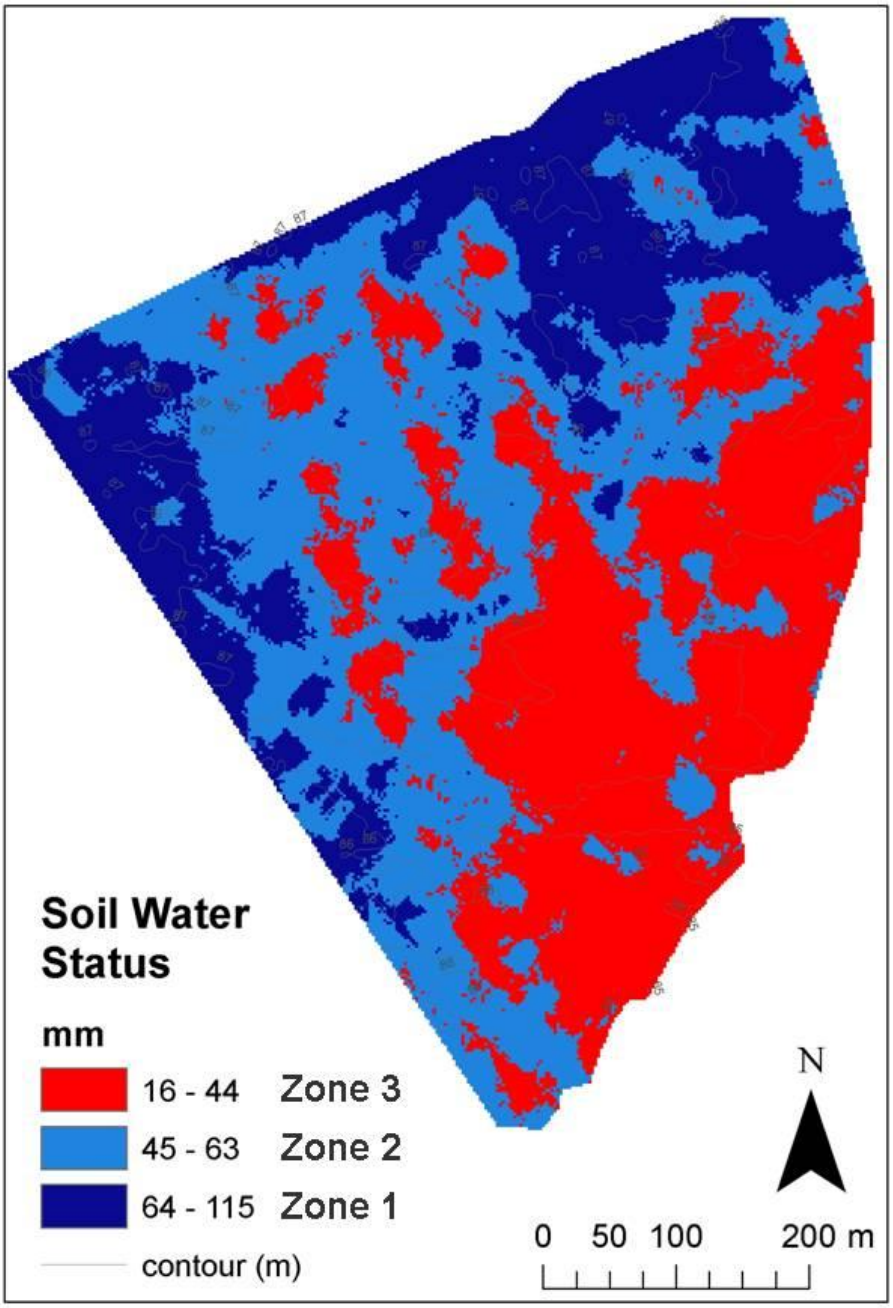

Fig. 8.10 **Soil water status map for 1 September 2007, indicating the mm available water in each zone on that day and delineating the management zone (Zone 3) that requires irrigation (in red)**

8.3.3 A comparison of VRI and URI key performance indicators

A key performance indicator of any irrigation system is it's water use efficiency, defined here as the millimetres of irrigation water applied per tonne of dry matter production. URI and VRI aim for maximum potential yield by maintaining soil water status above the plant stress point so that water is readily available to the plant. Other irrigation strategies, such as deficit irrigation, aim for efficient conversion of each millimetre of irrigation to DM production, with strategic timing, but withhold water at certain times beyond the SP, so that potential yield may not be achieved. Deficit irrigation strategies for pasture may be used when allocated freshwaters are limited, precluding URI or VRI. Section 8.3.2 discussed the potential water savings of VRI compared with URI, and this section explores further potential benefits of a VRI system compared with a URI system, using key performances indicators (KPIs).

KPIs considered are:

(i) water use

(ii) irrigation water lost as drainage and runoff

(iii) energy usage

(iv) irrigation water use efficiency (IWUE).

Water use and drainage/runoff KPIs are calculated from the soil water balance (see Table 8.3 for details). Energy use is calculated as kWhr m^{-3} water applied, using a factor of 0.42 kWhr m^{-3} irrigation water applied, based on a recent survey of New Zealand irrigation systems (FAR, 2008) and then converted to kg CO_2-eq using an implied emission factor of 0.18 kg CO_2-eq per kWhr electricity consumed (NZ MED, 2008). The IWUE index uses a reported dairy pasture production of 17.6 T DM ha^{-1} yr^{-1} for a similar soil in this region (LIC, 2008) to calculate millimetres of irrigation water applied per tonne DM produced (Table 8.3; Fig. 8.11).

Table 8.3 KPIs for VRI and URI of the case study irrigated dairy pasture in Canterbury, New Zealand

KPI	Units	Description
Water Use	mm season^{-1}	Total amount of irrigation water applied in one season (1 July 07 – 30 June 08)
Drainage/Runoff	mm season^{-1}	Drainage and runoff during one season (1 July 07 – 30 June 08), calculated as excess above FC by the soil water balance model; implications for nutrient leaching,
Energy usage	kg CO_2-eq	Energy usage (kWhr m^{-3}) for operation of irrigation system (largely cost of pumping water) converted to equivalent CO_2 emissions
Irrigation Water Use Efficiency	mm T^{-1} DM	Reports mm of irrigation water applied per tonne DM produced

An 8% reduction in water use by VRI compared with URI is accompanied by a 43% reduction in excess water lost as drainage and runoff over the 2007–2008 period. This implies that any potential nutrient leaching is reduced under VRI. Increased dissolved N concentrations in lowland rivers have been observed in this region over the past decade, associated with the introduction of high productivity dairy farming systems, and VRI is one method of mitigating against increasing levels of N leached into waterways, resulting in better utilisation of nutrients applied, by minimising drainage and runoff.

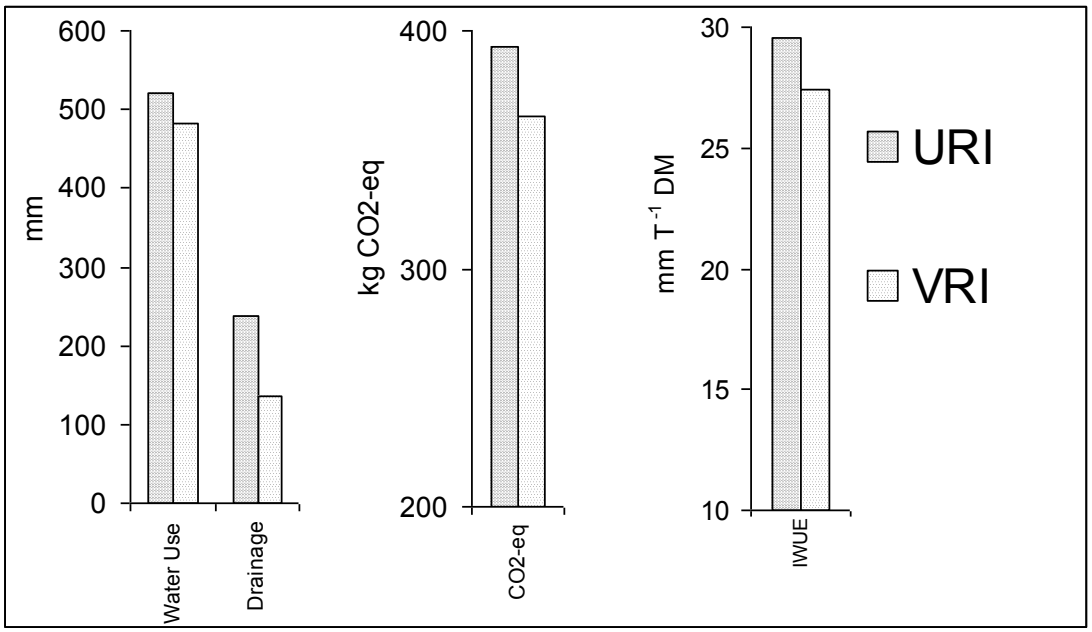

Fig. 8.11 A comparison of KPIs of VRI and URI for a 40 ha irrigated dairy pasture in North Canterbury, New Zealand

Energy used by VRI scheduling was 181 kWhr ha^{-1} (650 MJ ha^{-1}) less than URI, due primarily to the reduced requirement for pumping, directly related to water savings, with an estimated financial return of about NZ$86 ha^{-1}. This mitigates greenhouse gas emissions, with a saving of 33 kg CO_2-eq ha^{-1} yr^{-1}. The IWUE KPI indicates that VRI gave more dry matter production per mm of irrigation water applied.

These KPIs illustrate the overall benefits of VRI scheduling based on soil AWC differences.

8.4 Conclusions

Soil EC_a increased with decreasing percent stones in the soil profile at this irrigated dairy pasture site on Weathered Fluvial Recent, Waimakariri soils, in North Canterbury. In addition soil EC_a was strongly related to soil AWC (R^2 = 0.9) so that a linear regression model could be used to predict AWC from soil EC_a for the production of a AWC map. A daily time step was added to the AWC map using a soil water balance model to produce

daily soil water status maps. These maps are available to upload to an automated VRI system for spatial irrigation scheduling. At this site, VRI applies the first irrigation in late Spring to the very stony soil (AWC = 44 mm) on 1 September 2007 and delays irrigation to the intermediate AWC zone by 29 days and to the highest AWC soil zone by 54 days, optimising the use of stored soil water. Overall irrigation water savings using VRI scheduling was 8% for the season 1 July 2007 to 30 June 2008. This was accompanied by a 43% reduction in drainage and runoff, because VRI uses stored available water above the SP before applying irrigation, reducing the likelihood and frequency of soil moistures greater than FC. This implies that VRI will reduce the risk of nutrient leaching through the soil profile, with increased nutrient use efficiency compared with URI. This is an important mitigation strategy for N leaching in this region which has experiencing increases in groundwater N due to increased N leaching from dairy pastures over the last decade. In addition, in comparison with URI, VRI gave improved water use efficiency and reduced overall energy use, mitigating CO_2 emissions.

VRI optimises the amount, timing and positioning of irrigation scheduling under one irrigation system, and this optimisation is accompanied by a number of environmental and resource use benefits.

8.5 Appendix

The SWBsimple.xls file can be found in the Chapter 8 Folder on the CD accompanying this thesis. Worksheet One provides the soil water balance (with and without irrigation) for this case study. Worksheet Two provides a soil water balance template for the user to enter their own site-specific data.

Worksheet One:

1. Worksheet 1 “Soil WB” contains the Rainfall and PET climatic data for the Selwyn case study, and calculates and plots the daily soil moisture deficit (SMD, mm) for the period 3 August 2007 to the end of 2008 (with irrigation and without irrigation).

2. The soil water balance (SWB) example in “Soil WB” worksheet starts in mid-winter, after a heavy rainfall (34 mm), and assumes that the SMD is brought to 0 (i.e. field capacity, FC). At this time, the soil storage of plant available water (S) = 101 mm (i.e. AWC).

3. Hypothetical irrigation events are input to the spreadsheet to maintain the SMD above the Irrigation Trigger (S = 50.5 mm). The irrigation trigger in this example is set at a depletion factor of 0.5 AWC.

4. Different values for AWC and “Irrigation Trigger” are input to this worksheet to assess the total irrigation requirement for one season of each soil management zone (with a unique AWC value) for the Selwyn case study.

Worksheet Two:

5. Worksheet 2 “SoilWB_template” is available for calculating the SWB for any soil and climatic region. Input site name to cell C1, a value for soil AWC to cell C2 (≤ 250 mm), a value for the Irrigation Trigger to cell C3 and a depth of irrigation into cell I1 (≤ 50 mm).

6. Input daily rainfall data into column B and a regional or site-specific reference value for potential evapotranspiration (PET) into column D. Reference PET is calculated for a uniform grass sward cover and this can be adjusted for any crop type and stage (see Allen et al., 1998). Dates can be adjusted, but the SWB should start at a point where the soils are considered to be at field capacity, (SMD = 0).

7. Worksheet 2 will automatically calculate an irrigation schedule for this period of time. It also provides the total irrigation requirement for the period of interest in cell I4.

CHAPTER NINE

Key performance indicators for simulated variable rate irrigation of variable soils in humid regions

This chapter develops the discussion of key performance indicators (KPI), developed in Chapter 8, for comparison of VRI with URI. It uses biophysical models to estimate and compare nitrogen leaching, and introduces the concept of virtual water. The biodiversity value of New Zealand freshwaters is discussed, acknowledging and explaining the multiple ecological benefits of improving irrigation water use efficiency. This chapter uses the case study from the previous chapter [Canterbury pasture] and extends the number of KPIs used and the period of analysis (2004–2008). It also uses two new case studies (a Manawatu sand country maize grain site [Manawatu Sand Country maize]; and an Ohakune volcanic soils potato field [Ohakune potatoes]). It presents the KPIs on a radar chart to illustrate and compare the water and energy efficiencies of the three case studies. The radar chart and virtual water analysis provides a partial initial comparison of the life-cycle assessment of primary production at these three sites.

Research reported in this chapter has been accepted for presentation at three conferences, and accepted for publication in the Transactions of the American Society of Agricultural and Biological Engineers (ASABE):

Hedley CB, Yule IJ, Tuohy M, Collins A (2008) Development of high resolution proximal sensing methods for mapping daily soil water status for variable rate irrigation. In Proceedings Joint Conference of the New Zealand and Australian Soil Science Societies Soils 2008 Conference, 30 November – 5 December, 2008, Palmerston North, New Zealand.

Hedley CB, Yule IJ, Tuohy MP, Vogeler I (2009) Key performance indicators for variable rate irrigation implementation of variable soils. In Proceedings of ASABE Annual International Meeting, June 21–24, 2009, Reno, Nevada.

Hedley CB, Yule IJ, Tuohy MP, Vogeler I (2009) Key performance indicators for simulated variable rate irrigation of variable soils in humid regions. Transactions of ASABE 52(5): 1575–1584, Submitted June 09, Revised July 09, Accepted July 09.

Hedley CB, Yule IJ, Bradbury S, Scotter D, Vogeler I, Sinton S (2009) Water use efficiency indicators for variable rate irrigation of variable soils. Accepted for presentation at the 13th Symposium on Precision Agriculture in Australasia, 10–11 September, University of New England, Armidale, NSW, Australia.

Abstract

Decision support tools for precise irrigation scheduling are required to improve the efficiency of irrigation water use globally. This chapter presents a method for mapping soil variability and relating it to soil hydraulic properties so that soil management zones for variable rate irrigation can be defined. A soil–water balance is used to schedule hypothetical irrigation events based on (i) one blanket application of water to eliminate plant stress, (uniform rate irrigation, URI) and compares this to (ii) variable rate irrigation (VRI), where irrigation is tailored to specific soil zone available water-holding capacity (AWC) values. The key performance indicators: irrigation water use, drainage water loss, nitrogen leaching, energy use, irrigation water use efficiency (IWUE) and virtual water content are used to compare URI and VRI at three contrasting sites using 4 years climate data for a dairy pasture and maize crop and 2 years climate data for a potato crop. Our research found that VRI saved 9–19 % irrigation water, with accompanying energy saving. Loss of water by drainage, during the period of irrigation, was also reduced by 25–45% using VRI, which reduced the risk of nitrogen leaching. Virtual water content of these three primary products further illustrates potential benefits of VRI and shows that virtual water content of potato production used least water per unit of dry matter production.

9.1 Introduction

Variable rate irrigation (VRI) delivers different depths of irrigation water simultaneously to different parts of a field, preferably with high spatial resolution (<10 m or better). Lateral and centre-pivot sprinkler systems are well suited to VRI if modified with individual sprinkler control (King & Kincaid, 2004; Dukes & Perry, 2006; Pierce & Elliott, 2008; Bradbury, 2009), and other systems (e.g. surface and subsurface drip, towable spraylines, rain-guns) can also be employed but in general are less well suited with lower spatial resolution and accuracy of application.

The benefits of VRI include increased flexibility for mixed cropping (with different irrigation requirements), ease of chemigation and fertigation (reduced traffic reduces fuel costs and risk of soil compaction on wet soils; precision application), and the ability to shut-off water as the irrigator passes over farm tracks, ditches etc. In addition, where one irrigation system exists over an area of variable soils, VRI can help to maintain soil water status within the optimum range for maximum potential yields (Hedley & Yule, 2009), making best use of stored soil profile water, and minimizing run-off and deep percolation. VRI therefore enables strategic water use with improved water use efficiency.

Practitioner decisions to invest in VRI technologies will be driven by the perceived value of these benefits. Where water allocations are restricted (e.g. Kang et al., 2000: Kirda, 2002) and water charges exist (e.g., Burt, 2006) the economic benefits of improved water use efficiency (kg yield per amount of irrigation water applied) and reduced energy costs (less pumping) are easily quantified. Other potential benefits include less runoff and drainage with accompanying advantages of reduced risk of nutrient leaching, and protected biodiversity in waterways by reduced extraction. The “value” of this latter environmental benefit largely falls outside traditional cost-benefit analysis; however, it is now recognized that the traditional approach for assessing “value” is severely limited. “Value” should include not only direct benefits to the party who stands to gain from the product but also the wider ecological consequences of these decisions, and the social goals being served by the decision (Costanza, 2006). “Failure to think broadly enough about costs and benefits

leads to decisions that serve only narrow special interest not the sustainable well-being of society as a whole" (Costanza, 2006).

In New Zealand in recent decades an unprecedented demand for freshwater by irrigation to support increasing agricultural productivity, has led in some rivers to decreased flows compared with their long-term averages. Irrigation demands 77% of all allocated freshwaters in New Zealand, slightly higher than the global average of 70%, (NZ MfE, 2007). The Canterbury region of the South Island occupies 66% of total consented irrigated land, and river flows have dropped from long-term mean values at nearly all monitored sites, with drops of 10–25% at some sites (ECan, 2008). This example illustrates that freshwater extraction for irrigation has its limits, and these must be clearly defined. It exemplifies the reason why the New Zealand government formulated the "Sustainable Development Water Programme of Action" in 2003 (NZ MfE, 2007) focusing national policy on freshwater allocation with appropriate methods for setting both ecological flows as well as standards for mandatory measurement of actual water takes. Where freshwater supply is limited (frequently due to high irrigation demand) the full value of improved water use efficiency includes not only profit margins of crop production but also societal impacts by addressing issues of reduced freshwater supply, reduced water quality, and insufficient environmental river flow (reduced biodiversity, culture and heritage). The direct economic value of irrigation for New Zealand is estimated to be NZ$920m (US$580m) from 475 700 ha of land (NZ MAF, 2004). This is estimated as net contribution to GDP at the farm-gate for the year 2002/03, and was estimated using the formula:

Farm-gate GDP due to irrigation = GDP with irrigation – GDP without irrigation (NZ MAF, 2004).

The dollar return per hectare of agricultural land in New Zealand due to the use of irrigation is about NZ$1934 (US$1218).

In comparison, the total ecosystem services value of New Zealand's rivers and lakes has been defined and estimated by Patterson and Cole (1999). A full description of the

methods used is beyond the scope of this paper, and readers are referred to Patterson and Cole (1999) and Costanza et al. (1997) for more detail. Patterson and Cole (1999) assess the value of biodiversity (TEV) as:

$$TEV = DV + IV + PV \qquad (1)$$

where TEV = total economic value; DV = direct value of goods and services derived from direct use of biodiversity (i.e. the agricultural production); ID = indirect value derived from supporting or protecting direct use activities, (i.e. nutrient cycling, biological refugia, waste treatment, etc.); and PV = passive value, value not related to the actual use (i.e. existence and bequeath option).

Using the default methodology of values developed by Costanza et al. (1997), Patterson and Cole (1999) derived a first approximation of the direct and indirect value of ecosystem services provided by New Zealand lake and river ecosystems as NZ$7871m (US$4959m). Using an estimate of 303 977 ha for the total surface area covered by lake ecosystems and 225 750 ha covered by river systems (calculated using first order rivers and assuming a mean width of 500 metres) this equates to a biodiversity value of New Zealand's lakes and rivers of NZ$29 718 (US$18 722) per hectare.

An increase in the productivity of irrigation water, through changes in management and improvements in efficiency, offer the greatest potential for global water savings, because irrigated agriculture is the dominant consumptive user of freshwater world-wide (Jury & Vaux, 2007).

For the research presented in this paper, which assesses potential benefits of a VRI system compared with uniform rate irrigation (URI) in a humid climate, case studies were selected to represent two of the four major global irrigated crops (maize, potatoes) and pasture. Sustained productivity of the four major global crops – rice, wheat, maize and potatoes – is reliant on irrigation. In the USA, more than 50% of irrigation is used for growing cereals, with 29% used for maize (*Zea mays* L.) (Howell, 2001). In the UK 71% of irrigation is used for vegetable growing, with 43% used for potatoes (Weatherhead, 2007). In New Zealand,

75% of irrigation is used on pastoral soils (NZ MAF, 2004), and about 50% of this irrigated pastoral land is used for dairy farming, (NZ Statistics, 2009).

To assess any likely benefits of VRI on variable soils, soil variability must first be quantified. One method that is available for this is electromagnetic induction survey of soil apparent electrical conductivity (EC_a), which defines soil variability on a basis of texture and moisture in non-saline soils (e.g., Sudduth et al., 2005). Soil EC_a maps can then be used to select soil management zones for estimation of soil AWC (available water-holding capacity), (Hedley & Yule, 2009). Irrigation scheduling can then be optimized spatially to each specific soil zone AWC using a daily soil water balance.

The aim of this research is to: (1) determine the soil variability, under one irrigation system, by EMI survey; (2) use GIS and targeted soil sampling of EC_a-defined zones to spatially define soil zone AWCs; (3) investigate the potential advantages of using the soil AWC map to direct variable rate irrigation scheduling instead of a fixed depth of irrigation onto soil management zones; and (4) use key performance indicators to assess potential immediate and ecological benefits by optimizing and varying irrigation on a basis of geospatially defined soil differences.

9.2 Methodology

9.2.1 Case Studies

The three case studies used in this research are (1) a 40-ha irrigated dairy pasture (ryegrass-clover; *Lolium perenne* L. – *Trifolium repens* L.) [Canterbury pasture; Chapter 8], (2) a 24-ha potato (Solanum tuberosum) field [Ohakune potatoes], and (3) a 22-ha maize (Zea mays L) field [Manawatu Sand Country maize]. Centre-pivot irrigation schemes are employed at all three sites.

The 40-ha irrigated dairy pasture site is located near Christchurch, New Zealand. The soils here are variable stony alluvial soils, mapped as Waimakariri soils (Weathered Fluvial

Recent, Hewitt, 1998), formed on outwash gravel plains extending from the Southern Alp mountain range. The soils are characterized by varying depths of fine sandy material with wide-ranging stoniness. Irrigation is typically employed between at least the months of November and March, and regional statistics show that irrigation increases pasture production from 6.4 t DM ha^{-1} yr^{-1} to at least 11.1 t DM ha^{-1} yr^{-1} (Fleming and Burtt, 1991), which enables land-use change from dry-land sheep farming to irrigated dairy farming. Stocking rates are currently 3.3 cows ha^{-1} in this area; and nitrogen fertilizers are typically applied at a rate of 150–300 kg N ha^{-1} yr^{-1}, which is used strategically to address expected feed deficits.

The 23-ha potato field is near Ohakune, in the Central Volcanic Plateau region of the North Island of New Zealand. Here a 400-m centre-pivot is employed for strategic irrigation of potatoes during the summer months of November to February. The variable soils at this flat site are formed on mixed volcanic parent materials: air-fall andesitic tephra, water-borne laharic material and air-fall rhyolitic pumice.

The 22-ha irrigated maize field occurs in the Sand Country Region of Manawatu Province, New Zealand. The topography is a sand plain-sand dune catena sequence. The soils are somewhat excessively drained sandy soils, existing alongside low-lying poorly drained sandy soils, where the water table rises close to the soil surface in low-lying areas during the winter months. Irrigation is normally employed during the summer months of November–March, when there is a significant seasonal soil moisture deficit.

9.2.2 Assessing soil variability by electromagnetic soil survey

An electromagnetic induction (EMI) soil survey was employed to define soil variability spatially with respect to soil water supply characteristics at each site. A Geonics electromagnetic EM38 sensor (Geonics Ltd, Mississauga, Ontario, Canada) and real-time kinematic-differential global positioning system (RTK-DGPS) with Trimble Ag170 field computer (Trimble Navigation Ltd, Sunnyvale, California, USA) on-board an all-terrain vehicle (ATV) were used for on-the-go soil EM mapping. The ATV was driven at 12 km h^{-1}

at swath widths of 10 m. Soil apparent electrical conductivity (EC_a), measured by the EM sensor, was logged simultaneously with high resolution positional data every 1 second.

9.2.3 Soil apparent electrical conductivity map production

Soil EC_a survey points were filtered to remove: (i) RTK-GPS data classified as low accuracy, in order to ensure precise elevation information; and (ii) outlying EC_a values. Filtered data were then imported into ArcMap™ (Environmental Systems Research Institute, ESRI©1999) as latitude and longitude using a WGS84 projection, and subsequently converted to New Zealand Map Grid projection, using the (GD 1949) geodetic datum. The points were kriged using Geostatistical Analyst (ESRI©1999), using ordinary kriging and a spherical semivariogram model, to produce a map of soil EC_a. This map was used to target sites for soil description and sampling likely to reflect the widest range of soil water-holding characteristics. Intact soil cores were collected in high, medium and low EC_a zones, to assess the range of soil available water-holding content (AWC) at each site (Hedley & Yule, 2009).

9.2.4 Estimation of soil AWC in EC_a-defined management zones

The soil total available water-holding capacity (AWC) of each EC_a-defined management zone (high EC_a zone, intermediate EC_a zone, low EC_a zone) was estimated by soil sampling at three replicate sites within each zone. Intact cores were collected for laboratory estimation of soil water retention at 10 kPa (Field Capacity) and bags of loose soil were collected for laboratory estimation of soil water retention at 1500 kPa (Wilting Point) (Gradwell, 1972; Burt, 2004). AWC is defined as the difference between the equivalent depths of water that the effective root zone (or a sampling depth within that root zone) contains at field capacity (FC) and at Permanent Wilting Point (WP).

The soils were sampled to 60 cm depth to include the majority of roots, which extract soil water for plant use. Soil samples (0–15 cm, 15–30 cm, 30–45 cm, 45–60 cm) were also collected for estimation of percent sand, silt, clay and stones (Claydon, 1989).

9.2.5 Soil AWC map production

The EC_a map was interpreted on a basis of lab-estimated AWC or EAWC (Effective AWC) for each soil management zone. EAWC is the sum of AWC and Capillary Rise (CR) and was used where additional plant available water was supplied via capillary rise from a high water table. Capillary rise was estimated using a method developed by Scotter (1989), where soil moisture retentivity and conductivity data are used to predict millimetres of water contributed from different depths of water table in sandy soils.

9.2.6 Adding the daily time-step to soil AWC maps using a water balance model

The amount of plant-available water held in each EC_a-defined soil zone on any one day was calculated using a water balance model (Allen et al., 1998). This model determines soil water content in terms of root zone soil water depletion (S) relative to FC, and is expressed as a water depth in the root zone (mm).

$$S_i = S_{i-1} - R_i - I_i - C_i + Et_i + D_i \qquad (2)$$

where, S_i is root zone soil water depletion at the end of day i (mm), S_{i-1} is the depletion at the end of the previous day, i-1 (mm), R_i is the rainfall on day i (mm), I_i is the irrigation applied on day i (mm), C_i is the capillary rise from groundwater (GW), assumed to be zero when GW>1 m, on day i, Et_i is crop evapotranspiration on day i (mm) and D_i is drainage (runoff plus root zone water loss due to deep percolation) on day i.

Root zone soil water depletion at FC is zero (S = 0), and as soil water is extracted by E_t a critical soil moisture deficit (CSMD) is reached where E_t is limited to less than potential values, and pasture or crop E_t begins to decrease in proportion to the amount of water remaining in the root zone (Allen et al., 1998). The amount of water held in the soil between FC and CSMD is defined as the readily available water (RAWC), which was determined using the specific pasture (0.50 AWC), maize (0.55 AWC) and potato (0.35 AWC) depletion fractions defined by Allen et al. (1998). Daily rainfall data was obtained

from nearby weather stations and daily irrigation schedules were reported by the irrigator operators. These sprinkler irrigation system are expected to have an application efficiency of about 80%, based on a recent audit of these systems in New Zealand (McIndoe, 1999). Site-specific R and I were used to estimate E_t from the pastoral site using the Penman-Monteith equation, as outlined in Allen et al., (1998). This reference Et was then adjusted for crop stage at the irrigated maize and potato sites to provide crop E_t, using procedures outlined by Allen et al. (1998). Capillary rise, C, was assumed to be zero at two sites, but contributes additional plant-available water at the maize site, where the water table occurred within 1 metre of the root zone. At this site, retentivity and conductivity data were used to assess the contribution from capillary rise (Scotter, 1989). A value for D, which includes runoff and deep drainage below the root zone, was calculated as the excess water above FC by the soil water balance model. Deep drainage is calculated for any one day as R plus I minus E_t minus the soil moisture deficit present at the start of the day. Thus deep percolation is effectively assumed to occur at the end of the day, as it takes into account E_t for that day.

The water balance, calculated for each soil zone AWC, assesses soil water status, i.e. mm of available water present in each soil zone on any one day, indicating the day when the CSMD is reached and irrigation should commence.

In addition the water balance was used to estimate the total amount of drainage and E_t in any one season.

9.2.7 Variable rate irrigation scheduling

The soil water balance was also used to compare hypothetical uniform-rate irrigation (URI) scheduling with variable rate irrigation (VRI) schedules for each of four seasons (1 July 04–30 June 05; 1 July 05–30 June 06; 1 July 06–30 June 07; 1 July 07–30 June 08) at the pasture and maize site, and for two seasons (1 July 07–30 June 08; 1 July 08–1 June 09) in the potato field. To maintain potential E_t and therefore potential yield across the whole area, URI scheduling applies a hypothetical 10-mm irrigation event to the whole field

every time the most droughty soil zone (smallest AWC) reaches its CSMD. VRI scheduling adjusts irrigation according to soil zone AWC, so that 10 mm irrigation events are applied only to each soil zone on the day that its specific CSMD is reached.

9.2.8 Key performance indicators

The potential benefits of VRI compared to URI were compared using key performance indicators (KPI) (Table 9.1):

(i) Irrigation water use per season

(ii) Irrigation water lost as drainage and runoff

(iii) Nitrogen leaching

(iv) Energy usage per season

(v) Irrigation water use efficiency (IWUE) (mm irrigation applied per tonne dry matter produced)

(vi) Virtual water content (Hoekstra & Chapagain, 2008)

Both the amount of irrigation required to avoid any plant stress (i.e. by maintaining SMD above the CSMD), and the drainage/runoff have been calculated using the soil water balance model for 4 years of data for the pasture and maize sites and 2 years of data for the potato field. Nitrogen leaching is estimated using the nutrient budgeting model Overseer Version 5.4.3 (AgResearch®, 2009) for pasture, and biophysical models AMaizeN (Li, 2006) and The Potato Calculator, (Jamieson et al., 2004) for maize and potatoes. These models simulate crop growth using site-specific climate, soil and crop production inputs; with N leaching (kg N ha^{-1}) below the root zone being one output. The model outputs have not been validated in this study, and are a poor surrogate of on-site lysimeter measurement methodologies. However the models are useful for comparison of different nitrogen management strategies at any one farm. In this case they have been used to

compare any effects of different irrigation regimes (i.e. URI vs VRI) on drainage and runoff. The depth of the root zone was set at 0.6 m for pasture and potatoes and 1.5 m for maize. For the N leaching under pasture, production was 1100 kg MS ha^{-1} yr^{-1}, stocking rate 3.5 cows per hectare, and N fertiliser was applied once a month from September to June at a rate of 30 kg ha^{-1}. For the N leaching under potatoes, 200 kg/ha N fertiliser was applied (100 kg/ha at planting, 50 kg/ha at 3 weeks, and another 50 kg/ha at 6 weeks after planting). For the N leaching under maize, the model calculates optimum N fertiliser application rates for potential yield, with split application at planting and V6 growth stage.

Energy use is calculated as kWhr m^{-3} water applied, using a factor of 0.42 kWhr m^{-3} irrigation water applied, based on a recent survey of New Zealand irrigation systems (FAR, 2008) and then converted to kg CO_2-eq using an implied emission factor of 0.18 kg CO_2-eq per kWhr electricity consumed (NZ MED, 2008). The IWUE index calculates millimetres of irrigation water applied per tonne DM produced.

Virtual-water content is a concept developed by Hoekstra and Chapagain (2008) and defined as the water required for production. It is categorised into three components: blue, green and grey. Green water refers to the use of rainwater, while blue water refers to the use of ground-water or surface water (i.e. irrigation). Grey water is the amount of water required to dilute a certain amount of pollution (in this case leached N) so that it meets ambient water quality standards (in this example the permissible freshwater N concentration is 10 mg/L, a drinking water standard).

Green virtual-water (V_g) of a primary crop (m3/tonne) was calculated as crop water use divided by crop yield. Crop water use was estimated to be the smaller of cumulative crop Et (calculated using regional climate data and the Penman-Monteith equation; Allen et al., 1998) and effective rainfall (i.e. rainfall during the period of growth, minus any runoff and deep drainage during this period).

Blue virtual-water (V_b) of a primary crop (m^3/tonne) was calculated as effective crop irrigation water use divided by crop yield. Effective irrigation water use was calculated as

the irrigation requirement (estimated from the soil water balance model) minus any runoff and deep drainage during this period. Grey virtual-water (V_{gr}) is calculated as the load of pollutants that enters the water system (in this case leached nitrogen), divided by the maximum acceptable concentration for the pollutant and the crop production. The virtual water content on each primary product for any one year was then calculated in m^3 t^{-1} (Hoeskstra and Chapagain, 2008):

$$V = V_g + V_b + V_{gr} \qquad (3)$$

Table 9.1 Explanation of Key Performance Indicators for assessing potential benefits of VRI

KPI	Units	Description
Water Use	mm season^{-1}	Total amount of irrigation water applied in one season (1 July 07 – 30 June 08)
Drainage/Runoff	mm season^{-1}	Drainage and runoff during one growing season (pasture: 1 July – 30 June), calculated as excess above FC by the soil water balance model; implications for nutrient leaching,
Nitrogen leaching	kg ha^{-1} season^{-1}	Amount of nitrogen leached below the root zone and therefore wasted to crop production
Energy usage	kgCO_2-eq KWhr-energy consumed^{-1}	Energy usage (kWhr m^{-3}) for operation of irrigation system (largely cost of pumping water) converted to equivalent CO_2 emissions
Irrigation Water Use Efficiency	mm tonne DM^{-1}	Reports mm of irrigation water applied per tonne DM produced
Virtual water	m^3 tonne DM^{-1}	The water needed to produce a product

9.3 Results

9.3.1 Soil EC_a maps

The soil EC_a maps (Fig. 9.1) were classified into three zones that were investigated for visible soil differences, and sampled to assess soil AWC (Table 9.2). Soil EC_a zones at the pasture site were characterised by percent stones difference. Increasing percent stones in a sandy loam matrix decreased soil EC_a. There were significant differences in the soil water-holding characteristics of each EC_a-defined zone that could therefore be used as an irrigation management zone on a basis of its soil water-holding properties (see Table 9.2). At this pasture site, AWC increased linearly with soil EC_a, reflecting this percent stone increase (Fig. 9.2).

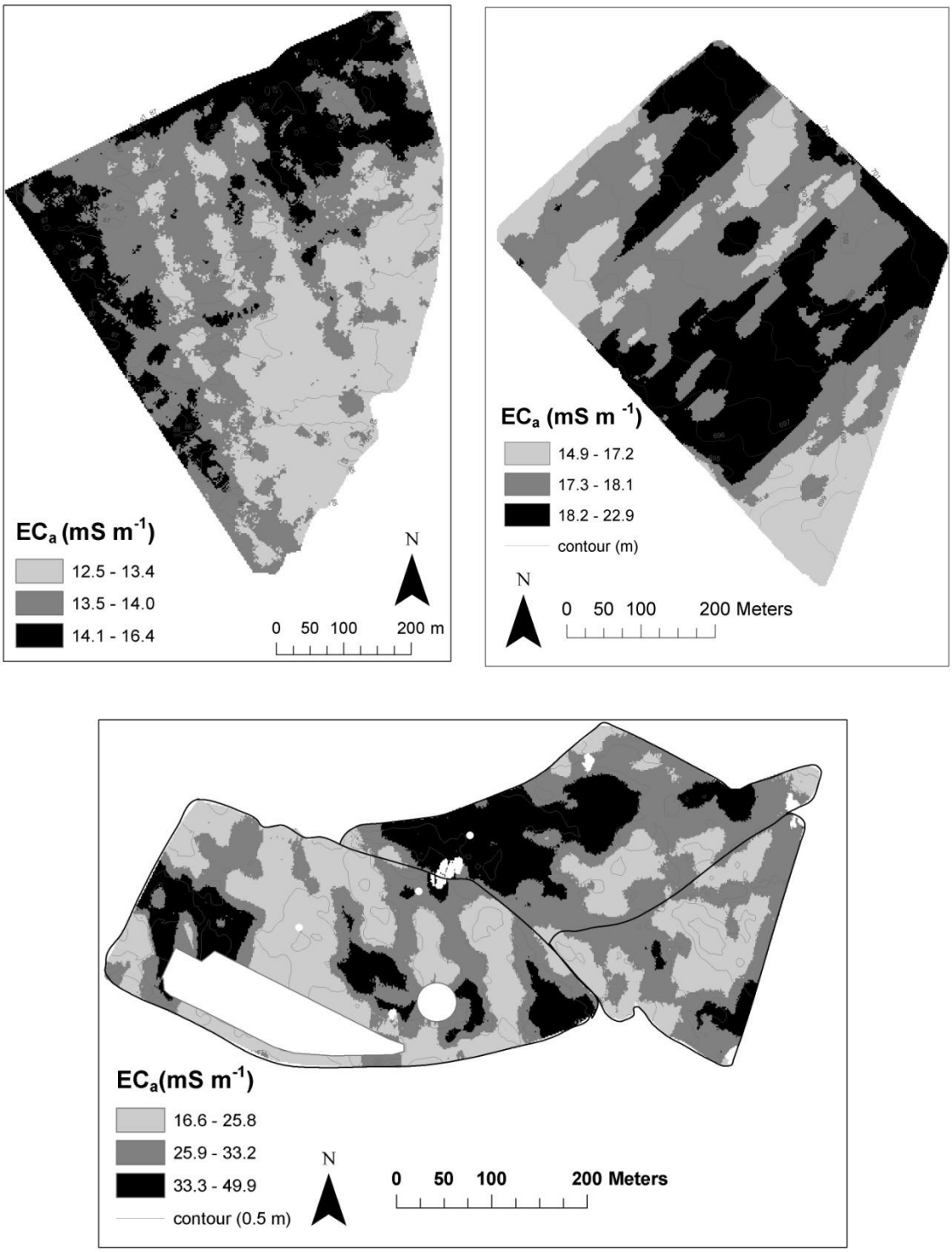

Fig. 9.1 **Soil EC_a maps delineate zones with contrasting AWC (a = Pasture; b = Potato; c = Maize site)**

The low EC_a soil management zone contains 70% stones, which reduced its AWC to 7% (44 mm in 60 cm of root zone) compared with the zone with no stones (AWC = 17%) and the intermediate EC_a zone with 39% stones (AWC= 12%).

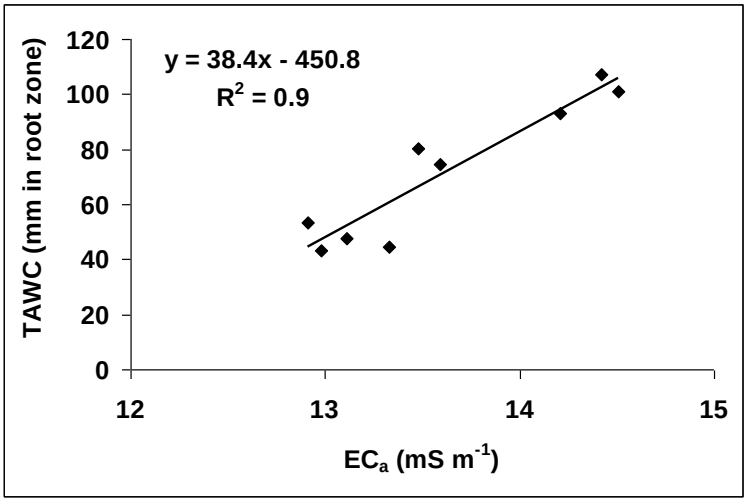

Fig. 9.2 Relation of soil apparent electrical conductivity (EC_a) to total available water-holding capacity (AWC) for Waimakariri soils, at the pastoral site

At the potato site, visual soil inspections at the three EC_a soil management zones revealed three contrasting volcanic parent materials reflecting the frequent episodic nature of volcanic eruptions and lahar events that have contributed to soil forming processes at this site. The low EC_a value zone is characterized by deep, freely draining, pumiceous, loamy silt soils. The soils in the intermediate EC_a zone have developed in andesitic ash (with gravels) inter-bedded with some laharic material. Soils in the high EC_a zone have developed on mixed andesitic and lahar parent materials, dominated by the more recent lahar material. Each zone is characterized by significantly different soil AWCs (Table 9.2). The lower AWC in Zone 2 is likely due to the observed soil compaction and the welded nature of the andesitic ash, which suggests that drying and wetting patterns modelled using a soil water balance for this soil with impeded drainage are likely to over-estimate rate of drainage, because the soil water balance assumes a freely draining soil.

The maize site is characterized by sandy soils in an undulating topography where the water-table rises to, or close to, the surface in low-lying areas, during the winter months. These wet low-lying areas occupy the high EC_a soil management zone, and the contribution of plant available water via capillary rise from the water table is an important contributor. Scotter (1989) showed that soil water retentivity and hydraulic conductivity data can be used to predict this contribution in these soils, and estimated that the equivalent depth of plant-available water increased substantially from 26 to 183 mm as the water table rises from 1.2 m to 0.4 m. Using this relationship, and our observations that the water table rises to within 0.8 m and 1.2 m of the root zone during the maize growing season in the high and medium EC_a-zones, respectively, we estimated a contribution of 130 mm and 30 mm respectively to soil AWC at these two sites. The high, medium and low soil EC_a management zones reflect decreasing AWC and EAWC (Table 9.2). There was a strong relationship between EC_a and AWC ($R^2 = 0.79$) and EC_a and EAWC ($R^2 = 0.94$).

At all three sites the range of AWC (mm available water in the root zone) under one irrigation system varied by more than a two-fold difference. Therefore the potential benefits of variable rate irrigation were assessed.

Table 9.2 Soil apparent electrical conductivity (EC_a), percent clay, sand and stones, and soil water-holding characteristics of each EC_a-defined soil zone at Sites 1, 2 and 3

Site	Soil description	Area	EC_a	Clay*	Sand*	Stones	Bulk density	Field Capacity	Wilting Point	AWC	CR#	EAWC	CSMD##
		(ha)	(mS/m)	(%)	(%)	(%)	(g/cc)	(%)	(%)	(%)	(mm)	mm in root zone**	(mm)
Site 1 – pasture													
Zone 1	Sandy loam	9	14.7–16.7	6	77	0	1.42 (0.02)	21 (2)	4 (1)	17 (1)	0	101	50
Zone 2	Stony sandy loam	20	13.7–14.6	6	77	39	1.22 (0.08)	15 (2)	3 (1)	12 (1)	0	74	37
Zone 3	Very stony sandy loam	11	12.5–13.6	6	77	70	1.13 (0.04)	10 (1)	3 (1)	7 (0)	0	44	22
Site 2 – potatoes													
Zone 1	Loamy silt	7	14.9–17.2	8	42	0	0.65 (0.07)	37 (2)	6 (1)	31 (1)	0	186	65
Zone 2	Loamy sand	9	17.3–18.1	6	74	3	1.09 (0.05)	24 (2)	11 (0)	13 (1)	0	81	28
Zone 3	Sandy loam	8	18.2–22.9	10	60	5	0.96 (0.09)	36 (2)	10 (1)	26 (1)	0	156	55
Site 3 – maize													
Zone 1	loamy sand	4	34.0–50.0	5	88	0	1.38 (0.04)	27 (3)	9 (1)	19 (2)	139	329	181
Zone 2	Sand	12	27.0–33.0	6	87	0	1.37 (0.06)	26 (2)	8 (0)	18 (2)	34	214	118
Zone 3	Sand	6	17.0–26.0	3	94	0	1.53 (0.06)	12 (0)	4 (1)	8 (0)	0	85	47

*% clay and sand are reported as lab-estimated % in the < 2 mm fine-earth soil fraction, and at Site 1 as a field-estimate

** Root zone depth for pasture and potatoes = 60 cm; maize = 100 cm

AWC: laboratory estimated total available water-holding capacity

CR: capillary rise

CSMD: critical soil moisture deficit

EAWC: Effective AWC is the sum of AWC and CR

Standard deviations in parantheses

9.3.2 Estimation of daily soil water status in soil management zones using the soil water balance model

The soil water balance was used to estimate daily soil moisture deficit (SMD) and run-off/drainage events for each zone AWC. Figure 9.3 illustrates changes in SMD and runoff/drainage events for the period 1 July 07 to 1 July 08 for each of the high AWC zones at the three sites. It also shows the hypothetical 10-mm irrigation events, scheduled using the soil water balance, when each specific zone AWC reaches its Stress Point (i.e. CSMD), the trigger point for irrigation (VRI). URI applies irrigation water to the whole site when the CSMD for the soil with the smallest AWC is reached, and therefore applies water needlessly to other zones with larger available water storage capacity. Under VRI the number of irrigation events are reduced (Fig. 9.3) because irrigation is tailored to each specific zone AWC and is only applied to that zone when its specific CSMD is reached. This soil water status information can be used to drive an automated variable rate irrigation system with irrigation scheduling optimized for each zone AWC.

Total volumes of irrigation water required and total volumes of water lost through drainage and run-off were also calculated for each zone for a whole season, using 2–4 years of climate data (Table 9.3)

(a)

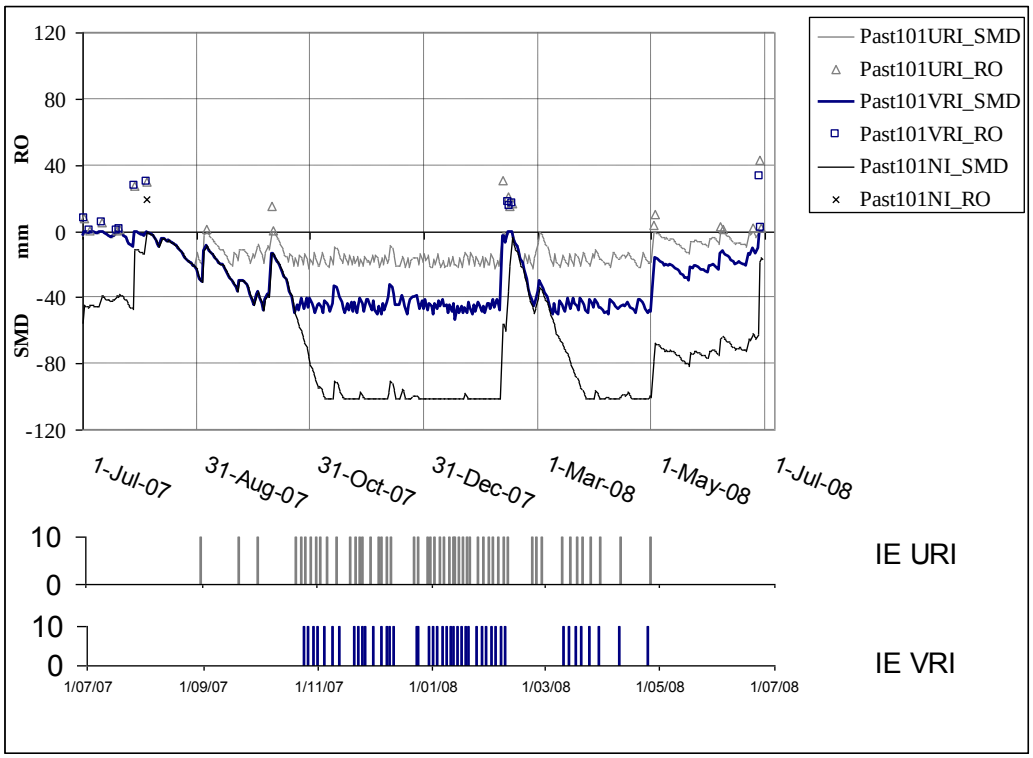
120
80
40
0
-40
-80
-120
RO
mm
SMD
Past101URI_SMD
Past101URI_RO
Past101VRI_SMD
Past101VRI_RO
Past101NI_SMD
Past101NI_RO
1-Jul-07
31-Aug-07
31-Oct-07
31-Dec-07
1-Mar-08
1-May-08
1-Jul-08
10
0
IE URI
10
0
IE VRI
1/07/07
1/09/07
1/11/07
1/01/08
1/03/08
1/05/08
1/07/08

(b)

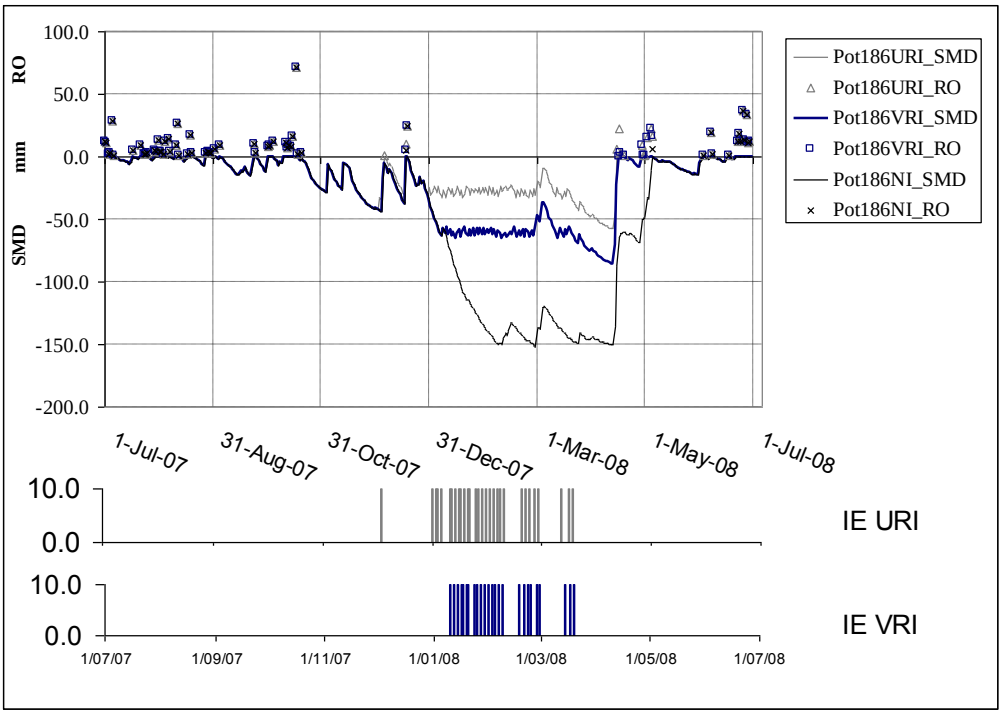
100.0
50.0
0.0
-50.0
-100.0
-150.0
-200.0
RO
mm
SMD
Pot186URI_SMD
Pot186URI_RO
Pot186VRI_SMD
Pot186VRI_RO
Pot186NI_SMD
Pot186NI_RO
1-Jul-07
31-Aug-07
31-Oct-07
31-Dec-07
1-Mar-08
1-May-08
1-Jul-08
10.0
0.0
IE URI
10.0
0.0
IE VRI
1/07/07
1/09/07
1/11/07
1/01/08
1/03/08
1/05/08
1/07/08

(c)

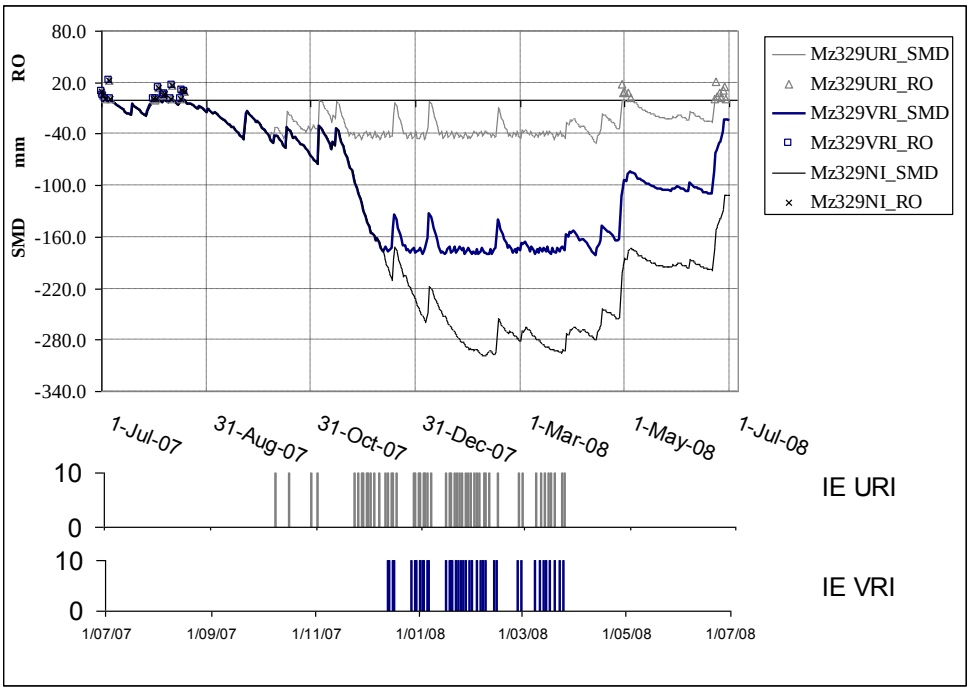

Fig. 9.3 Soil moisture deficit (SMD), drainage/runoff (RO) and irrigation events for 1 July 07 – 1 July 08 at (a) pasture site, (b) potato field and (c) maize grain site, using uniform rate irrigation (URI), variable rate irrigation (VRI) and no irrigation (NI) (IE = 10 mm irrigation events) (date format: day/month/year)

9.3.4 Assessing the potential benefits of VRI using key performance indicators

Table 9.3 compares VRI and URI for (1) total volume of irrigation water required, (2) total volume of water lost during irrigation due to runoff and deep drainage, (3) the amount of nitrogen leached from the soil profile, (4) energy savings due to reduced pumping of reduced water, (5) irrigation water use efficiency (IWUE) expressed as mm t^{-1} (using one mean yield value). KPI were calculated for each zone and these values were then proportioned for the whole site, using size (ha) of each zone. Virtual water content for each production site is also reported in Figure 9.5.

Table 9.3 A comparison of VRI and URI of pasture, potatoes and maize grain for total irrigation requirement, drainage, N leaching, energy use and irrigation water use efficiency (IWUE)

Site	Site 1 Dairy pasture	Site 2 Potatoes	Site 3 Maize grain
Irrigation		mm season^{-1}	
I_{uri}	510	215	385
I_{vri}	466	188	311
% saved	*9*	*13*	*19*
Drainage /Run-off (during period of irrigation)		mm season^{-1}	
D_{uri}	68	50	59
D_{vri}	37	35	45
% saved	*45*	*29*	*25*
N leached		kg ha^{-1}	
N_{uri}	29	11.9	22.1
N_{vri}	26	9.4	22.1
% saved	*10*	*21*	*0*
Energy used		kg CO_2-eq ha^{-1}	
E_{uri}	386	163	291
E_{vri}	352	142	235
% saved	*9*	*13*	*19*
Irrigation Water Use Efficiency		mm t^{-1}	
$IWUE_{uri}$	29	13	28
$IWUE_{vri}$	26	11	22

Our results show that VRI scheduling to soil zones using a water balance approach saves 9–19 % of irrigation water at these three sites, with accompanying energy savings due to reduced pumping. Based on an estimated operating cost for irrigation of NZ$2/mm/ha (US$1.26/mm/ha) (FAR, 2008), this equates to an operating cost saving of NZ$35/ha (US$22/ha) (potatoes), NZ$88/ha (US$55/ha) (pasture), and NZ$149 (US$94/ha) (maize). Maximum water savings are at the maize site, where the contribution of plant-available water via capillary rise in low-lying areas reduced the amount of irrigation water required by 743 m^3 ha^{-1} yr^{-1} (mean of 4 years). The 12% water saving at the potato field is a conservative estimate of potential water savings, because the water-balance modelling approach assumes drainage is not impeded. However, field observations showed significant compaction in the soil zone of smallest

AWC, suggesting further water savings could be made using real-time soil moisture monitoring at this site.

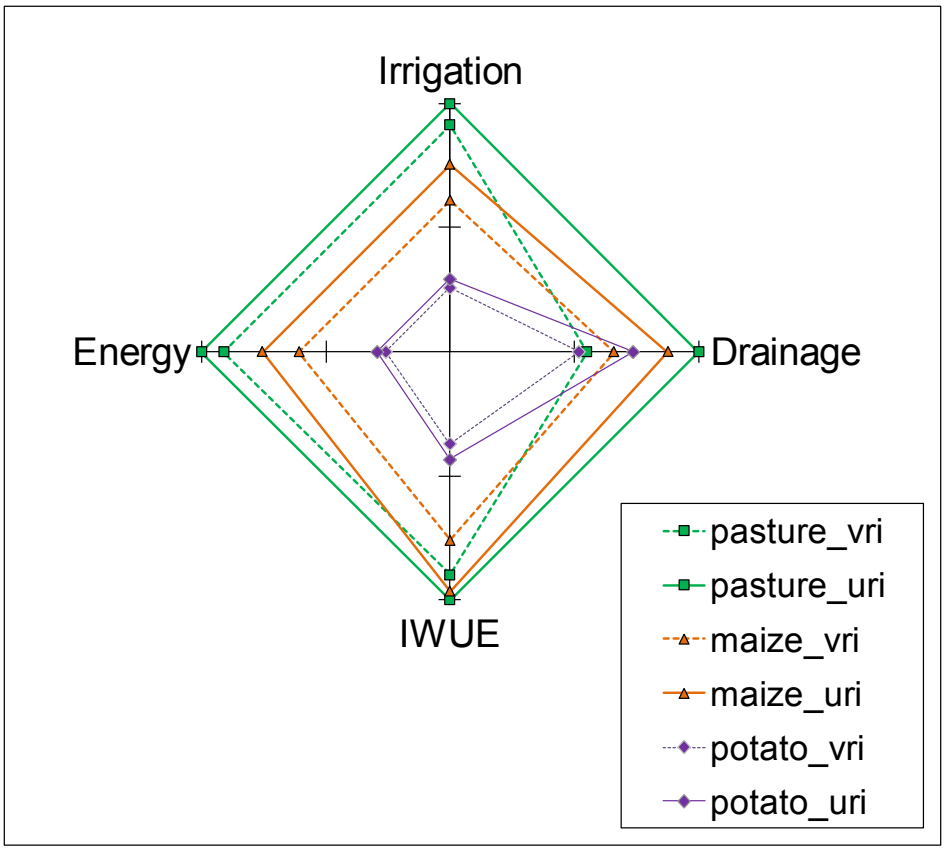

Fig. 9.4 Radar chart comparing potential benefits of variable rate irrigation (VRI) with uniform rate irrigation (URI) under pasture, maize grain and potatoes (IWUE: irrigation water use efficiency)

There was increased run-off and drainage under URI of variable soils and our results show a 25–45% reduction in drainage waters under VRI. Loss of irrigation water by drainage reduces IWUE (Table 9.4) and increases the likelihood of nitrogen leaching. Small decreases in nitrogen leaching were modelled for potatoes and pasture using VRI compared with URI, but no reduction was modelled at the maize site, perhaps reflecting that the maize crop model is modelling N leaching below 1.5 m compared with the depth of 0.6 m used by the other two models. However, the increased drainage implies there is greater risk of N leaching below the root zone during the period of irrigation, e.g., during a large rainfall event. These values will vary from year to year with increased savings due to VRI when there is increased rainfall during the period of irrigation. In arid regions where no rainfall may occur during the irrigation

season, the benefits of VRI (on a basis of soil differences) would be restricted to being able to delay irrigation to certain areas at the beginning of the dry season. For the period of study the mean E_t per season was 886 mm (pasture), 794 mm (maize grain) and 485 mm (potatoes).

The potential benefits of VRI of pasture, maize and potatoes is illustrated and compared in Figure 9.4, where each KPI index is expressed as a fraction of its largest value (in all cases URI of pasture). This comparison of the three sites shows the potato crop to be most water and energy efficient per unit of dry matter production. IWUE was 12.6 mm t^{-1}(URI) and 10.8 mm t^{-1}(VRI) for potatoes, compared with 28 mm t^{-1}(URI) and 22 mm t-1(VRI) for maize, and 29 mm t^{-1}(URI) and 26 mm t^{-1}(VRI) for pasture.

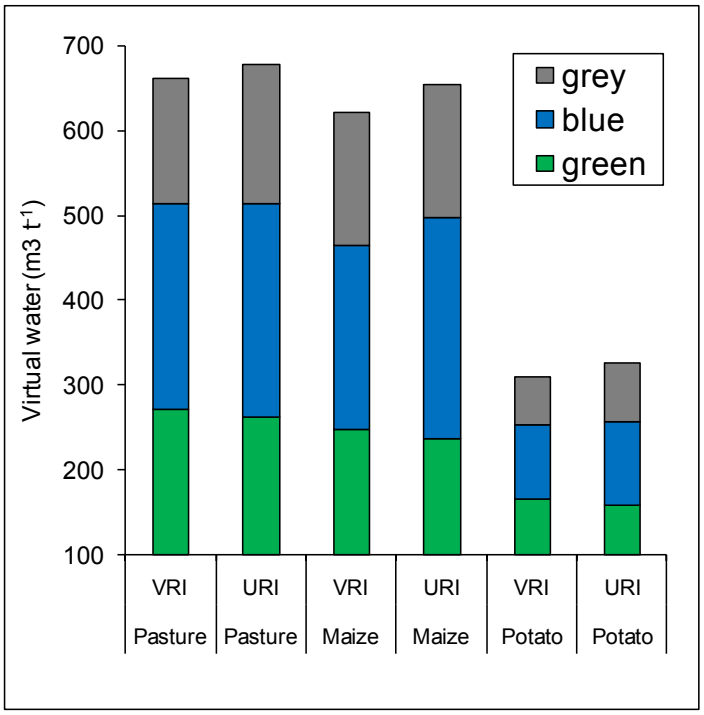

Fig. 9.5 Virtual water content (m^3 t^{-1}) of pasture, maize and potato crop produced over one season (pasture, maize = mean of 4 years; potato = mean of 2 years)

Figure 9.5 illustrates the relative proportions of virtual water contained in each product produced under VRI and URI. Primary production of potatoes (VRI: 308 m^3/t; URI: 325 m^3/t) includes less virtual water than maize (VRI: 622 m^3/t; URI 654 m^3/t), which includes less virtual water than pasture production (VRI: 661 m^3/t; URI: 678

m^3/t). Virtual water content of maize (622–654 m^3/t) compares favorably with a world average value of 900 m^3/t (Hoekstra & Chapagain, 2008), and virtual water content of potatoes (308–325 m3/t) compares favorably with a world average value of 500 m3/t reflecting differences in climate, fertilizer application and utilization, and technology. Grey water accounts for between 18 and 25% of the total water requirement for all sites. VRI increased the ratio of V_g to V_b at all sites and reduced V_{gr} at 2 of the 3 sites.

9.4 Conclusion

An electromagnetic induction survey delineated and quantified soil variability on a basis of soil texture and moisture. The EC_a map derived from the survey was used to target soil samples for characterization of each zone for its ability to supply plant available water. At each of the three sites (pasture, potatoes, maize grain) significant differences (at least two-fold) were found between zone AWCs, necessitating variable rate irrigation. A soil water balance was used to schedule hypothetical irrigation events at each site, and a blanket depth of irrigation water applied to the whole site (URI) determined by the soil with smallest AWC was compared with irrigation depths varied to each soil zone AWC, aiming to maintain each zone soil moisture between stress point and field capacity during the period of irrigation, to ensure maximum water use efficiency.

A number of key performance indicators have been used to investigate and quantify our simulated VRI and URI irrigation schedules. The simulation has assumed that the irrigators are performing within their expected range, i.e. 80% application efficiency, and that the soil water balance is accurately predicting actual soil moisture changes. Our research found that VRI gave 9–19% water and energy savings, and reduced drainage during the period of irrigation (25–45%), which in turn reduces the likelihood of nitrogen leaching, and improves IWUE. The analysis of virtual water content of the three products provided a useful means of comparison, showing that per unit of dry matter the water efficiency of primary production increases from dairy pasture to maize to potato, with an increase in the ratio of V_g to V_b under VRI.

The direct value of water savings using VRI is therefore estimated to be NZ$35–149/ha (US$22–94/ha) under these three contrasting primary productions, a significant saving to the producer. In addition, VRI reduces the pollution risk and extraction demand on freshwaters, two of the suite of freshwater ecosystem services, which are valued at approximately NZ$30 000 (US$18 900) per ha in New Zealand.

CHAPTER TEN

Summary, future research ideas and conclusions

This study has investigated the application of an on-the-go soil electromagnetic mapping system for quantifying soil variability, and has then used the information to target zones for characterizing the soil available water-holding properties of the study area. It has also investigated the use of the proximal sensing method, Vis-NIR DRS for rapid field collection of reflectance spectra. A spatial decision support tool has been developed for variable rate irrigation scheduling onto variable soils, and its potential benefits have been assessed. This final chapter reviews all results and then summarises and compares them enabling some overall conclusions to be made. The summary includes a new extended 4-year comparison of VRI and URI at all six research sites discussed in this thesis [Manawatu maize 1; Manawatu maize 2; Manawatu pasture; Canterbury pasture; Manawatu Sand Country maize; Ohakune potatoes].

The literature review (Chapter 2) highlights the wide range of proximal sensors being developed for ground-based soil sensing utilising each portion of the electromagnetic spectrum. Gamma sensors (wavelength: 3 x 1020 Hz) (e.g. Wong et al., 2008; van Egmond et al., 2008; Soderstrom et al., 2008) are one of the most recent ground-based sensors that have become available for soil investigation, and show considerable promise for real-time, simultaneous estimation of several soil properties, e.g. clay, organic matter and water. The electromagnetic sensor (Geonics EM38, Veris 3100 EC system) is currently the most widely adopted sensor for soil mapping. This sensor (Chapter 2, Section 2.3.2.1), initially developed in the 1980s to investigate soil salinity issues in North America is now extensively used for mapping soil variability, either for site-specific management or for improving existing soil survey maps (Lund et al., 1999). The review of literature also reveals that Vis-NIR diffuse reflectance spectroscopy has been adopted as a laboratory-based technique for rapid, non-destructive simultaneous assessment of a suite of soil properties, but that there has only been limited uptake for field analysis and soil parameter mapping (Chapter 2, Section 2.3.3.1).

The potential use of a (1) Geonics EM 38 sensor for mapping soil variability, and (2) Vis-NIR DRS for field soil analysis has been investigated in this thesis. The spatial structure of spatially defined EC_a sensor data is geostatistically investigated and defined before GIS interpolation of the data in ArcMap (2-dimensional) and ArcScene (3-dimensional (ArcGIS) (e.g. Fig. 10.1). The potential use of Vis-NIR DRS for rapid field analysis of soil carbon, nitrogen and moisture is also investigated.

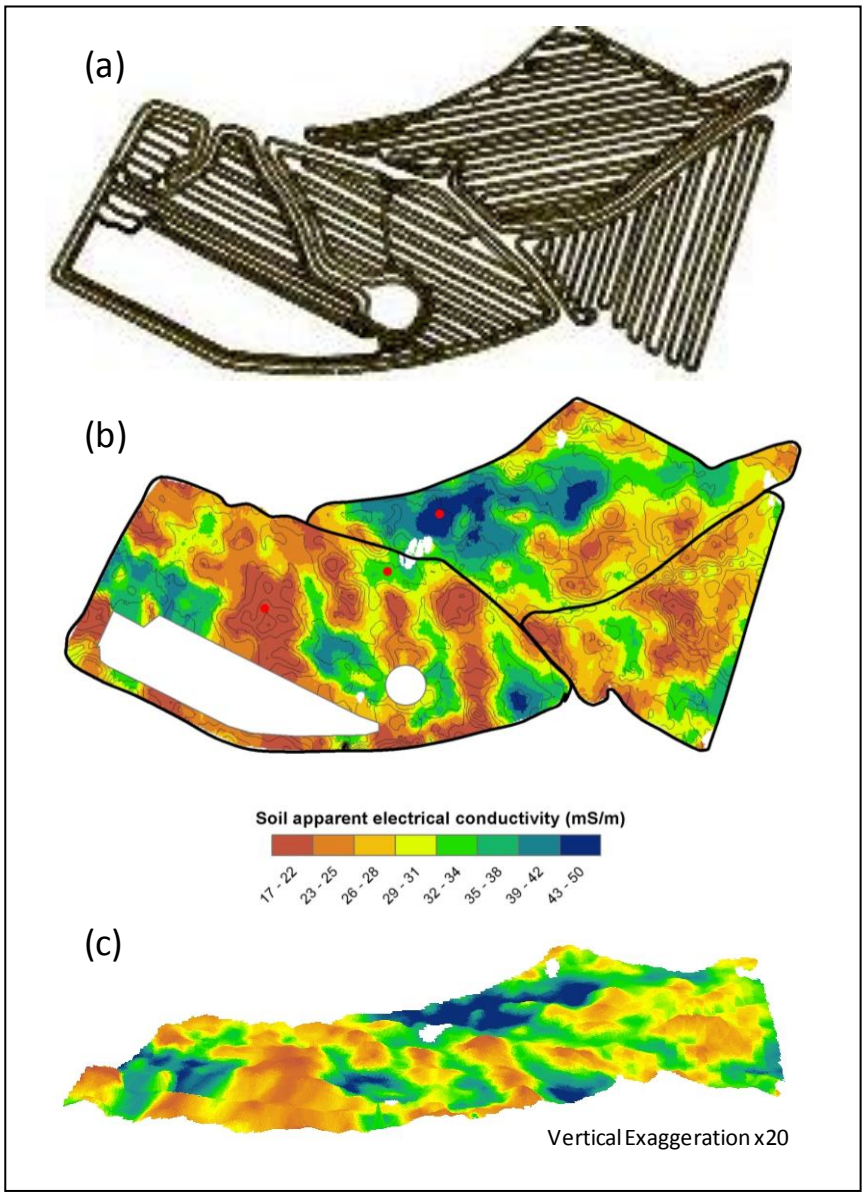

Fig. 10.1 Soil EC_a map of 23-ha maize field in the Manawatu Sand Country (a) EM survey swath tracks showing point logging positions for GPS and sensor data; (b) kriged EC_a prediction surface, note EC_a boundaries show close agreement with contour lines (red dots show 3 sampling positions); (c) 3D representation of the EC_a map to illustrate the relationship of EC_a with topography. High EC_a values (blue) reflect the low-lying wet soils and low EC_a values (brown) reflect the higher sandy knolls

Variogram analysis of EC_a sensor data at the Taupo-Rotorua forest-to-pasture conversion sites (Chapter 3) describes the spatial structure of the EC_a data with spherical and exponential variogram models. The variograms indicate that the optimum sampling distance to fully explore soil EC_a variability at all sites is ≤ 6m. Classical statistical analyses are also presented, and the inadequacy of classical statistics to describe spatial dependence of soil properties is discussed.

The EC_a maps reflect soil differences on a basis of slope and aspect, and targeted soil sampling of these land units give reasons for site-specific management (variable rate nitrogen application). There is less soil development (higher soil C:N ratio) and lower fertility (lower Olsen P values, lower herbage N) on north-facing slopes compared with south-facing slopes and flat areas. This suggests fertilizer N application rates could be reduced to these land units, with cost savings and little to no affect on productivity. More research is required to investigate the potential use of EC_a maps for site-specific management (SSM). Further research could also be conducted to quantify the benefits of SSM such as cost savings, productivity changes, fertilizer N use efficiency, N leaching benefits.

Field Vis-NIR DRS successfully predicted soil carbon, nitrogen and moisture, as well as herbage nitrogen (R^2 calibration ≥ 0.95; R^2 prediction ≥ 0.67) at these forest-to-farm sites, and further research is required to: (1) improve the ease of collection of reflectance spectra from the surface of soil cores in the field, and (2) develop this field analysis method into a soil mapping tool. The former could be addressed by designing and building an improved tool for rapid soil coring, either hand-held or vehicle mounted. A solely vehicle-mounted corer would be limited to use on relatively flat land. The effectiveness of Vis-NIR as a soil mapping tool, for example, for soil carbon mapping, would increase with faster collection of reflectance spectra and simultaneous positional data. In addition, further research is required to assess the usefulness of incorporating other sensor data layers, such as high resolution EC_a sensor data for improving the prediction model for soil parameter maps. Our findings show that soil carbon, nitrogen and moisture are soil parameters well suited to rapid soil mapping with the development of an on-the-go Vis-NIR soil mapping system.

The ability of Vis-NIR DRS to predict soil moisture is also tested at a second site, a 33-ha maize field near Bulls, in the Rangitikei River Catchment (Manawatu maize 1; Chapter 4). The soils were close to field capacity. In this experiment, soil cores were not collected, the prototype contact probe was instead placed directly onto a freshly cut soil surface at 20 mm depth, to collect the reflectance spectra (R^2 calibration = 0.79; R^2 prediction = 0.71). Soil moisture was predicted with less accuracy than in the previous trial, although reflectance spectra were collected more rapidly (n = 90). The accuracy of this method is similar to that reported for an on-the-go soil moisture monitoring trial (Mouazen et al., 2005). The need for such a rapid, accurate high resolution method for soil moisture mapping is discussed in Chapter 4, where a TDR survey (to 45 cm soil depth) (n = 47) of the 33-ha field showed that soil moisture content varied by 12.5–13.1% between sites at any one time, despite these soils having similar AWCs. The TDR data (n = 47) were co-kriged with the high resolution elevation data (n = 10,709) obtained during the EMI survey, improving the RMSE of prediction for a soil moisture map.

In addition, at this 33-ha site, the EC_a soil map was kriged into 3 zones: high, intermediate, and low EC_a zones. Three replicate measurements were made within each soil zone for soil AWC and soil texture. Hand-held EC_a values were collected at field capacity and when the soils were very dry (soil moisture deficit, SMD, 130 mm). Texture-moisture graphs were used to predict soil AWC for each zone, and this predicted value was then regressed against soil EC_a, following the procedure of Waine et al. (2000) and found to be appropriate for the New Zealand textural class ranges (Chapter 4). This provided a relationship between soil EC_a and soil AWC (R^2=0.8) which was used to krige a soil AWC prediction surface. This method is referred to as Method 1 (predicted AWC v EC_a) in this chapter. The difference in soil AWC between zones was very small (160–164 mm m^{-1}) in these medium-textured soils. The soil moisture spatial variability given by TDR results provides a measure of the accuracy of the soil AWC prediction surface at this site. Soil moisture differences at any one time within each EC_a zone are likely due to micro-topographic effects on soil moisture (i.e. wet to saturated poorly draining hollows, and dry rapidly draining sandy ridges). These land units have similar AWCs but drain at different rates. For further improvement of

prediction models further research is also required to investigate the use of point elevation datasets collected simultaneously with the EC_a datasets, for extracting topographic indices such as a wetness index, slope and aspect.

TDR data presented in Chapter 5 (Table 5.1) for this site shows greater soil moisture spatial variability (15.9–24.7 %CV) in the surface soil (0–15 cm) than in the 0–45 cm depth (12.5–13.1 %CV), with some soils wetter than field capacity in the 0-15 cm layer for the 13/12/06 survey. The water held in soil between saturation and field capacity (0–10kPa) is not included in an AWC estimate. It is largely unavailable to plants, because it drains too rapidly, or in this case, where the soil remains saturated for extended periods it indicates a poorly aerated soil where plant roots will not thrive.

Chapter 5 also investigates other methodologies required for accurate irrigation scheduling. These are (1) evaluation of the performance of the irrigation system, and (2) a method for prediction modelling of soil moisture wetting and drying patterns with knowledge of soil AWC, climate, crop type and crop stage, using a soil water balance model.

The New Zealand Code of Practice for Irrigator Evaluation (Bloomer, 2006) was used, and the 600 m centre-pivot sprinkler irrigation system was found to have a lower quartile distribution uniformity ratio (DU_{lq}) of 0.79 (0.68 including the end-gun), which is in the expected range for these systems (McIndoe, 1999). This evaluation is designed to measure how well an irrigation system can uniformly apply a depth of water. A new method would need to be developed for a variable rate irrigation system which aims to vary the amount applied, by a known amount, spatially.

The soil water balance concept (Scotter et al., 1979; Allen et al., 1998) is introduced, and site-specific factors are used to calculate a daily crop E_t, which is shown to vary between 0.3 and 7 mm per day for this irrigated maize crop on alluvial soils. The daily soil moisture deficit is tracked over the maize growing season, and predicts the first day for irrigation as 15 January (the farmer started to irrigate on 18 January), based on 0.55 depletion fraction of AWC for maize (Allen et al., 1998). The soil water balance is shown to be a useful tool for prediction of soil moisture deficit, and because it is

manipulated for soil AWC it has potential use for adding a daily time step to the soil AWC map, starting on a day when the soils are considered to be at field capacity. However the soil water balance assumes that soil drainage is not impeded, so its prediction would need to be modified for poorly draining soils, ideally by real-time monitoring (further research).

Chapter 6 explores methods for adding a daily time step to soil moisture maps, providing the ability to identify the day on which a soil zone reaches its trigger point for irrigation. The experiment is conducted using half of the previous site and a new adjacent field, used for wheat production in the previous year but under irrigated maize grain cultivation for the year of investigation [Manawatu maize 2]. The chapter defines variable rate irrigation (VRI) and selects this site because it has known variable yield, and is therefore a suitable choice to trial a method for producing daily soil water status maps for VRI. At this site a linear relationship is developed between EC_a and AWC (adj $R^2 = 0.76$); and EC_a and field capacity (adj $R^2 = 0.77$). This is a simpler method of prediction of AWC, and more practically applicable at this irrigated site, where the soils were not allowed to dry much beyond their trigger point for irrigation. This linear regression method is referred to as Method 2 (estimated AWC v EC_a). Method 2 was trialled and developed as a potential method for commercial application when a VRI system is installed. A wireless sensor network was installed into the 3 EC_a-defined management zones for real-time hourly logging of soil moisture. The EC_a sensor dataset (latitude, longitude, EC_a value) was used to predict soil moisture on any one day by adding columns for predicted AWC, predicted FC, irrigation trigger (using a known depletion factor or AWC) and soil moisture on day x for each spatially defined EC_a value (based on real-time soil moisture monitoring of the EC_a-defined zones).

Chapter 6 also further explores the use of TDR surveys (n = 50 at any one time) for investigating spatial and temporal variability of soil moisture. The results from the TDR survey show that soil moisture variability within each zone is greater than the difference between each zone at this site. If this variability cannot be captured by intense soil moisture monitoring then site-specific management is not possible. The appropriate zone size is investigated by variogram analysis of the EC_a dataset, and

indicated as at least half the range of spatial dependence (Kerry & Oliver, 2004); in this case 16 m.

The TDR surveys also show that the soil moisture pattern is moderately to strongly temporally stable (bivariate correlations range from 0.52 to 0.95). This supports other research (e.g. Kaleita et al., 2007; Vachaud et al., 1985) suggesting the temporal stability of soil moisture patterns is largely controlled by intrinsic properties of the soil and landscape, such as texture, structure and topographic unit. Therefore if the spatial variability of soil moisture can be defined and monitored, it can be used to manage irrigation events because the pattern is largely stable over time. However, an important finding at this site was that the difference in mean soil moisture between zones at any one time was ≤ 1 standard deviation. A greater density of soil moisture monitoring sites would be required for effective site-specific management.

In Chapter 7 (Method 1), the potential benefits of VRI compared with URI (uniform rate irrigation) are investigated at 2 sites (Site 1: 33-ha maize field [Chapter 4, 5; Manawatu maize 1]; Site 2: 156-ha part-Massey University farms [Manawatu pasture]). Hypothetical irrigation events are scheduled to each EC_a-defined soil AWC zone when each zone reaches its trigger point for irrigation, using a soil water balance model. The soil water balance was used to calculate soil moisture deficit (mm) on any one day for each soil AWC value, and to estimate the day when irrigation should occur. Real-time soil moisture monitoring was also used at the 33-ha maize field, and was used to check the accuracy of soil water balance predicted values of soil moisture. At Site 1, where there was little variation in soil AWC, VRI was used to shut off water to a zone of impeded drainage, which real-time soil moisture monitoring showed to be wetter than its irrigation trigger point for the whole season. At Site 2, the soil AWCs vary between 116 and 230 mm m^{-1}, and irrigation was scheduled according to the individual trigger points of each soil zone. Water savings were 26.3% at Site 1 and 21.8% at Site 2 per year, averaged over a 3-year period between 2004 and 2007. This large potential water saving illustrates the usefulness of VRI and its economic viability, with cost benefits of saved water being reduced pumping costs. The inability of many existing sprinkler systems to spatially vary irrigation water depth applied along their length precludes these potential savings being realized. However systems are being developed and built

in New Zealand (Bradbury, 2009) with individual sprinkler control. Existing sprinkler systems are modified for variable rate control of individual sprinklers, by fitting a latching solenoid valve to each sprinkler. The valve is pulsed on or off by a node, which is part of a wireless control system. Each node controls four sprinklers with individual control of each valve, and receives wireless inputs from a central controller to guide variable water delivery. These systems are being employed for several reasons (e.g., keeping water off raceways), and once installed have multiple benefits, including increased flexibility for mixed cropping, ease of chemigation and fertigation, ability to shut off water as the irrigator passes across farm tracks, wet poorly drained areas etc., improved application accuracy at either end of the pivot, and maintenance of soil water status in the optimum range for plant growth. This last is especially important where variable soils exist under one irrigation system, and/or soil zones exist with impeded drainage due to topographic and/or compaction effects.

Potential savings using VRI at a Canterbury dairy pastoral site (Chapter 8; Canterbury pasture, Method 2) were estimated to be 8% for the season 1 July 2007 to 30 June 2008. The amount of water saved by VRI will vary from year to year, depending on the rainfall pattern in any one year. Water savings with VRI are greatest when rainfall events occur early in the season to refill soil storage. VRI enables better use of available water stored in the soil profile. Chapter 8 also compares drainage and runoff losses under VRI with URI. Results show a 43% reduction in drainage and runoff, when VRI is employed. This is because VRI allows less frequent irrigation of soil zones with largest AWC values, so the SMD can be maintained at a greater deficit, minimizing the risk of runoff during rainfall events during the irrigation season. In addition energy savings are estimated and converted to kg CO_2-eq based on an implied emission factor of 0.18 kg CO_2-eq per kWhr electricity consumed to pump water. This figure is quoted by the NZ Ministry for Economic Development and is comparatively low compared with other countries (e.g. compare 0.54 kg CO_2 per kWhr for the UK [Carbontrust, 2009]) because of the relatively large contribution of renewable energy sources such as wind and water power generation in New Zealand. At this Canterbury site, the simplified Method 2 is employed for prediction of soil AWC from the EC_a data set, and

a strong linear relationship exists between soil EC_a and AWC (R2 = 0.9), thought to reflect the close relationship of percent stone increase with soil EC_a decrease.

A further analysis of potential benefits of VRI is provided in Chapter 9 at two new sites: a 23-ha potato field on volcanic soils [Ohakune potatoes] and a 22-ha maize grain field [Manawatu Sand Country maize] with the 40-ha pastoral Canterbury site [Chapter 8]. The key performance indicators: water use, drainage/runoff, N leaching, energy usage, irrigation water use efficiency and virtual water are investigated and compared for VRI and URI simulated scheduling, for a 4-year period (2-yr at the potato field). The results show water savings of 9–19%, with equivalent energy savings and improved irrigation water use efficiency (IWUE), and reduced drainage and runoff of 25–45 % (with inferred reduced risk of N leaching). N leaching was modelled at each site and results show reduced N leaching under pasture and potatoes. In addition the reduction in virtual water content of primary production using VRI compared with URI is calculated. The direct value of water savings using VRI is estimated to be NZ$35–149/ha.

IWUE is estimated as millimeters of irrigation water applied per tonne DM produced, using reported yields for the case study sites. Further research is required to more accurately assess IWUE by measuring yield differences under different irrigation regimes. This would be possible if a field-scale VRI trial were conducted, ideally with yield mapping of the crop, where known amounts of irrigation (URI and VRI) have been applied over one season. Also, it is recommended that IWUE is best calculated as the mm of irrigation water applied per tonne of additional DM produced compared with a non-irrigated crop.

Method 2 was used to predict soil AWC from soil EC_a at the 22-ha maize field, located in the Sand Country, Manawatu. Here the soils have loamy sand – sand texture (≥ 87% sand to 60 cm) and soil EC_a is predominantly controlled by soil moisture, because soil texture is largely uniform. Capillary rise of plant available water into the root zone occurs in the intermediate and high EC_a zone, as the water table rises close to the surface of the high EC_a zone during the winter months.

The 23-ha potato field is located at Tangiwai at the foot of an active volcano, Mt Ruapehu. Soil pit investigation of EC_a-defined soil zones revealed a complex soil pattern of mixed parent materials. The three major parent materials at this site are: air-fall rhyolitic pumice, air-fall andesitic tephra and water-borne laharic material. There were large differences between mean zone AWCs, although no overall relationship between EC_a and AWC was found. At this site the EC_a-defined zones can be used for site-specific irrigation scheduling. At other sites where a strong relationship exists between EC_a and AWC the data can be regressed and EC_a values then used to predict the AWC map.

Table 10.1 Summary table of soil properties in EC_a-defined zones at all research sites

Site	Soil texture	EC_a mS m^{-1}	Clay %	Sand %	Stones %	Bulk Density g cc^{-1}	Field Capacity m^3 m^{-3}	Capillary Rise mm	AWC* mm/root zone
Site 1 – Manawatu maize grain (on Alluvial terrace soils) (Chapter 4, 5, 7)									
Zone 1	Loamy sand	12.0–18.5	11	63	0	1.22 (0.14)	0.36 (0.01)	0	160 (15) a
Zone 2	Silt loam	18.5–22.0	24	22	0	1.47 (0.04)	0.38(0.04)	0	161 (21) a
Zone 3	Mottled Silt loam	22.0–31.4	14	38	0	1.51 (0.02)	0.39(0.03)	0	164 (32) a
Site 2 – Manawatu pasture (on Alluvial and High terraces soils) (Chapter 4, 7)									
Zone 1	Loamy gravel	14.0–20.0	4	65	30	1.35 (0.01)	0.16 (0.03)	0	77 (9) a
Zone 2	Sandy loam	20.0–30.0	10	53	0	1.38 (0.02)	0.30 (0.01)	0	99 (6) a b
Zone 3	Silt loam	30.0–37.0	20	19	0	1.50 (0.04)	0.41(0.06)	0	124 (28) b c
Zone 4	Silt loam	37.0–65.0	26	6	0	1.43 (0.06)	0.43(0.02)	0	132 (16) c
Site 3 – Manawatu maize grain (on Alluvial terrace soils) (Chapter 6)									
Zone 1	Loamy sand	14.0–19.6	8	61	0	1.47 (0.04)	0.30 (0.02)	0	190 (10) a
Zone 2	Silt loam	19.7–22.1	13	35	0	1.35 (0.07)	0.32 (0.01)	0	180 (15) a
Zone 3	Mottled silt loam	22.2–27.5	27	12	0	1.33 (0.06)	0.37 (0.01)	0	105 (21) b
Site 4 – Canterbury dairy pasture (on Alluvial terrace soils) (Chapter 8, 9)									
Zone 1	v. stony sandy loam	12.5–13.6	6	77	70	1.13 (0.04)	0.10 (0.01)	0	44 (6) a
Zone 2	Stony sandy loam	13.7–14.6	6	77	39	1.22 (0.08)	0.15 (0.02)	0	74 (19) a
Zone 3	Sandy loam	14.7–16.7	6	77	0	1.42 (0.02)	0.21 (0.02)	0	101(6) b
Site 5 – Manawatu maize grain (on Sand plains and dune soils) (Chapter 9)									
Zone 1	Sand	17.0–26.0	3	94	0	1.53 (0.06)	0.12 (0.00)	0	85 (6) a
Zone 2	Sand	27.0–33.0	6	87	0	1.37 (0.06)	0.26 (0.02)	34	214 (15)# b
Zone 3	loamy sand	34.0–50.0	5	88	0	1.38 (0.04)	0.27 (0.03)	139	329 (17)# c
Site 6 – Ohakune potatoes (in mixed volcanic air-fall and water-borne tephric soils) (Chapter 9)									
Zone 1	Loamy silt	14.9–17.2	8	42	0	0.65 (0.07)	0.37 (0.02)	0	186 (3) a
Zone 2	Loamy sand	17.3–18.1	6	74	3	1.09 (0.05)	0.24 (0.02)	0	81 (12) b
Zone 3	Sandy loam	18.2–22.9	10	60	5	0.96 (0.09)	0.36 (0.02)	0	156 (16) c

includes capillary rise; ( ) standard deviation in parentheses; * AWC with different letters are significantly different ($p \leq 0.05$)

10.1. Final synthesis of results comparing VRI and URI at six case study sites (Chapters 4, 6, 7, 8 and 9)

A final synthesis of results is presented in Tables 10.1 and 10.2. Previous chapters (Chapters 4, 5, 6, 7, 8, 9) discuss the relationship of soil EC_a to soil AWC at Sites 1–5 (R^2 ≥ 0.8), so that prediction models were developed to produce soil AWC maps. At Site 1 (Chapter 4, 5, 7), Site 2 (Chapter 4, 7), Site 3 (Chapter 6), Site 4 (Chapter 8, 9) and Site 5 (Chapter 9) the change in soil EC_a is related to soil moisture, texture and management differences.

At Site 4 (Chapter 8), changes in soil EC_a are controlled primarily by percent stones. At Site 5 (Chapter 9), where texture is largely uniform (≥88% sand) the soil EC_a map reflects soil moisture differences. At Site 6 (Chapter 9) no relationship was found between soil EC_a and soil AWC, but soil AWC was significantly different between zones (Table 10.1), so that zone management could be used for irrigation scheduling.

There were significant differences in zone AWC at all sites, except Site 1 (Table 10.1). These differences provide reasons at Sites 2–6 for variable irrigation scheduling to be considered in farm management planning. At Site 1, although AWC differences were insignificant, soil moisture monitoring showed that Zone 3 was a poorly draining area so that irrigation water could also be saved if VRI were employed (Chapter 7).

Table 10.2 shows the AWC range at any one site (defined as the difference between the smallest and largest zone AWC) and provides a further summary of water use efficiency indicators for VRI compared with URI (or no irrigation to Zone 3 at Site 1) for a 4-year period of study 2004–2008. AWC is calculated as the depth of available water in the root zone, using 60 cm for pasture and potatoes (Sites 2, 4 and 6) and 100 cm for maize grain (Sites 1, 3, 5). This provides a different analysis of VRI savings for Site 2 to those reported in Chapter 7 where a root zone of 100 mm was used for a different time period (2004–2007). This final 4-yr analysis (2004–2008) indicates that the amount of irrigation water saved using VRI is between 9 and 26% per year, being greatest at Site 1, where irrigation could be excluded for the whole season to a zone of

poorly draining soils (Chapter 7). At the other sites, where VRI is compared with URI, greatest water savings are observed where the AWC range is greatest (Site 5).

Table 10.2 Summary table of annual VRI water use efficiency indicators at 6 research sites (2004–2008)

Site	Land use	AWC range*	Irrigation water saved	Drainage/Runoff saved during period of irrigation	Energy saved	Reduced N leaching
		mm	%	%	$kgCO_2$-eq ha^{-1} y^{-1}	kg ha^{-1}
1	Maize grain	160–164	26	0	77	-
2	Pasture	77–132	10	19	27	-
3	Maize grain	105–190	12	22	38	-
4	Pasture	44–101	9	55	40	3
5	Maize grain	85–329	21	40	67	0
6	potatoes	81–186	15	29	30	2.5

*AWC = AWC + Capillary rise at Site 3; AWC range calculated for the root zone depth, which is 60 cm (pasture, potatoes) and 100cm (maize grain).

VRI conserves more water in years when there is increased rainfall during the period of irrigation. A wet Spring in 2006 (1 October to 31 December) delivered 400 mm of rain to the maize grain sites, and water savings from VRI increased from a mean of 12% to 14% at Site 3 and 21% to 26% at Site 5. Runoff (overland) and drainage (below the root zone) savings with VRI were up to 55%, compared with URI, during the period of irrigation. This occurs because VRI allows delayed irrigation to some zones so that soils reach greater soil moisture deficits with less likelihood of runoff and deep drainage. Reduced drainage implies more efficient utilisation of applied fertiliser N, with less N leached to groundwater and waterways. N leaching models substantiate these findings at 2 sites, with reduced N leaching under potatoes and pasture (Site 4) using VRI (Table 10.2). The amount of leached N per year under the Canterbury dairy pastoral system (Site 4, Chapter 8) was reduced with VRI (VRI: 26 kg ha^{-1}; URI: 29 kg ha^{-1}) but is slightly higher overall than for the other two systems (Site 5 maize grain VRI: 22 kg ha^{-1}; URI: 22 kg ha^{-1}; Site 6 potatoes VRI 9.4 kg ha^{-1}; URI 11.9 kg ha^{-1}).

Energy savings with VRI were 27–77 kg CO_2-eq ha^{-1} y^{-1}. Energy used during pumping varies with type of irrigation system, and total pumping head pressure, including the energy required for both lifting water and pushing the water against the pressure of sprinklers and friction loss. The exact energy consumed by any pumping system can be determined from flow rate, pressure head and pump efficiency (Chen & Baillie, 2009). Emission factors for energy generation also vary between countries, and Chen and Baillie (2009) report a value of 1.05 kg CO_2 kWh^{-1} for energy generation in Australia; and a factor of 0.54 is used in the UK (Carbontrust, 2009), compared with the 0.18 kg CO_2-eq kWh^{-1} used in this study. This implies greater potential greenhouse gas savings per unit of energy saved, when VRI is used in Australia and the UK.

In New Zealand, if irrigation is used, it accounts for about 50% of on-farm energy costs to the farm-gate in dairy farming systems, and 39% in arable and vegetable growing systems (Barber & Pellow, 2005). The energy saving benefits of VRI can be increased by ensuring the accuracy of delivery by the irrigator is optimised through regular maintenance. For example improving the precision of application from 70% to 90% is reported to reduce water and energy use by 30% (Barber & Pellow, 2005). Because VRI provides control of each sprinkler, some initial results suggest that accuracy of water delivery at either end of the pivot is improved compared with conventional systems (Bradbury, 2009).

Saved water can be diverted elsewhere when total water allocations are restricted allowing improved overall on-farm water use efficiency. Assuming that it costs NZ$2/ha to pump one mm irrigation water (FAR, 2008), these case studies show a cost saving of NZ$51–172/ha.

Site 1 exemplifies water savings under VRI where zone AWCs are similar but irrigation could be shut off or reduced to the zone of poor drainage. Figure 10.2 investigates the relationship between water savings and AWC range at the other sites where a significant difference occurs between zone AWCs.

Our results suggest that where the ability of the soil to store and supply water to plants varies by about 50 mm then the potential water savings are about 10%; and by

>100 mm gives a potential water saving of ≥15%. These values could be used as a rule-of-thumb when farm management decisions are to be made about installation of a VRI system.

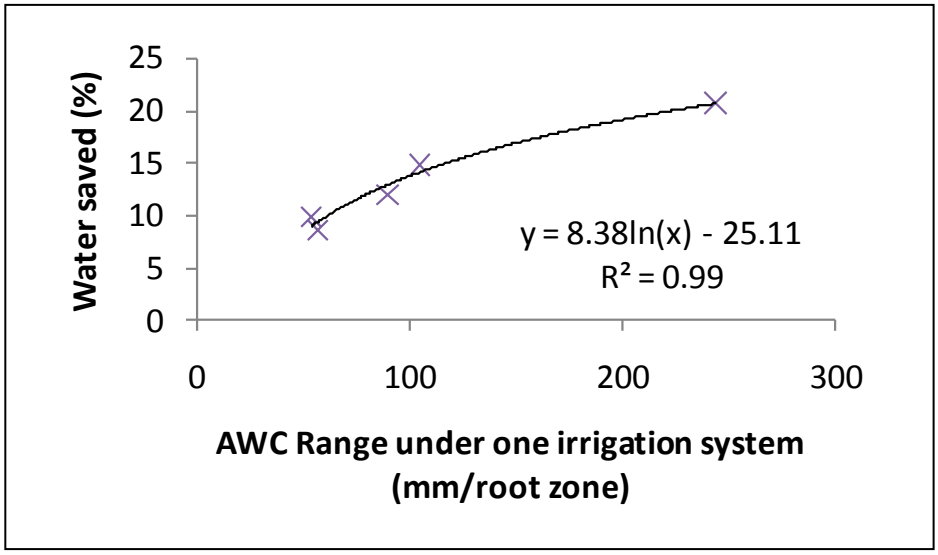

Fig. 10.2 Relation of water savings (%) with VRI to soil variability (defined as the difference between the smallest and largest soil AWC at each site) for five sites and a 4-yr period of study (2004–2008)

Existing best management practice for irrigation in New Zealand (Bloomer, 2007) ensures:

- A well maintained, accurate irrigation system ($DU_{lq} \geq 0.80$)
- Accurate scheduling, either by
  - Engaging a professional service agent (e.g., HydroServices) to monitor soil moisture weekly at a few locations on the farm, and receiving scheduling advice, or
  - Accessing relevant soils information, if available, (e.g., http://growotago.orc.govt.nz online maps) and following web-based (or daily published) climate and regional soil moisture deficit information (e.g. http://climate-explorer.niwa.co.nz) with installation of soil moisture sensors at carefully selected locations. Soil moisture is monitored and irrigation scheduling is determined by a soil water depletion factor.

Methods developed in this study investigate the spatial variability of soil properties and allow existing best management irrigation scheduling to be modified according to site-specific factors. Figure 10.2 provides some rule-of-thumb guidelines for management decisions concerning investment in a VRI system. Using this information to assist decision pathways, a flow chart (Fig. 10.3) illustrates five routes, four of which lead to a decision to use VRI. The flowchart includes the situation where VRI may not be necessary because soil moisture status and crop yields are uniform, and there is no requirement for mixed cropping or major requirement to shut off water to exclusion zones (shown as “E” in Fig. 10.3). A decision to use VRI may be made independent of soil differences where mixed cropping is desirable under one irrigation system, or where there are areas from which water should ideally be excluded, e.g. drains, water bodies, buildings and tracks etc. (Pathway D).

Pathways A, B and C are used where site conditions such as waterlogged zones, variable soil types, or undulating topography occur under one irrigation system. Pathway A exemplifies Sites 2, 3, 4, and 5 (Table 10.2). Pathway B exemplifies Site 6. Pathway C exemplifies Site 1. At Site 3, although soil water status maps were developed, the TDR survey showed that soil moisture variability within each zone was as great as between zones, so that a much larger number of zones would be required to accurately reflect the soil moisture pattern.

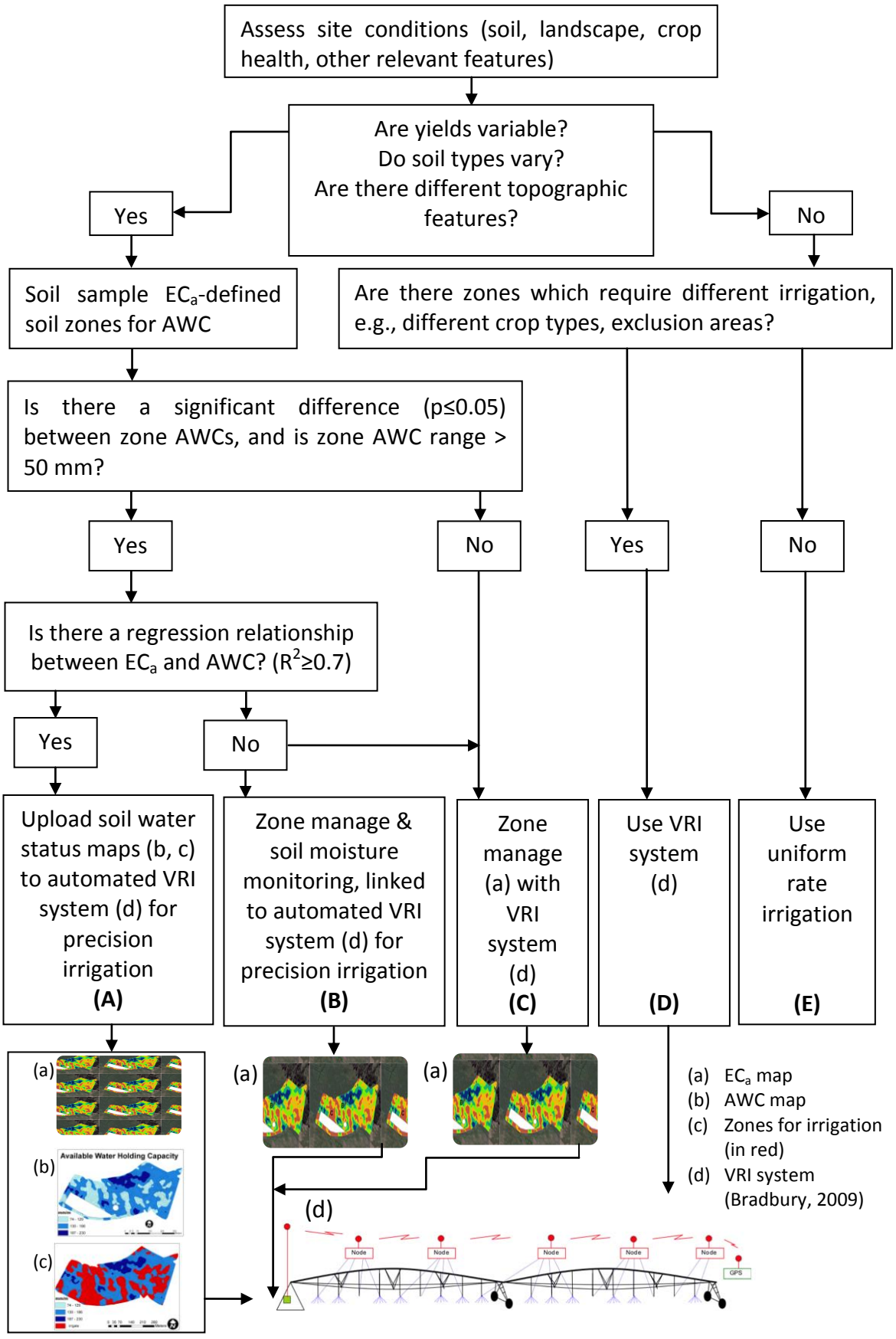

Fig. 10.3 Decision tree for assessing the need for VRI

10.2. Final conclusions

A new method has been developed for spatial irrigation scheduling to help address the urgent need for more efficient use of freshwaters, due to an unprecedented demand in recent years for irrigation to sustain and increase agricultural productivity to meet global food demands (Lal, 2009). This method spatially quantifies and manages soil variability on a basis of soil moisture differences. In addition it provides spatially defined digital data that can be uploaded to the central controller of a VRI system for automated control of irrigation scheduling to different zones.

Soil EC_a datasets have been related to and interpreted on a basis of soil AWC, because soil EC_a is largely controlled by soil texture and moisture differences in non-saline soils. To assess the potential benefits of VRI, hypothetical irrigation scheduling has been tailored to individual soil zones, using a water balance model. The multiple potential benefits of VRI that have been explored and quantified at these six contrasting sites suggest that a VRI field scale trial is now justified.

A future field-scale trial is required to validate the significant potential benefits of precision irrigation for New Zealand farm systems. These potential benefits include 9-26% water saving, NZ$51-172/ha/yr cost saving and 27-77 $kgCO_2$-eq/ha/yr energy saving, based on analysis at six case study sites for the period 2004-2008.

REFERENCES

Adamchuk VI (2008) Development of on-the-go soil sensor systems 2008. Proceedings of the 1st Global Workshop on High Resolution Digital Soil Sensing and Mapping, held under the auspices of the International Union of Soil Sciences (IUSS), Working Group on Digital Soil Mapping, Sydney, Australia, 5–8 February 2008. CDROM.

Adamchuk VI, Hummel JW, Morgan MT, Upadhyaya SK (2004) On-the-go soil sensors for precision agriculture. Computers and Electronics in Agriculture 44: 71–91.

Adamchuk VI, Lund ED, Sethuramasamyraja B, Morgan MT, Dobermann A, Marx DB (2005) Direct measurement of soil chemical properties on-the-go using ion-selective electrodes. Computers and Electronics in Agriculture 48: 272–294.

Allen RG, Periera LS, Raes D, Smith M (1998) Crop evapotranspiration. Guidelines for Computing Crop Water Requirements. FAO Irrigation and Drainage Paper 56. Rome: Food and Agriculture Organization of the United Nations.

Alumbaugh D, Chang PY, Paprocki L, Brainard JR, Glass RJ, Rautman CA (2002) Estimating moisture contents in the vadose zone using cross-borehole ground penetrating radar: a study of accuracy and repeatability. Water Resources Research 38 (12), 1309, doi:10.1029/2001WR000754.

Anderson-Cook CM, Alley MM, Roygard JKF, Khosla R, Noble RB, Doolittle JA (2002) Differentiating soil types using electromagnetic conductivity and crop yield maps. Soil Science Society of America Journal 66: 1562-1570.

ASAE (1993) Test procedure for determining uniformity of water distribution of centre-pivot, corner pivot and moving lateral irrigation machines equipped with spray or sprinkler nozzles. St Joseph, MI: ASAE.

ASCE (1978) Describing irrigation efficiency and uniformity. Journal of Irrigation and Drainage Division 104 (1): 35–41.

Ascough GW, Kiker GA (2002) The effect of irrigation uniformity on irrigation water requirements. Water South Africa 28 (2): 235–242.

Aslam T (2005) Investigations on growth and P uptake characteristics of maize and sweet corn as influenced by soil P status. PhD thesis, Massey University, Palmerston North, NZ.

Awiti AO, Walsh MG, Shepherd KD, Kinyamario J (2008) Soil condition classification using infrared spectroscopy: A proposition for assessment of soil condition along a tropical forest-cropland chronosequence. Geoderma 143: 73–84.

Barber A, Pellow G (2005) Energy use and efficiency measures for the New Zealand arable and outdoor vegetable industry. Prepared for Climate Change Office and Energy Efficiency and Conservation Authority. Where: Agrilink. 30 p.

Barnes EM, Sudduth KA, Hummel JW, Lesch SM, Corwin DL, Yang CH, Daughtry CST, Bausch WC (2003) Remote- and ground-based sensor techniques to map soil properties. Photogrammetric Engineering and Remote Sensing 69: 619–630.

Basset-Mens C, Ledgard S, Boyes M (2009) Eco-efficiency of intensification scenarios for milk production in New Zealand. Ecological Economics 68: 1615−1625.

Bazza M, Najib R (2003) Towards improved water demand management in agriculture in the Syrian Arab Republic. Paper presented to 1st National Symposium on Management and Rationalization of Water Resources Use in Agriculture, University of Damascus, Damascus, Arab Republic of Syria, 28–29 April 2003.

Beckett PHT, Webster R (1971) Soil variability: a review. Soils and Fertilizers 34: 1–15.

Bellamy PH, Loveland PJ, Bradley RI, Lark RM, Kirk GJD (2005) Carbon losses from all soils across England and Wales. Nature 437: 245−248.

Bishop TFA, Lark RM (2006) The geostatistical analysis of experiments at the landscape-scale. Geoderma 133: 87–106.

Blakemore LC, Searle PL, Daly BK (1987) Methods for chemical analysis of soils. New Zealand Soil Bureau Scientific Report 80. Wellington: NZSB. 103 p.

Blonquist JM, Jones SB, Robinson DA (2006) Precise irrigation scheduling for turfgrass using a subsurface electromagnetic soil moisture sensor. Agricultural Water Management 84: 153–165.

Bloomer DJ (2006) Irrigation Evaluation Code of Practice, February 2006, Page Bloomer Associates Ltd, 20 Selwyn Rd., Napier, New Zealand.

Bloomer DJ (2007) Irrigation evaluation code of practice and results of system evaluations. Australasian Precision Agriculture Conference, September 2007, Massey University, Palmerston North, Pp. 12−13.

Bork EW, West NE, Doolittle JA, Boettinger JL (1998) Soil depth assessment of sagebrush grazing treatments using electromagnetic induction. Journal of Range Management 51: 469–474.

Bos MG (1985) Summary of International Commission on Irrigation and Drainage definitions on irrigation efficiency. International Commission of Irrigation and Drainage Bulletin 34: 28–31.

Bradbury S (2009) Variable-rate irrigation for centre-pivot and linear move irrigators. http://www.precisionirrigation.co.nz/index.php Accessed 10 July 2009.

Bramley R, Panten K (2007) Optimising vineyard management through whole-of-block experimentation. Proceedings of the 11th Australasian Symposium on Precision Agriculture, 14 September 2007, Palmerston North, New Zealand. Pp. 18–21.

Brevik EC, Fenton TE, Lazari A (2006) Soil electrical conductivity as a function of soil water content and implications for soil mapping. Precision Agriculture 7: 393–404.

Brickelmeyer RS, Brown DJ, Clegg SM, Barefield J (2008) Simulated in situ soil carbon measurements using combined VisNIR and LIBS sensors. Proceedings of the 1st Global Workshop on High Resolution Digital Soil Sensing and Mapping, held under the auspices of the International Union of Soil Sciences (IUSS), Working Group on Digital Soil Mapping, Sydney, Australia, 5–8 February 2008. CDROM.

Brodnax R (2007) The next chapter in regional policy development to manage adverse effects of land use intensification. In: Currie LD, Yates L eds Proceedings of the FLRC Workshop 'Designing Sustainable Farms: Critical aspects of soil and water management', 8–9 February 2007. Occasional Report No. 20. Massey University, Palmerston North, New Zealand: Fertilizer and Lime Research Centre. P. 4.

Brown DJ (2007) Using a global Vis-NIR soil-spectral library for local soil characterization and landscape modeling in a 2nd-order Uganda watershed. Geoderma 140: 444–453.

Brown DJ, Shepherd KD, Walsh MG, Mays MD, Reinsch TG (2006) Global soil characterization with VNIR diffuse reflectance spectroscopy. Geoderma 132: 273–290.

Brus DJ, Knotters M, Vandooremolen WA, Vankernebeek P, Vanseeters RJM (1992) The use of electromagnetic measurements of apparent soil electrical-conductivity to predict the boulder clay depth. Geoderma 55: 79-93.

Burt CM, Clemmens AJ, Strelkoff TS, Solomon KH, Bliesner RD, Hardy LA, Howell TA, Members ASAE, Eisenhauer DE (1997) Irrigation performance measured: efficiency and uniformity. Journal of Irrigation and Drainage Engineering 123(6): 423–442.

Burt R ed. (2004) Soil survey laboratory methods manual. Soil Survey Investigations Report No. 42 Version 4.0 November 2004. USDA, Natural Resources Conservation Services, Lincoln, Nebraska, US, 700 p.

Burt CM (2006) Volumetric water pricing. ITRC Report No. R 06-002. San Luis Obispo, CA: California Polytechnic State University.

Canterbury Regional Council (2008) Canterbury Regional Environment Report (2008). Christchurch, NZ: ECan. Document available at www.ecan.govt.nz , 246 p.

Carbontrust (2009) Greenhouse gas conversion factors. www.carbontrust.co.uk Accessed 12 June 2009.

Carle JP, Vuorinen P, Del Lungo A (2002) Status and trends in global forest plantation development. Forest Products Journal 52(7/8) : 12–23.

Carroll ZL, Oliver MA (2005) Exploring the spatial relations between soil physical properties and apparent electrical conductivity. Geoderma 128: 354–374.

Cassel, FS (2007) Soil salinity mapping using ArcGIS. In: Pierce FJ, Clay D eds GIS Applications in Agriculture. Taylor & Francis Group, US: CRC Press. Pp. 141–162.

Chapagain AK, Hoekstra AY (2004) Water footprints of nations. Vol. 1: main report. Value of Water Research Report Series No.16. Delft, The Netherlands: UNESCO-IHE.

Chen G, Baillie C (2009) Development of a framework and tool to assess on-farm energy uses of cotton production. Energy Conversion and Management 50: 1256–1263.

Claydon JJ (1989) Determination of particle size in fine grained soils – Pipette method. DSIR Div. Land & Soil Sciences Technical Record LH5. Christchurch, NZ: Manaaki Whenua Press.

Cook SE, Bramley RGV (1998) Precision agriculture – opportunities, benefits and pitfalls of site-specific crop management in Australia. Australian Journal of Experimental Agriculture 38: 753–763.

Cook SE, Corner RJ, Groves PR, Grealish GJ (1996) Use of airborne gamma radiometric data for soil mapping. Australian Journal of Soil Research 34: 183–194.

Corwin DL, Lesch SM, Oster JD, Kaffka SR (2006) Monitoring management-induced spatio-temporal changes in soil quality through soil sampling directed by apparent electrical conductivity. Geoderma 131: 369–387.

Costanza, R (2006) Thinking broadly about costs and benefits in ecological management. Integrated Environmental Assessment and Management 2: 166–173.

Costanza, R, d'Arge R, deGroot R, Farber S, Grasso M, Hannon B, Limburg K, Naeem S, O'Neill RV, Paruelo J and others (1997) The value of the world's ecosystem services and natural capital. Nature 387(6630): 253–260.

Cowie, JD, Fitzgerald P, Owers W (1967) Soils of the Manawatu-Rangitikei sand country. Soil Bureau Bulletin 29. Manaaki Whenua Press, Lincoln. 58 p.

Craighead, MD, Yule IJ (2001) Opportunities for increased profitability from precision agriculture. First Australian Geospatial Information and Agriculture Conference, Sydney, Australia, 17-19 July 2001.

Da Silva, A, Nadler A, Kay BD (2001) Factors contributing to temporal stability on spatial patterns of water content in the tillage zone. Soil and Tillage Research 58: 207–218.

De Benedetto D, Castrignanò, Sollitto D, Campi P, Modugno F (2008) Non-intrusive mapping of subsoil properties in agricultural fields with GPR and EMI. Proceedings of the 1st Global Workshop on High Resolution Digital Soil Sensing and Mapping, held

under the auspices of the International Union of Soil Sciences (IUSS), Working Group on Digital Soil Mapping, Sydney, Australia, 5–8 February 2008. CDROM.

De Jonge KC, Kaleita AL, Thorp KR (2007) Simulating the effects of spatially variable irrigation on corn yields, costs, and revenue in Iowa. Agricultural Water Management 92: 99–109.

De Klein CAM, Ledgard SF (2005) Nitrous oxide emissions from New Zealand agriculture – key sources and mitigation strategies. Nutrient Cycling in Agroecosystems 72 : 77–85.

DIGISOIL (2009) http://eusoils.jrc.ec.europa.eu/ projects/ DIGISOIL, Accessed 5 July 2009.

Doolittle JA, Sudduth KA, Kitchen NR, Indorante SJ (1994) Estimating depths to claypans using electromagnetic induction methods. Journal of Soil and Water Conservation 49: 572–575.

Doolittle JA, Ealy E, Secrist G, Rector D, Crouch M (1995) Reconnaissance soil mapping of a small watershed using electromagnetic induction and global positioning system techniques. Soil Survey Horizons Fall: 86–93.

Doolittle JA, Murphy R, Parks G, Warner J (1996) Electromagnetic induction investigations of a soil delineation in Reno County, Kansas. Soil Survey Horizons Spring: 11–19.

Doolittle JA, Collins ME (1998) A comparison of EM induction and GPR methods in areas of karst. Geoderma 85: 83–102.

Dukes MD, Perry C (2006) Uniformity testing of variable-rate center pivot irrigation control systems. Precision Agriculture 7: 205–218.

Dunn BW, Beecher HG (2007) Using electro-magnetic induction technology to identify sampling sites for soil acidity assessment and to determine spatial variability of soil acidity in rice fields. Australian Journal of Experimental Agriculture 47: 208–214.

ECan Canterbury Regional Council (2009) Canterbury Regional Environment Report 2008. Christchurch, NZ: ECan. available at www.ecan.govt.nz 246 p.

Edkins R (2006) Irrigation efficiency gaps – review and stock take. Report No. L05264/2. Christchurch: Aqualinc Research Ltd.

Eigenberg RA, Doran JW, Nienaber JA, Ferguson RB, Woodbury BL (2002) Electrical conductivity monitoring of soil condition and available N with animal manure and a cover crop. Agriculture Ecosystems and Environment 88: 183–193.

Eigenberg RA, Nienaber JA, Woodbury BL, Ferguson RB (2006) Soil conductivity as a measure of soil and crop status – a four-year summary. Soil Science Society of America Journal 70: 1600–1611.

Esbensen KH, Guyot D, Westad F, Houmoller LP (2006) Multivariate data analysis – in practice : an introduction to multivariate data analysis and experimental design. Oslo, Norway : Camo.

Evett SR, Parkin GW (2005) Advances in soil water content sensing: The continuing maturation of technology and theory. Vadose Zone Journal 4: 986–991.

Evett SR, Tolk JA, Howell TA (2006) Soil profile water content determination: Sensor accuracy, axial response, calibration, temperature dependence, and precision. Vadose Zone Journal 5: 894–907.

Fleming PH, Burtt ES (1991) Farm technical manual. Lincoln, NZ: Lincoln University, Farm Management Department.

Fleskens L, Ataev A, Mamedov B, Spaan WP (2007) Desert water harvesting from Takyr surfaces: Assessing the potential of traditional and experimental technologies in the Karakum. Land Degradation and Development 18: 17–39.

Foundation for Arable Research (2008) Cost of irrigation: a survey report for growers. FAR brochure No. 73. 2 p.

Gehl RJ, Rice CW (2007) Emerging technologies for in situ measurement of soil carbon. Climatic Change 80: 43–54.

Godwin RJ (2001) Field condition mapping technologies. In: Amin MSE ed. Smart farming II: workshop on automation for agriculture, 13–15 March 2001, Putrajaya. Selangor Malaysia: MSAE/UPM Serdang.

Godwin RJ, Miller PCH (2003) A review of the technologies for mapping within-field variability. Biosystems Engineering 84: 393–407.

Goodwin I, O'Connell MG (2008) The future of irrigated production horticulture – world and Australian perspective. Acta Horticulturae 792: 449–458.

Goovaerts P (1997) Geostatistics for natural resources evaluation. Oxford University Press, New York.

Gradwell MW (1972) Methods for physical analysis of soils. Scientific Report 10C. Lower Hutt, New Zealand Soil Bureau (now Landcare Research).

Grandjean G, Cerdan O, Richard G, Cousin I, Lagacherie P, Tabbagh A, Van Wesemael B, Lambot S, Carré F, Maftei R, Hermann T, Thörnelöf L, Chiarantini L, Moretti S, McBratney A, Ben Dor E (2008) DIGISOIL: an integrated system of data collection technologies for mapping soil properties. Proceedings of the 1st Global Workshop on High Resolution Digital Soil Sensing and Mapping, held under the auspices of the International Union of Soil Sciences (IUSS), Working Group on Digital Soil Mapping, Sydney, Australia, 5–8 February 2008. CDROM.

Green SR, Kirkham MB, Clothier BE (2006) Root uptake and transpiration: from measurements and models to sustainable irrigation. Agricultural Water Management 86: 165–176.

Grunwald S (2006) Environmental soil-landscape modelling – geographic information technologies and pedometrics. London: Taylor and Francis. 448 p.

Hanks RJ (1974). Model for predicting plant yield as influenced by water use. Agronomy Journal 66: 660–664.

Hedley CB, Yule IJ, Bradbury S (2005) Using electromagnetic mapping to optimise irrigation water use by pastoral soils. In: Acworth RI, Macky G, Merrick NP eds Proceedings of the NZHS-IAH-NZSSS Conference, Auckland, 28 November – 2 December 2005. Wellington: NZ Hydrological Societ. CDROM.

Hedley CB, Yule IY, Eastwood CR, Shepherd TG, Arnold G (2004) Rapid identification of soil textural and management zones using electromagnetic induction sensing of soils. Australian Journal of Soil Research 42: 389–400.

Hedley CB, Yule IJ, Tuohy MP, Kusumo BH (2008a) Development of proximal sensing methods for mapping soil water status in an irrigated maize field. Proceedings of the 1st Global Workshop on High Resolution Digital Soil Sensing and Mapping, held under the auspices of the International Union of Soil Sciences (IUSS), Working Group on Digital Soil Mapping, Sydney, Australia, 5–8 February 2008. CDROM.

Hedley CB, Yule IJ, Bradbury S (2008b) Spatial irrigation scheduling with soil EM mapping. In: Irrigation New Zealand eds Handbook of 1st Irrigation New Zealand Conference, 14–15 October, 2008. Abstract CS5: 02 Christchurch NZ: Caxton Press.

Hedley CB, Yule IJ (2009) Soil water status mapping and two variable-rate irrigation scenarios. Precision Agriculture 10: 342–355.

Heywood I, Cornelius S, Carver S (2006) An introduction to geographic information systems. 3rd edition, 464p, Prentice Hall, USA.

Hewitt AE (1998) New Zealand soil classification. 2nd ed. Lincoln NZ: Manaaki Whenua Press.

Hezarjaribi A, Sourell H (2007) Feasibility study of monitoring the total available water content using non-invasive electromagnetic induction-based and electrode-based soil electrical conductivity measurements. Irrigation and Drainage 56: 53–65.

Hoekstra AY, Chapagain AK (2008) Globalization of water: sharing the planet's freshwater resources. UK: Blackwell Publishing Ltd.

Horizons Regional Council (2008) Proposed One Plan. www.horizons.govt.nz Retrieved 24 February 2008.

Howell TA (2001) Enhancing water use efficiency in irrigated agriculture. Agronomy Journal 93: 281–289.

Hueni A, Tuohy M (2006) Spectroradiometer data structuring, pre-processing and analysis – an IT-based approach. Journal of Spatial Science 51(2): 93–102.

Huisman JA, Hubbard SS, Redman JD, Annan AP (2003) Measuring soil water content with ground Penetrating radar: a review. Vadose Zone J 2: 476–491.

Humphreys E, White RJG, Smith DJ, Godwin DC (2008) Evaluation of strategies for increasing irrigation water productivity of maize in southern New South Wales using the MaizeMan model. Australian Journal of Experimental Agriculture. 48: 304–312.

Huth NI, Poulton PL (2007) An electromagnetic induction method for monitoring variation in soil moisture in agroforestry systems. Australian Journal of Soil Research 45: 63–72.

Hyslop N, Scott P (2008) The Opuha Dam. In: Irrigation New Zealand ed. Handbook of 1st Irrigation New Zealand Conference, 14–15 October 2008, Christchurch: Caxton Press.

James IT, Waine TW, Bradley RI, Taylor JC, Godwin RJ (2003) Determination of soil type boundaries using electromagnetic induction scanning techniques. Biosystems Engineering 86: 421–430.

Jamieson PD, Martin RJ, Francis GS (1995) Drought influences on grain yield of barley, wheat and maize. New Zealand Journal of Crop and Horticultural Science 23: 55–66.

Jamieson PD, Stone PJ, Zyskowski RF, Sinton S, Martin RJ (2004) Chapter 6: Implementation and testing of the potato calculator: a decision support system for nitrogen and irrigation management. In: MacKerron KL, Haverkort AJ eds Decision support systems in potato production, 85–99. D. Wageningen, The Netherlands: Academic Publishers. Pp. 85–99.

Jaynes DB (1996) Improved soil mapping using electromagnetic induction surveys. In: Robert PC, Rust RH, Larson WE eds Precision agriculture – Proceedings of the 3rd International Conference, Minneapolis, Minnesota, 23–26 June, 1986. Pp. 169–179.

Jiang PP, Anderson SH, Kitchen NR, Sudduth KA, Sadler EJ (2007) Estimating plant-available water capacity for claypan landscapes using apparent electrical conductivity. Soil Science Society of America Journal 71: 1902–1908.

Johnson CK, Mortensen DA, Wienhold BJ, Shanahan JF, Doran JW (2003) Site-specific management zones based on soil electrical conductivity in a semiarid cropping system. Agronomy Journal 95: 303–315.

Jury WA, Vaux HJ (2007) The emerging global water crisis: Managing scarcity and conflict between water users. Advances in Agronomy 95: 1–76.

Kachanoski RG, Gregorich EG, Vanwesenbeeck IJ (1988) Estimating spatial variations of soil-water content using noncontacting electromagnetic inductive methods. Canadian Journal of Soil Science 68: 715–722.

Kaleita AL., Tian LF, Hirschi MC (2005) Relationship between soil moisture content and soil surface reflectance. Transactions of the American Society of Agricultural Engineers 48: 1979–1986.

Kaleita AL, Hirschi MC, Tian LF (2007) Field-scale surface soil moisture patterns and their relationship to topographic indices. American Society of Agricultural and Biological Engineers 50: 557–564.

Kang S, Shi W, Zhang J (2000) An improved water-use efficiency for maize grown under regulated deficit irrigation. Field Crops Research 67: 207–214.

Kerry R, Oliver MA (2008) Determining nugget:sill ratios of standardized variograms from aerial photographs to krige sparse soil data. Precision Agriculture 9: 33–56.

Kgathi DL, Mmopelwa G, Mosepele K (2005) Natural resources assessment in the Okavango Delta, Botswana: Case studies of some key resources. Natural Resources Forum 29: 70–81.

Kgathi DL, Kniveton D, Ringrose S, Turton AR, Vanderpost CHM, Lundqvist J, Seely M (2006) The Okavango: a river supporting its people, environment and economic development. Journal of Hydrology 331: 3–17.

Kim Y, Evans RG, Iversen WM (2008) Remote sensing and control of an irrigation system using a distributed wireless sensor network. IEEE Transactions on Instrumentation and Measurement 57(7): 1379–1387.

Kimberley M, West G, Dean M, Knowles L (2005) The 300 Index – a volume productivity index for radiata pine. New Zealand Journal of Forestry 49: 13–18.

King BA, Kincaid DC (2004) A variable flow rate sprinkler for site-specific irrigation management. Applied Engineering in Agriculture 20(6): 765–770.

Kirda, C (2002) Deficit irrigation scheduling based on plant growth stages showing water stress tolerance. Deficit irrigation practices. FAO Water Reports No. 22. Rome: FAO. pp. 3–10.

Kitchen NR, Sudduth KA, Drummond ST (1996) Mapping of sand deposition from 1993 midwest floods with electromagnetic induction measurements. Journal of Soil and Water Conservation 51: 336–340.

Kitchen NR, Sudduth KA, Kremer RJ, Myers DB (2008) Sensor-based mapping of soil quality on degraded epiaqualf landscapes. Proceedings of the 1st Global Workshop on High Resolution Digital Soil Sensing and Mapping, held under the auspices of the International Union of Soil Sciences (IUSS), Working Group on Digital Soil Mapping, Sydney, Australia,5–8 February 2008. CDROM.

Korsaeth A (2005) Soil apparent electrical conductivity (ECa) as a means of monitoring changes in soil inorganic n on heterogeneous morainic soils in SE Norway during two growing seasons. Nutrient Cycling in Agroecosystems 72: 213–227.

Kusumo BH, Hedley CB, Hueni A, Hedley MJ, Tuohy M.P (2006) The use of reflectance spectroscopy for in situ carbon and nitrogen analysis of pastoral soils. Proceedings of the 2006 NZSSS Conference 'Soils and Society', 27–30 November 2006. Rotorua, NZ: NZSSS. P 67.

Kusumo BH, Hedley CB, Hedley MJ, Hueni A, Tuohy MP, Arnold GC (2008a) The use of reflectance spectroscopy for in situ carbon and nitrogen analysis of pastoral soils. Australian Journal of Soil Research 46: 623–635.

Kusumo BH, Hedley MJ, Tuohy MP, Hedley CB, Arnold GC (2008b) Predicting soil carbon and nitrogen concentrations and pasture root densities from proximally sensed soil spectral reflectance. Proceedings of the 1st Global Workshop on High Resolution Digital Soil Sensing and Mapping, held under the auspices of the International Union of Soil Sciences (IUSS), Working Group on Digital Soil Mapping, Sydney, Australia, 5–8 February 2008. CDROM.

Lal R (2009) Soils and world food security. Soil and Tillage Research 102: 1–4.

Lammers PS, Sun Y, Ma D, Zhu Z (2008) Combined sensor for soil resistance and water content. Proceedings of the 1st Global Workshop on High Resolution Digital Soil Sensing and Mapping, held under the auspices of the International Union of Soil Sciences (IUSS), Working Group on Digital Soil Mapping, Sydney, Australia, 5–8 February 2008. CDROM.

Lavado Contador JF, Maneta M, Schnabel S (2006) Prediction of near-surface soil moisture at large scale by digital terrain modeling and neural networks. Environmental Monitoring and Assessment 121: 213232.

Li FY, Jamieson PD, Pearson A, Arnold N (2007) Simulating soil mineral nitrogen dynamics during maize cropping under variable fertiliser management. In Currie LD, Yates LJ eds Designing sustainable farms: critical aspects of soil and water management. Occasional Report No. 20. Palmerston North, NZ: Fertiliser and Lime Research Centre, Massey University. Pp. 448–458.

LIC (2009) New Zealand Dairy Statistics 2007/08. Hamilton, NZ: Livestock Improvement Corporation (LIC). Document available from DairyNZ www.dairynz.co.nz/dairystatistic 51 p.

Liu W, Gaultney LD, Morgan MT (1993) Soil texture detection using acoustic methods. Paper No. 93-1015. St Joseph, MI: ASAE.

Lobsey C, Viscarra Rossel R, McBratney AB (2008) Proximal soil nutrient sensing using electrochemical sensors. Proceedings of the 1st Global Workshop on High Resolution Digital Soil Sensing and Mapping, held under the auspices of the International Union of

Soil Sciences (IUSS), Working Group on Digital Soil Mapping, Sydney, Australia, 5–8 February 2008. CDROM.

Lu Y-C, Sadler EJ, Camp CR (2005) Economic feasibility study of variable irrigation of corn production in southeast coastal plain. Journal of Sustainable Agriculture: 26, 69–81.

Lund ED, Colin PE, Christy CD, Drummond PE (1998) Applying soil electrical conductivity technology to precision agriculture. In: Robert PC, Rust RH, Larson WE eds Precision Agriculture – Proceedings of the 4th International Conference, St Paul, Minnesota, 22 July 1998. Pp. 1089–1100.

Lund ED, Christy CD, Drummond PE (1999) Practical applications of soil electrical conductivity mapping. Part 1 and Part 2. Papers presented at the 2nd European Conference on Precision Agriculture, Odense, Denmark, 11–15 July 1999: 771–779.

Lund E, Giyoung K, Maxton C, Drummond P, Jensen K (2008) Near-infrared soil spectroscopy: results from field trials using a commercially available spectrophotometer. Proceedings of the 1st Global Workshop on High Resolution Digital Soil Sensing and Mapping, held under the auspices of the International Union of Soil Sciences (IUSS), Working Group on Digital Soil Mapping, Sydney, Australia, 5–8 February 2008. CDROM.

Maier G, Scholger R, Schon J (2006) The influence of soil moisture on magnetic susceptibility measurements. Journal of Applied Geophysics 59: 162–175.

Maleki MR, Mouazen AM, Ramon H, De Baerdemaeker J (2007) Optimisation of soil VIS-NIR sensor-based variable rate application system of soil phosphorus. Soil and Tillage Research 94: 239–250.

Martin MZ, Labbe N, Andre N, Harris R, Ebinger M, Wullschleger SD, Vass AA (2007) High resolution applications of laser-induced breakdown spectroscopy for environmental and forensic applications. Spectrochimica Acta Part B-Atomic Spectroscopy 62: 1426–1432.

Martin DC, Stegman EC, Feres E (1990) Irrigation Scheduling Principles. In: Hoffman GJ et al. eds Management of farm irrigation systems. ASAE Monograph. St Joseph, MI: ASAE. Pp. 155–199.

McBratney AB, Webster R (1986) Choosing functions for semi-variograms and fitting them to sampling estimates. Journal of Soil Science 37: 617–639.

McBratney AB, Minasny B, Rossel RV (2006) Spectral soil analysis and inference systems: a powerful combination for solving the soil data crisis. Geoderma 136: 272–278.

McBride RA, Gordon AM, Shrive SC (1990) Estimating forest soil quality from terrain measurements of apparent electrical conductivity. Soil Science Society of America Journal 54: 290–293.

McCarty GW, Reeves JB, Reeves VB, Follett RF, Kimble JM (2002) Mid-infrared and near-infrared diffuse reflectance spectroscopy for soil carbon measurement. Soil Science Society of America Journal 66: 640–646.

McCarthy JJ, Canziani OF, Leary NA, Dokken DJ, White KS (2001) Climate Change 2001: Impacts, Adaptation, and Vulnerability. Contribution of Working Group II to the Third Assessment Report of the Intergovernmental Panel on Climate Change. Cambridge University Press, Cambridge, New York, Australia, Spain, South Africa.

McCutcheon MC, Farahani HJ, Stednick JD, Buchleiter GW, Green TR (2006) Effect of soil water on apparent soil electrical conductivity and texture relationships in a dryland field. Biosystems Engineering 94: 19–32.

McIndoe I (1999) Testing of irrigation best management guidelines 1998–1999. Report No. 4312/1, for MAF Policy. Lincoln: Lincoln Environmental.

McLaren RG, Cameron KC (1996) Soil science: sustainable production and environmental protection. 2nd ed. Auckland: Oxford University Press.

McNeill JD (1980) Electromagnetic terrain conductivity measurement at low induction numbers. Technical Note TN-6. Mississauga, Canada: Geonics Ltd.

McNeill JD (1992) Rapid, accurate mapping of soil salinity by electromagnetic ground conductivity meters. Advances in measurement of soil physical properties: bringing theory into practice. Special Publication 30. Madison, WI: SSSA. Pp. 209–229.

Milne JDG, Clayden B, Singleton PL, Wilson AD (1995) Soil description handbook. Lincoln: Manaaki Whenua Press, Landcare Research. 157 p.

Minasny B, McBratney AB, Whelan BM (2006) VESPER version 1.6. Variogram estimation and spatial software plus error. Sydney: Australian Centre for Precision Agriculture, The University of Sydney.

Ministry for the Environment (2004) Freshwater for a sustainable future: issues and options. A public discussion paper on the management of New Zealand's freshwater resources. Retrieved 24 February 2008 from www.maf.govt.nz

Ministry for the Environment (2007) Environment New Zealand 2007. Published by Ministry for the Environment, December 2007, Wellington, New Zealand.

Ministry for the Environment (2009) New Zealand's greenhouse gas inventory 1990-2007. Published April 2009, Available at www.mfe.govt.nz Accessed July 2009.

Ministry of Agriculture and Foresty (2004) The economic value of irrigation in New Zealand. MAF Technical Paper No; 04/01. ISBN No: 0-478-07798-X. Published April 2004. Available at www.maf.govt.nz/publications. Accessed July 2009.

Molloy L (1988) Soils of the New Zealand landscape – the living mantle. 2nd ed. Wellington, NZ: Mallinson Rendel.

Morgan M, Bidwell V, Bright J, McIndoe I, Robb C (2002) Canterbury strategic water study. Report No 4557/1, August 2002 prepared for MAF, ECan and MfE. Lincoln, NZ: Lincoln Environmental.

Morton JD, Roberts AHC (1999) Fertilizer use on New Zealand sheep and beef farms. Auckland, NZ: New Zealand Fertilizer Manufacturer's Association. 36 p.

Mouazen AM, De Baerdemaeker J, Ramon H (2005) Towards development of on-line soil moisture content sensor using a fibre-type NIR spectrophotometer. Soil and Tillage Research 80: 171–183.

Mouazen AM, Ramon H (2006) Development of on-line measurement system of bulk density based on on-line measured draught, depth and soil moisture content. Soil and Tillage Research 86: 218–229.

Mouazen AM, Maleki MR, De Baerdemaeker J, Ramon H (2007) On-line measurement of some selected soil properties using a VIS-NIR sensor. Soil and Tillage Research 93: 13–27.

MySQL AB (2005) MySQL, http://www.mysql.com

Mu J, Khan S, Hanjra MA, Wang H (2009) A food security approach to analyse irrigation efficiency improvement demands at the country level. Irrigation and Drainage 58: 1–16.

Neilson P (2008) The Best Solution for New Zealand's Water Problems. In: Irrigation New Zealand ed. Handbook of 1st Irrigation New Zealand Conference, 14–15 October 2008, Christchurch. Christchurch, NZ: Caxton Press.

New Zealand Ministry of Agriculture and Forestry. 2004. The economic value of irrigation in New Zealand. MAF Technical Paper no: 04/01, April 2004. Wellington, NZ: MAF. 62 p.

New Zealand Ministry of Economic Development (2008) New Zealand greenhouse gas emissions 1990–2007. Wellington, NZ: Ministry of Economic Development (MED). 31 p.

New Zealand Ministry for the Environment (2007) Environment New Zealand 2007. Wellington, NZ: Ministry for the Environment, Wellington, New Zealand. http://www.mfe.govt.nz/ [accessed 10 March 2009].

New Zealand Statistics (2009) Irrigable land by farm type (ANZSIC06). 2007 Agricultural Production Census. Wellington, NZ: Statistics NZ.

NIWA (2007) http://www.niwa.cri.nz/ncc

O'Leary G, Peters J (2004) Standards for electromagnetic induction mapping in the grains industry. Horsham, Victoria, Australia: Grains Research and Development Corporation, CSIRO Land and Water, DPI. 51 p.

Oliver MA, Webster R (1991) How geostatistics can help you. Soil Use and Management 7(4): 206–217.

Ortiz BA, Sullivan DG, Perry C, Vellidis G (2007) Spatial variability of root knot nematodes in relation to within field variability of soil properties. 2007 ASAE Annual Meeting Paper 071096, St Joseph, MI: ASABE.

Parliamentary Commissioner for the Environment (PCE) (2004) Growing for good – summary of key messages. Retrieved 24 February 2008 from www.pce.govt.nz

Patrick C, Kechavarzi C, James IT, O'Dogherty M, Godwin RJ (2007) Developing reservoir tillage technology for semi-arid environments. Soil Use and Management 23: 185–191.

Patterson M, Cole A, (1999) Assessing the value of New Zealand's biodiversity. Massey University School of Resource and Environmental Planning Occasional Paper No. 1. Palmerston North: Massey University. 88 p.

Pellerin S, Pages L (1996) Evaluation in field conditions of a three-dimensional architectural model of the maize root system: comparison of simulated and observed horizontal root maps. Plant and Soil 178: 101–112.

Pennock DJ, Veldkamp A (2006) Advances in landscape-scale soil research. Geoderma 133: 1–5.

Peters RT, Evett SR (2007) Spatial and temporal analysis of crop conditions using multiple canopy temperature maps created with center-pivot-mounted infrared thermometers. Transactions of the ASABE 50: 919–927.

Peters RT, Evett SR (2008) Automation of a centre pivot using the temperature-time-threshold method of irrigation scheduling. Journal of Irrigation and Drainage Engineering ASCE 134 (3): 286-291.

Pierce FJ, Elliott TV (2008) A modbus RTU, multidrop bus design for precision irrigation. Proceedings 9th International Precision Agriculture Conference, 20–23 July 2008, Denver. P. 68.

Pires da Silva A, Nadler A, Kay BD (2001) Factors contributing to temporal stability on spatial patterns of water content in the tillage zone. Soil and Tillage Research 58: 207–218.

Pirie A, Singh B, Islam K (2005) Ultra-violet, visible, near-infrared, and mid-infrared diffuse reflectance spectroscopic techniques to predict several soil properties. Australian Journal of Soil Research 43: 713–721.

Plant RE (2001) Site-specific management: the application of information technology to crop production. Computers and Electronics in Agriculture 30: 9–29.

Postel S (1999) Pillar of sand. New York: WW Norton and Company.

Postel S (2005) Liquid assets: the critical need to safeguard freshwater ecosystems. Worldwatch Paper 170. Washington, DC: Worldwatch Institute.

Reedy RC, Scanlon BR (2003) Soil water content monitoring using electromagnetic induction. Journal of Geotechnical and Geoenvironmental Engineering 129: 1028–1039.

Reeves JB III, McCarty GW, Hively WD (2008) Mid-versus near-infrared reflectance spectroscopy for on-site determination of soil carbon. Proceedings of the 1st Global Workshop on High Resolution Digital Soil Sensing and Mapping, held under the auspices of the International Union of Soil Sciences (IUSS), Working Group on Digital Soil Mapping, Sydney, Australia, 5–8 February 2008. CDROM.

Rhoades JD (1981) Predicting bulk soil electrical conductivity vs saturation paste extract electrical conductivity calibrations from soil properties. Soil Science Society of America Journal 45: 43–44.

Rhoades JD (1993) Electrical conductivity methods for measuring and mapping soil salinity. Advances in Agronomy 49: 201–251.

Rhoades JD, Corwin DL (1981) Determining soil electrical conductivity depth relations using an inductive electromagnetic soil conductivity meter. Soil Science Society of America Journal 45: 255-260.

Rhoades JD, Corwin DL (1990) Soil electrical conductivity: Effects of soil properties and application to soil salinity appraisal. Communications in Soil Science and Plant Analysis 21: 837–860.

Richard G, Rouveure R, Chanzy A, Faure P, Chanet M, Marionneau A, Régnier P, Duval Y (2008) Continuous monitoring of agricultural soil physical conditions sing proximal sensors for soil tillage management. Proceedings of the 1st Global Workshop on High Resolution Digital Soil Sensing and Mapping, held under the auspices of the International Union of Soil Sciences (IUSS), Working Group on Digital Soil Mapping, Sydney, Australia, 5–8 February 2008. CDROM.

Rijsdijk A, Bruijnzeel LAS, Prins TM (2007) Sediment yield from gullies, riparian mass wasting and bank erosion in the Upper Konto catchment, East Java, Indonesia. Geomorphology 87: 38–52.

Rosegrant MW, Cai X, Cline SA (2002) Global water outlook to 2025: averting an impending crisis. International Food Policy Research Institute, Food Policy Repor., Colombo, Sri Lanka: International Water Management Institute. Retrieved 5 November 2007 from www.ifpri.org Rossi RE, Mulla DJ, Journel AG, Franz EH (1992) Geostatistical

tools for modeling and interpreting ecological spatial dependence. Ecological Monographs 62(2): 277−314.

Rossi RE, Mulla DJ, Journel AG, Franz EH (1992) Geostatistical Tools for Modeling and Interpreting Ecological Spatial Dependence Ecological Monographs, Vol. 62, No. 2 (Jun., 1992), pp. 277-314 Published by: Ecological Society of America.

Russo D (1986) A stochastic approach to the crop yield-irrigation relationships in heterogeneous soils: I. Analysis of the field spatial variability. Soil Science Society of America Journal 50: 736–745.

Sadler EJ, Camp CR, Evans DE, Millen JA (2002) Spatial variation of corn response to irrigation. Transactions of the ASAE 45(6): 1869–1881.

Sadler EJ, Evans RG, Stone KC, Camp CR (2005) Opportunities for conservation with precision irrigation. Journal of Soil and Water Conservation 60: 371–379.

Sanches ID, Tuohy M, Hedley MJ (2006) Measuring pasture biomass and nitrogen with a spectroradiometer. 13th Australasian Remote Sensing and Photogrammetry Conference. Canberra, Australia, 20–24 November 2006. CDROM.

Schipper LA, Baisden WT, Parfitt RL, Ross C, Claydon JJ, Arnold G† (2007) Large losses of soil C and N from soil profiles under pasture in New Zealand during the past 20 years. Global Change Biology 13: 1138−1144.

Scott NA, Tate KR, Ross DJ, Parshotam A (2006) Processes influencing soil carbon storage following afforestation of pasture with Pinus radiata at different stocking densities in New Zealand. Australian Journal of Soil Research 44(2): 85–96.

Scotter DR, Clothier BE, Turner MA (1979) The soil-water balance in a Fragiaqualf and its effect on pasture growth in central New Zealand. Australian Journal of Soil Research 17: 455–465.

Scotter DR (1989) An analysis of the effect of water table depth on plant-available soil water and its application to a yellow-brown sand. New Zealand Journal of Agricultural Research 32: 71−76.

Seckler D, Amarasinghe U, Molden D, de Silva R, Barker R (1998) World water demand and supply 1990 to 2025: scenarios and issues. International Water Management Institute Research Report 19. Colombo, Sri Lanka: International Water Management Institute.

Seckler D, Barker R, Amarasinghe U (1999) Water scarcity in the twenty-first century. International Journal of Water Research Development 15: 29–42.

Shepherd KD, Walsh MG (2002) Development of reflectance spectral libraries for characterization of soil properties. Soil Science Society of America Journal 66: 988–998.

Sherlock MD, McDonnell JJ (2003) A new tool for hillslope hydrologists: spatially distributed groundwater level and soil water content measured using electromagnetic induction. Hydrological Processes 17: 1965-1977.

Shonk JL, Gaultney LD, Schulze DG, Vanscoyoc GE (1991) Spectroscopic sensing of soil organic-matter content. Transactions of the ASAE 34: 1978-1984.

Smith HF (1938) An empirical law describing heterogeneity of agricultural crops. Journal of Agricultural Science 28: 1–23.

Söderström M, Eriksson JE (2008) Gamma-ray sensing for cadmium risk assessment in agricultural soil and grain – a case study in eastern Sweden. Proceedings of the 1st Global Workshop on High Resolution Digital Soil Sensing and Mapping, held under the auspices of the International Union of Soil Sciences (IUSS), Working Group on Digital Soil Mapping, Sydney, Australia, 5–8 February 2008. CDROM.

Sommer M, Wehrhan M, Zipprich M, Weller U, Castell WZ, Ehrich S, Tandler B, Selige T (2003) Hierarchical data fusion for mapping soil units at field scale. Geoderma 112: 179–196.

Starr GC (2005) Assessing temporal stability and spatial variability of soil water patterns with implications for precision water management. Agricultural Water Management 72: 223–243.

Statistics New Zealand Agricultural Production Census (2002) http://www.stats.govt.nz/tables/2002-ag-prod/default.htm 19 June 2009.

Stokes JR, Horvath A (2009) Energy and air emission effects of water supply. Environmental Science and Technology 43: 2680–2687.

Stronge J (2001) Field efficiency of border strip irrigation in Canterbury, New Zealand. Masters thesis, Lincoln University, Lincoln, New Zealand.

Sudduth KA, Hummel JW (1993) Soil organic-matter, CEC, and moisture sensing with a portable nir spectrophotometer. Transactions of the ASAE 36: 1571–1582.

Sudduth KA, Drummond ST, Kitchen NR (2001) Accuracy issues in electromagnetic induction sensing of soil electrical conductivity for precision agriculture. Computers and Electronics in Agriculture 31: 239–264.

Sudduth KA, Kitchen NR, Bollero GA, Bullock DG, Wiebold WJ (2003) Comparison of electromagnetic induction and direct sensing of soil electrical conductivity. Agronomy Journal 95: 472–482.

Sudduth KA, Kitchen NR, Wiebold WJ, Batchelor WD, Bollero GA, Bullock DG, Clay DE, Palm HL, Pierce FJ, Schuler RT, Thelen KD (2005) Relating apparent electrical conductivity to soil properties across the north-central USA. Computers and Electronics in Agriculture 46: 263–283.

Sudduth RS, Kitchen NR, Sadler EJ, Drummond ST, Myers DB (2008) VNIR spectroscopy for estimation of within-field variability on soil properties. Proceedings of the 1st Global Workshop on High Resolution Digital Soil Sensing and Mapping, held under the auspices of the International Union of Soil Sciences (IUSS), Working Group on Digital Soil Mapping, Sydney, Australia, 5–8 February 2008. CDROM.

Swaminathan MS (2007) Can science and technology feed the world in 2025? Field Crops Research 104: 3–9.

Taylor J (2004) Digital terroirs and precision viticulture: investigations into the application of information technology in Australian vineyards. PhD thesis, Australian Center for Precision Agriculture, Faculty of Agriculture, Food and Natural Resources, University of Sydney, NSW, Australia.

Taylor JA, McBratney AB, Whelan BM (2007) Establishing management classes for broadacre agricultural production. Agronomy Journal 99: 1366–1376.

Taylor J, Short M, McBratney A, Wilson J (2008) Comparison of the ability of multiple soil sensors to predict soil properties in a Scottish potato production system. Proceedings of the 1st Global Workshop on High Resolution Digital Soil Sensing and Mapping, held under the auspices of the International Union of Soil Sciences (IUSS), Working Group on Digital Soil Mapping, Sydney, Australia, 5–8 February 2008. CDROM.

Thompson RB, Gallardo M, Valdez LC, Fernandez MD (2007) Determination of lower limits for irrigation management using in situ assessments of apparent crop water uptake made with volumetric soil water content sensors. Agricultural Water Management 92: 13–28.

Tomer MD, Anderson JH (1995) Variation of soil water storage across a sand plain hillslope. Soil Science Society of America Journal 38: 1091–1100.

Topp GC, Davis JL, Annan AP (1980) Electromagnetic determination of soil-water content - measurements in coaxial transmission-lines. Water Resources Research 16: 574–582.

Triantafilis J, Laslett GM, McBratney AB (2000) Calibrating an Electromagnetic Induction Instrument to Measure Salinity in Soil under Irrigated Cotton. Soil Science Society of America Journal 64: 1009–1017.

Triantafilis J, Odeh IOA, McBratney AB (2001a) Five Geostatistical Models to Predict Soil Salinity from Electromagnetic Induction Data Across Irrigated Cotton. Soil Science Society of America Journal 65: 869–878.

Triantafilis J, Huckel AI, Odeh IOA (2001b) Comparison of statistical prediction methods for estimating field-scale clay content using different combinations of ancillary variables. Soil Science 166: 415–427.

Trimble (2009) Centimetre accuracy and RTK. Last accessed 5 July 2009 from www.trimble.com.

UN/WWAP (United Nations/World Water Assessment Programme) (2003) 1st UN world water development report: water for people, water for life. Paris, New York and Oxford: UNESCO (United Nations Educational, Scientific and Cultural Organization) and Bergham Books.

Vachaud G, Passerat de Silans A, Balabanis P, Vauclin M (1985) Temporal stability of spatially measured soil water probability density function. Soil Science Society of America Journal 49: 822–828.

Van Egmond FM, Loonstra EH, Limburg J (2008) Gamma-ray sensor for topsoil mapping: the Mole. Proceedings of the 1st Global Workshop on High Resolution Digital Soil Sensing and Mapping, held under the auspices of the International Union of Soil Sciences (IUSS), Working Group on Digital Soil Mapping, Sydney, Australia, 5–8 February 2008. CDROM.

Vellidis G, Tucker M, Perry C, Kvien C, Bednarz C (2008) A real-time wireless smart sensor array for scheduling irrigation. Computers and Electronics in Agriculture 61: 44–50.

Viscarra Rossel RA (2007) Robust modelling of soil diffuse reflectance spectra by "bagging-partial least squares regression". Journal of Near Infrared Spectroscopy 15: 39–47.

Viscarra Rossel RA, McBratney AB (1998) Laboratory evaluation of a proximal sensing technique for simultaneous measurement of soil clay and water content. Geoderma 85: 19–39.

Viscarra Rossel RA, Walvoort DJJ, McBratney AB, Janik LJ, Skjemstad JO (2006) Visible, near infrared, mid-infrared or combined diffuse reflectance spectroscopy for simultaneous assessment of various soil properties. Geoderma 131: 59–75.

Viscarra Rossel and others (2008) The soil spectroscopy group: making a global soil spectral library. Presentation at 3rd global workshop on Digital Soil Mapping, Logan, Utah 30/9–3/10 2008. http://groups.google.com/group/soil-spectroscopy

Vitharana UWA, Meirvenne MV, Simpson D, Cockx L, De Baerdemaeker J (2008) Key soil and topographic properties to delineate potential management classes for precision agriculture in the European loess area Geoderma 143: 206–215.

Vucetich CG, Wells N (1978) Soils, agriculture and forestry of Waiotapu Region, Central North Island, New Zealand. New Zealand Soil Bureau Bulletin 31. Wellington, NZ.

Waine TW, Blackmore BS, Godwin RJ (2000) Mapping available water content and estimating soil textural class using electromagnetic induction. EurAgEng 2000,

Warwick, UK. Paper Number: 00-SW-044 UK: European Society of Agricultural Engineers.

Walker TW (1968) Changes induced in the soil by pastoral farming. In Soils of New Zealand. Soil Bureau Bulletin 26(1): 104–109.

Wallace JS, Batchelor CH (1997) Managing water resources for crop production. Philosophical Transactions of the Royal Society of London B 352: 937–947.

Weatherhead EK (2007) Survey of irrigation of outdoor crops in 2005 – England and Wales. Silsoe, UK: Cranfield University. 30 p.

Webster R, Oliver MA (2006) Modeling spatial variation of soil as random functions. In: Grunwald S ed. Environmental soil-landscape modeling – geographic information technologies and pedometrics. London: Taylor and Francis. Pp. 241–287.

Webster R, Oliver MA (2007) Geostatistics for environmental scientists. 2nd Ed. UK: John Wiley and Sons.

Weller U, Zipprich M, Sommer M, Castell WZ, Wehrhan M (2007) Mapping clay content across boundaries at the landscape scale with electromagnetic induction. Soil Science Society of America Journal 71: 1740–1747.

Wells C, Barber A (1998) Field testing indicators of sustainable irrigated agriculture study. MAF Policy Technical Paper 00/04 prepared by Agriculture NZ Ltd in association with John Greer and Sue Cumberworth and Lincoln Ventures. 40 p.

Wesseling JG, Feddes RA (2006) Assessing crop water productivity from field to regional scale. Agricultural Water Management 86: 30–39.

Wheadon M, Adam B (2006) Forest converter's guide: South Waikato/Bay of Plenty forest to farming project. – fieldbook. Forest to Farming Group Field Day, 27 April 2006. Wellington, NZ: Sustainable Farming Fund.

Whelan B, McBratney A (2000) The "Null Hypothesis" of precision agriculture management. Precision Agriculture 2: 265–279.

Whelan B, Sun Y, Zeng Q, Shulze Lammers P, Hassall J (2008) Paddock-scale draught resistance and soil moisture measurement in Australia using a tine-based force/capacitance sensing system. Proceedings of the 1st Global Workshop on High Resolution Digital Soil Sensing and Mapping, held under the auspices of the International Union of Soil Sciences (IUSS), Working Group on Digital Soil Mapping, Sydney, Australia, 5–8 February 2008. CDROM.

Williams M (2006) Many Rivers to Cross. AgScience 24: 6–8.

Wong MTF, Asseng S (2006) Determining the causes of spatial and temporal variability of wheat yields at sub-field scale using a new method of upscaling a crop model. Plant and Soil 283: 203–215.

Wong MTF, Harper RJ (1999) Use of on-ground gamma-ray spectrometry to measure plant-available potassium and other topsoil attributes. Australian Journal of Soil Research 37: 267–277.

Wong MTF, Wittwer K, Oliver Y, Robertson MJ (2008) Use of EM38 and gamma-ray spectrometry as complementary sensors for high resolution soil property mapping. Proceedings of the 1st Global Workshop on High Resolution Digital Soil Sensing and Mapping, held under the auspices of the International Union of Soil Sciences (IUSS), Working Group on Digital Soil Mapping, Sydney, Australia, 5–8 February 2008. CDROM.

Wood M, Wang QJ, Bethune M (2007) An economic analysis of conversion from border-check to centre-pivot irrigation on dairy farms in the Murray Dairy Region, Australia. Irrigation Science 26: 9–20.

Young M, Hatton DH (2000) Inter-state water trading: a 2-year review. Natural Resource Management Economics 00_001, Policy and Economic Research Unit. Adelaide: CSIRO Land and Water.

Yule IJ, Kohnen G, Nowak M (1999) A tractor performance monitor with DGPS capability. Computers and Electronics in Agriculture 23: 155–174.

Yule IJ, Murray RI, Irwin M, Hedley MJ, Jones J (2005) Variable-rate application technology for aerial topdressing aircraft. Paper No. 051121. 2005 ASAE International Meeting, Tampa, Florida, USA.

Yule, IJ, Lawrence HG, Jago J (2008). Precision management for dairy farming and automation. Proceedings of the 9th International Conference on Precision Agriculture, Denver, Colorado, USA, 20-23 July, 2008.

Zhang H (2003) Improving water productivity through deficit irrigation: examples from Syria, the North China plain and Oregon, USA. In Kijne JW, Barker R, Molden D eds Water productivity in agriculture: limits and opportunities for improvement. Wallingford, UK: CAB Publishing.

Zhang ML, Crocker RL, Mankin RW, Flanders KL, Brandhorst-Hubbard JL (2003) Acoustic estimation of infestations and population densities of white grubs (Coleoptera: Scarabaeidae) in turf grass. Journal of Economic Entomology 96: 1770–1779.